EUROPEAN ORGANIZATION FOR NUCLEAR RESEARCH (CERN)

LHCb-PUB-2012-006
August 8, 2012

Implications of LHCb measurements and future prospects

The LHCb collaboration[†]

and

A. Bharucha[a], I.I. Bigi[b], C. Bobeth[c], M. Bobrowski[d], J. Brod[e], A.J. Buras[f], C.T.H. Davies[g], A. Datta[h], C. Delaunay[i], S. Descotes-Genon[j], J. Ellis[i,k], T. Feldmann[l], R. Fleischer[m,n], O. Gedalia[o], J. Girrbach[f], D. Guadagnoli[p], G. Hiller[q], Y. Hochberg[o], T. Hurth[r], G. Isidori[i,s], S. Jäger[t], M. Jung[q], A. Kagan[e], J.F. Kamenik[u,v], A. Lenz[i], Z. Ligeti[w], D. London[x], F. Mahmoudi[i,y], J. Matias[z], S. Nandi[l], Y. Nir[o], P. Paradisi[i], G. Perez[i,o], A.A. Petrov[aa,ab], R. Rattazzi[ac], S.R. Sharpe[ad], L. Silvestrini[ae], A. Soni[af], D.M. Straub[ag], J. Virto[z], Y.-M. Wang[l], A. Weiler[ah], J. Zupan[e]

[a] *Institut für Theoretische Physik, University of Hamburg, Hamburg, Germany*
[b] *Department of Physics, University of Notre Dame du Lac, Notre Dame, USA*
[c] *Technical University Munich, Excellence Cluster Universe, Garching, Germany*
[d] *Karlsruhe Institute of Technology, Institut für Theoretische Teilchenphysik, Karlsruhe, Germany*
[e] *Department of Physics, University of Cincinnati, Cincinnati, USA*
[f] *TUM-Institute for Advanced Study, Garching, Germany*
[g] *School of Physics and Astronomy, University of Glasgow, Glasgow, United Kingdom*
[h] *Department of Physics and Astronomy, University of Mississippi, Oxford, USA*
[i] *European Organization for Nuclear Research (CERN), Geneva, Switzerland*
[j] *Laboratoire de Physique Théorique, CNRS/Univ. Paris-Sud 11, Orsay, France*
[k] *Physics Department, Kings College London, London, UK*
[l] *Theoretische Elementarteilchenphysik, Naturwissenschaftlich Techn. Fakultät, Universität Siegen, Siegen, Germany*
[m] *Nikhef, Amsterdam, The Netherlands*
[n] *Department of Physics and Astronomy, Vrije Universiteit Amsterdam, Amsterdam, The Netherlands*
[o] *Department of Particle Physics and Astrophysics, Weizmann Institute of Science, Rehovot, Israel*
[p] *LAPTh, Université de Savoie, CNRS/IN2P3, Annecy-le-Vieux, France*

[†]Authors are listed on the following pages.

[q] Institut für Physik, Technische Universität Dortmund, Dortmund, Germany
[r] Institute for Physics, Johannes Gutenberg University, Mainz, Germany
[s] Laboratori Nazionali dell'INFN di Frascati, Frascati, Italy
[t] Department of Physics & Astronomy, University of Sussex, Brighton, UK
[u] J. Stefan Institute, Ljubljana, Slovenia
[v] Department of Physics, University of Ljubljana, Ljubljana, Slovenia
[w] Ernest Orlando Lawrence Berkeley National Laboratory, University of California, Berkeley, USA
[x] Physique des Particules, Université de Montréal, Montréal, Canada
[y] Clermont Université, Université Blaise Pascal, CNRS/IN2P3, Clermont-Ferrand, France
[z] Universitat Autonoma de Barcelona, Barcelona, Spain
[aa] Department of Physics and Astronomy, Wayne State University, Detroit, USA
[ab] Michigan Center for Theoretical Physics, University of Michigan, Ann Arbor, USA
[ac] Institut de Théorie des Phénomènes Physiques, EPFL, Lausanne, Switzerland
[ad] Physics Department, University of Washington, Seattle, USA
[ae] INFN, Sezione di Roma, Roma, Italy
[af] Department of Physics, Brookhaven National Laboratory, Upton, USA
[ag] Scuola Normale Superiore and INFN, Pisa, Italy
[ah] DESY, Hamburg, Germany

Abstract

During 2011 the LHCb experiment at CERN collected $1.0\,\text{fb}^{-1}$ of $\sqrt{s} = 7\,\text{TeV}$ pp collisions. Due to the large heavy quark production cross-sections, these data provide unprecedented samples of heavy flavoured hadrons. The first results from LHCb have made a significant impact on the flavour physics landscape and have definitively proved the concept of a dedicated experiment in the forward region at a hadron collider. This document discusses the implications of these first measurements on classes of extensions to the Standard Model, bearing in mind the interplay with the results of searches for on-shell production of new particles at ATLAS and CMS. The physics potential of an upgrade to the LHCb detector, which would allow an order of magnitude more data to be collected, is emphasised.

The LHCb collaboration

I. Bediaga[1], J.M. De Miranda[1], F. Ferreira Rodrigues[1], J. Magnin[1], A. Massafferri[1], I. Nasteva[1], A.C. dos Reis[1]
[1] *Centro Brasileiro de Pesquisas Físicas (CBPF), Rio de Janeiro, Brazil*

S. Amato[2], K. Carvalho Akiba[2], L. De Paula[2], O. Francisco[2], M. Gandelman[2], A. Gomes[2], J.H. Lopes[2], J.M. Otalora Goicochea[2], E. Polycarpo[2], M.S. Rangel[2], B. Souza De Paula[2], D. Vieira[2]
[2] *Universidade Federal do Rio de Janeiro (UFRJ), Rio de Janeiro, Brazil*

C. Göbel[3], J. Molina Rodriguez[3]
[3] *Pontifícia Universidade Católica do Rio de Janeiro (PUC-Rio), Rio de Janeiro, Brazil*

P. Chen[4,39], Y. Gao[4], G. Gong[4], H. Gong[4], F. Jing[4], L. Li[4], Y. Li[4], B. Liu[4], H. Lu[4], B. Shao[4], S. Wu[4], T. Xue[4], Z. Yang[4], X. Yuan[4], M. Zeng[4], F. Zhang[4], Y. Zhang[4], L. Zhong[4]
[4] *Center for High Energy Physics, Tsinghua University, Beijing, China*

I. De Bonis[5], D. Decamp[5], C. Drancourt[5], Ph. Ghez[5], P. Hopchev[5], J.-P. Lees[5], I.V. Machikhiliyan[5,31], M.-N. Minard[5], B. Pietrzyk[5], S. T'Jampens[5], V. Tisserand[5], E. Tournefier[5,53], G. Vouters[5]
[5] *LAPP, Université de Savoie, CNRS/IN2P3, Annecy-Le-Vieux, France*

Z. Ajaltouni[6], H. Chanal[6], E. Cogneras[6], O. Deschamps[6], I. El Rifai[6], P. Henrard[6], M. Hoballah[6], M. Jahjah Hussein[6], R. Lefèvre[6], L. Li Gioi[6], S. Monteil[6], V. Niess[6], P. Perret[6], D.A. Roa Romero[6], K. Sobczak[6]
[6] *Clermont Université, Université Blaise Pascal, CNRS/IN2P3, LPC, Clermont-Ferrand, France*

C. Adrover[7], E. Aslanides[7], J.-P. Cachemiche[7], J. Cogan[7], P.-Y. Duval[7], F. Hachon[7], B. Khanji[7], R. Le Gac[7], O. Leroy[7], G. Mancinelli[7], E. Maurice[7], M. Perrin-Terrin[7], F. Rethore[7], M. Sapunov[7], J. Serrano[7], A. Tsaregorodtsev[7]
[7] *CPPM, Aix-Marseille Université, CNRS/IN2P3, Marseille, France*

S. Barsuk[8], C. Beigbeder-Beau[8], T. Cacérès[8], O. Callot[8], D. Charlet[8], O. Duarte[8], J. He[8], B. Jean-Marie[8], O. Kochebina[8], J. Lefrançois[8], F. Machefert[8], A. Martín Sánchez[8], M. Nicol[8], P. Robbe[8], M.-H. Schune[8], M. Teklishyn[8], V. Tocut[8], B. Viaud[8], I. Videau[8]
[8] *LAL, Université Paris-Sud, CNRS/IN2P3, Orsay, France*

E. Ben-Haim[9], M. Benayoun[9], P. David[9], L. Del Buono[9], A. Martens[9], F. Polci[9]
[9] *LPNHE, Université Pierre et Marie Curie, Université Paris Diderot, CNRS/IN2P3, Paris, France*

T. Brambach[10], Ch. Cauet[10], M. Deckenhoff[10], M. Domke[10], R. Ekelhof[10], M. Kaballo[10], T.M. Karbach[10], F. Kruse[10], J. Merkel[10], K. Rudloff[10], S. Schleich[10], M. Schlupp[10], B. Spaan[10], S. Swientek[10], K. Warda[10], J. Wishahi[10]
[10] *Fakultät Physik, Technische Universität Dortmund, Dortmund, Germany*

C. Bauer[11], M. Britsch[11], C. Föhr[11], M. Fontana[11], H. Fuchs[11], W. Hofmann[11], T. Kihm[11],

D. Popov[11], M. Schmelling[11], D. Volyanskyy[11], H. Voss[11], M. Zavertyaev[11,a]
[11] *Max-Planck-Institut für Kernphysik (MPIK), Heidelberg, Germany*

S. Bachmann[12], A. Bien[12], J. Blouw[12], F. Dordei[12], C. Färber[12], E. Gersabeck[12], S. Hansmann-Menzemer[12], A. Jaeger[12], K. Kreplin[12], G. Krocker[12], C. Linn[12], J. Marks[12], M. Meissner[12], T. Nikodem[12], P. Seyfert[12], S. Stahl[12], J. van Tilburg[12], U. Uwer[12], S. Wandernoth[12], D. Wiedner[12], A. Zhelezov[12]
[12] *Physikalisches Institut, Ruprecht-Karls-Universität Heidelberg, Heidelberg, Germany*

O. Grünberg[13], T. Hartmann[13], C. Voß[13], R. Waldi[13]
[13] *Institut für Physik, Universität Rostock, Rostock, Germany*

S. Bifani[14], S. Farry[14], P. Ilten[14], T. Kechadi[14], Z. Mathe[14], R. McNulty[14], R. Wallace[14], W.C. Zhang[14]
[14] *School of Physics, University College Dublin, Dublin, Ireland*

D.A. Milanes[15], A. Palano[15,b]
[15] *Sezione INFN di Bari, Bari, Italy*

A. Carbone[16,c], I. D'Antone[16], D. Derkach[16,38], A. Falabella[16,e], D. Galli[16,c], I. Lax[16], U. Marconi[16], S. Perazzini[16,c], V. Vagnoni[16], G. Valenti[16], M. Zangoli[16]
[16] *Sezione INFN di Bologna, Bologna, Italy*

W. Bonivento[17], S. Cadeddu[17], A. Cardini[17], A. Lai[17], G. Manca[17,d], R. Oldeman[17,d,38], B. Saitta[17,d]
[17] *Sezione INFN di Cagliari, Cagliari, Italy*

W. Baldini[18], C. Bozzi[18], F. Evangelisti[18], L. Landi[18,e], A. Mazurov[18,33,38], M. Savrie[18,e], S. Squerzanti[18], S. Vecchi[18]
[18] *Sezione INFN di Ferrara, Ferrara, Italy*

A. Bizzeti[19,h], M. Frosini[19,f], G. Graziani[19], G. Passaleva[19], M. Veltri[19,g]
[19] *Sezione INFN di Firenze, Firenze, Italy*

M. Anelli[20], F. Archilli[20,38], G. Bencivenni[20], P. Campana[20,38], P. Ciambrone[20], P. De Simone[20], G. Felici[20], G. Lanfranchi[20,38], M. Palutan[20], A. Saputi[20], A. Sarti[20,l], B. Sciascia[20], F. Soomro[20,38]
[20] *Laboratori Nazionali dell'INFN di Frascati, Frascati, Italy*

R. Cardinale[21,i,38], F. Fontanelli[21,i], C. Patrignani[21,i], A. Petrolini[21,i]
[21] *Sezione INFN di Genova, Genova, Italy*

M. Calvi[22,j], S. Furcas[22], A. Giachero[22], C. Gotti[22], M. Kucharczyk[22,26,38,j], M. Maino[22], C. Matteuzzi[22], G. Pessina[22]
[22] *Sezione INFN di Milano Bicocca, Milano, Italy*

G. Carboni[23,k], S. De Capua[23,k], G. Sabatino[23,k], E. Santovetti[23,k], A. Satta[23]
[23] *Sezione INFN di Roma Tor Vergata, Roma, Italy*

A.A. Alves Jr[24], G. Auriemma[24,m], V. Bocci[24], G. Martellotti[24], G. Penso[24,l], D. Pinci[24],

R. Santacesaria[24], C. Satriano[24,m], A. Sciubba[24]
[24] *Sezione INFN di Roma La Sapienza, Roma, Italy*

S. Nisar[25]
[25] *Institute of Information Technology, COMSATS, Lahore, Pakistan*

P. Morawski[26], G. Polok[26], M. Witek[26]
[26] *Henryk Niewodniczanski Institute of Nuclear Physics Polish Academy of Sciences, Kraków, Poland*

B. Muryn[27], A. Oblakowska-Mucha[27], K. Senderowska[27], T. Szumlak[27]
[27] *AGH University of Science and Technology, Kraków, Poland*

Z. Guzik[28], A. Nawrot[28], M. Szczekowski[28], A. Ukleja[28]
[28] *Soltan Institute for Nuclear Studies, Warsaw, Poland*

I. Burducea[29], C. Coca[29], M. Dogaru[29], A. Grecu[29], F. Maciuc[29], R. Muresan[29], M. Orlandea[29], C. Pavel-Nicorescu[29], B. Popovici[29], S. Stoica[29], M. Straticiuc[29], E. Teodorescu[29]
[29] *Horia Hulubei National Institute of Physics and Nuclear Engineering, Bucharest-Magurele, Romania*

G. Alkhazov[30], B. Bochin[30], N. Bondar[30], A. Dzyuba[30], S. Gets[30], V. Golovtsov[30], A. Kashchuk[30], O. Maev[30,38], M. Matveev[30], N. Sagidova[30], Y. Shcheglov[30], S. Volkov[30], A. Vorobyev[30]
[30] *Petersburg Nuclear Physics Institute (PNPI), Gatchina, Russia*

V. Balagura[31], S. Belogurov[31], I. Belyaev[31], V. Egorychev[31], D. Golubkov[31], T. Kvaratskheliya[31,38], D. Savrina[31], A. Semennikov[31], P. Shatalov[31], V. Shevchenko[31], A. Zhokhov[31]
[31] *Institute of Theoretical and Experimental Physics (ITEP), Moscow, Russia*

A. Berezhnoy[32], G. Bogdanova[32], I. Komarov[32], M. Korolev[32], A. Leflat[32,38], N. Nikitin[32], V. Volkov[32], E. Zverev[32]
[32] *Institute of Nuclear Physics, Moscow State University (SINP MSU), Moscow, Russia*

S. Filippov[33], E. Gushchin[33], O. Karavichev[33], L. Kravchuk[33], Y. Kudenko[33], S. Laptev[33], A. Tikhonov[33]
[33] *Institute for Nuclear Research of the Russian Academy of Sciences (INR RAN), Moscow, Russia*

A. Bondar[34], S. Eidelman[34], P. Krokovny[34], V. Kudryavtsev[34], L. Shekhtman[34], V. Vorobyev[34]
[34] *Budker Institute of Nuclear Physics (SB RAS) and Novosibirsk State University, Novosibirsk, Russia*

A. Artamonov [35], K. Belous[35], R. Dzhelyadin[35], Yu. Guz[35], A. Likhoded[35], A. Novoselov[35], V. Obraztsov[35], A. Ostankov[35], V. Romanovsky[35], M. Shapkin[35], O. Stenyakin[35], O. Yushchenko[35]
[35] *Institute for High Energy Physics (IHEP), Protvino, Russia*

C. Abellan Beteta[36,n], M. Calvo Gomez[36,n], A. Camboni[36], A. Casajus Ramo[36], A. Comerma-Montells[36], F. Domingo Bonal[36,n], L. Garrido[36], D. Gascon[36], M. Grabalosa Gándara[36], R. Graciani Diaz[36], E. Graugés[36], E. Lopez Asamar[36], J. Mauricio[36], V. Mendez-Munoz[36,o], A. Pérez-Calero Yzquierdo[36], E. Picatoste Olloqui[36], B. Pie Valls[36], C. Potterat[36], A. Puig Navarro[36], M. Rosello[36,n], H. Ruiz[36], R. Vazquez Gomez[36], X. Vilasis-Cardona[36,n]
[36] *Universitat de Barcelona, Barcelona, Spain*

B. Adeva[37], P. Alvarez Cartelle[37], X. Cid Vidal[37], A. Dosil Suárez[37], D. Esperante Pereira[37], V. Fernandez Albor[37], A. Gallas Torreira[37], J.A. Hernando Morata[37], A. Pazos Alvarez[37], E. Perez Trigo[37], M. Plo Casasus[37], P. Rodriguez Perez[37], J.J. Saborido Silva[37], B. Sanmartin Sedes[37], C. Santamarina Rios[37], M. Seco[37], P. Vazquez Regueiro[37], J. Visniakov[37]
[37] *Universidad de Santiago de Compostela, Santiago de Compostela, Spain*

J. Albrecht[38], F. Alessio[38], C. Barschel[38], T. Blake[38], E. Bonaccorsi[38], L. Brarda[38], J. Buytaert[38], M. Cattaneo[38], B. Chadaj[38], Ph. Charpentier[38], M. Chebbi[38], K. Ciba[38], M. Clemencic[38], J. Closier[38], P. Collins[38], B. Corajod[38], G. Corti[38], B. Couturier[38], C. D'Ambrosio[38], G. Decreuse[38], H. Dijkstra[38], R. Dumps[38], M. Ferro-Luzzi[38], R. Forty[38], C. Fournier[38], M. Frank[38], C. Frei[38], C. Gaspar[38], M. Gersabeck[38], V.V. Gligorov[38], L.A. Granado Cardoso[38], T. Gys[38], C. Haen[38], E. van Herwijnen[38], R. Jacobsson[38], O. Jamet[38], B. Jost[38], M. Karacson[38], R. Kristic[38], D. Lacarrere[38], E. Lanciotti[38], C. Langenbruch[38], R. Lindner[38], G. Liu[38], D. Martinez Santos[38], R. Matev[38], N. Neufeld[38], J. Panman[38], M. Pepe Altarelli[38], D. Piedigrossi[38], N. Rauschmayr[38], S. Roiser[38], L. Roy[38], T. Ruf[38], H. Schindler[38], B. Schmidt[38], T. Schneider[38], A. Schopper[38], R. Schwemmer[38], F. Stagni[38], V.K. Subbiah[38], F. Teubert[38], E. Thomas[38], D. Tonelli[38], M. Ubeda Garcia[38], O. Ullaland[38], M. Vesterinen[38], J. Wicht[38], W. Witzeling[38], K. Wyllie[38], A. Zvyagin[38]
[38] *European Organization for Nuclear Research (CERN), Geneva, Switzerland*

Y. Amhis[39], A. Bay[39], F. Bernard[39], F. Blanc[39], J. Bressieux[39], G.A. Cowan[39], H. Degaudenzi[39,38], F. Dupertuis[39], V. Fave[39], R. Frei[39], N. Gauvin[39], G. Haefeli[39], P. Jaton[39], A. Keune[39], M. Knecht[39], V.N. La Thi[39], N. Lopez-March[39], J. Luisier[39], R. Märki[39], B. Muster[39], T. Nakada[39], A.D. Nguyen[39], C. Nguyen-Mau[39,p], J. Prisciandaro[39], B. Rakotomiaramanana[39], J. Rouvinet[39], O. Schneider[39], P. Szczypka[39], S. Tourneur[39], M.T. Tran[39], G. Veneziano[39]
[39] *Ecole Polytechnique Fédérale de Lausanne (EPFL), Lausanne, Switzerland*

J. Anderson[40], R. Bernet[40], A. Büchler-Germann[40], A. Bursche[40], N. Chiapolini[40], M. De Cian[40], Ch. Elsasser[40], K. Müller[40], J. Palacios[40], C. Salzmann[40], S. Saornil Gamarra[40], N. Serra[40], O. Steinkamp[40], U. Straumann[40], M. Tobin[40], A. Vollhardt[40]
[40] *Physik-Institut, Universität Zürich, Zürich, Switzerland*

R. Aaij[41], S. Ali[41], H. Band[41], Th. Bauer[41], M. van Beuzekom[41], V. van Beveren[41], H. Boer Rookhuizen[41], L. Ceelie[41], V. Coco[41], P.N.Y. David[41], K. De Bruyn[41], P. De Groen[41], D. van Eijk[41], C. Farinelli[41], V. Gromov[41], B. van der Heijden[41], V. Heijne[41], W. Hulsbergen[41], E. Jans[41], F. Jansen[41], L. Jansen[41], P. Jansweijer[41], R. Kluit[41], P. Koppenburg[41], A. Kozlinskiy[41], J. van Leerdam[41], M. Martinelli[41], M. Merk[41], I. Mous[41],

B. Munneke[41], S. Oggero[41], M. van Overbeek[41], A. Pellegrino[41], O. van Petten[41], E. Roeland[41], K. de Roo[41], A. Schimmel[41], H. Schuijlenburg[41], T. Sluijk[41], B. Storaci[41], P. Tsopelas[41], N. Tuning[41], W. Vink[41], P. Wenerke[41], L. Wiggers[41], F. Zappon[41], A. Zwart[41]
[41] *Nikhef National Institute for Subatomic Physics, Amsterdam, The Netherlands*

J. van den Brand[42], F. Dettori[42], T. Ketel[42], R.F. Koopman[42], J. Kos[42], R.W. Lambert[42], F. Mul[42], G. Raven[42], M. Schiller[42], S. Tolk[42]
[42] *Nikhef National Institute for Subatomic Physics and VU University Amsterdam, Amsterdam, The Netherlands*

A. Dovbnya[43], S. Kandybei[43], I. Raniuk[43], I. Shapoval[43,38], O. Shevchenko[43]
[43] *NSC Kharkiv Institute of Physics and Technology (NSC KIPT), Kharkiv, Ukraine*

V. Iakovenko[44], Y. Nikolaiko[44], O. Okhrimenko[44], M. Pugatch[44], V. Pugatch[44]
[44] *Institute for Nuclear Research of the National Academy of Sciences (KINR), Kyiv, Ukraine*

P.J.W. Faulkner[45], I.R. Kenyon[45], C. Lazzeroni[45], J. McCarthy[45], M.W. Slater[45], N.K. Watson[45]
[45] *University of Birmingham, Birmingham, United Kingdom*

M. Adinolfi[46], J. Benton[46], N.H. Brook[46], A. Cook[46], M. Coombes[46], T. Hampson[46], S.T. Harnew[46], P. Naik[46], J.H. Rademacker[46], A. Solomin[46], D. Souza[46], J.J. Velthuis[46], D. Voong[46]
[46] *H.H. Wills Physics Laboratory, University of Bristol, Bristol, United Kingdom*

W. Barter[47], M.-O. Bettler[47], H.V. Cliff[47], J. Garra Tico[47], V. Gibson[47], S. Gregson[47], S.C. Haines[47], C.R. Jones[47], S. Sigurdsson[47], D.R. Ward[47], S.A. Wotton[47], S. Wright[47]
[47] *Cavendish Laboratory, University of Cambridge, Cambridge, United Kingdom*

J.J. Back[48], D. Craik[48], D. Dossett[48], T. Gershon[48,38], M. Kreps[48], T. Latham[48], T. Pilař[48], A. Poluektov[48,34], M.M. Reid[48], R. Silva Coutinho[48], M. Whitehead[48], M.P. Williams[48,49]
[48] *Department of Physics, University of Warwick, Coventry, United Kingdom*

S. Easo[49], R. Nandakumar[49], A. Papanestis[49], G.N. Patrick[49], S. Ricciardi[49], F.F. Wilson[49]
[49] *STFC Rutherford Appleton Laboratory, Didcot, United Kingdom*

S. Benson[50], P.E.L. Clarke[50], R. Currie[50], S. Eisenhardt[50], C. Fitzpatrick[50], D. Lambert[50], H. Luo[50], H. Mejia[50], F. Muheim[50], M. Needham[50], S. Playfer[50], A. Sparkes[50], Y. Xie[50]
[50] *School of Physics and Astronomy, University of Edinburgh, Edinburgh, United Kingdom*

M. Alexander[51], J. Beddow[51], S. Borghi[51,54], L. Eklund[51], D. Hynds[51], S. Ogilvy[51], M. Pappagallo[51], E. Rodrigues[51,54], P. Sail[51], F.J.P. Soler[51], P. Spradlin[51]
[51] *School of Physics and Astronomy, University of Glasgow, Glasgow, United Kingdom*

T.J.V. Bowcock[52], H. Brown[52], G. Casse[52], S. Donleavy[52], K. Hennessy[52], E. Hicks[52], T. Huse[52], D. Hutchcroft[52], M. Liles[52], G.D. Patel[52], K. Rinnert[52], T. Shears[52], N.A. Smith[52]
[52] *Oliver Lodge Laboratory, University of Liverpool, Liverpool, United Kingdom*

L. Carson[53], G. Ciezarek[53], S. Cunliffe[53], U. Egede[53], A. Golutvin[53,31,38], S. Hall[53], P. Owen[53],

C.J. Parkinson[53], M. Patel[53], K. Petridis[53], A. Richards[53], T. Savidge[53], I. Sepp[53], A. Shires[53], D. Websdale[53], M. Williams[53]
[53] *Imperial College London, London, United Kingdom*

R.B. Appleby[54], R.J. Barlow[54], T. Bird[54], P.M. Bjørnstad[54], D. Brett[54], J. Harrison[54], G. Lafferty[54], G. McGregor[54], D. Moran[54], C. Parkes[54], M. Smith[54], A.D. Webber[54]
[54] *School of Physics and Astronomy, University of Manchester, Manchester, United Kingdom*

M. Brock[55], M. Charles[55], N. Harnew[55], J.J. John[55], M. John[55], S. Malde[55], A. Nomerotski[55,38], A. Powell[55], C. Thomas[55], S. Topp-Joergensen[55], G. Wilkinson[55]
[55] *Department of Physics, University of Oxford, Oxford, United Kingdom*

B. Meadows[56], M.D. Sokoloff[56]
[56] *University of Cincinnati, Cincinnati, OH, United States*

M. Artuso[57,38], S. Blusk[57], A. Borgia[57], T. Britton[57], J. Garofoli[57], B. Gui[57], C. Hadjivasiliou[57], R. Mountain[57], B.K. Pal[57], A. Phan[57], W. Qian[57], T. Skwarnicki[57], S. Stone[57,38], J. Wang[57], Z. Xing[57], L. Zhang[57].
[57] *Syracuse University, Syracuse, NY, United States*

[a] *P.N. Lebedev Physical Institute, Russian Academy of Science (LPI RAS), Moscow, Russia*
[b] *Università di Bari, Bari, Italy*
[c] *Università di Bologna, Bologna, Italy*
[d] *Università di Cagliari, Cagliari, Italy*
[e] *Università di Ferrara, Ferrara, Italy*
[f] *Università di Firenze, Firenze, Italy*
[g] *Università di Urbino, Urbino, Italy*
[h] *Università di Modena e Reggio Emilia, Modena, Italy*
[i] *Università di Genova, Genova, Italy*
[j] *Università di Milano Bicocca, Milano, Italy*
[k] *Università di Roma Tor Vergata, Roma, Italy*
[l] *Università di Roma La Sapienza, Roma, Italy*
[m] *Università della Basilicata, Potenza, Italy*
[n] *LIFAELS, La Salle, Universitat Ramon Llull, Barcelona, Spain*
[o] *Port d'Informació Científica (PIC), Barcelona, Spain*
[p] *Hanoi University of Science, Hanoi, Viet Nam*

Contents

Executive summary

This executive summary was submitted as a standalone document to the European Strategy Preparatory Group [1].

Background to the document

During 2011 both the LHC machine and the LHCb detector performed superbly, allowing LHCb to accumulate $1.0\,\text{fb}^{-1}$ of $\sqrt{s} = 7\,\text{TeV}$ pp collisions that is available for physics analysis. Due to the large production cross-sections, these data provide unprecedented samples of heavy flavoured hadrons. The first results from LHCb have made a significant impact on the flavour physics landscape and have definitively proved the concept of a dedicated experiment in the forward region at a hadron collider.

The results to date cover several topics in the core flavour physics programme of LHCb in rare decays and *CP* violation. This programme is focussed on searching for physics beyond the Standard Model (SM) — referred to as "New Physics" (NP) — with an approach that is complementary to that used by the ATLAS and CMS experiments. While the high-p_{T} experiments search for on-shell production of new particles, LHCb can look for their effects in processes that are precisely predicted in the SM. In particular, the SM has a highly distinctive flavour structure, with no tree-level flavour-changing neutral currents, and quark mixing described by the Cabibbo-Kobayashi-Maskawa matrix [2] which has a single source of *CP* violation. This structure is not necessarily replicated in extended models. Historically, new particles have first been seen through their virtual effects since this approach allows to probe mass scales beyond the energy frontier. For example, the observation of *CP* violation in the kaon system [3] was, in hindsight, the discovery of the third family of quarks, well before the observations of the bottom and top quarks. Crucially, measurements of both high-p_{T} and flavour observables are necessary in order to decipher the nature of NP.

In many channels, the LHCb results are already the world's most precise, and begin to reach the sensitivity where small deviations from SM predictions may be observed. In several areas hints of large anomalies from previous measurements have not been confirmed: the branching fraction of $B^0_s \to \mu^+\mu^-$ [4], the forward-backward asymmetry of $B^0 \to K^{*0}\mu^+\mu^-$ [5] and the *CP*-violation phase in B^0_s oscillations [6] are all found to be consistent with the SM, within current uncertainties. The situation regarding *CP* violation in B^0 and B^0_s mixing is still ambiguous [7]. Nevertheless, in all these cases more precise measurements are mandatory. Moreover, in other channels there are strengthened, or new, hints of unexpected effects: for example, evidence of *CP* violation in the charm system [8] and anomalous isospin asymmetry in $B \to K\mu^+\mu^-$ decays [9]. These also demand to be followed up with more data, and with studies of complementary decay channels.

The physics output of LHCb also extends beyond this core programme. Examples of other topics include measurements of the production of electroweak gauge bosons in the forward kinematic region covered by the LHCb acceptance [10], studies of double parton

scattering [11], measurements of the properties of newly discovered hadrons [12], and searches for exotic hadrons [13], for lepton number and lepton flavour violation [14, 15], and for long-lived new particles [16].

In order to discuss the implications of its first measurements, and possibilities for future analysis directions, the LHCb collaboration arranged two workshops with theorists as satellite meetings of the series on implications of LHC results for TeV-scale physics. The first was held on 10–11 November 2011, the second on 16–18 April 2012. These meetings focussed on the observables that are sensitive to physics beyond the SM, such as models that predict new particles at the TeV scale. They were arranged in three main strands: rare charm and beauty decays, *CP* violation in the B system, and mixing and *CP* violation in the charm sector. The interplay with the results of searches for on-shell production of new particles at ATLAS and CMS is therefore highly relevant and was discussed both in the LHCb meetings as well as in the main series of "Implications" workshops.

This document gives a detailed summary of these workshops. It highlights the impact of the first results from LHCb, and emphasises the need to exploit fully the flavour physics potential of the LHC. This motivates a reassessment of the potential sensitivity of the upgraded LHCb experiment in the light of the latest results, as discussed below.

Highlights of LHCb measurements and their implications

Rare decays

Among rare decays, the LHCb limit on the rate of the decay $B_s^0 \to \mu^+\mu^-$ [4] places stringent limits on NP models that enhance the branching fraction. The measurement

$$\mathcal{B}(B_s^0 \to \mu^+\mu^-) < 4.5 \times 10^{-9} \text{ (95 \% confidence level)}, \tag{1}$$

can be compared to the SM prediction $\mathcal{B}(B_s^0 \to \mu^+\mu^-)_{\rm SM} = (3.1 \pm 0.2) \times 10^{-9}$ [17].[1] This result puts severe constraints — far beyond the ATLAS and CMS search limits — on supersymmetric models with large values of $\tan\beta$, *i.e.* of the ratio of vacuum expectation values of the Higgs doublets (see, for example, Refs. [17,19,20]). The impact of the result is illustrated in Fig. 1. Models where the branching fraction of $B_s^0 \to \mu^+\mu^-$ is reduced below its SM value are starting to receive serious consideration.

The measurement of the forward-backward asymmetry in $B^0 \to K^{*0}\mu^+\mu^-$ [5] has to be viewed as the start of a programme towards a full angular analysis of these decays. The full analysis will allow determination of numerous NP-sensitive observables (see, for example, Refs. [22, 23]). The measurements that will be obtained from such an analysis, as well as similar studies of related channels, such as $B_s^0 \to \phi\mu^+\mu^-$ [24], allow model-independent constraints on NP, manifested as limits on the operators of the effective Hamiltonian (see, for example, Refs. [25,26]). Indeed, the first results already impose important constraints, as shown in Fig. 2. Studies of radiative decays such as $B_s^0 \to \phi\gamma$ [27,28] provide additional

[1] It should be noted that the measured value is the time-integrated branching fraction, and the SM prediction should be increased by around 10 % to allow a direct comparison [18].

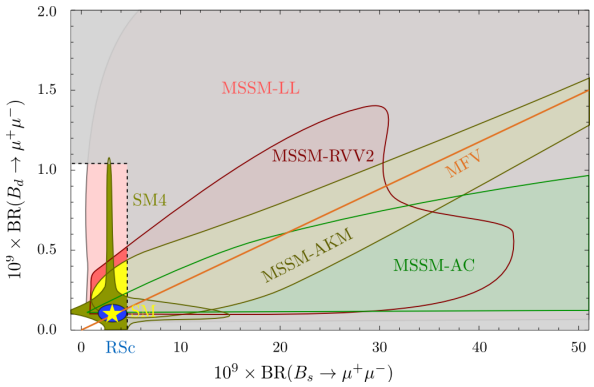

Figure 1: Correlation between the branching ratios of $B_s^0 \to \mu^+\mu^-$ and $B^0 \to \mu^+\mu^-$ in various models. The grey area is ruled out experimentally. The SM point is marked by a star. From Ref. [21].

information since they allow to measure the polarisation of the emitted photon, and are therefore especially sensitive to models that predict new right-handed currents. Similarly, studies of observables such as isospin asymmetries [9] are important since they allow to pin down in which operators the NP effects occur.

Several new opportunities with rare decays at LHCb are becoming apparent. The observation of $B^+ \to \pi^+\mu^+\mu^-$ [29], the rarest B decay yet discovered, enables a new approach to measure the ratio of CKM matrix elements $|V_{td}/V_{ts}|$. Decays to final states containing same-sign leptons [14] allow searches for Majorana neutrinos complementary to those based on neutrinoless double beta decay. LHCb can also reach competitive sensitivity for some lepton flavour violating decays such as $\tau^+ \to \mu^+\mu^-\mu^+$ [15].

CP violation in the *B* sector

Measurements of the neutral B meson mixing parameters provide an excellent method to search for NP effects, due to the low theoretical uncertainties associated to several observables. The LHCb measurements of the *CP*-violating phase, ϕ_s, and the width difference, $\Delta\Gamma_s$, in the B_s^0 system [6, 30–32] significantly reduce the phase space for NP:

$$\phi_s = -0.002 \pm 0.083 \pm 0.027 \text{ rad}\,, \quad \Delta\Gamma_s = 0.116 \pm 0.018\,(\text{stat}) \pm 0.006\,(\text{syst})\,\text{ps}^{-1}\,. \quad (2)$$

However, as shown in Fig. 3, deviations from the SM predictions [33, 34] are still possible. Deviations of $\mathcal{O}(0.1)$ are typical of some well-motivated NP models that survive the present ATLAS and CMS bounds (such as in Ref. [35]). The experimental uncertainty on ϕ_s is still a factor of 40 larger than that on the prediction, therefore improved measurements are needed to reach the level of sensitivity demanded by theory. It should also be noted that compared to the *CP*-violating phase in the B^0 system (2β), ϕ_s is much more precisely predicted, and therefore presents stronger opportunities for NP searches.

In addition, to understand the origin of the anomalous dimuon asymmetry seen by D0 [36], improved measurements of semileptonic asymmetries in both B_s^0 and B^0 systems

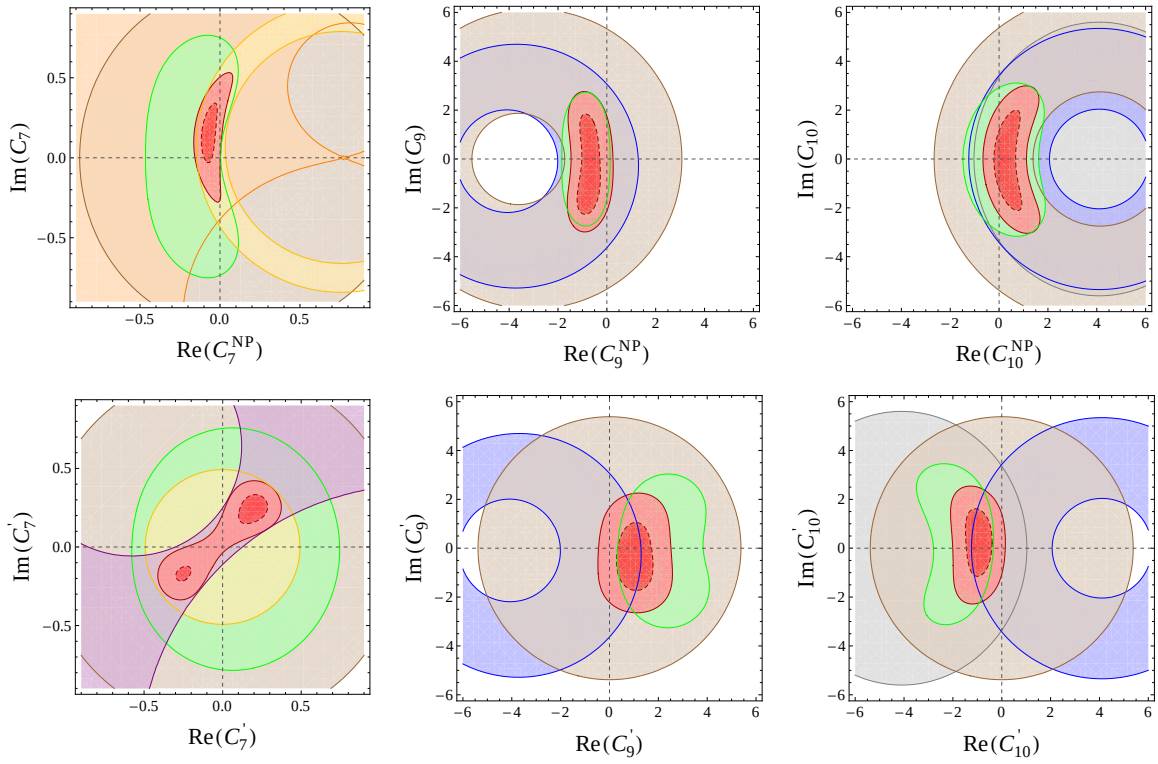

Figure 2: Individual 2σ constraints in the complex planes of Wilson coefficients, coming from $B \to X_s \ell^+ \ell^-$ (brown), $B \to X_s \gamma$ (yellow), $A_{CP}(b \to s\gamma)$ (orange), $B \to K^* \gamma$ (purple), $B \to K^* \mu^+ \mu^-$ (green), $B \to K \mu^+ \mu^-$ (blue) and $B_s \to \mu^+ \mu^-$ (grey), as well as combined 1 and 2σ constraints (red). From Ref. [25].

are needed. LHCb has just released its first results on the B_s^0 asymmetry [7], demonstrating the potential to search for NP effects with more precise measurements. Moreover, a constraint on, or a measurement of, the rate of the decay $B_s^0 \to \tau^+ \tau^-$ is important to provide knowledge of possible NP contributions to Γ_{12} (see, for example, Refs. [37, 38]).

Among the B^0 mixing parameters, improved measurements of both ϕ_d (*i.e.*, $\sin(2\beta)$) and $\Delta\Gamma_d$ are needed. Reducing the uncertainty on the former will help to improve the global fits to the CKM matrix [40, 41], and may clarify the current situation regarding the tension between various inputs to the fits (see, for example, Ref. [42]). Another crucial observable is the angle γ, which, when measured in the tree-dominated $B \to DK$ processes, provides a benchmark measurement of *CP* violation. The first measurements from LHCb already help to improve the uncertainty on γ [43]: further improvements are both anticipated and needed.

Knowledge of γ from tree-dominated processes is also essential to test the consistency with measurements from loop-dominated processes. In particular, the study of $B_s^0 \to K^+ K^-$ and $B^0 \to \pi^+ \pi^-$ decays [44], which are related by U-spin, allows a powerful test of the consistency of the observables with the SM [45, 46]. Similarly, the U-spin partners $B_s^0 \to K^{*0} \overline{K}^{*0}$ [47] and $B^0 \to K^{*0} \overline{K}^{*0}$ are among the golden channels to search for

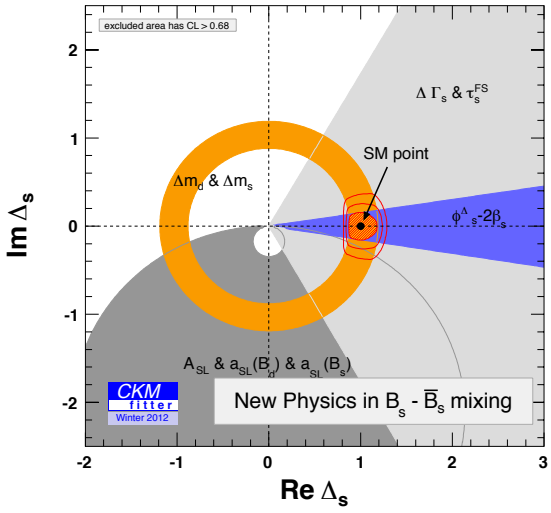

Figure 3: Model independent fit to search for NP in B_s^0 mixing. The coloured areas represent regions with CL $< 68.3\,\%$ for the individual constraints. The red area shows the region with CL $< 68.3\,\%$ for the combined fit, with the two additional contours delimiting the regions with CL $< 95.45\,\%$ and CL $< 99.73\,\%$. From Ref. [39]

NP contributions in $b \to sq\bar{q}$ penguin amplitudes [48]. Another important channel in this respect is $B_s^0 \to \phi\phi$ [49], for which the *CP* violating observables are predicted with low theoretical uncertainty in the SM. Studies of *CP* violation in multibody b hadron decays [50] offer additional possibilities to search for both the existence and features of NP.

Charm mixing and *CP* violation

In the charm sector, the evidence for *CP* violation in the observable ΔA_{CP} has prompted a large amount of theoretical work. The measurement

$$\Delta A_{CP} = A_{CP}(K^+K^-) - A_{CP}(\pi^+\pi^-) = (-0.82 \pm 0.21 \pm 0.11)\,\%\,, \tag{3}$$

is 3.5 standard deviations from zero [8]. While A_{CP} represents a time-integrated *CP* asymmetry, ΔA_{CP} originates predominantly from direct *CP* violation. The emergent consensus, as shown in Fig. 4 is that while an asymmetry of the order of $1\,\%$ is rather unlikely in the SM, it cannot be ruled out that QCD effects cause enhancements of that size. Further measurements are needed in order to establish if NP effects are present in the charm sector. Among the anticipated results are updates of the ΔA_{CP} measurement as well as of the individual *CP* asymmetries in $D^0 \to K^+K^-$ and $D^0 \to \pi^+\pi^-$. It is of great interest to look for direct *CP* violation in decays to other final states, and in decays of other charmed hadrons (D^+, D_s^+ and Λ_c^+).

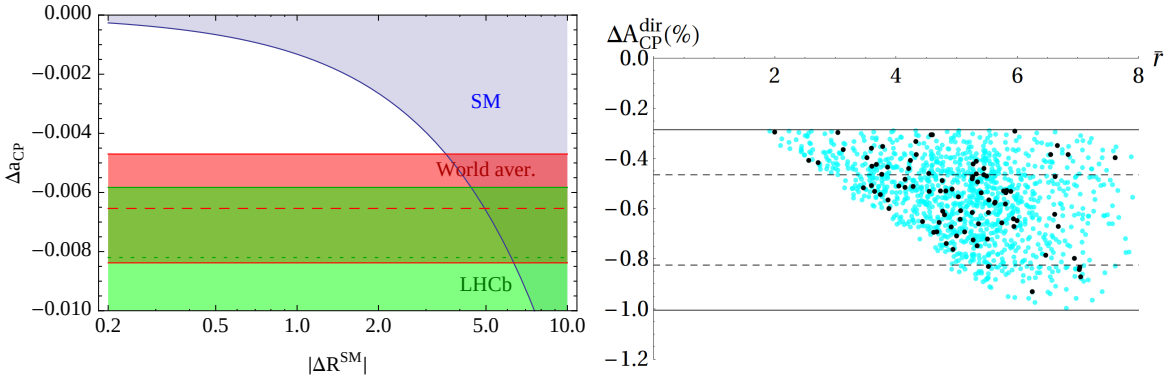

Figure 4: Possible values of ΔA_{CP} in the SM as functions of hadronic parameters, from (left) Ref. [51], (right) Ref. [52]. The experimental constraints are shown as horizontal bands in both plots.

The SM predictions are somewhat cleaner for indirect *CP* violation effects, and therefore it is also essential to search for *CP* violation in charm mixing. New results from time-dependent analyses of $D^0 \to K^+K^-$ [53] and $D^0 \to K^0_S\pi^+\pi^-$ will improve the current knowledge, and additional channels will also be important with high statistics.

Several authors have noted correlations between *CP* violation in charm and various other observables (for example, Refs. [51, 54]). These correlations appear in, and differ between, certain theoretical models, and can therefore be used to help identify the origin of the effects. Observables of interest in this context include those that can be measured at high-p_T experiments, such as $t\bar{t}$ asymmetries, as well as rare charm decays. Among the latter, it has been noted that *CP* asymmetries are possible in radiative decays such as $D^0 \to \phi\gamma$ [55], and that searches for decays involving dimuons, such as $D^0 \to \mu^+\mu^-$ [56] and $D^+ \to \pi^+\mu^+\mu^-$ are well motivated.

Measurements exploiting the unique kinematic acceptance of LHCb

The workshops mentioned above focussed on the observables, mainly in the flavour sector, most sensitive to physics beyond the SM, but the physics programme of LHCb includes additional topics. These will continue to be important in the upgrade era, since the unique kinematic region covered by the LHCb acceptance enables measurements that cannot be performed at other experiments. These include probes of QCD both in production, such as studies of multi-parton scattering [11, 57], and in decay, such as studies of exotic hadrons like the $X(3872)$ [58] and the putative $Z(4430)^+$ state. Conventional hadrons can also be studied with high precision: one important goal will be to establish the existence of doubly heavy baryons. Central exclusive production of conventional and exotic hadrons can also be studied; the sensitivity of the upgraded experiment will be significantly enhanced due to the software trigger. LHCb may also be able to make a unique contribution to the field of heavy ion physics, by studying soft QCD and heavy flavour production in pA collisions. The first pA run of the LHC will clarify soon the potential of LHCb in this field.

Measurements of production rates and asymmetries of electroweak gauge bosons in the LHCb acceptance are important to constrain parton density functions (PDFs) [10]. With high statistics, LHCb will be well placed to make a precision measurement of the sine of the effective electroweak mixing angle for leptons, $\sin^2\theta^{\rm lept}_{\rm eff}$, from the forward-backward asymmetry of leptons produced in the $Z \to \mu^+\mu^-$ decay. Improved knowledge of PDFs, as can be obtained from studies of production of gauge bosons in association with jets [59], will help to reduce limiting uncertainties on the measurement of the W boson. These studies are also an important step towards a top physics programme at LHCb, which will become possible once the LHC energy approaches the nominal 14 TeV.

The importance of having a detector in the forward region can be illustrated with the recent discovery by ATLAS and CMS of a new particle that may be the Higgs boson. It is now essential to determine if this particle has the couplings to bosons, leptons and quarks expected in the SM. In particular, at the observed mass the highest branching ratio is expected to be for $H \to b\bar{b}$ — however this is a difficult channel for ATLAS and CMS due to the large SM background. LHCb with its excellent b-hadron sensitivity will be able to search for such decays. The forward geometry of LHCb is also advantageous to observe new long-lived particles that are predicted in certain NP models, including some with extended Higgs sectors. Although limits can be set with the current detector [16], this is an area that benefits significantly from the flexible software trigger of the upgraded experiment. Models with extended Higgs sectors also produce characteristic signals in flavour physics observables, which emphasises the need for the LHCb upgrade as part of the full exploitation of the LHC.

Sensitivity of the upgraded LHCb experiment to key observables

Given the strong motivation to exploit fully the flavour physics potential of the LHC, it is timely to update the estimated sensitivities for various key observables based on the results to date. A detailed description of the upgraded LHCb experiment can be found in the Letter of Intent (LoI) [60], complemented by the recent framework technical design report (FTDR) [61], which sets out the timeline and costing for the project. A summary has been prepared for the European Strategy Preparatory Group [62]. The upgrade is necessary to progress beyond the limitations imposed by the current hardware trigger that, due to its maximum output rate of 1 MHz, restricts the instantaneous luminosity at which data can most effectively be collected. To overcome this, the upgraded detector will be read out at the maximum LHC bunch-crossing frequency of 40 MHz so that the trigger can be fully implemented in software. With such a flexible trigger strategy, the upgraded LHCb experiment can be considered as a general purpose detector in the forward region. The upgraded detector will be installed during the long shutdown of the LHC planned for 2018.

Several important improvements compared to the current detector performance can be expected in the upgrade era, as detailed in the LoI and FTDR. However, the sensitivity studies that have been performed assume detector performance as achieved during 2011 data taking. The exception is in the trigger efficiency, where channels selected at hardware

trigger level by hadron, photon or electron triggers are expected to have their efficiencies double (channels selected by muon triggers are expected to have marginal gains, that have not been included in the extrapolations). Several other assumptions are made:

- LHC collisions will be at $\sqrt{s} = 14\,\text{TeV}$, with heavy flavour production cross-sections scaling linearly with $\sqrt{s}$;
- the instantaneous luminosity in LHCb will be $\mathcal{L}_{\text{inst}} = 10^{33}\,\text{cm}^{-2}\,\text{s}^{-1}$: this will be achieved with 25 ns bunch crossings and an average number of visible interactions per crossing $\mu = 2$;
- LHCb will change the polarity of its dipole magnet with similar frequency as in 2011/12 data taking, to approximately equalise the amount of data taken with each polarity for better control of certain potential systematic biases;
- the integrated luminosity will be $\mathcal{L}_{\text{int}} = 5\,\text{fb}^{-1}$ per year, and the experiment will run for 10 years to give a total sample of $50\,\text{fb}^{-1}$.

The sensitivity to various flavour observables is summarised in Table 1, which is taken from the FTDR [61]. This is an updated version of a similar summary that appears as Table 2.1 in the LoI [60]. The measurements considered include *CP*-violating observables, rare decays and fundamental parameters of the CKM Unitarity Triangle. More details about these observables are given below. The current precision, either from LHCb measurements or averaging groups [40,41,63] is given and compared to the estimated sensitivity with the upgrade. As an intermediate step, the estimated precision that can be achieved prior to the upgrade is also given for each observable. For this, a total integrated luminosity of 1.0 (1.5, 4.0) fb^{-1} at pp centre-of-mass collision energy $\sqrt{s} = 7$ (8, 13) TeV recorded in 2011 (2012, 2015–17) is assumed. Another assumption is that the current efficiency of the muon hardware trigger can be maintained at higher $\sqrt{s}$, but that higher thresholds will be necessary for other triggers, reducing the efficiency for the relevant channels by a factor of 2 at $\sqrt{s} = 13\,\text{TeV}$.

In LHCb measurements to date, the *CP*-violating phase in B_s^0 mixing, measured in both $J/\psi\,\phi$ and $J/\psi\,f_0(980)$ final states, has been denoted ϕ_s. In the upgrade era it will be necessary to remove some of the assumptions that have been made in the analyses to date, related to possible penguin amplitude contributions, and therefore we denote the observables in $b \to c\bar{c}s$ transitions by $2\beta_s = -\phi_s$, while in $b \to q\bar{q}s$ ($q = u, d, s$) transitions we use $2\beta_s^{\text{eff}}$. This parallels the established notation used in the B^0 system (we use α, β, γ for the CKM Unitarity Triangle angles). The penguin contributions are expected to be small, and therefore we quote a theory uncertainty on $2\beta_s\,(B_s^0 \to J/\psi\,\phi) \sim 0.003$, comparable to the theory uncertainty on $2\beta\,(B^0 \to J/\psi\,K_{\text{S}}^0)$. However, larger effects cannot be ruled out at present. Data-driven methods to determine the penguin amplitudes are also possible [65,66]: at present these given much larger estimates of the uncertainty, but improvement can be anticipated with statistics. The flavour-specific asymmetry in the B_s^0 system, a_{sl}^s in Tab. 1, probes *CP* violating in mixing. The "sl" subscript is used because the measurement uses semileptonic decays.

Type	Observable	Current precision	LHCb 2018	**Upgrade** ($50\,\text{fb}^{-1}$)	Theory uncertainty
B_s^0 mixing	$2\beta_s$ $(B_s^0 \to J/\psi\,\phi)$	0.10 [30]	0.025	0.008	~ 0.003
	$2\beta_s$ $(B_s^0 \to J/\psi\, f_0(980))$	0.17 [32]	0.045	0.014	~ 0.01
	$a_{\rm sl}^s$	6.4×10^{-3} [63]	0.6×10^{-3}	0.2×10^{-3}	0.03×10^{-3}
Gluonic penguins	$2\beta_s^{\rm eff}(B_s^0 \to \phi\phi)$	–	0.17	0.03	0.02
	$2\beta_s^{\rm eff}(B_s^0 \to K^{*0}\bar{K}^{*0})$	–	0.13	0.02	< 0.02
	$2\beta^{\rm eff}(B^0 \to \phi K_S^0)$	0.17 [63]	0.30	0.05	0.02
Right-handed currents	$2\beta_s^{\rm eff}(B_s^0 \to \phi\gamma)$	–	0.09	0.02	< 0.01
	$\tau^{\rm eff}(B_s^0 \to \phi\gamma)/\tau_{B_s^0}$	–	5 %	1 %	0.2 %
Electroweak penguins	$S_3(B^0 \to K^{*0}\mu^+\mu^-; 1 < q^2 < 6\,\text{GeV}^2/c^4)$	0.08 [64]	0.025	0.008	0.02
	$s_0\, A_{\rm FB}(B^0 \to K^{*0}\mu^+\mu^-)$	25 % [64]	6 %	2 %	7 %
	$A_{\rm I}(K\mu^+\mu^-; 1 < q^2 < 6\,\text{GeV}^2/c^4)$	0.25 [9]	0.08	0.025	~ 0.02
	$\mathcal{B}(B^+ \to \pi^+\mu^+\mu^-)/\mathcal{B}(B^+ \to K^+\mu^+\mu^-)$	25 % [29]	8 %	2.5 %	~ 10 %
Higgs penguins	$\mathcal{B}(B_s^0 \to \mu^+\mu^-)$	1.5×10^{-9} [4]	0.5×10^{-9}	0.15×10^{-9}	0.3×10^{-9}
	$\mathcal{B}(B^0 \to \mu^+\mu^-)/\mathcal{B}(B_s^0 \to \mu^+\mu^-)$	–	~ 100 %	~ 35 %	~ 5 %
Unitarity triangle angles	γ $(B \to D^{(*)}K^{(*)})$	~ 10–12° [40, 41]	4°	0.9°	negligible
	γ $(B_s^0 \to D_s K)$	–	11°	2.0°	negligible
	β $(B^0 \to J/\psi\, K_S^0)$	0.8° [63]	0.6°	0.2°	negligible
Charm *CP* violation	A_Γ	2.3×10^{-3} [63]	0.40×10^{-3}	0.07×10^{-3}	–
	ΔA_{CP}	2.1×10^{-3} [8]	0.65×10^{-3}	0.12×10^{-3}	–

Table 1: Statistical sensitivities of the LHCb upgrade to key observables. For each observable the current sensitivity is compared to that which will be achieved by LHCb before the upgrade, and that which will be achieved with $50\,\text{fb}^{-1}$ by the upgraded experiment. Systematic uncertainties are expected to be non-negligible for the most precisely measured quantities. Note that the current sensitivities do not include new results presented at ICHEP 2012.

Sensitivity to the emitted photon polarisation is encoded in the effective lifetime, $\tau^{\rm eff}$ of $B^0_s \to \phi\gamma$ decays, together with the effective *CP*-violation parameter $2\beta^{\rm eff}_s$. Two of the most interesting of the full set of angular observables in $B^0 \to K^{*0}\mu^+\mu^-$ decays [67], are S_3, which is related to the transverse polarisation asymmetry [68], and the zero-crossing point (s_0) of the forward-backward asymmetry. As discussed above, isospin asymmetries, denoted A_I, are also of great interest.

In the charm sector, it is important to improve the precision of ΔA_{CP}, described above, and related measurements of direct *CP* violation. One of the key observables related to indirect *CP* violation is the difference in inverse effective lifetimes of $D^0 \to K^+K^-$ and $\overline{D}^0 \to K^+K^-$ decays, A_Γ.

The extrapolations in Tab. 1 assume the central values of the current measurements, or the SM where no measurement is available. While the sensitivities given include statistical uncertainties only, preliminary studies of systematic effects suggest that these will not affect the conclusions significantly, except in the most precise measurements, such as those of $a^s_{\rm sl}$, A_Γ and ΔA_{CP}. Branching fraction measurements of B^0_s mesons require knowledge of the ratio of fragmentation fractions f_s/f_d for normalisation [69]. The uncertainty on this quantity is limited by knowledge of the branching fraction of $D^+_s \to K^+K^-\pi^+$, and improved measurements of this quantity will be necessary to avoid a limiting uncertainty on, for example, $\mathcal{B}(B^0_s \to \mu^+\mu^-)$. The determination of $2\beta_s$ from $B^0_s \to J/\psi\,\phi$ provides an example of how systematic uncertainties can be controlled for measurements at the LHCb upgrade. In the most recent measurement [30], the largest source of systematic uncertainty arises due to the constraint of no direct *CP* violation that is imposed in the fit. With larger statistics, this constraint can be removed, eliminating this source of uncertainty. Other sources, such as the background description and angular acceptance, are already at the 0.01 rad level, and can be reduced with more detailed studies.

Although other experiments will study flavour-physics observables in a similar timeframe to the LHCb upgrade, the sample sizes in most exclusive B and D final states will be far larger than those that will be collected elsewhere, for example at the upgraded e^+e^- B factories. The LHCb upgrade will have no serious competition in its study of B^0_s decays, b-baryon decays, charm mixing and *CP* violation. Similarly the yields in charmed-particle decays to final states consisting of only charged tracks cannot be matched by any other experiment.

Importance of the LHCb upgrade

The study of deviations from the SM in quark flavour physics provides key information about any extension of the SM. We already know that the NP needed to stabilise the electroweak sector must have a non-generic flavour structure in order to be compatible with the tight constraints of flavour-changing processes, even if the precise form of this structure is still unknown. Hopefully, ATLAS and CMS will detect new particles belonging to these models, but the couplings of the theory and, in particular, its flavour structure, cannot be determined only using high-$p_{\rm T}$ data.

Therefore, the LHCb upgrade will play a vital role in any of these scenarios, including

the possibility of covering NP phase space, which *a priori* cannot be exploited by high energy searches. Future plans for full exploitation of the LHC should be consistent with a co-extensive LHCb programme.

1 Introduction

During 2011 the LHCb experiment [70] at CERN collected $1.0\,\text{fb}^{-1}$ of $\sqrt{s} = 7\,\text{TeV}$ pp collisions. Due to the large production cross-section, $\sigma(pp \to b\bar{b}X) = (89.6 \pm 6.4 \pm 15.5)\,\mu\text{b}$ in the LHCb acceptance [71], with the comparable number for charm production about 20 times larger [72], these data provide unprecedented samples of heavy flavoured hadrons. The first results from LHCb have made a significant impact on the flavour physics landscape and have definitively proved the concept of a dedicated experiment in the forward region at a hadron collider.

The physics objectives of the first phase of LHCb were set out prior to the commencement of data taking in the "roadmap document" [73]. They centred on six main areas, in all of which LHCb has by now published its first results: (i) the tree-level determination of γ [43], (ii) charmless two-body B decays [74], (iii) the measurement of mixing-induced CP violation in $B^0_s \to J/\psi\,\phi$ [6], (iv) analysis of the decay $B^0_s \to \mu^+\mu^-$ [4, 75, 76], (v) analysis of the decay $B^0 \to K^{*0}\mu^+\mu^-$ [5], (vi) analysis of $B^0_s \to \phi\gamma$ and other radiative B decays [27]. In addition, the search for CP violation in the charm sector was established as a priority, and interesting results in this area have also been published [8, 53].

The early data also illustrated the potential for LHCb to expand its physics programme beyond these "core" measurements. In particular, the development of trigger algorithms that select events inclusively based on properties of b-hadron decays [77] facilitates a much broader output than previously foreseen. On the other hand, limitations imposed by the hardware trigger lead to a maximum instantaneous luminosity at which data can most effectively be collected (higher luminosity requires tighter trigger thresholds, so that there is no gain in yields, at least for channels that do not involve muons). To overcome this limitation, an upgrade of the LHCb experiment has been proposed to be installed during the long shutdown of the LHC planned for 2018. The upgraded detector will be read out at the maximum LHC bunch-crossing frequency of 40 MHz so that the trigger can be fully implemented in software. With such a flexible trigger strategy, the upgraded LHCb experiment can be considered as a general purpose detector in the forward region.

The Letter of Intent for the LHCb upgrade [60], containing a detailed physics case, was submitted to the LHCC in March 2011 and was subsequently endorsed. Indeed, the LHCC viewed the physics case as "compelling." Nevertheless, the LHCb collaboration continues to consider further possibilities to enhance the physics reach, and to refine its sensitivity studies based on the latest data available. These studies are described in this document, and summarised in the framework technical design report for the LHCb upgrade [61], submitted to the LHCC in June 2012.

Several important improvements compared to the detector performance can be expected in the upgrade era, as detailed in the framework TDR. However, to be conservative, the sensitivity studies reported in this document all assume detector performance as achieved during 2011 data taking. The exception is in the trigger efficiency, where channels selected at hardware level by hadron, photon or electron triggers are expected to have their efficiencies double (channels selected by muon triggers are expected to have marginal gains, that have not been included in the extrapolations). Several other assumptions are

made:

- LHC collisions will be at $\sqrt{s} = 14\,\text{TeV}$, with heavy flavour production cross-sections scaling linearly with $\sqrt{s}$;
- the instantaneous luminosity in LHCb will be $\mathcal{L}_{\text{inst}} = 10^{33}/\,\text{cm}^2/\,\text{s}$: this will be achieved with 25 ns bunch crossings and an average number of visible interactions per crossing $\mu = 2$;
- LHCb will change the polarity of its dipole magnet with similar frequency as in 2011/12 data taking, to approximately equalise the amount of data taken with each polarity for better control of certain potential systematic biases;
- the integrated luminosity will be $\mathcal{L}_{\text{int}} = 5\,\text{fb}^{-1}$ per year, and the experiment will run for 10 years to give a total sample of $50\,\text{fb}^{-1}$.

In order to discuss the implications of its first measurements, and possibilities for future analysis directions, the LHCb collaboration arranged two workshops with theorists as satellite meetings of the series on implications of LHC results for TeV-scale physics. The first was held on 10-11 November 2011, the second on 16–18 April 2012. These meetings focussed on the observables that are sensitive to physics beyond the Standard Model, such as models that predict new particles at the TeV scale. The interplay with the results of direct searches at ATLAS and CMS is therefore highly relevant and was discussed both in the LHCb meetings as well as in the main series of "Implications" workshops.

This document summarises the outcome of these discussions, together with the latest upgrade sensitivity studies. The workshops were arranged in three main strands, and these are discussed in turn: rare charm and beauty decays in Sec. 2, *CP* violation in the B system in Sec. 3 and mixing and *CP* violation in the charm sector in Sec. 4. There are several other important topics, not covered in any of these sections, that can be studied at LHCb and its upgrade, and these are discussed in Sec. 5. A brief summary is given in Sec. 6.

2 Rare decays

2.1 Introduction

The term rare decay is used within this document to refer loosely to two classes of decays:

- flavour changing neutral current (FCNC) processes that are mediated by electroweak box and penguin type diagrams in the SM;
- more exotic decays, including searches for lepton flavour or number violating decays of B or D mesons and for light scalar particles.

The first broad class of decays includes the rare radiative process $B_s^0 \to \phi\gamma$ and rare leptonic and semi-leptonic decays $B_{(d,s)} \to \mu^+\mu^-$ and $B^0 \to K^{*0}\mu^+\mu^-$. These were listed as priorities for the first phase of the LHCb experiment in the roadmap document [73]. In many well motivated new physics models, new particles at the TeV-scale can enter in diagrams that compete with the SM processes, leading to modifications of branching fractions or angular distributions of the daughter particles in these decays.

For the second class of decay, there is either no SM contribution or the SM contribution is vanishingly small and any signal would indicate evidence for physics beyond the SM. Grouped in this class of decay are searches for GeV-scale new particles that might be directly produced in B or D meson decays. This includes searches for light scalar particles that are motivated by the HyperCP anomaly [78] and for B meson decays to pairs of same-charge leptons that can arise, for example, in models containing Majorana neutrinos [79–81].

The focus of this section is on rare decays involving leptons or photons in the final states. There are also several interesting rare decays involving hadronic final states that can be pursued at LHCb, such as $B^+ \to K^-\pi^+\pi^+$, $B^+ \to K^+K^+\pi^-$ [82, 83], $B_s^0 \to \phi\pi^0$ and $B_s^0 \to \phi\rho^0$ [84]; however, these are not discussed in this document.

Section 2.2 introduces the theoretical framework (the operator product expansion) that is used when discussing rare electroweak penguin processes. The observables and experimental constraints coming from rare semileptonic, radiative and leptonic B decays are then discussed in Secs. 2.3, 2.4 and 2.5 respectively. The implications of these experimental constraints for NP contributions are discussed in Sec. 2.6 and 2.7. Possibilities with rare charm and kaon decays are then discussed in Secs. 2.8 and 2.10. Finally, the second class of decays are discussed in Secs. 2.9 (lepton number and flavour violating decays) and 2.11 (light scalar particles).

2.2 Model-independent analysis of new physics contributions to leptonic, semi-leptonic and radiative decays

Contributions from physics beyond the SM to the observables in rare radiative, semi-leptonic and leptonic B decays can be described by the modification of Wilson coefficients

of local operators in an effective Hamiltonian of the form

$$\mathcal{H}_{\rm eff} = -\frac{4\,G_F}{\sqrt{2}} V_{tb}V_{tq}^* \frac{e^2}{16\pi^2} \sum_i (C_i O_i + C_i' O_i') + \text{h.c.}\,, \tag{4}$$

where $q = d, s$. In many concrete models, the operators that are most sensitive to new physics (NP) are a subset of

$$\begin{aligned}
O_7^{(\prime)} &= \frac{m_b}{e}(\bar{q}\sigma_{\mu\nu}P_{R(L)}b)F^{\mu\nu}, & O_8^{(\prime)} &= \frac{g m_b}{e^2}(\bar{q}\sigma_{\mu\nu}T^a P_{R(L)}b)G^{\mu\nu\,a}, \\
O_9^{(\prime)} &= (\bar{q}\gamma_\mu P_{L(R)}b)(\bar{\ell}\gamma^\mu \ell)\,, & O_{10}^{(\prime)} &= (\bar{q}\gamma_\mu P_{L(R)}b)(\bar{\ell}\gamma^\mu\gamma_5 \ell)\,, \\
O_S^{(\prime)} &= \frac{m_b}{m_{B_q}}(\bar{q}P_{R(L)}b)(\bar{\ell}\ell)\,, & O_P^{(\prime)} &= \frac{m_b}{m_{B_q}}(\bar{q}P_{R(L)}b)(\bar{\ell}\gamma_5 \ell)\,,
\end{aligned} \tag{5}$$

which are customarily denoted as magnetic ($O_7^{(\prime)}$), chromomagnetic ($O_8^{(\prime)}$), semi-leptonic ($O_9^{(\prime)}$ and $O_{10}^{(\prime)}$), pseudoscalar ($O_P^{(\prime)}$) and scalar ($O_S^{(\prime)}$) operators.[2] While the radiative $b \to q\gamma$ decays are sensitive only to the magnetic and chromomagnetic operators, semi-leptonic $b \to q\ell^+\ell^-$ decays are, in principle, sensitive to all these operators.[3]

In the SM, models with Minimal Flavour Violation [85, 86] and models with a flavour symmetry relating the first two generations [35], the Wilson coefficients appearing in Eq. 4 are equal for $q = d$ or s and the ratio of amplitudes for $b \to d$ relative to $b \to s$ transitions is suppressed by V_{td}/V_{ts}. Due to this suppression, at the current level of experimental precision, constraints on decays with a $b \to d$ transition are much weaker than those on decays with a $b \to s$ transition for constraining $C_i^{(\prime)}$. In the future, precise measurements of $b \to d$ transitions will allow powerful tests to be made of this universality which could be violated by NP.

The dependence on the Wilson coefficients, and the set of operators that can contribute, is different for different rare B decays. In order to put the strongest constraints on the Wilson coefficients and to determine the room left for NP, it is therefore desirable to perform a combined analysis of all the available data on rare leptonic, semi-leptonic and radiative B decays. A number of such analyses have recently been carried out for subsets of the Wilson coefficients [25, 26, 87–90].

The theoretically cleanest branching ratios probing the $b \to s$ transition are the inclusive decays $B \to X_s\gamma$ and $B \to X_s\ell^+\ell^-$. In the former case, both the experimental measurement of the branching ratio and the SM expectation have uncertainties of about 7 % [63, 91]. In the latter case, semi-inclusive measurements at the B factories still have errors at the 30 % level [63]. At hadron colliders, the most promising modes to constrain new physics are exclusive decays. In spite of the larger theory uncertainties on the branching fractions as compared to inclusive decays, the attainable experimental precision can lead to stringent constraints on the Wilson coefficients. Moreover, beyond simple branching fraction measurements, exclusive decays offer powerful probes of $C_7^{(\prime)}$, $C_9^{(\prime)}$ and $C_{10}^{(\prime)}$

[2] In principle there are also tensor operators, $O_{T(5)} = (\bar{q}\sigma_{\mu\nu}b)(\bar{\ell}\sigma^{\mu\nu}(\gamma_5)\ell)$, which are relevant for some observables.

[3] In radiative and semi-leptonic decays, the chromomagnetic operator O_8 enters at higher order in α_s.

through angular and *CP* violating observables. These are discussed in Sec. 2.3 below. The exclusive decays most sensitive to new physics in $b \to s$ transitions are $B \to K^*\gamma$, $B_s \to \mu^+\mu^-$, $B \to K\mu^+\mu^-$ and $B \to K^*\mu^+\mu^-$. These decays are discussed in more detail below.

2.3 Rare semi-leptonic B decays

The richest set of observables sensitive to NP are accessible through rare semileptonic decays of B mesons to a vector or pseudoscalar meson and a pair of leptons. In particular the angular distribution of $B \to K^*\mu^+\mu^-$ decays, discussed in Sec. 2.3.2, provides strong constraints on $C_7^{(\prime)}$, $C_9^{(\prime)}$ and $C_{10}^{(\prime)}$.

2.3.1 Theoretical treatment of rare semileptonic $B \to M\ell^+\ell^-$ decays

The theoretical treatment of exclusive rare semi-leptonic B decays is possible in two kinematic regimes for the meson: where the meson has a large recoil and the dilepton system is soft and collinear with the B (low dimuon invariant mass squared, q^2) and where the meson has a small-recoil (high q^2). Calculations are difficult outside these regimes, in particular in the q^2 region close to the narrow $c\bar{c}$ resonances (the J/ψ and $\psi(2S)$).

In the low q^2 region, these decays can be described by QCD-improved Factorisation (QCDF) and the field theory formulation of Soft-Collinear Effective Theory (SCET). The combined limit of a heavy b-quark and an energetic meson M, leads to the schematic form of the decay amplitude [92, 93]:

$$\mathcal{T} = C\,\xi + \phi_B \otimes T \otimes \phi_M + \mathcal{O}(\Lambda_{\rm QCD}/m_b)\,. \tag{6}$$

which is accurate to leading order in $\Lambda_{\rm QCD}/m_b$ and to all orders in α_s. It factorises the calculation into process-independent non-perturbative quantities, $B \to M$ form factors, ξ, and light-cone distribution amplitude (LCDAs), $\phi_{B(M)}$, of the heavy (light) mesons, and perturbatively calculable quantities, C and T which are known to $\mathcal{O}(\alpha_s^1)$ [92, 93]. Further, the seven (three) *a priori* independent $B \to V$ ($B \to P$) form factors reduce to two (one) universal *soft* form factors $\xi_{\perp,\parallel}$ (ξ_P) in QCDF/SCET [94]. The factorisation formula applies well in the range of the dilepton mass range, $1\,\text{GeV}^2 < q^2 < 6\,\text{GeV}^2$.[4]

For $B \to K^*\ell^+\ell^-$, the three K^* spin amplitudes, corresponding to longitudinal and transverse polarisations of the K^*, are linear in the soft form factors $\xi_{\perp,\parallel}$,

$$A_{\perp,\parallel}^{L,R} \propto C_{\perp}^{L,R}\,\xi_{\perp}, \qquad\qquad A_0^{L,R} \propto C_{\parallel}^{L,R}\,\xi_{\parallel}, \tag{7}$$

at leading order in $\Lambda_{\rm QCD}/m_b$ and α_s. The $C_{\perp,\parallel}^{L,R}$ are combinations of the Wilson coefficients $\mathcal{C}_{7,9,10}$ and the L and R indices refer to left- and right-handed K^* spin amplitudes.

[4] Light resonances at q^2 below $1\,\text{GeV}^2$ cannot be treated within QCDF, and their effects have to be estimated using other approaches. In addition, the longitudinal amplitude in the QCDF/SCET approach generates a logarithmic divergence in the limit $q^2 \to 0$, indicating problems in the description below $1\,\text{GeV}^2$ [92].

Symmetry breaking corrections to these relationships of order α_s are known [92,93]. This simplification of the amplitudes as linear combinations of $C_{\perp,\parallel}^{L,R}$ and form factors, makes it possible to design a set of optimised observables in which any soft form factor dependence cancels out for all low dilepton masses q^2 at leading order in α_s and $\Lambda_{\rm QCD}/m_b$ [22,23,95], see Sec. 2.3.2.

Within the QCDF/SCET approach, a general, quantitative method to estimate the important $\Lambda_{\rm QCD}/m_b$ corrections to the heavy quark limit is missing. In semileptonic decays, a simple dimensional estimate of 10 % is often used, largely from matching of the soft form factors to the full-QCD form factors (see also Ref. [96]).

The high q^2 (low hadronic recoil) region, corresponds to the dilepton invariant masses above the two narrow resonances of J/ψ and $\psi(2S)$, with $q^2 \gtrsim (14-15)\,{\rm GeV}^2$. In this region, broad $c\bar{c}$-resonances are treated using a local operator product expansion [97, 98]. The OPE predicts small sub-leading corrections which are suppressed by either $(\Lambda_{\rm QCD}/m_b)^2$ [98] or $\alpha_s\Lambda_{\rm QCD}/m_b$ [97] (depending on whether full QCD or subsequent matching on HQET in combination with form factor symmetries [99] is adopted). The sub-leading corrections to the amplitude have been estimated to be below 2 % [98] and those due to form factor relations are suppressed numerically by $C_7/C_9 \sim \mathcal{O}(0.1)$. Moreover, duality violating effects have been estimated within a model of resonances and found to be at the level of 2 % of the rate, if sufficiently large bins in q^2 are chosen [98]. Consequently, like the low-q^2 region, this region is theoretically well under control.

At high q^2 the heavy-to-light form factors are known only as extrapolations from LCSR calculations at low q^2. Results based on lattice calculations are being derived [100], but may play an important role in the near future in reducing the form factor uncertainties.

2.3.2 Angular distribution of $B \to K^{*0}\mu^+\mu^-$ and $B_s^0 \to \phi\mu^+\mu^-$ decays

The physics opportunities of $B \to V\ell^+\ell^-$ ($\ell = e, \mu$, $V = K^*, \phi, \rho$) can be maximised through measurements of the angular distribution of the decay. Using the decay $B \to K^*(\to K\pi)\ell^+\ell^-$, with K^* on the mass shell, as an example, the angular distribution has the differential form [67, 101]

$$\frac{d^4\Gamma[B \to K^*(\to K\pi)\ell^+\ell^-]}{dq^2\, d\cos\theta_l\, d\cos\theta_K\, d\phi} = \frac{9}{32\pi}\sum_i J_i(q^2)\, g_i(\theta_l, \theta_K, \phi)\,, \tag{8}$$

with respect to the dilepton invariant mass squared, q^2, and three decay angles θ_l, θ_K, and ϕ (as defined in [22]). There are twelve angular terms appearing in the distribution and it is a long-term experimental goal to measure the J_i associated with these twelve terms, from which all other $B \to K^{(*)}\ell^+\ell^-$ observables can be derived.

In the SM, with massless leptons, the J_i depend on bi-linear products of six complex K^* spin amplitudes $A_{\perp,\parallel,0}^{L,R}$,[5] such as

$$J_{1s} = \frac{3}{4}\left[|A_\perp^L|^2 + |A_\parallel^L|^2 + |A_\perp^R|^2 + |A_\parallel^R|^2\right]\,. \tag{9}$$

[5] Further amplitudes have to be taken into account if the mass of the leptons or scalar/tensor operators are present in the analysis.

The expressions for the eleven other J_i terms are given for example in Refs. [23, 68]. Depending on the number of operators that are taken into account in the analysis, it is possible to relate some of the J_i terms. The full derivation of these symmetries can be found in Ref. [23]. The symmetries provide crucial information that can dramatically affect the stability of a fit to the full angular distribution.

When combining B and $\overline{B}$ decays, it is possible to form both *CP*-averaged and *CP*-asymmetric quantities: $S_i = (J_i + \bar{J}_i)/[d(\Gamma + \bar{\Gamma})/dq^2]$ and $A_i = (J_i - \bar{J}_i)/[d(\Gamma + \bar{\Gamma})/dq^2]$, from the J_i [22, 23, 67, 68, 102–104]. The terms $J_{5,6,8,9}$ in the angular distribution are *CP*-odd and, consequently, the associated *CP*-asymmetry, $A_{5,6,8,9}$ can be extracted from an untagged analysis (making it possible for example to measure $A_{5,6,8,9}$ in $B_s^0 \to \phi\mu^+\mu^-$ decays). Moreover, the terms $J_{7,8,9}$ are T-odd and avoid the usual suppression of the corresponding *CP*-asymmetries by small strong phases [102]. The decay $B^0 \to K^{*0}\mu^+\mu^-$, where the K^{*0} decays to $K^+\pi^-$, is self-tagging and it is therefore possible to measure both the A_i and S_i for the twelve angular terms.

In addition, a measurement of the T-odd *CP* asymmetries, A_7, A_8 and A_9, which are zero in the SM and are not suppressed by small strong phases in the presence of NP, would be useful to constrain non-standard *CP* violation. This is particularly true since the direct *CP* asymmetry in the inclusive $B \to X_s\gamma$ decay is plagued by sizable long-distance contributions and is therefore not very useful as a constraint on NP [105].

2.3.3 Short term physics opportunities with $B \to K^*(\to K\pi)\ell^+\ell^-$ decays

In $1.0\,\text{fb}^{-1}$ of integrated luminosity, LHCb has collected the world's largest samples of $B^0 \to K^{*0}\mu^+\mu^-$ (with $K^{*0} \to K^+\pi^-$) and $B_s^0 \to \phi\mu^+\mu^-$ decays, with around 900 and 80 signal candidates respectively [24, 64]. These candidates are however sub-divided into six q^2-bins, with the largest bin containing only $\mathcal{O}(300)$ candidates (for the $B^0 \to K^{*0}\mu^+\mu^-$ decay). With the present statistics it has therefore not been possible to perform a full angular analysis of these decays. The analyses are instead simplified by integrating over two of the three angles or by applying a folding technique to the ϕ angle, $\phi \to \phi + \pi$ for $\phi < 0$, to cancel terms in the angular distribution.

In the case of massless leptons, one finds:

$$\frac{d\Gamma'}{d\phi} = \frac{\Gamma'}{2\pi}\left(1 + S_3\cos 2\phi + A_9 \sin 2\phi\right), \tag{10}$$

$$\frac{d\Gamma'}{d\theta_K} = \frac{3\Gamma'}{4}\sin\theta_K\left(2F_L\cos^2\theta_K + (1 - F_L)\sin^2\theta_K\right), \tag{11}$$

$$\frac{d\Gamma'}{d\theta_\ell} = \Gamma'\left(\frac{3}{4}F_L\sin^2\theta_\ell + \frac{3}{8}(1 - F_L)(1 + \cos^2\theta_\ell) + A_{\text{FB}}\cos\theta_\ell\right)\sin\theta_\ell. \tag{12}$$

where $\Gamma' = \Gamma + \bar{\Gamma}$. The observables appear linearly in the expressions. Experimentally, the fits are performed in bins of q^2 and the measured observables are rate averaged over the q^2-bin. The observables appearing in the angular projections are the fraction of longitudinal polarisation of the K^*, F_L, the lepton system forward-backward asymmetry, A_{FB}, S_3 and A_9.

The differential branching ratio, $A_{\rm FB}$ and F_L have already been measured by the B factories, CDF and LHCb [64, 106, 107]. The observable S_3 is related to the asymmetry between the parallel and perpendicular K^* spin amplitudes[6] and is sensitive to right-handed operators (C_7') at low q^2. In the future, the decay $B^0 \to K^{*0} e^- e^-$ could play an important role in constraining C_7' through S_3 since it allows to probe to smaller values of q^2 than the $B^0 \to K^{*0}\mu^+\mu^-$ decay. The observables S_3 and A_9 are sensitive to right-handed currents only and are negligibly small in the SM. First measurements have been performed by CDF and LHCb [64, 106].[7] The current experimental status of these $B^0 \to K^{*0}\mu^+\mu^-$ angular observables at LHCb, the B factories and CDF is shown in Fig. 5. Improved measurements of these quantities would be useful to constrain the chirality-flipped Wilson coefficients ($C_7^{(\prime)}$, $C_9^{(\prime)}$ and $C_{10}^{(\prime)}$).

Whilst $A_{\rm FB}$ is not free from form factor uncertainties at low q^2, the value of the dilepton invariant mass q_0^2, for which the differential forward-backward asymmetry $A_{\rm FB}$ vanishes, can be predicted in a clean way.[8] The zero crossing-point is highly sensitive to the ratio of the two Wilson coefficients C_7 and C_9. In particular the model-independent upper bound on $|C_9|$ implies $q_0^2 > 1.7\,{\rm GeV}^2/c^4$, which improves to $q_0^2 > 2.6\,{\rm GeV}^2/c^4$, assuming the sign of C_7 to be SM-like [89]. At next-to-leading order one finds [93]:[9]

$$q_0^2[K^{*0}\ell^+\ell^-] = 4.36^{+0.33}_{-0.31}\ {\rm GeV}^2/c^4, \quad q_0^2[K^{*+}\ell^+\ell^-] = 4.15^{+0.27}_{-0.27}\ {\rm GeV}^2/c^4. \tag{13}$$

where the first value is in good agreement with the recent result from LHCb of $q_0^2 = 4.9\ ^{+1.3}_{-1.1}\,{\rm GeV}^2/c^4$ [64] for the $B^0 \to K^{*0}\mu^+\mu^-$ decay.

In the medium term, it is possible to access information from other terms in the angular distribution by integrating over one of the angles and making an appropriate folding of the remaining two angles. From ϕ and θ_K only [109] it is possible to extract:

$$S_5 = -\frac{4}{3}\left[\int_{\pi/2}^{3\pi/2} - \int_0^{\pi/2} - \int_{3\pi/2}^{2\pi}\right] d\phi \left[\int_0^1 - \int_{-1}^0\right] d\cos\theta_K \frac{d^3(\Gamma-\bar\Gamma)}{dq^2\, d\cos\theta_K d\phi} \Big/ \frac{d(\Gamma+\bar\Gamma)}{dq^2}. \tag{14}$$

Analogously to $A_{\rm FB}$, the zero-crossing point of this observable is shown to be also theoretically clean. S_5 is sensitive to the ratio of Wilson coefficients, $(C_7+C_7')/(C_9+\hat m_b(C_7+C_7'))$, and if measured would add complementary information to $A_{\rm FB}$ and S_3 about new right-handed currents.

[6] The quantity $S_3 = (1-F_L)/2 \times A_T^{(2)}$ (in the massless case) allows access to one of the theoretically clean quantities, namely $A_T^{(2)}$. The observable A_T^2 is a theoretiically cleaner observable than S_3 due to the cancellation of some of the form-factor dependence [108].

[7] Depending on the convention for the angle ϕ, $d\Gamma'/d\phi$ of Eq. (10) can also depend on S_9, which is tiny in the SM and beyond. We note that, due to different angular conventions, the quantity $A_{\rm Im}$ reported in Ref. [64] corresponds to S_9, while $A_{\rm Im}$ in Ref. [106] corresponds to A_9.

[8] In the QCDF approach at leading order in $\Lambda_{\rm QCD}/m_b$, the value of q_0^2 is free from hadronic uncertainties at order α_s^0. A dependence on the soft form factor and on the light-cone wave functions of the B and K^* mesons appears only at order α_s^1.

[9] A recent determination of q_0^2 in B^0 decays gives $4.0 \pm 0.3\,{\rm GeV}^2/c^4$ [89]. The shift with respect to Ref. [93] is of parametric origin and is driven in part by the choice of the renormalisation scale ($\mu = 4.2\,{\rm GeV}$ instead of $4.8\,{\rm GeV}$), but also due to differences in the implementation of higher $\mathcal{O}(\alpha_s)$ short-distance contributions.

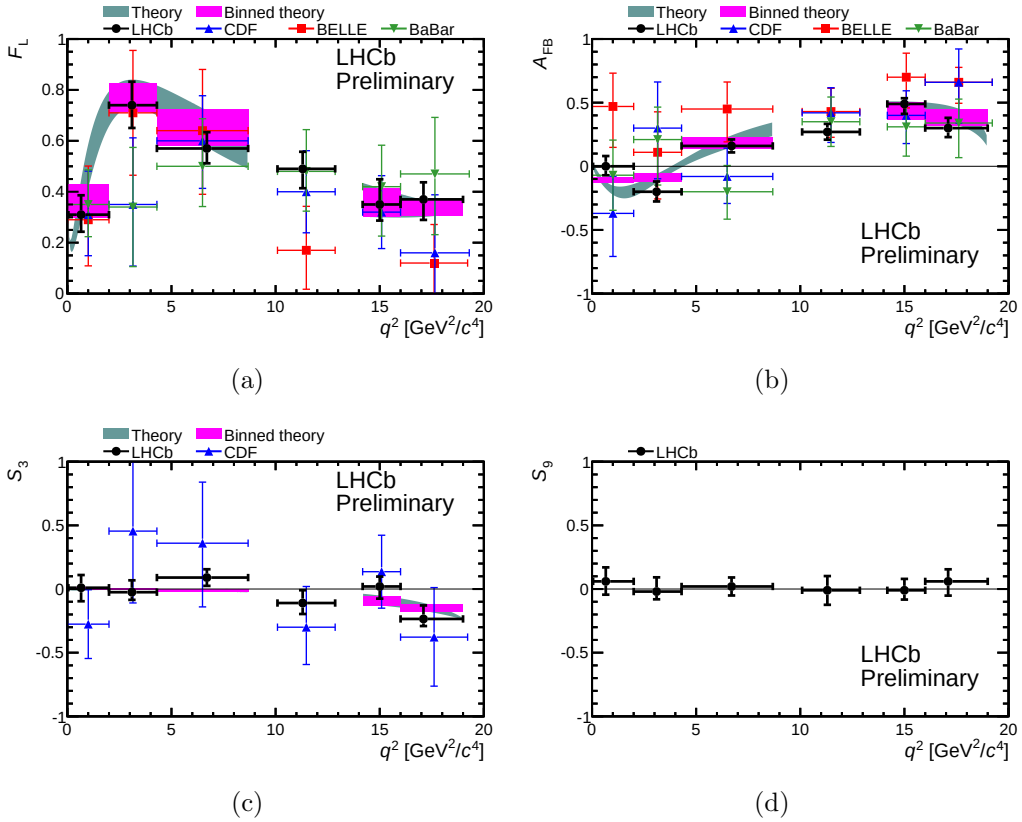

Figure 5: Summary of recent measurements of the angular observables $A_{\rm FB}$, F_L, S_3 and S_9 in $B \to K^* \mu^+ \mu^-$ decays at LHCb, CDF and the B factories. A description of these observables is provided later in the text. The theory predictions at low- and high-dimuon invariant masses are indicated by the coloured bands and are also described in detail in the text.

2.3.4 Theoretically clean observables in $B \to K^*(\to K\pi)\ell^+\ell^-$ decays

With 2–5 fb^{-1} of integrated luminosity at LHCb it will be possible to exploit the complete new physics sensitivity of the $B \to K^* \ell^+ \ell^-$ both in the low- and high-q^2 regions, by performing a full angular analysis. The increasing size of the experimental samples makes it important to design optimised observables (by using specifically chosen combinations of the J_i) to reduce theoretical uncertainties. In the low-q^2 region, the linear dependence of the amplitudes on the soft form factors allows for a complete cancellation of the hadronic uncertainties due to the form factors at leading order. This consequently increases the sensitivity to the structure of new physics models [22, 23].

In the low-q^2 region, the so-called transversity observables $A_T^{(i)}, i = 2, 3, 4, 5$ are an example of set of observables that are constructed such that the soft form factor dependence cancels out at leading order. They represent the complete set of angular observables and are chosen to be highly sensitive to new right handed currents via C_7' [22, 23]. A second, complete, set of optimised angular observables was constructed (also in the cases of non-

vanishing lepton masses and in the presence of scalar operators) in Ref. [95]. Recently the effect of binning in q^2 on these observables has been considered [108]. In these sets of observables, the unknown $\Lambda_{\rm QCD}/m_b$ corrections are estimated to be of order 10 % on the level of the spin amplitudes and represent the dominant source of theory uncertainty.

In general, the angular observables are shown to offer high sensitivity to NP in the Wilson coefficients of the operators O_7, O_9, and O_{10} and of the chirally flipped operators [22, 23, 67, 102]. In particular, the observables S_3, A_9 and the *CP*-asymmetries A_7 and A_8 vanish at leading order in $\Lambda_{\rm QCD}/m_b$ and α_s in the SM operator basis [102]. Importantly, this suppression is absent in extensions with non-vanishing chirality-flipped $C'_{7,9,10}$, giving rise to contributions proportional to $\mathrm{Re}(C_i C_j^{*\prime})$ or $\mathrm{Im}(C_i C_j^{*\prime})$ and making these terms ideal probes of right-handed currents [22, 23, 67, 102]. *CP* asymmetries are small in the SM, because the only *CP*-violating phase affecting the decay is doubly Cabibbo-suppressed, but can be significantly enhanced by NP phases in $C_{9,10}$ and $C'_{9,10}$, which at present are poorly constrained. In a full angular analysis it can also be shown that *CP*-conserving observables provide indirect constraints on *CP*-violating NP contributions [23].

At large q^2, the dependence on the magnetic Wilson coefficients $C_7^{(\prime)}$ is suppressed, allowing, in turn, a cleaner extraction of semi-leptonic coefficients ($C_9^{(\prime)}$ and $C_{10}^{(\prime)}$). As a consequence of symmetry relations of the OPE [89,103,104,110], at high q^2, combinations of the angular observables J_i can be formed within the SM operator basis (*i.e.* with $C'_i = 0$), which depend:

- only on short-distance quantities (*e.g.* $H_T^{(2,3)}$) ;
- only on long-distance quantities (F_L and low-q^2 optimised observables $A_T^{(2,3)}$).

Deviations from these relations are due to small sub-leading corrections at order $(\Lambda_{\rm QCD}/m_b)^2$ from the OPE.

In the SM operator basis it is interesting to note that $A_T^{(2,3)}$, which are highly sensitive to short distance contributions (from C'_7) at low-q^2, instead become sensitive to long-distance quantities (the ratio of form factors) at high q^2. The extraction of form factor ratios is already possible with current data on S_3 ($A_T^{(2)}$) and F_L and leads to a consistent picture between LCSR calculations, lattice calculations and experimental data [90, 110]. In the presence of chirality-flipped Wilson coefficients, these observables are no longer short-distance free, but are probes of right-handed currents [25]. At high q^2, the OPE framework predicts $H_T^{(2)} = H_T^{(3)}$ and $J_7 = J_8 = J_9 = 0$. Any deviation from these relationships, would indicate a problem with the OPE and the theoretical predictions in the high-q^2 region.

2.3.5 $B^+ \to K^+\mu^+\mu^-$ and $B^+ \to K^+e^-e^-$

The branching fractions of $B^{(+)} \to K^{(+)}\mu^+\mu^-$ have been measured by BaBar, Belle and CDF [107, 111, 112]. In 1.0 fb^{-1} LHCb observes 1250 $B^+ \to K^+\mu^+\mu^-$ candidates [9], and in the future will dominate measurements of these decays.

Since the $B \to K$ transition does not receive contributions from an axial vector current, the primed Wilson coefficients enter the $B^{(+)} \to K^{(+)}\mu^+\mu^-$ observables always in conjunction with their unprimed counterparts as $(C_i + C_i')$. This is in contrast to the $B \to K^*\mu^+\mu^-$ decay and therefore provides complementary constraints on the Wilson coefficients and their chirality-flipped counterparts.

An angular analysis of the $\mu^+\mu^-$ pair in the $B^{(+)} \to K^{(+)}\mu^+\mu^-$ decay would allow the measurement of two further observables, the forward-backward asymmetry $A_{\rm FB}$ and the so-called flat term F_H [113]. The angular distribution of a B meson decaying to a pseudoscalar meson, P, and a pair of leptons involves just q^2 and a single angle in the dilepton system, θ_l [113]

$$\frac{1}{\Gamma_\ell}\frac{d\Gamma_\ell[B \to P\ell^+\ell^-]}{d\cos\theta_l} = \frac{3}{4}(1 - F_{\rm H})(1 - \cos^2\theta_l) + \frac{1}{2}F_{\rm H} + A_{\rm FB}\cos\theta_l \qquad (15)$$

which depends on two parameters discussed above.

In the SM, the forward-backward asymmetry of the dilepton system is expected to be zero. Any non-zero forward backward asymmetry would point to a contribution from new particles that extend the SM operator basis. Allowing for generic (pseudo-)scalar and tensor couplings, there is sizable room for new physics contributions in the range $|A_{\rm FB}| \lesssim 15\,\%$. The flat term, $F_{\rm H}/2$, that appears with $A_{\rm FB}$ in the angular distribution, is non-zero, but small (for $\ell = e, \mu$) in the SM. This term can also see large enhancements in models with (pseudo-)scalar and tensor couplings of up to $F_{\rm H} \sim 0.5$. Recent SM predictions at low- and high-q^2 can be seen in Refs. [89, 96, 113, 114]. The current experimental limits on $\mathcal{B}(B_s^0 \to \mu^+\mu^-)$ now largely preclude large C_S and C_P, and if NP is present only in tensor operators then new physics contributions are expected to be in the range $|A_{\rm FB}| \lesssim 5\,\%$ and $F_{\rm H} \lesssim 0.2$.

In addition to $A_{\rm FB}$, $F_{\rm H}$ and the differential branching fraction of the decays, it is possible to probe the universality of lepton interactions by comparing the branching fraction of decays $B \to K^{(+)}\ell^+\ell^-$ with two different lepton flavours (*e.g.* electrons versus muons):

$$R_K = \Gamma_\mu/\Gamma_e \qquad \text{(with same } q^2\text{-cuts)}. \qquad (16)$$

Lepton universality may be violated in extensions to the SM, such as R-parity violating SUSY models.[10] In the SM, the ratio $R_K^{\rm SM}$ is expected to be close to unity $R_K^{\rm SM} = 1 + \mathcal{O}(m_\mu^2/m_B^2)$ [118].

It is also interesting to note that at low recoil (high q^2) the differential decay rates and CP asymmetries of $B^{(+)} \to K^{(+)}\ell^+\ell^-$ and $B \to K^*\ell^+\ell^-$ ($\ell = e, \mu$) are correlated [89] and exhibit the same short-distance dependence (in the SM operator basis). Any deviation would point to a problem for the OPE used in the high q^2 region.

2.3.6 Rare semileptonic $b \to d\ell^+\ell^-$ decays

Rare $b \to d$ radiative decay processes $B \to \rho\gamma$, have been previously observed at the B factories [119]. In the 2011 data sample, the very rare decay $B^+ \to \pi^+\mu^+\mu^-$ was

[10] There are hints of lepton universality violation in recent measurements of $B \to D^{(*)}\tau\nu$ by BaBar [115] and Belle [116, 117].

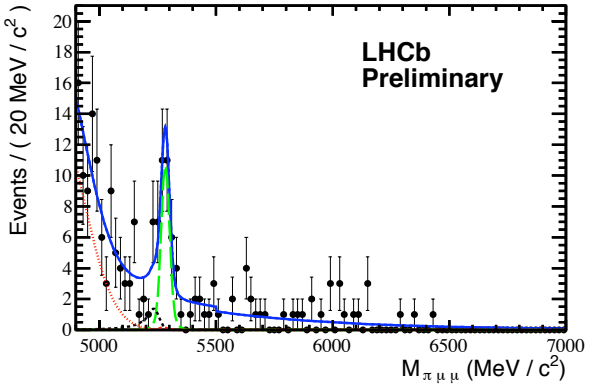

Figure 6: The $\pi^+\mu^+\mu^-$ invariant mass of selected $B^+ \to \pi^+\mu^+\mu^-$ candidates in $1\,\text{fb}^{-1}$ of integrated luminosity. The (green) long-dashed line indicates the signal, the (black) short-dashed line reflected background from $B^+ \to K^+\mu^+\mu^-$ and the (red) dotted line low-mass partially reconstructed background from $B \to \pi^+\mu^+\mu^- + X$ decays.

observed at the LHCb experiment for the first time. This is a rare $b \to d\ell^+\ell^-$ transition, which is in the SM suppressed by loop and CKM factors proportional to $|V_{td}|/|V_{ts}|$. In the 1.0 fb^{-1} data sample, LHCb observes $25.3\,^{+6.7}_{-6.4}$ signal candidates corresponding to a branching fraction of $\mathcal{B}(B^+ \to \pi^+\mu^+\mu^-) = 2.4 \pm 0.6 \pm 0.2 \times 10^{-8}$ [29]. This measurement is in good agreement with the SM prediction, which is consistent with there being no large NP contribution to the $b \to d\ell^+\ell^-$ processes and with the MFV hypothesis.

The $b \to d$ transitions can show potentially larger *CP*- and isospin violating effects than their $b \to s$ counterparts due to the different CKM hierarchy [93]. These studies would need the large statistics provided by the future LHCb upgrade. A 5-50 fb^{-1} data sample will also enable a precision measurement of the ratio of the branching fractions of B^+ meson decays to $\pi^+\mu^+\mu^-$ and $K^+\mu^+\mu^-$. This ratio would enable a useful comparison of $|V_{td}/V_{ts}|$ to be made using penguin processes (with form factors from lattice QCD) and box processes (using $\Delta m_s/\Delta m_d$ and bag-parameters from lattice QCD) and provide a powerful test of MFV.

2.3.7 Isospin asymmetry of $B^{(+)} \to K^{(+)}\mu^+\mu^-$ and $B^{(+)} \to K^{*(+)}\mu^+\mu^-$ decays

Analyses at hadron colliders (at LHCb and CDF) have mainly focused on decay modes with charged tracks in the final state. B meson decays involving K^0 mesons are experimentally much more challenging due to the long lifetimes of K^0_S and K^0_L mesons (the K^0_L is not reconstructable within LHCb). Nevertheless, LHCb has been able to select 60 $B^0 \to K^0\mu^+\mu^-$ decays, reconstructed as $K^0_S \to \pi^+\pi^-$, and 80 $B^+ \to K^{*+}\mu^+\mu^-$, reconstructed as $K^{*+} \to K^0_S\pi^+$, which are comparable in size to the samples that are available for these modes in the full data sets of the B factories. The isolation of these rare decay

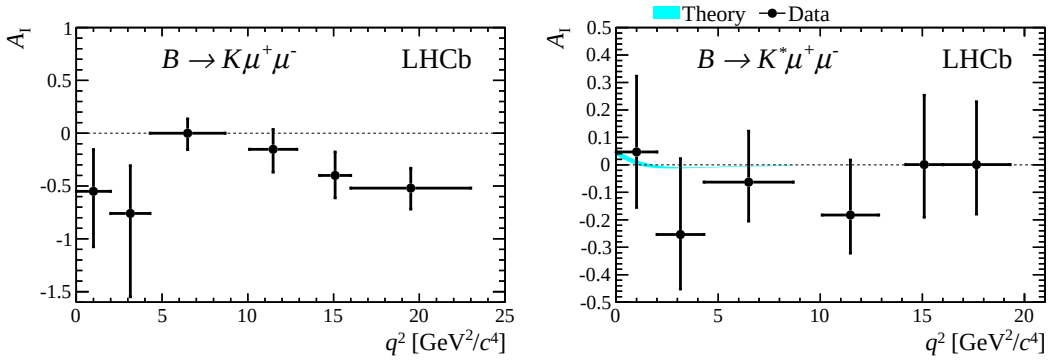

(a) (b)

Figure 7: $B \to K\mu^+\mu^-$ (a) and $B \to K^*\mu^+\mu^-$ isospin asymmetries in 1.0 fb^{-1} of data collected by the LHCb collaboration in 2011 [9].

modes enables a measurement of the isospin asymmetry of $B \to K^{(*)}\mu^+\mu^-$ decays:

$$A_{\rm I} = \frac{\mathcal{B}(B^0 \to K^0\mu^+\mu^-) - (\tau_{B^0}/\tau_{B^\pm})\mathcal{B}(B^\pm \to K^\pm\mu^+\mu^-)}{\mathcal{B}(B^0 \to K^0\mu^+\mu^-) - (\tau_{B^0}/\tau_{B^\pm})\mathcal{B}(B^\pm \to K^\pm\mu^+\mu^-)} \quad .$$

At leading order, isospin asymmetries (which involve the spectator quark) are expected to be zero in the SM. Isospin breaking effects are sub leading Λ/m_b effects, which are difficult to estimate due to unknown power corrections. Nevertheless isospin breaking effects are expected to be small and these observables may be useful in NP searches because they offer complementary information on specific Wilson coefficients [120].

The LHCb measurement of the K and K^* isospin asymmetries in bins of q^2 are shown in Fig. 7. For the K^* modes $A_{\rm I}$ is compatible with the SM expectation that $A_{\rm I}^{SM} \simeq 0$, but for the K^+/K^0 modes, $A_{\rm I}$ is seen to be negative at low- and high-q^2 [9]. This is consistent with what has been seen at previous experiments, but is inconsistent with the naive expectation of $A_{\rm I} \sim 0$ at the four sigma level.

2.4 Radiative B decays

While the branching ratio of the $B \to K^*\gamma$ decay is problematic (from the theory side) due to large form factor uncertainties, the mixing-induced CP asymmetry $S_{K^*\gamma}$ is an important constraint due to its sensitivity to the chirality-flipped magnetic Wilson coefficient C_7'. At leading order it vanishes for $C_7' \to 0$, so the SM prediction is tiny and experimental evidence for a large $S_{K^*\gamma}$ would be a clear indication of NP effects through right handed currents [121, 122]. Unfortunately it is experimentally very challenging to measure $S_{K^*\gamma}$ in a hadronic environment, requiring both flavour tagging and the ability to reconstruct the K^{*0} in the decay mode $K^{*0} \to K^0\pi^0$. However, the channel $B_s^0 \to \phi\gamma$, which is much more attractive experimentally, offers the same physics opportunities, with additional sensitivity due to the non-negligible width difference in the B_s^0 system. Moreover, LHCb can study several other interesting radiative b-hadron decays.

2.4.1 Experimental status and short term outlook for rare radiative decays

In 1.0 fb^{-1} and 370 pb^{-1} of integrated luminosity LHCb observes 5300 $B^0 \to K^{*0}\gamma$ [28] and 240 $B_s^0 \to \phi\gamma$ [27] candidates respectively. These are the largest samples of rare radiative B^0 and B_s^0 decays collected by a single experiment. The large sample of $B^0 \to K^{*0}\gamma$ decays has enabled LHCb to make the world's most precise measurement of the direct CP-asymmetry $A_{CP}(K^*\gamma) = 0.8 \pm 1.7 \pm 0.9\,\%$, compatible with zero as expected in the SM [28].

In the medium term it will be possible to add additional constraints on the $C_7 - C_7'$ plane through measurements of $b \to s\gamma$ processes. This includes a time-dependent analysis of $B_s^0 \to \phi\gamma$ [123], as described in detail in the LHCb roadmap document [73]. Furthermore, the large Λ_b^0 production cross-section will allow for measurements of the photon polarisation through the decays $\Lambda_b^0 \to \Lambda^{(*)}\gamma$ [124, 125]. In fact, the study of $\Lambda_b^0 \to \Lambda$ transitions is quite attractive from the theoretical point of view, since the hadronic uncertainties are under good control [126–128]. However, because the Λ_b^0 has $J^P = \frac{1}{2}^+$ and can be polarised at production, it will be important to measure first the Λ_b^0 polarisation.

$B \to VP\gamma$ decays with a photon, a vector and a pseudoscalar particle in the final state can also provide sensitivity to C_7' [129–132]. The decays $B \to \phi K\gamma$ and $B^+ \to K_1(1270)^+\gamma$ have been previously observed at the B factories [133, 134] and large samples will be available for the first time at LHCb.

2.5 Leptonic B decays

2.5.1 $B_s^0 \to \mu^+\mu^-$ and $B^0 \to \mu^+\mu^-$

The decays $B_s^0 \to \mu^+\mu^-$ are a special case amongst the electroweak penguin processes, as they are chirality-suppressed in the SM and are most sensitive to scalar and pseudoscalar operators. The branching fraction of $B_{s(d)}^0 \to \mu^+\mu^-$ can be expressed as [135–138]:

$$\begin{aligned} \mathcal{B}(B_q^0 \to \mu^+\mu^-) &= \frac{G_F^2\alpha^2}{64\pi^3} f_{B_q}^2 \tau_{B_q} m_{B_q} |V_{tb}V_{tq}^*|^2 \sqrt{1 - \frac{4m_\mu^2}{m_{B_q}^2}} \\ &\times \left\{ \left(1 - \frac{4m_\mu^2}{m_{B_q}^2}\right) |C_S - C_S'|^2 + \left| (C_P - C_P') + 2\frac{m_\mu}{m_{B_q}} (C_{10} - C_{10}') \right|^2 \right\} , \end{aligned} \tag{17}$$

where $q = s, d$.

Within the SM, C_S and C_P are negligibly small and the dominant contribution of C_{10} is helicity suppressed. The coefficients C_i are the same for B_s^0 and B^0 in any physics scenario that obeys Minimal Flavour Violation (MFV). The large suppression of $\mathcal{B}(B^0 \to \mu^+\mu^-)$ with respect to $\mathcal{B}(B_s^0 \to \mu^+\mu^-)$ in MFV scenarios means that $B_s^0 \to \mu^+\mu^-$ is often of more interest than $B^0 \to \mu^+\mu^-$ for NP searches. The ratio $\mathcal{B}(B_s^0 \to \mu^+\mu^-)/\mathcal{B}(B^0 \to \mu^+\mu^-)$ is however a very useful probe of MFV.

The SM branching fraction depends on the exact values of the input parameters: f_{B_q}, τ_{B_q} and $|V_{tb}V_{tq}^*|^2$. The B_s^0 decay constant, f_{B_s}, constitutes the main source of uncertainty on $\mathcal{B}(B_s^0 \to \mu^+\mu^-)$. As of the year 2009 there were two unquenched lattice QCD calculations of f_{B_s}, by the HPQCD [139] and FNAL/MILC [140] collaborations, which, when averaged, gave the value $f_{B_s} = 238.8 \pm 9.5\,\text{MeV}$ [141]. The FNAL/MILC calculation was updated in Ref. [142], which increased the world average to $f_{B_s} = 250 \pm 12\,\text{MeV}$ in 2010. In 2011, the ETM collaboration reported a value of $f_{B_s} = 232 \pm 10\,\text{MeV}$ [143] and FNAL/MILC, $f_{B_s} = 242 \pm 9.5\,\text{MeV}$ [144, 145]. The HPQCD collaboration result of $f_{B_s} = 227 \pm 10\,\text{MeV}$ [146] has recently been improved upon with an independent calculation that gives $f_{B_s} = 225 \pm 4\,\text{MeV}$ [147].

If we consider the 2010/11 results by the three lattice groups, ETMC, FNAL/MILC and HPQCD (excluding for the moment the most recent HPQCD result), we remark that their uncertainties agree, as do their results within these uncertainties, so that one can take an average of these three results, giving $f_{B_s} = 234 \pm 10$ MeV [148]. This implies 8.7 % uncertainty on the branching ratio, and leads to the SM prediction [148]:

$$\mathcal{B}(B_s^0 \to \mu^+\mu^-)_{\text{SM}} = (3.53 \pm 0.38) \times 10^{-9} \tag{18}$$

where the other sources of uncertainty are due to the B_s^0 lifetime, the CKM matrix element V_{ts}, the top mass m_t, the electroweak corrections and scale variations.

A weighted average of FNAL/MILC '11 [144], HPQCD '11 [147] and HPQCD '12 [146] was presented recently [141], giving $f_{B_s} = 227.6 \pm 5.0$ MeV. Using this value instead, the SM prediction for the branching ratio is [17]:

$$\mathcal{B}(B_s^0 \to \mu^+\mu^-)_{\text{SM}} = (3.1 \pm 0.2) \times 10^{-9}\,. \tag{19}$$

Note that the two predictions of (18) and (19) agree within uncertainties. We use the latter value as our nominal $\mathcal{B}(B_s^0 \to \mu^+\mu^-)_{\text{SM}}$. For a more detailed discussion of the SM prediction, see Ref. [149]. It is also possible to obtain predictions for $\mathcal{B}(B_s^0 \to \mu^+\mu^-)_{\text{SM}}$ with reduced sensitivity to the value of f_{B_s} using input from either Δm_s [150] or from a full CKM fit [34].

Likewise for f_{B_d}, using the average of ETMC-11 ($f_{B_d} = 195 \pm 12$ MeV) [143], Fermilab-MILC-11 ($f_B = 197 \pm 9$ MeV) [144,145] and HPQCD-12 ($f_{B_d} = 191 \pm 9$ MeV) [146] results, which amounts to $f_B = 194 \pm 10$ MeV [148], the branching ratio of $B^0 \to \mu^+\mu^-$ is:

$$\mathcal{B}(B^0 \to \mu^+\mu^-)_{\text{SM}} = (1.1 \pm 0.1) \times 10^{-10} \quad . \tag{20}$$

New Physics models, especially those with an extended Higgs sector, can significantly enhance the $B_{s(d)}^0 \to \mu^+\mu^-$ branching fraction even in the presence of other existing constraints. In particular, it has been emphasised in many works [151–158] that the decay $B_s^0 \to \mu^+\mu^-$ is very sensitive to the presence of SUSY particles. At large $\tan\beta$, the SUSY contribution to this process is dominated by the exchange of neutral Higgs bosons, and both C_S and C_P can receive large contributions from scalar exchange.

In constrained SUSY models such as CMSSM and NUHM1, predictions can be made for the $\mathcal{B}(B_s^0 \to \mu^+\mu^-)$ that take into account the existing constraints from the general

purpose detectors. These models predict [20]:

$$1 < \frac{\mathcal{B}(B_s^0 \to \mu^+\mu^-)_{\rm CMSSM}}{\mathcal{B}(B_s^0 \to \mu^+\mu^-)_{\rm SM}} < 2$$

$$1 < \frac{\mathcal{B}(B_s^0 \to \mu^+\mu^-)_{\rm NUHM1}}{\mathcal{B}(B_s^0 \to \mu^+\mu^-)_{\rm SM}} < 3$$

The LHCb (and CMS) measurements of $B_s^0 \to \mu^+\mu^-$ have already excluded the upper range of these predictions.

Other NP models such as composite models (*e.g.* Littlest Higgs model with T-parity or Topcolour-assisted Technicolor), models with extra dimensions (*e.g.* Randall Sundrum models) or models with a fourth generation fermions can modify $\mathcal{B}(B_s^0 \to \mu^+\mu^-)$ [17,159–163]. The BSM contributions from these models usually arise via $(C_{10} - C'_{10})$, and they are therefore correlated with the constraints from other $b \to s\ell^+\ell^-$ processes, *e.g.* with $\mathcal{B}(B^+ \to K^+\mu^+\mu^-)$ which depends on $(C_{10} + C'_{10})$. The term $(C_P - C'_P)$ in the branching fraction adds coherently with the SM contribution from $(C_{10} - C'_{10})$, and therefore can also destructively interfere. In such cases, if $(C_S - C'_S)$ remains small, $\mathcal{B}(B_s^0 \to \mu^+\mu^-)$ could be smaller than the SM prediction. A measurement of $\mathcal{B}(B_s^0 \to \mu^+\mu^-)$ well below the SM prediction would be a clear indication of NP and would be symptomatic of a model with a large non-degeneracy in the scalar sector (where $C_P^{(\prime)}$ is enhanced but $C_S^{(\prime)}$ is not). If only C_{10} is modified, these constraints currently require the branching ratio to be above 1.1×10^{-10} [25]. In the presence of NP effects in both C_{10} and C'_{10}, even stronger suppression is possible in principle.

At the beginning of 2012, the LHCb experiment set the world best limits on the $\mathcal{B}(B_{s(d)}^0 \to \mu^+\mu^-)$. At 95 % C.L.:

$$\begin{aligned} \mathcal{B}(B_s^0 \to \mu^+\mu^-) &< 4.5 \times 10^{-9} \\ \mathcal{B}(B^0 \to \mu^+\mu^-) &< 1.0 \times 10^{-9} \end{aligned}$$

Experimentally the measured branching fraction is the time-averaged (TA) branching fraction, which differs from the theoretical value because of the sizable width difference between the heavy and light B_s^0 mesons [18,164].[11] In general,

$$\mathcal{B}(B_s^0 \to \mu^+\mu^-)_{\rm TH} = [(1 - y_s^2)/(1 + \mathcal{A}_{\Delta\Gamma} y_s)] \times \mathcal{B}(B_s^0 \to \mu^+\mu^-)_{\rm TA} \qquad (21)$$

where $\mathcal{A}_{\Delta\Gamma} = +1$ in the SM and $y_s = 0.088 \pm 0.014$ [30]. Thus the experimental measurements have to be compared to the following SM prediction for the time-averaged branching fraction:

$$\mathcal{B}(B_s^0 \to \mu^+\mu^-)_{\rm SM,TA} = \mathcal{B}(B_s^0 \to \mu^+\mu^-)_{\rm SM,TH}/(1 - y_s) = (3.5 \pm 0.2) \times 10^{-9}\,. \qquad (22)$$

[11] This was previously observed in a different context [165].

With $50\,\text{fb}^{-1}$ of integrated luminosity, taken with an upgraded LHCb experiment, a precision better than 10 % can be achieved in $\mathcal{B}(B_s^0 \to \mu^+\mu^-)$, and $\sim 35\,\%$ on the ratio $\mathcal{B}(B_s^0 \to \mu^+\mu^-)/\mathcal{B}(B^0 \to \mu^+\mu^-)$. The dominant systematic uncertainty is likely to come from knowledge of the ratio of fragmentation fractions, f_d/f_s, which is currently known to a precision of 8 % [69].[12] This uncertainty originates mainly from the measurement of $\mathcal{B}(D_s^+ \to K^+K^+\pi^+)$, which in the PDG is given to 4.9 % (coming from a single measurement from CLEO [166]). A new result from Belle has recently been presented [167] – inclusion of this measurement in the world average will improve the uncertainty on $\mathcal{B}(D_s^+ \to K^+K^+\pi^+)$ to $\sim 3.5\,\%$. With the samples available with the LHCb upgrade, it will be possible to go beyond branching fraction measurements and study the effective lifetime, that provides additional sensitivity to NP [18].

In Sec. 2.7, the NP implications of the current measurements of $\mathcal{B}(B_s^0 \to \mu^+\mu^-)$ and the interplay with other observables, including results from direct searches, are discussed for a selection of specific NP models. In general, the strong experimental constraints on $\mathcal{B}(B_s^0 \to \mu^+\mu^-)$ [4,168–170] largely preclude any visible effects from scalar or pseudoscalar operators in other $b \to s\ell^+\ell^-$ decays.[13]

2.5.2 $B_s^0 \to \tau^+\tau^-$

The leptonic decay $B_s^0 \to \tau^+\tau^-$ provides interesting information on the interaction of the third generation quarks and leptons. In many new physics models, contributions to third generation quarks/leptons can be dramatically enhanced with respect to the first and second generation. This is true in, for example, scalar and pseudoscalar interactions in supersymmetric scenarios, for large values of $\tan\beta$. Interestingly, there is also an interplay between $b \to s\tau^+\tau^-$ processes and the lifetime difference Γ_{12}^s in B_s^0 mixing (see Sec. 3). The correlation of both processes has been discussed model-independently [38, 171] and in specific scenarios, such as Lepto-Quarks [37, 172] or Z'-models [173–175]. There are presently no experimental limits on $B_s^0 \to \tau^+\tau^-$, however the interplay with Γ_{12}^s, and the latest LHCb-measurement of Γ_d/Γ_s would imply a limit of $\mathcal{B}(B_s^0 \to \tau^+\tau^-) < 3\,\%$ at 90 % CL. Any improvement on this limit, which might be in reach with the existing LHCb dataset, would yield strong constraints on models that couple strongly to third generation leptons. A large enhancement in $b \to s\tau^+\tau^-$ could help to understand the anomaly observed by the D0 experiment in their measurement of A_{SL} [36] and could also reduce the tension that exists with other mixing observables [38, 171].

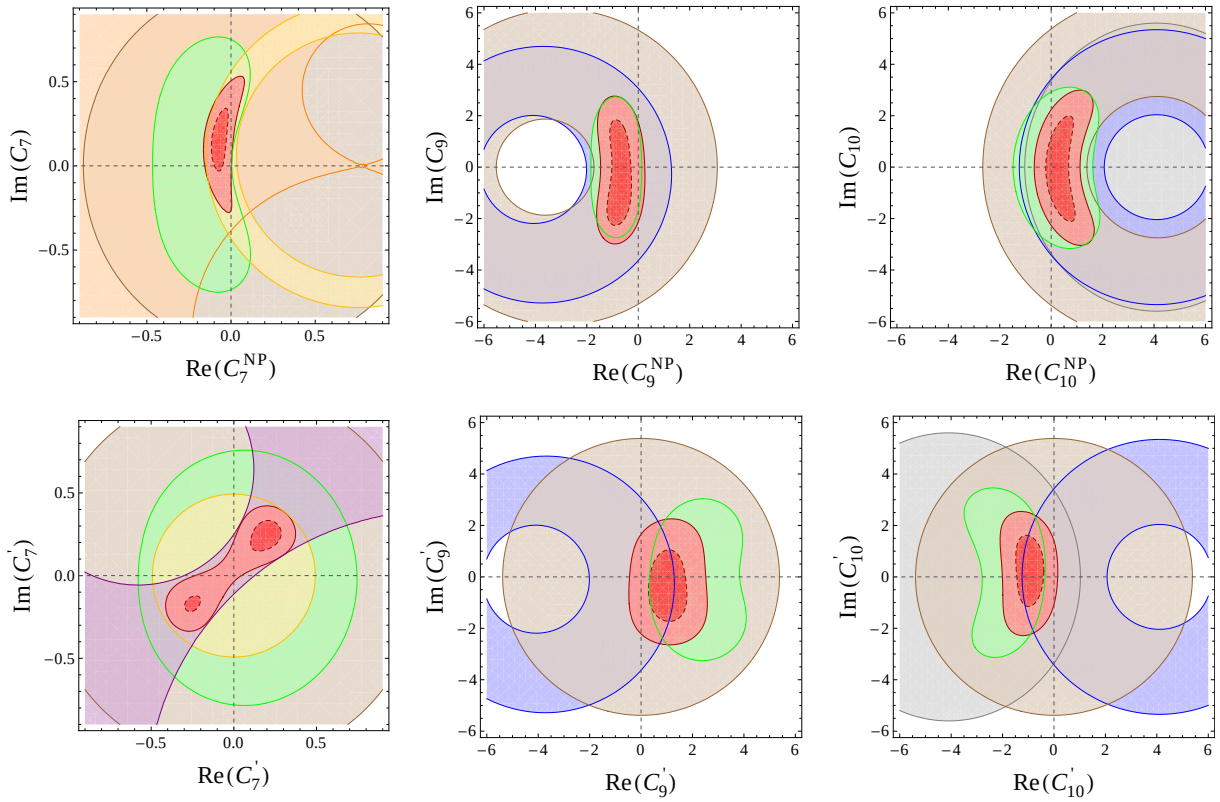

Figure 8: Individual 2σ constraints in the complex planes of Wilson coefficients, coming from $B \to X_s\ell^+\ell^-$ (brown), $B \to X_s\gamma$ (yellow), $A_{CP}(b \to s\gamma)$ (orange), $B \to K^*\gamma$ (purple), $B \to K^*\mu^+\mu^-$ (green), $B \to K\mu^+\mu^-$ (blue) and $B_s \to \mu^+\mu^-$ (grey), as well as combined 1 and 2σ constraints (red). Figure taken from Ref. [25].

2.6 Model-independent constraints

Figure 8, taken from Ref. [25], shows the current constraints on the NP contributions to the Wilson coefficients $C_7^{(\prime)}$, $C_9^{(\prime)}$ and $C_{10}^{(\prime)}$, varying only one coefficient at a time. The experimental constraints included here are: the branching fractions of $B \to X_s\gamma$, $B \to X_s\ell^+\ell^-$, $B \to K\mu^+\mu^-$ and $B_s \to \mu^+\mu^-$, the time-dependent CP asymmetries in $B \to K^*\gamma$ and $b \to s\gamma$ and the branching fraction and angular observables in $B \to K^*\mu^+\mu^-$. One can make the following observations:

- At 95 % C.L., all Wilson coefficients are compatible with their SM values.
- For the coefficients present in the SM, *i.e.* C_7, C_9 and C_{10}, the constraints on the imaginary part are looser than on the real part.

[12] This value is valid for B mesons produced from $\sqrt{s} = 7$ TeV pp collisions within the LHCb acceptance. It will, in principle, need to be remeasured at each different LHC collision energy. However, once any B_s^0 branching fraction, such as that for $B_s^0 \to J/\psi\,\phi$, is known to good precision, normalisation can be carried out without direct need for an f_d/f_s value.

[13] Barring a sizable, fortuitous cancellation among $C_{S,P}$ and $C'_{S,P}$ [114].

- For the Wilson coefficients $C_{10}^{(\prime)}$, the latest constraint on $\mathcal{B}(B_s^0 \to \mu^+\mu^-)$ is starting to become competitive with the constraints from the angular analysis of $B \to K^{(*)}\mu^+\mu^-$.

- The constraints on C_9' and C_{10}' from $B \to K\mu^+\mu^-$ and $B \to K^*\mu^+\mu^-$ are complementary and lead to a more constrained region, and better agreement with the SM, than with $B \to K^*\mu^+\mu^-$ alone.

- A second allowed region in the C_7-C_7' plane characterised by large positive contributions to both coefficients, which was found previously to be allowed *e.g.* in Refs. [87, 88], is now disfavoured at 95 % C.L. by the new $B \to K^*\mu^+\mu^-$ data, in particular the measurements of the forward-backward asymmetry from LHCb.

The second point above can be understood from the fact that in the branching fractions and *CP* averaged angular observables which give the strongest constraints, only NP contributions aligned in phase with the SM can interfere with the SM contributions. As a consequence, NP with non-standard *CP* violation is in fact constrained more weakly than NP where *CP* violation stems only from the CKM phase. This highlights the need for improved measurements of *CP* asymmetries directly sensitive to non-standard phases. A measurement of the *CP* asymmetries in $B^0 \to K^{*0}\mu^+\mu^-$ decays is currently being prepared by the LHCb collaboration.

Significant improvements of these constraints – or first hints for physics beyond the SM – can be obtained in the future by both improved measurements of the observables discussed above and by improvements on the theoretical side. From the theory side, there is scope for improving the estimates of the hadronic form factors from lattice calculations, which will reduce the dominant source of uncertainty on the exclusive decays. On the experimental side there are also a large number of theoretically clean observables that can be extracted with a full angular analysis of $B^0 \to K^{*0}\mu^+\mu^-$.

2.7 Interplay with direct searches and model-dependent constraints

The search for SUSY is the main focus of NP searches in ATLAS and CMS, which, with no signal so far, has put strong limits in the constrained SUSY scenarios. The understanding of the parameters of the SUSY models also depends on other measurements, such as the anomalous dipole moment of the muon, limits from dark matter direct detection experiments, measurements of the dark matter relic density and various B physics observables which provide important information. As discussed in Sec. 2.5, the rare decay channels studied in LHCb, such as $B_{s(d)}^0 \to \mu^+\mu^-$, are stringent tests of SUSY. In addition, the decays $B \to K^{(*)}\mu^+\mu^-$ offer many complementary observables which are sensitive to different sectors of the theory. In this section, we will explain the implications of the current LHCb measurements in different SUSY models, both in constrained scenarios and in a more general case (pMSSM).

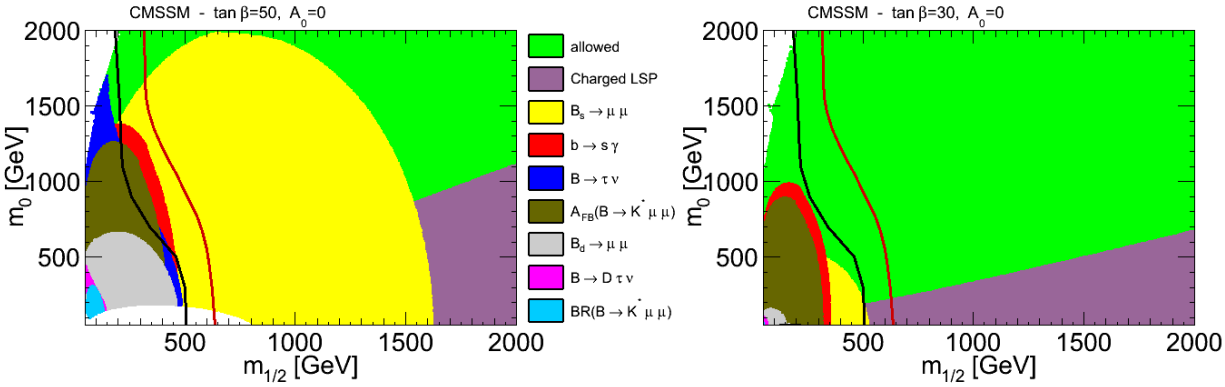

Figure 9: Constraints from flavour observables in CMSSM in the plane $(m_{1/2}, m_0)$ with $A_0 = 0$, for $\tan\beta = 50$ (left) and 30 (right) [19], using `SuperIso` [138, 176]. The black line corresponds to the CMS exclusion limit with 1.1 fb^{-1} of data [177] and the red line to the CMS exclusion limit with 4.4 fb^{-1} of data [178].

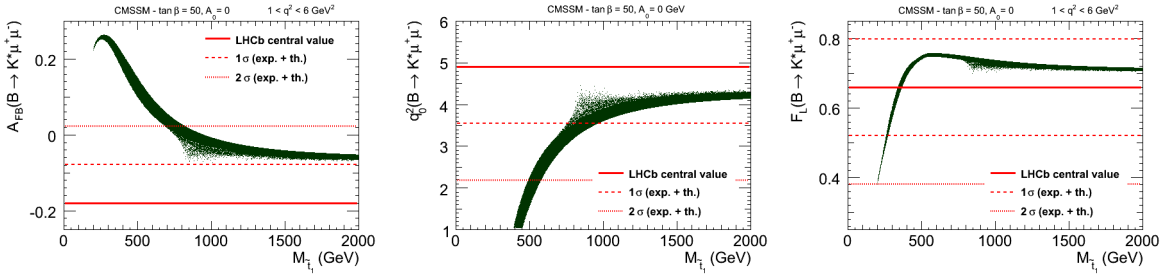

Figure 10: SUSY spread of $A_{\rm FB}(B \to K^*\mu^+\mu^-)$ (left), $q_0^2(B \to K^*\mu^+\mu^-)$ (middle) and $F_L(B \to K^*\mu^+\mu^-)$ (right) as a function of the lightest stop mass, for $A_0 = 0$ and $\tan\beta = 50$, using `SuperIso` [138,176]. The solid red lines correspond to the LHCb central value with 1.0 fb^{-1} [64], while the dashed and dotted lines represent the 1 and 2σ bounds respectively, including both theoretical and experimental errors.

We first consider the constrained MSSM (CMSSM) and non-universal Higgs Masses of type 1 (NUHM1). The CMSSM is characterised by the set of parameters $\{m_0, m_{1/2}, A_0, \tan\beta, \mathrm{sgn}(\mu)\}$ and invokes unification boundary conditions at a very high scale $m_{\rm GUT}$ where the universal mass parameters are specified. NUHM1 relaxes the universality condition for the Higgs bosons which are decoupled from the other scalars, adding then one extra parameter to the CMSSM.

Fig. 9 shows the plane $(m_{1/2}, m_0)$ for large and moderate $\tan\beta$ in the CMSSM where, for comparison, direct search limits from CMS are superimposed. It can be seen that, at large $\tan\beta$, the constraints from flavour observables – in particular $\mathcal{B}(B_s^0 \to \mu^+\mu^-)$– are more constraining than those from direct searches. As soon as one goes down to smaller values of $\tan\beta$, the flavour observables start to lose importance compared to direct searches. On the other hand, $B \to K^*\mu^+\mu^-$ related observables, in particular

the forward backward asymmetry, lose less sensitivity and could play a complementary role. To better see the effect of $A_{\rm FB}(B \to K^* \mu^+ \mu^-)$, the $A_{\rm FB}$ zero-crossing point q_0^2 and $F_L(B \to K^* \mu^+ \mu^-)$, in Fig. 10 we show their SUSY spread as a function of the lightest stop mass for $\tan\beta = 50$ [19]. As can be seen from the figure, small stop masses are excluded and in particular $m_{\tilde{t}_1} \lesssim 800$ GeV is disfavoured by $A_{\rm FB}$ at the 2σ level.

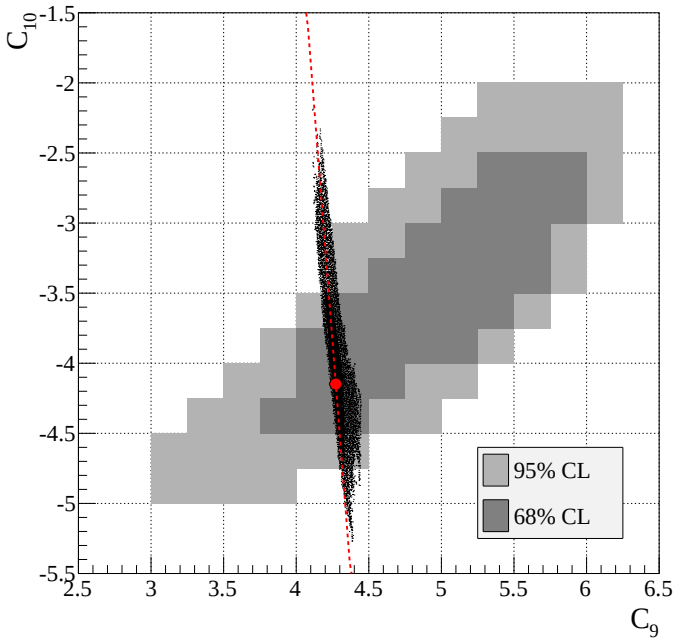

Figure 11: SUSY spread in NMFV-models. The light (dark) grey shaded areas are the 95 % (68 %) confidence limit bounds from $B \to K^{(*)} l^+ l^-$ data [89]. The red dotted line denotes the Z-penguin correlation $C_{10}^{Z-\rm p}/C_9^{Z-\rm p} = 1/(4\sin^2\theta_W - 1)$. The SM point $(C_9^{\rm SM}, C_{10}^{\rm SM})$ is marked by the red dot. Figure taken from Ref. [179].

The impact of the recent $B \to K^{(*)} l^+ l^-$ decay data on SUSY models beyond MFV (NMFV) with moderate $\tan\beta$ is shown in Fig. 11. The largest effect stems from left-right mixing between top and charm super-partners. Due to the Z-penguin dominance of the SUSY-flavour contributions the constraints are most effective for the Wilson coefficient C_{10}, see Section 2.2. SUSY effects in C_{10} are reduced from about 50 % to 16 %(28 %) at 68(95) % C.L. by the recent semileptonic rare decay data [179]. The constraints are relevant to flavour models based on radiative flavour violation (see, *e.g.*, [181]), and exclude solutions to the flavour problem with flavour generation in the up-sector and sub-TeV spectra. The flavour constraints are stronger for lighter stops, hence there is an immediate interplay with direct searches.

Fig. 12 shows the (M_A , $\tan\beta$) plane from a fit of the NUHM1 parameter space to the current data from SUSY and Higgs searches in ATLAS and CMS, as well as dark matter

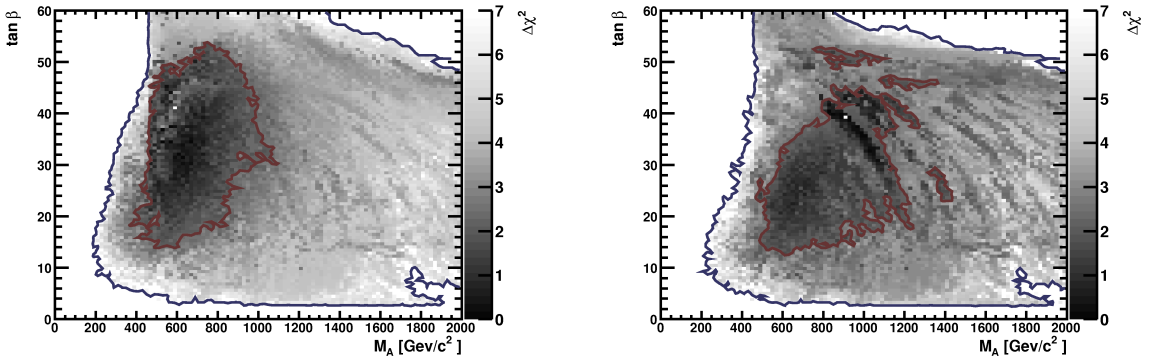

Figure 12: The $(M_A\ ,\tan\beta)$ plane in the NUHM1 with shading displaying the contribution to the global fit, using the 2010 (in the left) and 2011 (in the right) limits of $B_s^0 \to \mu^+\mu^-$. Figures obtained updating the analyses in Refs. [20, 180].

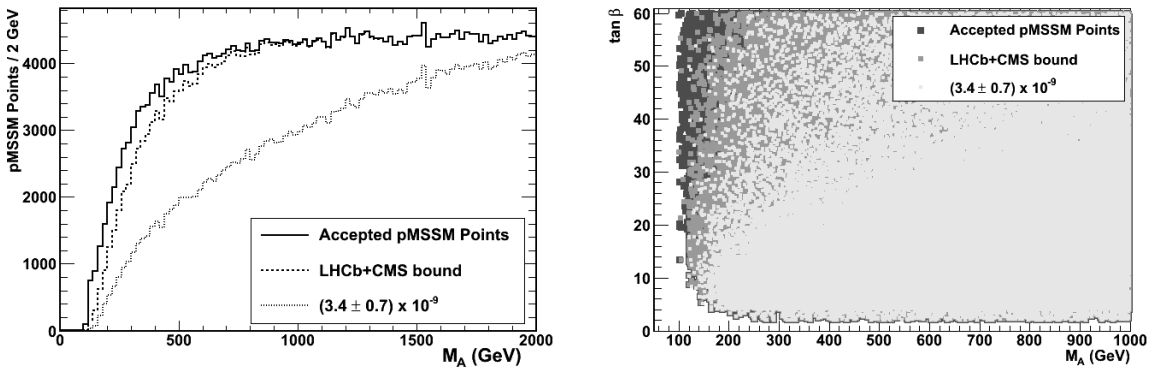

Figure 13: Distribution of pMSSM points after the $B_s \to \mu^+\mu^-$ constraint projected on the M_A (left) and $(M_A, \tan\beta)$ plane (right) for all accepted pMSSM points (medium grey), points not excluded by the combination of the 2010 LHCb and CMS analyses (dark grey) and the projection for the points compatible with the measurement of the SM expected branching fractions with a 20 % total uncertainty (light grey) [183].

relic density [20, 180]. As can be seen, the overall picture changes when adding the latest $B_s^0 \to \mu^+\mu^-$ constraint.

The study in constrained MSSM scenarios is illustrative but not representative of the full MSSM. Also, such scenarios are highly constrained by the current data, while this is not the case in more general scenarios. To go beyond the constrained scenarios, we consider the phenomenological MSSM (pMSSM) [182]. This model is the most general *CP* and R–parity conserving MSSM, assuming MFV at the weak scale and the absence of FCNCs at the tree level. It contains 19 free parameters: 10 sfermion masses, 3 gaugino masses, 3 trilinear couplings and 3 Higgs masses.

The left panel of Fig. 13 shows the density of points as a function of M_A before and after applying the combined 2010 LHCb and CMS $B_s^0 \to \mu^+\mu^-$ limit (1.1×10^{-8} at 95 % C.L.), as well as the projection for a SM–like measurement with an overall 20 % theoretical and experimental uncertainty. As can be seen the density of the allowed pMSSM points is reduced by a factor of 3, in the case of a SM–like measurement. The right panel shows the same distribution in the (M_A, $\tan\beta$) plane. Similar to the CMSSM case, the region with large $\tan\beta$ and small M_A is the most affected one.

The interplay with the Higgs searches can also be very illuminating as any viable model point has to be in agreement with all the direct and indirect limits. As an example, if a Higgs is confirmed at $\sim 125\,\text{GeV}$,[14] the MSSM scenarios in which the excess would correspond to the heaviest *CP*-even Higgs (as opposed to the lightest Higgs) is ruled out by the $B_s^0 \to \mu^+\mu^-$ limit, since they would lead to a too light pseudoscalar Higgs.

It is clear that with more precise measurements a large part of the supersymmetric parameter space could be disfavoured. In particular the large $\tan\beta$ region is strongly affected by $B_s^0 \to \mu^+\mu^-$ as can be seen in Fig. 9. Also, a measurement of $\text{BR}(B_s^0 \to \mu^+\mu^-)$ lower than the SM prediction would rule out a large variety of supersymmetric models. In addition, $B \to K^*\mu^+\mu^-$ observables could play a complementary role especially for smaller $\tan\beta$ values. With reduced theoretical and experimental errors, the exclusion bounds in Fig. 10 and Fig. 11 for example would shrink leading to important consequences for SUSY parameters. The $B \to K^*\mu^+\mu^-$ decay provides many other clean observables, not yet measured, which could also bring substantial additional information.

2.8 Rare charm decays

So far the focus of this chapter has been on rare B decays, but the charm sector also provides excellent probes for new physics in the form of very rare decays. Unlike the B decays described in the previous sections, the smallness of the u, d and s quark masses makes the Glashow-Iliopoulos-Maiani (GIM) cancellation in loop processes very effective. Branching ratios governed by FCNC are hence expected not to exceed $O(10^{-10})$ in the SM. These processes can then receive contributions from New Physics scenarios which can be several orders of magnitude larger than the SM expectation.

2.8.1 Search for $D^0 \to \mu^+\mu^-$

The branching fraction of the $D^0 \to \mu^+\mu^-$ decay is dominated in the SM by the long distance contributions due to the two photon intermediate state, $D^0 \to \gamma\gamma$. The experimental upper limit on the two photon mode can be combined with theoretical predictions to constrain $\mathcal{B}(D^0 \to \mu^+\mu^-)$ in the framework of the SM: $\mathcal{B}(D^0 \to \mu^+\mu^-) < 6 \times 10^{-11}$ at 90 % C.L. [186]. Particular NP models where this decay is enhanced include Supersymmetric models with R-parity violation (RPV), which provides tree-level contributions that would enhance the branching fraction. In such models, the branching fraction would be

[14] At ICHEP 2012 the observation of a new particle consistent with the SM Higgs boson was reported by ATLAS and CMS [184, 185].

related the D^0–$\overline{D}^0$ mixing parameters. Once the experimental constraints on the mixing parameters are taken into account, the corresponding tree-level couplings can still give rise to $\mathcal{B}(D^0 \to \mu^+\mu^-)$ of up to $\mathcal{O}(10^{-9})$ [187].

A search for these rare decays has been performed by the LHCb collaboration [56]. The upper limit obtained with $0.9\,\text{fb}^{-1}$ of data taken in 2011 is:

$$\mathcal{B}(D^0 \to \mu^+\mu^-) \leq 1.3\,(1.1) \times 10^{-8} \text{ at } 95\ (90)\,\%\ \text{C.L.} \tag{23}$$

This upper limit on the branching fraction, already an improvement of an order of magnitude on previous results, is expected to improve down to 5×10^{-9} by the end of the first data-taking phase of the LHCb experiment.

2.8.2 Search for $D^+_{(s)} \to h^+\mu^+\mu^-$ and $D^0 \to hh'\mu^+\mu^-$

The $D^+_{(s)} \to h^+\mu^+\mu^-$ decay rate is also dominated by long distance contributions from tree-level $D^+_{(s)} \to h^+V$ decays, where V is a light, resonant state ($V = \phi, \rho, \omega$). The long-distance contributions have an effective branching fraction (with $V \to \mu^+\mu^-$) above 10^{-6} in the SM. Large deviations in the total decay rate due to New Physics are therefore unlikely. However, the regions of the dimuon mass spectrum far enough from these resonances are interesting probes. Here, the SM contribution stems only from FCNC processes, that should yield no partial branching ratio above 10^{-11} [188]. New physics contributions could enhance the branching fraction away from the resonances by several orders of magnitude: *e.g.* in the RPV model mentioned above, or in models involving a fourth quark generation [188, 189].

The LHCb collaboration can also search for $D^+_{(s)} \to h^\mp\mu^+\mu^\pm$ decays. The long distance contributions can be used to normalise the decays searched for at high and low dimuon mass: their decay rate will be measured relative to that of $D^+_{(s)} \to \pi^+\phi(\mu^+\mu^-)$. These resonant decays have a clean experimental signature and their final state only differs from the signal in the kinematic distributions, which helps to reduce the systematic uncertainties. The sensitivity of the LHCb experiment can be estimated by comparing the yields of $D^+_{(s)} \to \pi^+\phi(\mu^+\mu^-)$ decays observed in LHCb with those obtained by the D0 experiment, which established the best limit on this modes so far [190]. With an integrated luminosity corresponding to $1.0\,\text{fb}^{-1}$, upper limits on the D^+ (D^+_s) modes are expected close to 10^{-8} (10^{-7}) at 90 % CL.

In analogy to the B sector, there are a wealth of observables potentially available in four body rare decays of D mesons. In $D^0 \to hh'\mu^+\mu^-$ (with $h^{(\prime)} = K$ or π), forward-backward asymmetries or asymmetries based on T-odd quantities could reveal new physics effects [188, 191]. Clearly the first challenge is to observe the decays – depending on their branching fractions, this may be possible with the 2011 data set. However, the 50 fb^{-1} collected by the upgraded LHCb detector will be necessary to analyse the full set of observables in these modes.

2.9 Lepton flavour and lepton number violation

The experimental observation of neutrino oscillations was the first evidence of lepton flavour violation (LFV). The consequent addition of mass terms for the neutrinos in the Standard Model already implies LFV also in the charged sector, but with branching fractions smaller than 10^{-40}. New physics (NP) could significantly enhance the rates but, despite steadily improving experimental sensitivity, charged lepton flavour violating (cLFV) decays like $\mu^- \to e^-\gamma$, $\mu^- \to e^+e^-e^-$, $\tau^- \to \ell^-\gamma$ and $\tau^- \to \ell^+\ell^-\ell^-$ (with $\ell^- = e^-, \mu^-$) have not been observed. Numerous beyond the Standard Model theories predict larger LFV effects in τ^- decays than μ^- decays, with branching fractions within experimental reach [192]. An observation of cLFV would thus be a clear sign for NP, while lowering the experimental upper limit will help to further constrain exotic theories.

Another approach to search for NP is via lepton number violation (LNV). Decays with LNV are sensitive to Majorana neutrino masses — their discovery would answer the question of whether neutrinos are Dirac or Majorana particles. The strongest constraints on minimal models including neutrino mass come from neutrinoless double beta decay processes, but searches in heavy flavour decays provide competitive and complementary limits in models with extended neutrino sectors.

In this section, LFV and LNV decays of τ leptons and B mesons with only charged tracks in the final state are discussed.

2.9.1 Lepton flavour violation

The neutrinoless decay $\tau^- \to \mu^+\mu^-\mu^-$ is a particular sensitive mode in which to search for LFV at LHCb as the inclusive τ^- production cross-section at the LHC is large ($\sim 80\,\mu$b, coming mainly from D_s^+ decays[15]) and muon final states provide clean signatures in the detector. This decay is experimentally favoured with respect to the decays $\tau^- \to \mu^-\gamma$ and $\tau^- \to e^+e^-e^-$ due to the considerably better particle identification of the muons and better possibilities for background discrimination. LHCb has performed a search for the decay $\tau^- \to \mu^+\mu^-\mu^-$ using $1.0\,\text{fb}^{-1}$ of data. The upper limit on the branching fraction was found to be $\mathcal{B}(\tau^- \to \mu^+\mu^-\mu^-) < 7.8\ (6.3) \times 10^{-8}$ at 95 % (90 %) C.L, to be compared with the current best experimental upper limit from Belle: $\mathcal{B}(\tau^- \to \mu^+\mu^-\mu^-) < 2.1 \times 10^{-8}$ at 90 % C.L. As the data sample increases this limit is expected to scale as $\sqrt{\mathcal{L}}$, with possible further reduction depending on improvements in the analysis. The large integrated luminosity that will be collected by the upgraded experiment will provide a sensitivity corresponding to an upper limit of a few times 10^{-9}. Searches will also be conducted in modes such as $\tau^- \to p^-\mu^+\mu^-$ or $\tau^- \to \phi\mu^-$, where the existing limits are much weaker, and low background contamination is expected in the data sample.

The pseudoscalar meson decays probe transitions of the type $q \to q'\ell\ell'$ and hence are particularly sensitive to lepton-quark-models and thus provide complementarity to leptonic decay LFV processes [194, 195]. For the LHCb experiment, both decays from

[15] Calculated from the $b\bar{b}$ and $c\bar{c}$ cross-sections measured at the LHCb experiment and the inclusive branching ratios $b \to \tau$ and $c \to \tau$ [193].

D and B mesons are accessible. Sensitivity studies for the decays $B_{s,d} \to e^-\mu^+$ and $D^0 \to e^-\mu^+$ are ongoing. Present estimates indicate that LHCb will be able to match the sensitivity of the existing limits from the B factories and CDF in the near future.

2.9.2 Lepton number violation

In lepton number violating B and D meson decays a search can be made for Majorana neutrinos with a mass of $\mathcal{O}(1\,\text{GeV})$. These indirect searches are performed by analysing the production of same sign charged leptons in D or B decays such as $D_s^+ \to \pi^-\mu^+\mu^+$ or $B^+ \to \pi^-\mu^+\mu^+$ [80, 196]. These same sign dileptonic decays can only occur via exchange of heavy Majorana neutrinos. Resonant production may be possible if the heavy neutrino is kinematically accessible, which could put the rates of these decays within reach of the future LHCb luminosity. Even non-observation of these LNV processes, together with low energy neutrino data, would lead to better constraints for neutrino masses and mixing parameters in models with extended neutrino sectors.

Using $0.4\,\text{fb}^{-1}$ of integrated luminosity from LHCb, limits have been set on the branching fraction of $B^+ \to D^-_{(s)}\mu^+\mu^+$ decays at the level of a few times 10^{-7} and on $B^+ \to \pi^-\mu^+\mu^-$ at the level of 1×10^{-8} [14, 197]. These branching fraction limits imply a limit on, for example, the coupling $|V_{\mu 4}|$ between ν_μ and a Majorana neutrino with a mass in the range $1 < m_N < 4\,\text{GeV}/c^2$ of $|V_{\mu 4}|^2 < 5 \times 10^{-5}$.

2.10 Rare kaon decays

The LHC K^0_S cross-section is such that $\sim 10^{12}$ $K^0_S \to \pi^+\pi^-$ would be reconstructed and selected in LHCb with a fully efficient trigger. This provides a good opportunity to search for rare K^0_S decays in channels with high trigger efficiency, in particular $K^0_S \to \mu^+\mu^-$.

The decay $K^0_S \to \mu^+\mu^-$ is a flavour changing neutral current that has not yet been observed. This decay is strongly suppressed in the Standard Model (SM), with an expected branching fraction of [198, 199]

$$\mathcal{B}(K^0_S \to \mu^+\mu^-) = (5.0 \pm 1.5) \times 10^{-12}\,, \tag{24}$$

while the current experimental upper limit is 3.2×10^{-7} at 90 % C.L. [200]. The study of $K^0_S \to \mu^+\mu^-$ has been suggested as a possible way to look for new light scalars [198], and indeed New Physics (NP) contributions up to one order of magnitude above the SM expectation are perfectly allowed [199]. Enhancements above 10^{-10} are less likely. Bounds on $\mathcal{B}(K^0_S \to \mu^+\mu^-)$ close to 10^{-11} could be useful to discriminate among NP scenarios if other modes, such as $K^+ \to \pi^+\nu\bar{\nu}$, indicated a non-standard enhancement of the $s \to dll$ transition. It is expected that LHCb could easily improve over existing limits, and, with improved triggers on low mass dimuons, reach branching fractions of the order 10^{-11} or below with the luminosity of the upgrade. K^0_L decays into charged tracks can also be reconstructed, but with much less ($\sim 1\,\%$) efficiency compared to a similar decay coming from a K^0_S. This is due to the long distance of flight of the K^0_L state, which tends to decay outside the tracking system.

2.11 Search for NP in other rare decays

Many extensions of the SM predict weakly interacting particles with masses from a few MeV to a few GeV [201] and there is some experimental hints for these particles from astrophysical and collider experiments [202, 203]. For example, the HyperCP collaboration has reported an excess of $\Sigma^+ \to p\mu^+\mu^-$ events with dimuon invariant masses around $214\,\mathrm{MeV}/c^2$. These decays are consistent with the decay $\Sigma^+ \to pX$ with the subsequent decay $X \to \mu^+\mu^-$. Phenomenologically, X can be interpreted as pseudoscalar or axial-vector particle with lifetimes for the pseudoscalar case estimated to be about $10^{-14}\,\mathrm{s}$ [204, 205]. Such a particle can, for example, be interpreted as a pseudoscalar sgoldstino particle [206] or light pseudoscalar Higgs bosons [207].

The LHCb experiment has recorded the worlds largest data sample of B and D mesons which provide a unique opportunity to search for these light particles. For the first time, a search for decays of $B_{s,d} \to \mu^+\mu^-\mu^+\mu^-$ has been performed. No excess has been found and limits of 1.3 and 0.5×10^{-8} at 95 % CL have been set for the B_s^0 and B^0 modes respectively. The analysis can naturally be extended to $D^0 \to \mu^+\mu^-\mu^+\mu^-$ decays, as well as $B_{s,d} \to K^{(*)}(\rho, \phi)\mu^+\mu^-$, where the dimuon mass spectrum can be tested for any resonant structure. Such an analysis has been performed by the Belle collaboration [208]. With the larger data sample and flexible trigger of the LHCb upgrade, it will be possible to exploit several new approaches to search for exotic particles produced in decays of heavy flavoured hadrons (see, *e.g.* [209]).

3 *CP* violation in the *B* system

3.1 Introduction

CP violation, *i.e.* violation of the combined symmetry of charge conjugation and parity, is one of three necessary conditions to generate a baryon asymmetry in the Universe [210]. Understanding the origin and mechanism of *CP* violation is a key question in physics. In the Standard Model, *CP* violation is fully described by the CKM mechanism [2]. While this paradigm has been successful in explaining the current experimental data, it is known to generate insufficient *CP* violation to explain the observed baryon asymmetry of the Universe. Therefore, additional sources of *CP* violation are required. Many extensions of the SM naturally contain new sources of *CP* violation.

The b hadron systems provide excellent laboratories to search for new sources of *CP* violation, since new particles beyond the SM may enter loop-mediated processes such as $b \to q$ FCNC transitions with $q = s$ or d, leading to discrepancies between measurements of *CP* asymmetries and other quantities with their SM expectations. Two types of $b \to q$ FCNC transitions are of special interest: neutral B meson mixing ($\Delta B = 2$) processes, and loop-mediated B decay ($\Delta B = 1$) processes.

The LHCb experiment exploits the large number of b hadrons, including the particularly interesting B_s^0 mesons, produced in proton-proton collisions at the LHC to search for *CP* violating NP effects. Sec. 3.2 provides a review of the status and prospects in the area of searches for NP in $B_{s,d}^0$ mixing, in particular through measurements of the mixing phases $\phi_{s,d}$ and the semileptonic asymmetries $a_{\rm sl}^{s,d}$. The LHCb efforts to search for NP in hadronic $b \to s$ penguin decays, such as $B_s^0 \to \phi\phi$, are discussed in Sec. 3.3. Sec. 3.4 describes the LHCb programme to measure the angle γ of the CKM unitarity triangle in decay processes described only by tree amplitudes, such as $B^\pm \to DK^\pm$, $B^0 \to DK^{*0}$ and $B_s^0 \to D_s^\mp K^\pm$. These measurements allow precise tests of the SM description of quark-mixing via global fits to the parameters of the CKM matrix, as well as direct comparisons with alternative determinations of γ in decay processes involving loop diagrams, such as $B_s^0 \to K^+K^-$. At the end of each section, a brief summary of the most promising measurements with the upgraded LHCb detector and their expected/projected sensitivities is provided.

3.2 B mixing measurements

3.2.1 B_q–$\bar{B}_q$ mixing observables

The effective Hamiltonian of the B_q–$\bar{B}_q$ ($q = d\,, s$) system can be written as

$$\mathbf{H_q} = \begin{pmatrix} M_{11}^q & M_{12}^q \\ M_{12}^{q*} & M_{22}^q \end{pmatrix} - \frac{i}{2} \begin{pmatrix} \Gamma_{11}^q & \Gamma_{12}^q \\ \Gamma_{12}^{q*} & \Gamma_{22}^q \end{pmatrix} . \tag{25}$$

where $M_{11}^q = M_{22}^q$ and $\Gamma_{11}^q = \Gamma_{22}^q$ hold under the assumption of *CPT* invariance. The off-diagonal elements M_{12}^q and Γ_{12}^q are responsible for B_q–$\bar{B}_q$ mixing phenomena. The

"dispersive" part M_{12}^q corresponds to virtual $\Delta B = 2$ transitions dominated by heavy internal particles (top quarks in the SM) while the "absorptive" part Γ_{12}^q arises from on-shell transitions due to decay modes common to B_q and $\bar{B}_q$ mesons. Diagonalising the Hamiltonian matrix leads to the two mass eigenstates $B_{\rm H,L}^q$ (H and L denote heavy and light, respectively), with mass $M_{\rm H,L}^q$ and decay width $\Gamma_{\rm H,L}^q$, being linear combinations of flavour eigenstates with complex coefficients p and q that satisfy $|p|^2 + |q|^2 = 1$[16]

$$|B_{\rm L,H}^q\rangle = p|B_q\rangle \pm q|\bar{B}_q\rangle \,. \tag{26}$$

The magnitudes of M_{12}^q and Γ_{12}^q and their phase difference are physical observables and can be determined from measurements of the following quantities (for more details, see, *e.g.* Ref. [211]):

- the mass difference between the heavy and light mass eigenstates

$$\Delta m_q \equiv M_{\rm H}^q - M_{\rm L}^q \approx 2|M_{12}^q| \left(1 - \frac{|\Gamma_{12}^q|^2}{8|M_{12}^q|^2} \sin^2\phi_{12}^q\right) , \tag{27}$$

  where $\phi_{12}^q = \arg(-M_{12}^q/\Gamma_{12}^q)$ is convention-independent;

- the decay width difference between the light and heavy mass eigenstates

$$\Delta\Gamma_q \equiv \Gamma_{\rm L}^q - \Gamma_{\rm H}^q \approx 2|\Gamma_{12}^q| \cos\phi_{12}^q \left(1 + \frac{|\Gamma_{12}^q|^2}{8|M_{12}^q|^2} \sin^2\phi_{12}^q\right) ; \tag{28}$$

- the flavour-specific asymmetry[17]

$$a_{\rm sl}^q \equiv \frac{|p/q|^2 - |q/p|^2}{|p/q|^2 + |q/p|^2} \approx \frac{|\Gamma_{12}^q|}{|M_{12}^q|} \sin\phi_{12}^q \approx \frac{\Delta\Gamma_q}{\Delta m_q} \tan\phi_{12}^q \,. \tag{29}$$

The correction terms in Eqs. (27) and (28) proportional to $\sin^2\phi_{12}^q$ are tiny. In addition, the ratio of q and p can be written

$$\left(\frac{q}{p}\right) = \frac{\Delta m_q + \frac{i}{2}\Delta\Gamma_q}{2(M_{12}^q - \frac{i}{2}\Gamma_{12}^q)} \,, \tag{30}$$

and hence in both B^0 and B_s^0 systems one obtains, to a good approximation, a convention-dependent expression (for an unobservable quantity) $\arg(q/p) \approx -\arg(M_{12}^q)$. Since B–$\bar{B}$ mixing is dominated by the box diagram with internal top quarks, this leads to an expression in terms of CKM matrix elements $\arg(q/p) = -2\arg(V_{tb}^* V_{tq})$.

[16] Strictly, the coefficients p and q should also have subscripts q to indicate that they can be different for B^0 and B_s^0, but we omit these to simplify the notation.

[17] We use the notation $a_{\rm sl}^q$ to denote flavour-specific asymmetries, reflecting the fact that the measurements of these quantities use semileptonic decays.

Further information can be obtained by measuring the phase difference between the amplitude for a direct decay to a final state f and the amplitude for decay after oscillation. In the case that the decay is dominated by $b \to c\bar{c}s$ tree amplitudes we denote this phase as

$$\phi_q \equiv -\arg\left(\frac{q}{p}\frac{\bar{A}_f}{A_f}\right) , \tag{31}$$

where A_f and $\bar{A}_f$ are the decay amplitudes of $B \to f$ and $\bar{B} \to f$, respectively. In the absence of direct *CP* violation, and for a *CP* eigenstate f with eigenvalue η_f, $\bar{A}_f/A_f = \eta_f$. With these approximations, the *CP* violating phases in B mixing give the unitarity triangle angles, $\phi_d \approx 2\beta$ and $\phi_s \approx -2\beta_s$,[18] where the angles are defined as [63]

$$\beta \equiv \arg\left(-\frac{V_{cd}V_{cb}^*}{V_{td}V_{tb}^*}\right) , \quad \beta_s \equiv \arg\left(-\frac{V_{ts}V_{tb}^*}{V_{cb}V_{cs}^*}\right) . \tag{32}$$

Clearly, if there is NP in M_{12}^q or in the decay amplitudes, the measured value of ϕ_q can differ from the true values of $\beta_{(s)}$. Similarly, NP in either M_{12}^q or Γ_{12}^q can make the observed value of $a_{\rm sl}^q$ differ from its SM predictcion. Note, however, that even within the SM, there is a difference between ϕ_q and ϕ_{12}^q [212].

The ϕ_s notation that has been used in the LHCb measurements to date of the *CP*-violating phase in B_s^0 mixing, using $J/\psi\,\phi$ [6, 30] and $J/\psi\,f_0(980)$ [32, 213] final states. By using the same notation for different decays, we are making an assumption that $\arg(\bar{A}_f/A_f)$ is common for different final states, which corresponds to an assumption that the penguin contribution to these decays is negligible. Although this is reasonable with the current precision, as the measurements improve it will be necessary to remove such assumptions – therefore for measurements in the upgrade era we denote the observables in $b \to c\bar{c}s$ transitions by $2\beta_s = -\phi_s$, while in $b \to q\bar{q}s$ ($q = u, d, s$) transitions we use $2\beta_s^{\rm eff}$. This parallels the established notation used in the B^0 system.

In the SM, these observables can be predicted using CKM parameters from a global fit to other observables and hadronic parameters (decay constants and bag parameters) from lattice QCD calculation. These predictions can be compared to their direct measurements to test the SM and search for new physics in neutral B mixing.

3.2.2 Current experimental status and short term outlook

The current measurements and SM predictions for the mixing observables are summarised in Table 2.

The HFAG average of the B_s^0 mass difference Δm_s in Table 2 is based on measurements performed at CDF [218] and LHCb [216, 219]. It is dominated by the most recent LHCb result obtained using 0.34 fb^{-1} of data [216], which is also given in Table 2. These are all consistent with the SM prediction. Improving the precision of the SM prediction is desirable to further constrain NP in M_{12}^s, and requires improving the accuracy of lattice

[18] Note the conventional sign-flip between β and β_s ensures that both are positive in the SM.

Table 2: Status of B mixing measurements and corresponding SM predictions. New results presented at ICHEP 2012 are not included. The inclusive same-sign dimuon asymmetry $A^b_{\rm SL}$ is defined below and in Ref. [36].

Observable	Measurement	Source	SM prediction	References
B^0_s system				
Δm_s ($\rm ps^{-1}$)	17.719 ± 0.043 $17.725 \pm 0.041 \pm 0.026$	HFAG 2012 [63] LHCb (0.34 $\rm fb^{-1}$) [216]	17.3 ± 2.6	[33, 214, 215]
$\Delta\Gamma_s$ ($\rm ps^{-1}$)	0.105 ± 0.015 $0.116 \pm 0.018 \pm 0.006$	HFAG 2012 [63] LHCb (1.0 $\rm fb^{-1}$) [30]	0.087 ± 0.021	[33, 214, 215]
ϕ_s (rad)	$-0.044^{+0.090}_{-0.085}$ $-0.002 \pm 0.083 \pm 0.027$	HFAG 2012 [63] LHCb (1.0 $\rm fb^{-1}$) [30]	-0.036 ± 0.002	[33, 34, 215]
$a^s_{\rm sl}$ (10^{-4})	$-17 \pm 91^{+14}_{-15}$ -105 ± 64	D0 (no $A^b_{\rm SL}$) [217] HFAG 2012 (including $A^b_{\rm SL}$) [63]	$0.29^{+0.09}_{-0.08}$	[33, 34, 215]
Admixture of B^0 and B^0_s systems				
$A^b_{\rm SL}$ (10^{-4})	$-78.7 \pm 17.1 \pm 9.3$	D0 [36]	-2.0 ± 0.3	[33, 214, 215]
B^0 system				
Δm_d ($\rm ps^{-1}$)	0.507 ± 0.004	HFAG 2012 [63]	0.543 ± 0.091	[33, 211, 215]
$\Delta\Gamma_d/\Gamma_d$	0.015 ± 0.018	HFAG 2012 [63]	0.0042 ± 0.0008	[33, 214, 215]
$\sin\phi_d$	0.679 ± 0.020	HFAG 2012 [63]	$0.832^{+0.013}_{-0.033}$	[33, 34, 215]
$a^d_{\rm sl}$ (10^{-4})	-5 ± 56	HFAG 2012 [63]	$-6.5^{+1.9}_{-1.7}$	[33, 34, 215]

QCD evaluations of the decay constant and bag parameter (see Ref. [211] and references therein).

The observables ϕ_s and $\Delta\Gamma_s$ have been determined simultaneously from $B^0_s \to J/\psi\,\phi$ decays using time-dependent flavour tagged angular analyses [220, 221]. The first LHCb tagged analysis using 0.34 $\rm fb^{-1}$ of data [6] already provided a significant constraint on ϕ_s and led to the first direct evidence for a non-zero value of $\Delta\Gamma_s$. LHCb has also published a paper which determined the sign of $\Delta\Gamma_s$ to be positive at 4.7σ confidence level [31] by exploiting the interference between the K^+K^- S-wave and P-wave amplitudes in the $\phi(1020)$ mass region [222]. This resolved the two-fold ambiguity in the value of ϕ_s for the first time. Recently, LHCb updated the $B^0_s \to J/\psi\,\phi$ analysis using the full data sample of 1.0 $\rm fb^{-1}$ collected before 2012 [30]. The results from this analysis,

$$\phi_s = -0.001 \pm 0.101 \pm 0.027\,\text{rad}\,, \qquad \Delta\Gamma_s = 0.116 \pm 0.018 \pm 0.006\,\text{ps}^{-1}\,, \tag{33}$$

are shown in Fig. 14 (left), and are in good agreement with the SM expectations.

LHCb has also studied $B^0_s \to J/\psi\,\pi^+\pi^-$. This decay process is expected to proceed dominantly via $b \to c\bar{c}s$ (the $s\bar{s}$ produced in the decay rescatters to $\pi^+\pi^-$ through either a resonance such as $f_0(980)$ or a nonresonant process). Therefore, these events can be used to measure ϕ_s. The $\pi^+\pi^-$ mass range 775–1550 MeV shown in Fig. 15 (left) is used for the measurement. In contrast to $B^0_s \to J/\psi\,\phi$, no angular analysis is needed to disentangle the *CP* eigenstates, since the final state is determined to be dominantly *CP*-odd in this mass range [223]. On the other hand, $\Delta\Gamma_s$ cannot be determined in this decay channel alone.[19] Using as input the value of $\Delta\Gamma_s$ obtained from $B^0_s \to J/\psi\,\phi$, the measurement

[19] The effective lifetime of $B^0_s \to J/\psi\,f_0(980)$ is sensitive to $\Delta\Gamma_s$ and *CP* violation parameters [224]

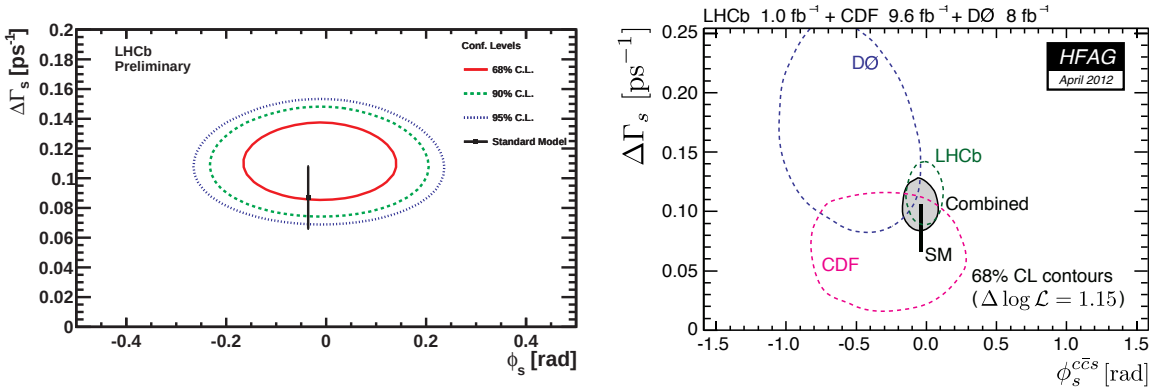

Figure 14: (Left) LHCb measurement of ϕ_s and $\Delta\Gamma_s$ from $B_s^0 \to J/\psi\,\phi$ decays using 1.0 fb^{-1} [30]. (Right) HFAG 2012 combination of ϕ_s and $\Delta\Gamma_s$ results, where the 1 σ confidence region is shown for each experiment and the combined result [63]. Note the different scales.

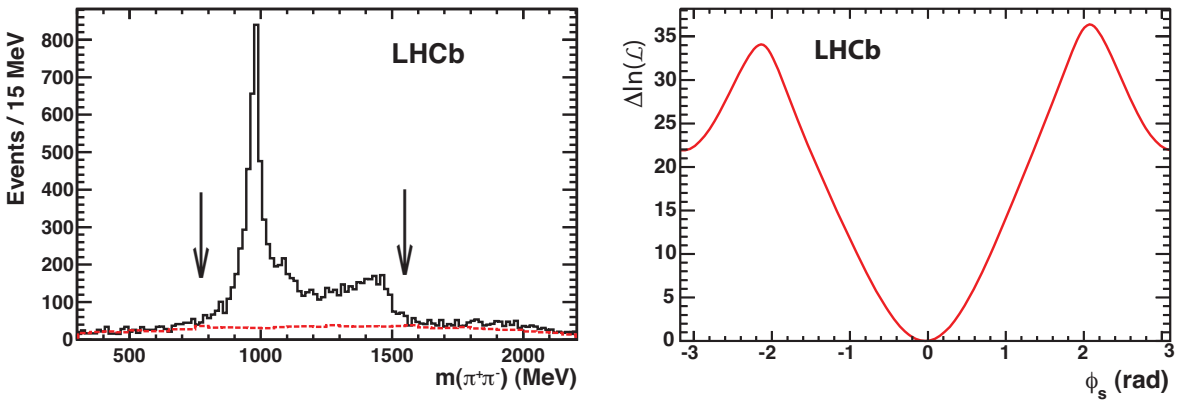

Figure 15: (Left) $\pi^+\pi^-$ mass distribution of selected $B_s^0 \to J/\psi\,\pi^+\pi^-$ candidates and range used for the ϕ_s measurement. (Right) log-likelihood difference as a function ϕ_s [32].

from the analysis of $B_s^0 \to J/\psi\,\pi^+\pi^-$ with 1.0 fb^{-1} is [32]

$$\phi_s = -0.019\,^{+0.173\ +0.004}_{-0.174\ -0.003}\,\text{rad}\,. \tag{34}$$

Fig. 15 (right) shows the log-likelihood scan for the ϕ_s parameter for the $B_s^0 \to J/\psi\,\pi^+\pi^-$ analysis. The latest HFAG average in Table 2 combines the LHCb results with the $B_s^0 \to J/\psi\,\phi$ analysis results from CDF using 9.6 fb^{-1} [226] and D0 using 8.0 fb^{-1} [227]. The LHCb result dominates the combination, which is in good agreement with the SM predictions, as seen in Fig. 14 (right).

The LHCb $B_s^0 \to J/\psi\,\phi$ and $B_s^0 \to J/\psi\,\pi^+\pi^-$ analyses discussed above only used opposite side flavour tagging [228, 229]. Future updates of these analyses will gain in sensitivity by also using the same side kaon tagging information, which so far has been

and has recently been measured by LHCb [225].

used in the determination of Δm_s [216]. Currently, the systematic uncertainty on ϕ_s is dominated by imperfect knowledge of the background, angular acceptance effects and by neglecting potential contributions of direct *CP* violation. All of these uncertainties are expected to be reduced with more detailed understanding and some improvements in the analysis. Therefore we expect that the determination of ϕ_s will remain statistics limited, even with the data samples available after the upgrade of the LHCb detector. In addition to $B_s^0 \to J/\psi\,\phi$ and $B_s^0 \to J/\psi\,\pi^+\pi^-$, other $b \to c\bar{c}s$ decay modes of B_s^0 mesons, such as $J/\psi\eta$, $J/\psi\eta'$ [230] and $D_s^+ D_s^-$ [231] will also be investigated. The latter has recently been measured at LHCb [232].

The SM prediction $\phi_s = -0.036 \pm 0.002$ rad could receive a small correction from doubly CKM-suppressed penguin contributions in the decay. The value of this correction is not precisely known, and may depend on the decay mode. Moreover, NP in the $b \to c\bar{c}s$ decay may also affect the results. Although such effects are already constrained by results from B^+ and B^0 decays, NP in the decay amplitudes can lead to polarisation-dependent mixing-induced *CP* asymmetries and triple product asymmetries in $B_s^0 \to J/\psi\,\phi$ [66]. Such effects will be searched for in future analyses.

The flavour-specific asymmetries provide important complementary constraints on $\Delta B = 2$ processes. D0 has performed a direct measurement of $a^s_{\rm sl}$ in semileptonic B_s^0 decays [217], which is very weakly constraining due to its limited precision.[20] However, a measurement of the inclusive same-sign dimuon asymmetry provides better precision, and shows evidence of a large deviation from its SM prediction [36]. The inclusive measurement is sensitive to a linear combination of the flavour-specific asymmetries, $A^b_{\rm SL} = C_d\, a^d_{\rm sl} + C_s\, a^s_{\rm sl}$, where C_q depend on the production fractions and mixing probabilities, and are determined to be $C_d = 0.594 \pm 0.022$, $C_s = 0.406 \pm 0.022$ [36]. As discussed in Sec. 3.2.3, this is in tension with other $\Delta B = 2$ observables. Improved measurements of $a^s_{\rm sl}$ and $a^d_{\rm sl}$ from LHCb are needed to solve this puzzle.

In LHCb, $a^s_{\rm sl}$ can be determined from the asymmetry between the time-integrated untagged decay rates of B_s^0 decays to $D_s^+\mu^- X$ and $D_s^-\mu^+ X$, with $D_s^\pm \to \phi\pi^\pm$ (or with the full $K^+K^-\pi^\pm$ Dalitz plot). Detector- and trigger-induced asymmetries can be calibrated in control channels, and the fact that data is taken with both magnet dipole polarities can be used as a handle to reduce systematic uncertainties. The effect of B_s^0 production asymmetry is cancelled due to the fast oscillation, and the resulting asymmetry is trivially related to $a^s_{\rm sl}$. The first LHCb result on $a^s_{\rm sl}$ has been reported at ICHEP 2012, and is the most precise measurement of this quantity to date [7],

$$a^s_{\rm sl} = (-0.24 \pm 0.54 \pm 0.33)\ \%\,. \tag{35}$$

It will also also possible to measure $a^d_{\rm sl}$ using $D^+\mu^- X$ final states with $D^+ \to K^-\pi^+\pi^+$. In this case extra care must be taken to calibrate the difference between K^+ and K^- detection efficiencies and an independent measurement of the B^0 production asymmetry is needed as input.

In the B^0 system, Δm_d and $\sin\phi_d$ have been measured precisely by the B factories [63]. The measurements of $\Delta\Gamma_d$ and $a^d_{\rm sl}$ are consistent with their SM predictions, but their

[20] An updated measurement has been presented by D0 at ICHEP 2012 [233].

uncertainties are at least an order larger than those of the predictions. Hence a large improvement in precision is needed to test the SM using these observables. In the B^0 sector there has been for some time a tension between the measurements of $\sin\phi_d$ [63] and the branching ratio $\mathcal{B}(B^+ \to \tau^+\nu)$ [234, 235], as shown in Fig. 16,[21] and discussed in Sec. 3.2.4. This motivates improved measurements of $\sin\phi_d$ and improved understanding of the possible effects of penguin contributions to this observable.

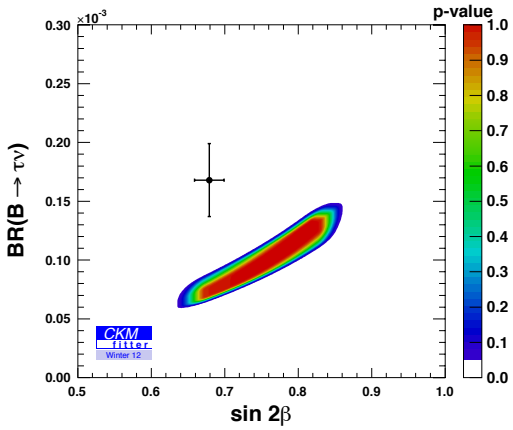

Figure 16: Comparison of direct and indirect determinations of $\sin\phi_d \equiv \sin 2\beta$ *vs.* $\mathcal{B}(B^+ \to \tau^+\nu)$, from Ref. [40].

LHCb has already presented first results on Δm_d [219] and $\sin\phi_d$ [237]. The precision of these observables will be competitive with the B factory results using the data sample that will be collected by the end of 2012. LHCb can also search for enhancements in the value of $\Delta\Gamma_d$ above the tiny value expected in the SM, *e.g.* by comparing the effective lifetimes of $B^0 \to J/\psi K^0_S$ and $B^0 \to J/\psi K^{*0}$ [238]. Significantly improving the precisions of the B^0 mixing observables is an important goal of the LHCb upgrade, as will be discussed in Sec. 3.2.6.

The SM predictions of b-hadron lifetimes and $\Delta\Gamma_q$ are all obtained within the framework of heavy quark expansion. LHCb is actively working on measurements of b-hadron lifetimes and lifetime ratios, which will be used to test these predictions. The knowledge obtained from this work will allow to improve the SM predictions of $\Delta\Gamma_q$ for the purpose of searching for NP. Furthermore, a more precise measurement of the ratio of B^0_s to B^0 lifetimes could either support or strongly constrain the existence of new physics in Γ^s_{12} [38, 39, 171, 211, 214].

[21] An updated measurement of $\mathcal{B}(B^+ \to \tau^+\nu)$ using the hadronic tag method was presented by Belle at ICHEP 2012 [236]: this new result reduces, but does not completely remove, the tension in the fits. The analyses discussed here do not include this new result.

3.2.3 Model independent constraints on new physics in B mixing

Neutral B_q meson mixing is described in terms of the three parameters $|M_{12}^q|$, $|\Gamma_{12}^q|$ and $\phi_q = \arg(-M_{12}^q/\Gamma_{12}^q)$ for each of the two systems $q = d, s$. In the context of model independent analyses, the NP contributions can be parametrised in the form of two complex quantities Δ_q and Λ_q [38, 239]

$$M_{12}^q = M_{12}^{q,\mathrm{SM}}\,|\Delta_q|\,e^{i\phi_q^\Delta}\,, \qquad\qquad \Gamma_{12}^q = \Gamma_{12}^{q,\mathrm{SM}}\,|\Lambda_q|\,e^{i\phi_q^\Lambda}\,, \tag{36}$$

i.e., 4 real degrees of freedom. The observables which depend on these parameters are the mass and decay width differences and flavour-specific *CP*-asymmetries. They can be expressed in terms of the SM predictions and NP parameters as

$$\Delta m_q = (\Delta m_q)_{\mathrm{SM}}\,|\Delta_q|\,, \qquad \Delta\Gamma_q = (\Delta\Gamma_q)_{\mathrm{SM}}\,|\Lambda_q|\,\frac{\cos\left(\phi_{12}^{q,\mathrm{SM}} + \phi_q^\Delta - \phi_q^\Lambda\right)}{\cos\phi_{12}^{q,\mathrm{SM}}}, \tag{37}$$

$$a_{\mathrm{sl}}^q = (a_{\mathrm{sl}}^q)_{\mathrm{SM}}\,\frac{|\Lambda_q|}{|\Delta_q|}\,\frac{\sin\left(\phi_{12}^{q,\mathrm{SM}} + \phi_q^\Delta - \phi_q^\Lambda\right)}{\sin\phi_{12}^{q,\mathrm{SM}}}\,, \tag{38}$$

up to corrections suppressed by tiny $(\Gamma_{12}^q/M_{12}^q)^2$. Note that the expressions of Eqs. (37) and (38) depend only on the difference $(\phi_q^\Delta - \phi_q^\Lambda)$. The SM predictions of Δm_q, $\Delta\Gamma_q$ and a_{sl}^q can be found in Table 2 and for ϕ_{12}^q [214]

$$\phi_{12}^{d,\mathrm{SM}} = (-0.075 \pm 0.024)\,\mathrm{rad}\,, \qquad\qquad \phi_{12}^{s,\mathrm{SM}} = (0.0038 \pm 0.0010)\,\mathrm{rad}. \tag{39}$$

The values of Δm_q have been precisely measured, giving rather strong constraints on $|\Delta_q|$ which are limited by the knowledge of hadronic matrix elements. The new $\Delta\Gamma_s$ measurement of LHCb starts to provide useful constraints. As discussed above, the *CP*-asymmetries a_{sl}^q are currently rather weakly constrained.

Further information can be extracted from the mixing-induced *CP*-asymmetries in $B^0 \to J/\psi\,K_{\mathrm{S}}^0$ and $B_s^0 \to J/\psi\,\phi$ decays

$$\phi_d = 2\beta + \phi_d^\Delta - \delta_d, \qquad\qquad \phi_s = -2\beta_s + \phi_s^\Delta - \delta_s, \tag{40}$$

where δ_d and δ_s denote shifts of ϕ_d and ϕ_s induced by either SM penguin diagrams or NP contributions in the decay process. In the SM ϕ_d and ϕ_s are related to the angles β and β_s of the according unitarity triangles. When short-distance NP contributions are introduced, ϕ_q depends on the phase ϕ_q^Δ of M_{12}^q, whereas the phase ϕ_q^Λ of Γ_{12}^q does not enter. The phase δ_q can be split schematically into different sources: SM penguin pollution and contribution due to NP in the decay. The SM penguin pollution is expected to be negligible for the current precision of ϕ_q, and is discussed in detail in Sec. 3.2.5. Beyond the SM, NP can contribute in principle to both the tree $b \to c\bar{c}s$ decay and the penguin process. However, in the model-independent analysis described here, NP contributions

in the $b \to c\bar{c}s$ decay are neglected and any observed deviation from the SM will be interpreted as effects of NP in neutral B meson mixing. When δ_q is neglected, Eqs. (37), (38) and (40) allow to determine the NP parameters $|\Delta_q|$, ϕ_q^Δ, $|\Lambda_q|$ and ϕ_q^Λ.

The assumption of NP in M_{12}^q only, or equivalently in $\Delta B = 2$ processes only, implies that there is no NP in $\Delta B = 1$ processes which contribute to the absorptive part Γ_{12}^q. Consequently, NP can only decrease $\Delta\Gamma_q$ (since $\cos(\phi_{12}^{q,\mathrm{SM}})$ is maximal, see Eq. (37)) with respect to the SM [221, 240]. This scenario has been studied in extensions of the CKM fit of the SM which includes $\Delta B = 2$ measurements to constrain the CKM elements V_{tq} [39, 241], in combination with many other flavour-changing processes. Including the latest LHCb measurements[22] [30, 219] the SM point $\Delta_d = \Delta_s = 1$ is disfavoured by $2.4\,\sigma$ [39] (prior to the LHCb results being available, a similar analysis gave a discrepancy of $3.6\,\sigma$ driven mainly by the anomalous dimuon asymmetry [241]). The analysis gives Δ_s consistent with the SM, within large uncertainties, whereas the more precise data in the B^0 system hint at a deviation in Δ_d (see Fig. 17). Moreover, NP effects up to 30–40 % are still allowed in both systems at the $3\,\sigma$ level. It should be noted, that the large deviations in the B^0 sector are not only due to A_{SL}^b, but also due to the tension between $\sin\phi_d$ and $\mathcal{B}(B^+ \to \tau^+\nu)$.

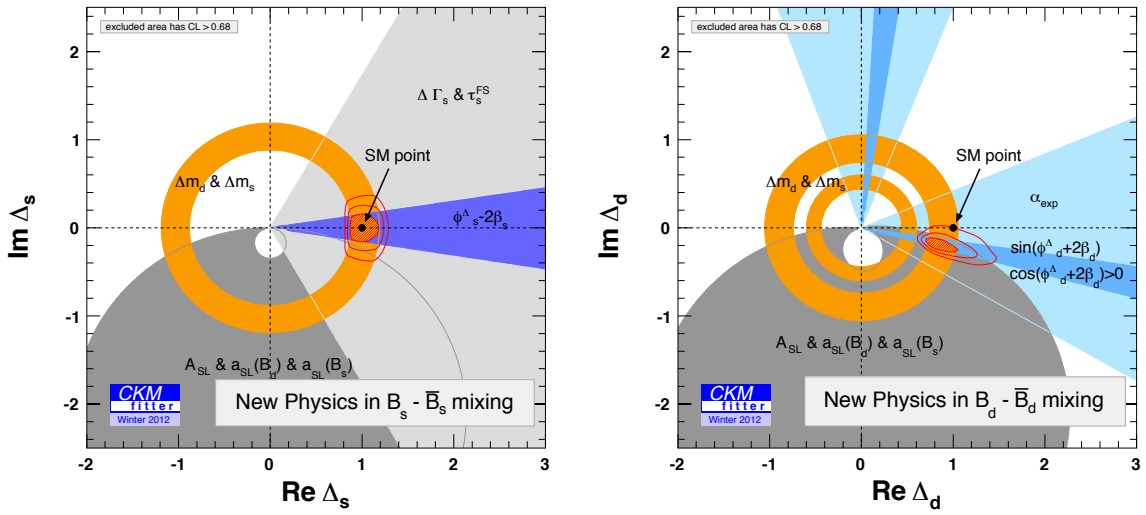

Figure 17: Model-independent fit [39] in the scenario that NP affects M_{12}^q separately. The coloured areas represent regions with CL $< 68.3\,\%$ for the individual constraints. The red area shows the region with CL $< 68.3\,\%$ for the combined fit, with the two additional contours delimiting the regions with CL $< 95.45\,\%$ and CL $< 99.73\,\%$.

NP contributions to the absorptive part Γ_{12}^q of B mixing can enter through $\Delta B = 1$ decays $b \to qX$ with light degrees of freedom X of total mass below m_B. In some particular

[22] But not including new results shown at ICHEP 2012.

models such contributions can arise [172,242] and interfere constructively or destructively with the SM contribution. The recent measurements of $\Delta\Gamma_q$ and of $A_{\rm SL}^b$ revived interest in this possibility. Model-independent analyses have confirmed that the $A_{\rm SL}^b$ measurement cannot be accommodated within the SM [243,244]. A model-independent fit assuming NP in both M_{12}^q and Γ_{12}^q has been considered in the framework of an extended CKM fit [39]. In this case, the experimental data can be accommodated, and the B_s^0 system remains rather SM-like, but large NP contributions in the B^0 system are required.

Model-independent analyses based on Eq. (36) are restricted to a particular set of observables, mainly those with $\Delta B = 2$, since correlations with $\Delta B = 1$ measurements are difficult to quantify. Either additional assumptions on the nature of X in $b \to qX$ or explicit NP models will allow to exploit better the wealth of future experimental information. In fact, such analyses have found it difficult to accommodate the hypothesis of large NP in Γ_{12}^q with current $\Delta B = 1$ measurements, therefore NP in Γ_{12}^q seems unlikely to provide a full explanation of the measured value of $A_{\rm SL}^b$. In the case of $X = f\bar{f}$, the $\Delta B = 1$ operators $b \to (d,s) f\bar{f}$ ($f = q$ or ℓ) are strongly constrained [171], with the exception of $b \to sc\bar{c}$ and $b \to s\tau^+\tau^-$. Currently, only a weak upper bound on $\mathcal{B}(B^+ \to K^+\tau^+\tau^-) \lesssim 3.3 \cdot 10^{-3}$ at 90 % CL [245] exists whereas other decays $B_s^0 \to \tau^+\tau^-$, $B \to X_s\tau^+\tau^-$ might be indirectly constrained with additional assumptions (see also the discussion in Sec. 2.5.2). As an example, the improved LHCb measurement of $\tau_{B_s^0}/\tau_{B^0}$ allowed to derive a stronger bound on $\mathcal{B}(B_s^0 \to \tau^+\tau^-)$. Still, a model-independent analysis of the complete set of $b \to s\tau^+\tau^-$ operators does not allow for deviations larger than 35 % from the SM in Γ_{12}^s [38], which is by far not sufficient to resolve the tension with $A_{\rm SL}^b$. For $b \to d\tau^+\tau^-$ operators there exists a stronger constraint $\mathcal{B}(B^0 \to \tau^+\tau^-) \lesssim 4 \cdot 10^{-3}$ and even smaller NP effects are expected in Γ_{12}^d. Other proposed solutions such as the existence of new light spin-0 [246] or spin-1 [247] X states could be seriously challenged by improved measurements of quantities, such as ratios of lifetimes, which are theoretically under good control [214].

In summary, NP contributions to $|\Delta_q|$ are currently already quite constrained due to Δm_q measurements and theoretical progress is required in order to advance. Although the phases ϕ_q^Δ are constrained by the recent LHCb measurement of ϕ_s, and B factory measurements of ϕ_d, there is a mild hint of NP in model-independent fits of $\Delta B = 2$ measurements [38,39,243,244], especially when allowing for NP in Γ_{12}^q. On the other hand, NP effects in Γ_{12}^q are expected to be limited when constraints from $\Delta B = 1$ observables are taken into account. Independent improved measurements of $a_{\rm sl}^q$ are needed in order to resolve the nature of the current discrepancies between the $\Delta B = 2$ observables with their SM expectations and other observables entering global CKM fits. Further, improved measurements of Γ_q and $\Delta\Gamma_q$, as well as of control channels are needed to constrain NP in Γ_{12}^q.

3.2.4 CKM unitarity fits in SM and Beyond

In this section, we present the results of the Unitarity Triangle Analysis (UTA) performed by two groups: UTfit [41] and CKMfitter [40].[23] The main aim of the UTA is the determination of the values of the Cabibbo-Kobayashi-Maskawa matrix (CKM) parameters, by comparing experimental measurements and theoretical predictions for several observables. The popular Wolfenstein parametrisation allows for a transparent expansion of the CKM matrix in terms of the sine of the small Cabibbo angle, λ, with the other three parameters being A, $\bar{\rho}$ and $\bar{\eta}$. Assuming the validity of the Standard Model (SM), one can perform a fit to the available measurements. LHCb results already make important contributions to the constraints on γ and Δm_s. With more statistics, LHCb results are expected to also impact on other CKM fit inputs, including α and $\sin(2\beta)$. It is important to note the crucial role of lattice QCD calculations as input to the CKM fits. For example, the parameters $f_{B_s}\sqrt{B_{B_s}}$ and ξ enter the constraints on Δm_s and $\Delta m_d/\Delta m_s$. At the end of 2011, the precision of the calculations was at the level of 5.4 % and 2.6 %, respectively [141]. The necessary further progress to obtain the full benefit of the LHCb measurements appears to be in hand exploiting algorithmic advances as well as ever increasing computing power for the lattice calculations.

The overall quality of the fit can be judged using the projection of the likelihoods on the $\{\bar{\rho}, \bar{\eta}\}$ plane. This projection is shown in Fig. 18. The fit can also be made removing one of the inputs, giving a prediction for the removed parameter, which then can be compared to the experimental value. The results of this study are presented in Table 3. Both groups find a tension between $\mathcal{B}(B \to \tau\nu)$ and $\sin(2\beta)$, as can be seen in Fig. 16. (As discussed in Sec. 3.2.2 this tension will be reduced once the latest Belle result on $\mathcal{B}(B^+ \to \tau^+\nu_\tau)$ [236] is included in the fits.) Improved measurements of $\sin(2\beta)$ can shed further light on this problem.

In order to estimate the origin of the tensions, the UTfit and CKMfitter groups have performed analyses including model-independent NP contributions to $\Delta F = 2$ processes (see Refs. [39, 249] for details). The NP effects are introduced through the real valued C and ϕ parameters in case of UTfit and the complex valued Δ parameter for CKMfitter. The parameters are added separately for the B_s^0 and B^0 sectors. In the absence of NP, the expected values are $C = 1$, $\phi = 0°$, and $\Delta = 1 + i \cdot 0$. For the B^0 sector the fits return $C = 0.94 \pm 0.14$ and $\phi = (-3.6 \pm 3.7)°$, and $\Delta = (0.823\,^{+0.143}_{-0.095}) + i(-0.199\,^{+0.062}_{-0.048})$. The results for both groups show some disagreement with the SM, driven by tensions in the input parameters mentioned above. In the B_s^0 sector, on the other hand, the situation is much closer to the SM than before the LHCb measurements were available: $C = 1.02 \pm 0.10$ and $\phi = (-1.1 \pm 2.2)°$, and $\Delta = (0.925\,^{+0.133}_{-0.078}) + i(-0.00 \pm 0.10)$.

The results of the studies by both groups point to the absence of big NP effects in $\Delta B = 2$ processes. Nevertheless there is still significant room for NP in mixing in both B^0 and B_s^0 systems. More precise results, in particular from LHCb, can enable more careful studies. Besides providing null tests of the SM hypothesis, improved ϕ_s and $a^s_{\rm sl}$ measurements are crucial to quantity effects of NP in mixing. In addition a precise γ

[23] A similar approach has been developed in Ref. [42].

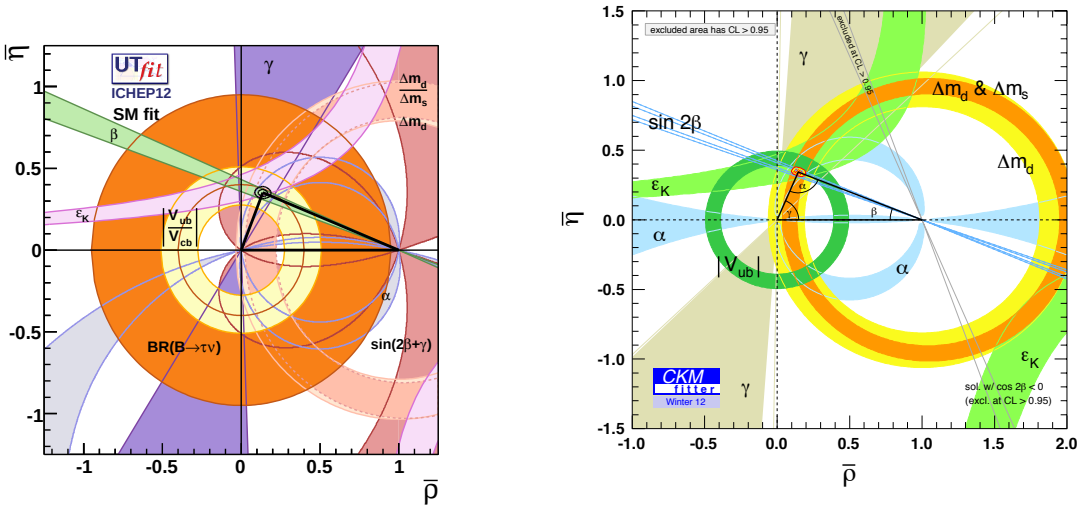

Figure 18: Result of the UT fit within the SM: $\{\bar{\rho}, \bar{\eta}\}$ plane obtained by UTfit (left) and CKMfitter (right). The 95 % probability regions selected by the single constraints are also shown with various colours for the different constraints.

Table 3: Predictions for some parameters of the SM fit and their measurements as combined by the UTfit and CKMfitter groups. The lines marked with (*) are not used in the full fit. Details of the pull calculation can be found in Refs. [241, 248]. New results presented at ICHEP2012 are not included in these analyses.

Parameter	UTfit			CKMfitter		
	prediction	measurement	pull	prediction	measurement	pull
$\alpha\,(^\circ)$	87.5 ± 3.8	91.4 ± 6.1	$+0.5\sigma$	$95.9^{+2.2}_{-5.6}$	$88.7^{+2.2}_{-5.9}$	-1.0σ
$\sin(2\beta)$	0.809 ± 0.046	0.667 ± 0.024	-2.7σ	$0.820^{+0.024}_{-0.028}$	0.679 ± 0.020	-2.6σ
$\gamma\,(^\circ)$	67.8 ± 3.2	75.5 ± 10.5	$+0.7\sigma$	$67.2^{+4.4}_{-4.6}$	66^{+12}_{-12}	-0.1σ
$V_{ub}\,(10^{-3})$	3.62 ± 0.14	3.82 ± 0.56	$+0.3\sigma$	$3.55^{+0.15}_{-0.14}$	$3.92 \pm 0.09 \pm 0.45$	0.0σ
$V_{cb}\,(10^{-3})$	42.26 ± 0.89	41 ± 1	-0.9σ	$41.3^{+0.28}_{-0.11}$	$40.89 \pm 0.38 \pm 0.59$	0.0σ
$\varepsilon_k\,(10^{-3})$	1.96 ± 0.20	2.229 ± 0.010	$+1.3\sigma$	$2.02^{+0.53}_{-0.52}$	2.229 ± 0.010	0.0σ
$\Delta m_s\,(\,\mathrm{ps}^{-1})$	18.0 ± 1.3	17.69 ± 0.08	-0.2σ	$17.0^{+2.1}_{-1.5}$	17.731 ± 0.045	0.0σ
$\mathcal{B}(B \to \tau\nu)\,(10^{-4})$	0.821 ± 0.0077	1.67 ± 0.34	$+2.5\sigma$	$0.733^{+0.121}_{-0.073}$	1.68 ± 0.31	$+2.8\sigma$
β_s rad (*)	0.01876 ± 0.0008			$0.01822^{+0.00082}_{-0.00080}$		
$\mathcal{B}(B_s^0 \to \mu\mu)\,(10^{-9})$ (*)	3.47 ± 0.27			$3.64^{+0.21}_{-0.32}$		

determination is essential, not only for a SM global consistency test, but also to fix the apex of the UT in the extended fits.

3.2.5 Penguin pollution in $b \to c\bar{c}s$ decays

In addition to the very clear experimental signature, precise determination of the B^0 and B_s^0 mixing phases is possible due to the fact that in the "golden modes", $B^0 \to J/\psi\, K_S^0$ and $B_s^0 \to J/\psi\, \phi$, explicit calculation of the relevant matrix elements can be avoided, once subleading doubly Cabibbo suppressed and loop suppressed terms are assumed to vanish [250]. Estimates yield corrections of the order $O(10^{-3})$ only [251–253]; it is however notoriously difficult to actually calculate the relevant matrix elements, and non-perturbative enhancements cannot be excluded. Given the experimental precision presently aimed at for these and related modes, a critical reconsideration of this assumption is mandatory.

The main problem lies in the fact that once the assumption of negligible penguin contributions is dropped, the evaluation of hadronic matrix elements again becomes necessary, which still does not seem feasible to an acceptable precision for the decays in question. Therefore, to avoid explicit calculation, typically symmetry relations are used, exploiting either flavour SU(3) or U-spin symmetry [65, 254–259]. Without taking into account any QCD evaluation and only using control channels to estimate the size of the penguin amplitude, the analyses in Refs. [256, 259] still allow a phase shift of up to a few degrees for ϕ_d, which would correspond to a very large non-perturbative enhancement of the penguin size. In Ref. [256] a negative sign is preferred which (slightly) reduces the tension in the unitarity triangle fit shown in Fig. 16. The reason for the large allowed range of the shift of ϕ_d is due to the limited precision to which the corresponding control channels $B^0 \to J/\psi\, \pi^0$ and $B_s^0 \to J/\psi\, K^0$, which are Cabibbo suppressed compared to the golden modes, are known. For ϕ_s, an analogous analysis [65] cannot constrain yet the penguin contribution, due to absent $B \to J/\psi\, V$ control channel data for $B_s^0 \to J/\psi\, \phi$. However, in principle the effects in the $B \to J/\psi\, V$ modes are expected to be of the same order of magnitude as in the $B \to J/\psi\, P$ modes. The control channel $B_s^0 \to J/\psi\, K^{*0}$ has already been observed at CDF [260] and LHCb [261], and work is ongoing to measure its decay rate, polarisations and direct *CP* asymmetries. This will enable the first direct constraint on the shift of ϕ_s due to penguin contributions in the decay $B_s^0 \to J/\psi\, \phi$. For $B_s^0 \to J/\psi\, f_0(980)$ there is an additional complication due to the unknown hadronic structure of the $f_0(980)$ [224].

In addition to insufficient data, there are also theoretical aspects limiting the precision of this method at present, the most important of which is the violation of SU(3) symmetry. Regarding the B^0 mixing phase, a very recent paper [262] extends the analysis to a full SU(3) analysis (instead of using only one control channel) to be able to model-independently include SU(3) breaking. There, the importance of SU(3)-breaking contributions in this procedure is demonstrated: their neglect can lead to an overestimation of the subleading effects. Including recent data for two of the relevant modes [263, 264], the analysis shows that the data are at the moment actually compatible with vanishing penguin contributions, with SU(3)-breaking contributions of the order 20 %. Including

the penguin contributions, an upper limit on the shift of the mixing-induced *CP* asymmetry $\Delta S = \sin\phi_d - \sin 2\beta$ is derived: $|\Delta S| \lesssim 0.01$, with a negative sign for ΔS slightly preferred.[24] This is the most stringent limit available, despite the more general treatment of SU(3) breaking. In this analysis still some (conservatively chosen) theoretical inputs are needed to exclude fine-tuned solutions: SU(3) breaking effects have been restricted to at most 40 % for a few parameters which are not well determined by the fit and also have only small influence on the *CP* violation observables, and the penguin matrix elements are constrained to be at most 50 % of the leading contributions. Importantly, these theory inputs can be replaced by experimental measurements, namely of the *CP* asymmetries in the decay $B_s^0 \to J/\psi\, K_S^0$, the decay rate of which has already been measured at LHCb [264] after its observation at CDF [260]. Furthermore, data from all the corresponding modes (*i.e.* $B_{d,u,s} \to J/\psi\, P$, with light pseudoscalar meson $P = \pi, \eta^{(\prime)}$ or K) can be used to determine the shift more precisely, *i.e.* the related uncertainty is not irreducible, but can be reduced with coming data.

Turning to the second golden mode, $B_s^0 \to J/\psi\,\phi$, in general, the absolute shift is not expected to be larger than in the B^0 case. At the moment the data are not yet available to make a comparable analysis. While the penguin decay mode $B_s^0 \to \phi\phi$ is not related by symmetry with $B_s^0 \to J/\psi\,\phi$, comparing their decay rates indicates that the penguin contributions are small, and there are no huge enhancements to be expected for the penguin matrix elements in question.

Ultimately however, a quantitative analysis is warranted here as well. In principle, these methods can be adapted to extract the B_s^0 mixing phase including penguin contributions and model-independent SU(3) breaking, thereby improving the method proposed in Ref. [65]. The corresponding partners of the golden mode $B_s^0 \to J/\psi\,\phi$ are all the decays $B_{u,d,s} \to J/\psi\, V$, with the light vector mesons $V = K^*$, ρ, ϕ or ω. However, the complete analysis requires results on the polarisation fractions and *CP* asymmetries for each of these final states, and for some of them the experimental signature is quite challenging. In addition, the ϕ meson is a superposition of octet and singlet, therefore the "control channels" involving K^* and ρ are not as simply related as in the case with a pseudoscalar meson, but require the usage of nonet symmetry, whose precision has to be investigated in turn.

Nevertheless, significant progress can be expected. Several $B \to J/\psi\, V$ modes, including $B_{d,s} \to J/psiK^{*0}$ [265], are being studied at LHCb. While measurements of the modes involving $b \to d$ transitions are expected to exhibit rather large uncertainties at first, the advantage of the proposed method is the long "lever arm" in form of the relative enhancement $\sim 1/\lambda^2$ in the control channels, so that even moderate precision will be very helpful.

3.2.6 Future prospects with LHCb upgrade

Current measurements of ϕ_s carried out by LHCb in the $J/\psi\,\phi$ and $J/\psi\,\pi^+\pi^-$ final states show no deviation from the SM prediction within uncertainties [30, 32], putting strong

[24] Note the definition of ΔS here has a sign difference to that in Ref. [262].

constraints on new physics in B_s^0 mixing, as discussed in Sec. 3.2.3. Table 4 shows the current results with 1.0 fb^{-1} and the projected precision for 50 fb^{-1} with the upgraded detector. Based on the uncertainty of 83 (stat) + 27 (syst) mrad with 1.0 fb^{-1} combining the two decay modes, a precision of < 10 mrad is expected for 50 fb^{-1} with the upgraded detector. It is expected that even with this data sample, the main limitation will be statistical: the largest systematic uncertainties on the current measurement (background description, angular acceptance, effect of fixed physics parameters) [30] are expected to be removed with more sophisticated analyses or to scale with statistics. Thus changes as small as a factor of two with respect to the SM should be observable. This precision will make it possible either to measure a significant deviation from the SM prediction or otherwise to place severe constraints on NP scenarios.

Table 4: LHCb measurements of $\phi_s^{c\bar{c}s}$. The quoted uncertainties are statistical and systematic, respectively.

Final State	Current value (rad) with 1.0 fb^{-1}	Projected uncertainty (50 fb^{-1})
$J/\psi\phi$	$-0.001 \pm 0.101 \pm 0.027$	0.008
$J/\psi\pi^+\pi^-$	$-0.019\,^{+0.173\ +0.004}_{-0.174\ -0.003}$	0.014
Both	$-0.002 \pm 0.083 \pm 0.027$	0.007

As discussed in Sec. 3.2.5, contributions from doubly CKM-suppressed SM penguin diagrams could have a non-negligible effect on the mixing-induced *CP* asymmetry and bias the extracted value of ϕ_s. Naive estimates of the bias are of the order $O(10^{-3})$ only [251–253], but this must be examined with experimental data using flavour symmetries to exploit control channels. LHCb can perform an SU(3) analysis using measurements of the decays rates and *CP* asymmetries in $B_s^0 \to J/\psi K^{*0}$, $B^0 \to J/\psi\rho^0$ and $B^0 \to J/\psi\phi$ as control channels for $B_s^0 \to J/\psi\phi$. The necessary high precision can only be reached using the large data sample that will be collected with the upgraded LHCb detector. The 50 fb^{-1} data sample will also allow to measure ϕ_s in the penguin-free ($b \to c\bar{u}s/u\bar{c}s$) $B_s^0 \to D\phi$ decay [266, 267].

Another important goal is a more precise determination of $\sin 2\beta$ in the B^0 system, motivated by the tension between the direct and indirect determinations of $\sin 2\beta$ seen by both UTfit and CKMfitter groups, as shown in Table 3. With the upgraded detector, using the $B^0 \to J/\psi\ K^0_{\rm S}$ final state alone, a statistical precision of ± 0.006 is expected, to be compared to the current error from the B factories of ± 0.023 [193]. Given experience with the current detector it seems feasible to control the systematic uncertainties to a similar level. Such precision, together with better control of the penguin pollution, will allow us to pin down any NP effects in B^0 mixing. In addition, the penguin-free ($b \to c\bar{u}d/u\bar{c}d$) $B^0 \to D\rho^0$ channel can be used to get another handle on $\sin 2\beta$ [268, 269].

In addition, measurements of $\sin 2\beta^{\rm eff}_{(s)}$ can be made using loop dominated $b \to s$ transitions. For example, the decay $B^0 \to \phi K^0_{\rm S}$ has been used to probe $\sin 2\beta$ in penguin modes [270, 271], and improved measurements from time-dependent Dalitz plot analyses of $B^0 \to K^+K^-K^0_{\rm S}$ can be anticipated with the LHCb upgrade. Similarly, high precision

measurements of $B_s^0 \to \phi\phi$ and related modes will be possible for the first time. These penguin decays are discussed in detail in Sec. 3.3.

The importance of improved measurements of $\Delta\Gamma_q$ has been emphasised in Sections 3.2.1–3.2.3. LHCb has measured $\Delta\Gamma_s$ in $B_s^0 \to J/\psi\,\phi$ using a 1.0 fb^{-1} data sample [30]. The effective lifetime of $B_s^0 \to J/\psi f_0(980)$ [272] has also been measured [225]. Based on this, the statistical precision on $\Delta\Gamma_s$ with 50 fb^{-1} is projected to be ~ 0.003 ps^{-1}. It is hoped that the systematic uncertainty can be controlled to the same level.

A measurement of $\Delta\Gamma_d$ is of interest as any result larger than the tiny value expected in the SM would clearly signal new physics [172, 238, 273]. To determine this quantity, LHCb will compare the effective lifetimes of the two decay modes $B^0 \to J/\psi\, K^0_{\rm S}$ with $B^0 \to J/\psi\, K^{*0}$. The estimated precision for 1.0 fb^{-1} is ~ 0.02 ps^{-1}. With the upgraded detector a statistical precision of ~ 0.002 ps^{-1} on $\Delta\Gamma_d$ can be achieved. The systematic uncertainty is under study.

The LHCb upgrade will also have sufficient statistics to make novel tests of *CPT* symmetry. Any observation of *CPT* violation indicates physics beyond the SM. An example of a unique test in the B^0 system uses $B^0 \to J/\psi\, K^0$ and its charge-conjugate decay, where the K^0 decays semileptonically [274–276]. Thus this involves looking at 4 separate decay paths that can interfere. While several tests can be performed, one can be done without flavour tagging. The asymmetry A_{bk} is measured where

$$A_{bk} = \frac{\Gamma(B^0 + \overline{B}^0 \to J/\psi\,[\pi^-\mu^+\nu] - \Gamma(B^0 + \overline{B}^0 \to J/\psi\,[\pi^+\mu^-\overline{\nu}])}{\Gamma(B^0 + \overline{B}^0 \to J/\psi\,[\pi^-\mu^+\nu] + \Gamma(B^0 + \overline{B}^0 \to J/\psi\,[\pi^+\mu^-\overline{\nu}])} \tag{41}$$

In terms of the *CPT* violation parameter θ', the kaon decay time t_K, the B^0 decay time t_B, the B^0 mass difference Δm_d and *CP* violating phase 2β, and kaon decay widths Γ_S^K and Γ_L^K, we have

$$A_{bk} = \mathrm{Re}(\theta')\frac{2e^{-\frac{1}{2}\left(\Gamma_S^K+\Gamma_L^K\right)t_K}\sin(2\beta)\,(1-\cos\Delta m_d t_B)}{e^{-\Gamma_S^K t_K} + e^{-\Gamma_L^K t_K}}. \tag{42}$$

A signature of *CPT* violation would be a $1-\cos\Delta m_B t_B$ dependence of the decay rate after integrating over kaon decay times. Roughly we expect to collect 5000 such decays with the upgrade. It is possible to detect these decays with low background level, even with the missing neutrino, using the measured B^0 direction, the detected J/ψ four-momentum, and the kaon decay vertex. Other methods to test *CPT* symmetry are also under investigation.

3.3 *CP* violation measurements with hadronic $b \to s$ penguins

3.3.1 Probes for new physics in penguin-only $b \to sq\bar{q}$ decays

The presence of physics beyond the SM can be detected by looking for their contributions to $b \to sq\overline{q}$ ($q = s,\, d$) decays, which in the SM can only proceed via FCNC loop diagrams that are dynamically suppressed. These decays provide a rich set of observables that are rather precisely known in the SM but could potentially receive sizable corrections from new heavy particles appearing in the loop.

- **Direct *CP* asymmetries**. In the SM $b \to sq\overline{q}$ decays are dominated by the penguin diagram with an internal top quark. As a consequence, the direct *CP* asymmetry is expected to be small. If there is a new physics amplitude with comparable size interfering with the SM amplitude, and it has different strong and weak phases than the SM amplitude, a much larger direct *CP* asymmetry can arise.

- **Polarisation and triple product asymmetries**. For B decays into two vector mesons V_1 and V_2, followed by vector to two pseudoscalar decays $V_1 \to P_1 P_1'$ and $V_2 \to P_2 P_2'$, there are three polarisations, labelled "longitudinal" (0), "perpendicular" ($\perp$) and "parallel" ($\parallel$). The fractions of the total decay rate in each of these polarisation states provide useful information about the chiral structure of the electroweak currents, as well about non-perturbative effects such as rescattering and penguin annihilation. In the SM each polarisation is dominated by a single amplitude with magnitude $|A_j|$, weak phase Φ_j and strong phase δ_j, then the *CP* violating observables $\mathrm{Im}(A_\perp A_j^* - \bar{A}_\perp \bar{A}_j^*)$ are

$$\mathrm{Im}(A_\perp A_j^* - \bar{A}_\perp \bar{A}_j^*) = 2|A_\perp||A_j| \cos(\delta_\perp - \delta_j) \sin(\Phi_\perp - \Phi_j),\ j = 0, \parallel\ . \tag{43}$$

  The values of these observables are tiny since in the SM the weak phases are the same to a very good approximation, but $\mathrm{Im}(A_\perp A_j^* - \bar{A}_\perp \bar{A}_j^*)$ can significantly differ from zero if there is a sizable *CP*-violating NP contribution in the loop.

  These observables can be extracted from the differential distributions in terms of the angles θ_1, θ_2 and ϕ, where θ_1 (θ_2) is the polar angle of P_1 (P_2) in the rest frame of V_1 (V_2) with respect to the opposite of the direction of motion of the B meson, and ϕ is the angle between the decay planes of $V_1 \to P_1 P_1'$ and $V_2 \to P_2 P_2'$ in the rest frame of the B meson. The two observables can also be related to two triple product asymmetries for *CP* averaged decays[25] which are equal to asymmetries between the number of events with positive and negative values of $U = \sin 2\phi$ and $V = \mathrm{sign}(\cos\theta_1 \cos\theta_2) \sin\phi$:

$$\mathrm{Im}(A_\perp A_\parallel^* - \bar{A}_\perp \bar{A}_\parallel^*) \propto A_U = \frac{N(U>0) - N(U<0)}{N(U>0) + N(U<0)}\,, \tag{44}$$

$$\mathrm{Im}(A_\perp A_0^* - \bar{A}_\perp \bar{A}_0^*) \propto A_V = \frac{N(V>0) - N(V<0)}{N(V>0) + N(V<0)}\,. \tag{45}$$

  A review of this subject can be found in Ref. [277] and references therein.

- **Mixing-induced *CP* asymmetries**. Mixing-induced *CP* asymmetries in $b \to sq\overline{q}$ decays of neutral B to *CP* eigenstates are precisely predicted. Due to the fact that the penguin diagram with an internal top quark is expected to dominate, the values of $2\beta^{\rm eff}$ determined using $B^0 \to \phi K^0_{\rm S}$, $B^0 \to \eta' K^0_{\rm S}$, $B^0 \to f_0(980) K^0_{\rm S}$, *etc.*, are all

[25] The triple product asymmetries in $B_s^0 \to \phi\phi$ and $B_s^0 \to K^{*0}\overline{K}^{*0}$ decay could in principle also receive contribution from non-zero mixing-induced *CP* asymmetries arising from NP in B_s^0 mixing. However, this contribution is suppressed by $\Delta\Gamma_s/\Gamma_s$ and is already highly constrained.

expected to give $\approx \sin 2\beta$ (see, *e.g.* Refs. [278, 279] and the discussion in Ref. [63]). Similarly, the values of $2\beta_s^{\rm eff}$ determined from $B_s^0 \to \phi\phi$, $B_s^0 \to K^{*0}\bar{K}^{*0}$, *etc.*, are expected to vanish due to cancellation of weak phases between mixing (top box) and decay (top penguin) amplitudes. Higher order corrections from subleading diagrams are expected to be small compared to the precision that can be achieved in the near-term, but further theoretical studies will be needed as we approach the upgrade era. NP with a flavour structure different from the SM will alter these *CP* asymmetries through the decay amplitudes, even if there is no new physics in B mixing. A number of quasi-two-body or three-body decay modes can be studied. Due to the resonant structure in multibody decays, these can offer additional possibilities to search for both the existence and features of NP.

- **Correlations between direct and mixing-induced asymmetries**. Penguin-only decay modes are particularly interesting as the difference between formal "tree" and "penguin" contributions boils down to a difference in the quark-flavour running in the loop of the penguins. This difference, dominated by short distances, can be assessed accurately using QCD factorisation, and it can be used to correlate the branching ratio and the *CP* asymmetries of penguin-mediated modes. As discussed in Refs. [165, 280, 281], these observables can be correlated not only within the SM, but can also be used to extract the B_s^0 mixing phase even in the presence of NP affecting only this phase.

3.3.2 Current status and short term outlook of LHCb measurements

Interesting hadronic $b \to sq\bar{q}$ decays that have been studied or will be studied at LHCb include $B_s^0 \to \phi\phi$, $B_s^0 \to \phi f_0(980)$, $B_s^0 \to K^{*0}\overline{K}^{*0}$, $B^0 \to \phi K^{*0}$, $B^0 \to \phi K_{\rm S}^0$ *etc.*

LHCb has recently published the first observation and measurement of the branching ratio and polarisation amplitudes in the $B_s^0 \to K^{*0}\overline{K}^{*0}$ decay mode [47] using 35 pb^{-1} of data collected in 2010. A clean mass peak corresponding to 50 ± 8 $B_s^0 \to (K^+\pi^-)(K^+\pi^+)$ decays is seen (Fig. 19 (left)), mostly from resonant $B_s^0 \to K^{*0}\overline{K}^{*0}$ decays. Using this signal the longitudinal polarisation amplitude is measured to be $f_L = 0.31 \pm 0.12({\rm stat}) \pm 0.04({\rm syst})$ and the branching ratio to be $\mathcal{B}(B_s^0 \to K^{*0}\overline{K}^{*0}) = (2.81 \pm 0.46({\rm stat}) \pm 0.45({\rm syst}))\,\%$.

LHCb also published the measurement of the polarisation amplitudes and triple product asymmetries in $B_s^0 \to \phi\phi$ [49] using the 2011 dataset of 1.0 fb^{-1}. In this dataset 801 ± 29 events are observed with excellent signal-to-background ratio (see Fig. 19 (right)). The polarisation amplitudes are measured to be

$$\begin{aligned} |A_0|^2 &= 0.365 \pm 0.022\,({\rm stat}) \pm 0.012\,({\rm syst})\,, \\ |A_\perp|^2 &= 0.291 \pm 0.024\,({\rm stat}) \pm 0.010\,({\rm syst})\,, \\ |A_\parallel|^2 &= 0.344 \pm 0.024\,({\rm stat}) \pm 0.014\,({\rm syst})\,, \end{aligned} \tag{46}$$

where the sum of the square of the amplitudes is constrained to unity. The triple product

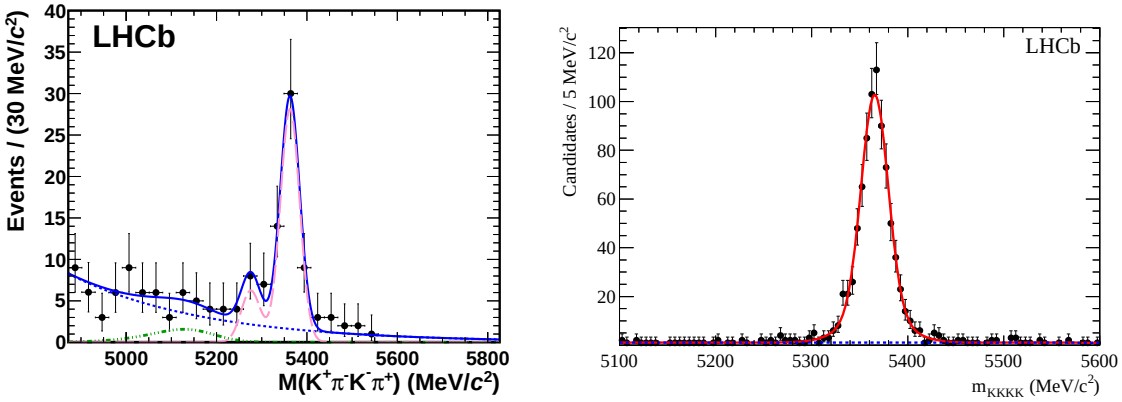

Figure 19: Fit of the $K^+\pi^-K^-\pi^+$ mass distribution taken from Ref. [47] (left) and fit of the $K^+K^-K^-K^+$ invariant mass distribution taken from Ref. [49] (right).

asymmetries in this mode are measured to be

$$\begin{aligned} A_U &= -0.055 \pm 0.036\,(\text{stat}) \pm 0.018\,(\text{syst})\,, \\ A_V &= 0.010 \pm 0.036\,(\text{stat}) \pm 0.018\,(\text{syst})\,. \end{aligned} \tag{47}$$

The results of this analysis are in agreement with, and more precise than, the previous measurement [282], and are also consistent with the SM.

First measurements of *CP* asymmetries in these modes from a time-dependent flavour-tagged angular analysis are expected to follow soon. With high statistics, it will be possible to measure polarisation-dependent direct and mixing-induced *CP* asymmetries, but for the first analysis it will be more convenient to determine a single complex observable common to all polarisations (as done for $B_s^0 \to J/\psi\,\phi$)

$$\lambda = \eta_j \frac{q}{p} \frac{\bar{A}_j}{A_j} \tag{48}$$

where j denotes one of the three transversity states, which are also *CP* eigenstates with eigenvalues η_j, and A_j ($\bar{A}_j$) is the decay amplitude of B_s^0 ($\overline{B}_s^0$) to the corresponding state. With this approximation it will be possible to determine the magnitude $|\lambda|$ and phase $\phi_s^{\rm eff} \equiv -\arg(\lambda)$. The SM expectation is $|\lambda| \approx 1$ and $\phi_s^{\rm eff} \approx 0$ due to the dominance of the top-quark loop, and any observed deviation from these expectations would be a signature of NP. Since NP in B_s^0 mixing is already constrained by measurement of ϕ_s from $B_s^0 \to J/\psi\,\phi$, the main interest in these $b \to s$ penguin modes is to look for NP in the decay processes. Based on simulation studies, a sensitivity on $\phi_s^{\rm eff}$ of 0.3–0.4 radians with 1.0 fb^{-1} is expected for both $B_s^0 \to \phi\pi$ and $B_s^0 \to K^{*0}\overline{K}^{*0}$.

3.3.3 Future prospects with LHCb upgrade

The latest results on mixing-induced *CP* violation in $b \to s$ transitions show no significant deviation from the SM, as seen in Fig. 20, which compares the mixing-induced *CP* violation parameter $\sin 2\beta^{\rm eff}$ measured in penguin-dominated $b \to s$ decays with the value of

sin 2β measured in the tree-dominated $b \to c\bar{c}s$ decays. In the absence of NP these observables should only differ by a small number. Due to these results, large NP contributions in $b \to sq\bar{q}$ decays are unlikely but further tests with higher precision remain interesting. LHCb will be able to make competitive measurements of $\sin 2\beta^{\rm eff}$ in $B^0 \to \phi K^0_{\rm S}$ and several other $b \to sq\bar{q}$ decays, but a significant improvement in precision requires the 50 fb^{-1} of the LHCb upgrade. With this data sample, the statistical error of $\sin 2\beta^{\rm eff}(B^0 \to \phi K^0_{\rm S})$ is estimated to be roughly 0.06, which is still above the SM uncertainty of ~ 0.02 [283].

There are several more NP probes in $b \to sq\bar{q}$ decays that can be exploited at LHCb and its upgrade, such as mixing-induced CP asymmetries and triple product asymmetries in both $B^0_s \to \phi\phi$ and $B^0_s \to K^{*0}\overline{K}^{*0}$ decays. The statistical precision of $\phi_s^{\rm eff}$ with each channel is estimated to be 0.3–0.4 rad for 1 fb^{-1}. The projected precision for 50 fb^{-1} is about 0.03 rad each. This can be compared with the uncertainties of their SM predictions of about 0.02 rad. It is also possible to perform a combined analysis of $B^0_s \to K^{*0}\overline{K}^{*0}$ and its U-spin related channel $B^0 \to K^{*0}\overline{K}^{*0}$, which will put strong constraint on the subleading penguin diagrams in $B^0_s \to K^{*0}\overline{K}^{*0}$, thus further reducing the theoretical uncertainty in the measurement of $\phi_s^{\rm eff}$ [48, 284]. The statistical precision of A_U and A_V is estimated to be about 0.004, compared with an upper bound of 0.02 on their possible sizes in the SM.

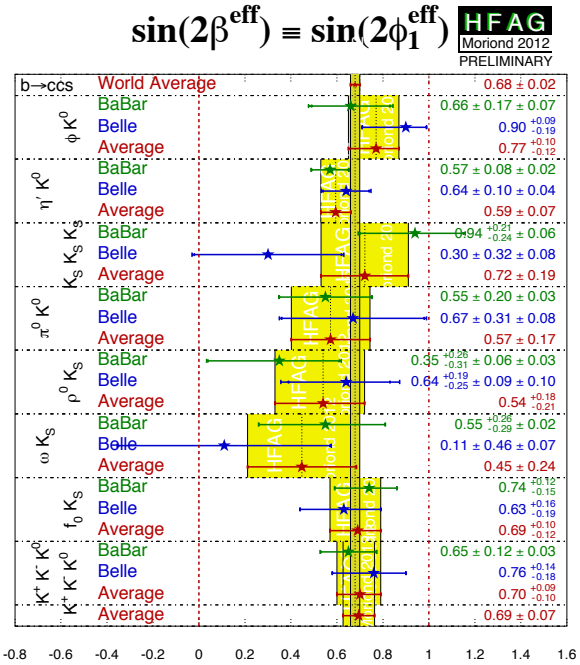

Figure 20: HFAG compilation of results for $\sin 2\beta^{\rm eff}$ in $b \to sq\bar{q}$ decays [63].

In summary, the LHCb upgrade will allow to exploit the full potential of the NP probes in $b \to sq\bar{q}$ decays. Table 5 compares the current and projected (LHCb upgrade 50 fb^{-1})

precisions of the key observables with the theory uncertainties of their SM predictions.

Table 5: Current and projected precisions of the key observables in $b \to sq\overline{q}$ decays.

Observable	Current	LHCb upgrade (50 fb^{-1})	Theory uncertainty
$A_{U,V}(B_s^0 \to \phi\phi)$	0.04 (LHCb 1.0 fb^{-1})	0.004	0.02 [285]
$\phi_s^{\rm eff}(B_s^0 \to \phi\phi)$	–	0.03	0.02 [283]
$\phi_s^{\rm eff}(B_s^0 \to K^{*0}\bar{K}^{*0})$	–	0.03	0.02 [283]
$\sin 2\beta^{\rm eff}(B^0 \to \phi K_{\rm S}^0)$	0.12 (B factories)	0.06	0.02 [188]

3.4 Measurements of the CKM angle γ

3.4.1 Measurements of γ using tree-mediated decays

The CKM angle γ, defined as the phase $\gamma = \arg\left[-V_{ud}V_{ub}^*/(V_{cd}V_{cb}^*)\right]$, is one of the angles of the unitarity triangle formed from the hermitian product of the first (d) and third (b) columns of the CKM matrix V. It is one of the least well known parameters of the quark mixing matrix. However, since it can be determined entirely through decays of the type $B \to DK$ [26] that involve only tree amplitudes — an unusual, even unique, property amongst all CP violation parameters — it provides a benchmark measurement. The determination from tree level decays has essentially negligible theoretical uncertainty, at the level of $\delta\gamma/\gamma = O(10^{-6})$, as we will show in the next section. This makes γ a very appealing "standard candle" of the CKM sector. It serves as a reference point for comparison with γ values measured from loop decays (see Sec. 3.4.4).

Moreover, the determination of γ is crucial input to improve the precision of the global CKM fits, and resulting limits on (or evidence for) NP contributions (see Sec. 3.2.4). In particular, the measurement of Δm_d and the oscillation phase $\sin 2\beta$ in B^0–$\overline{B}^0$ mixing can be converted to a measurement of γ (in the SM). This can be compared to the reference value from $B \to DK$ – their consistency verifies that the Kobayashi-Maskawa mechanism of CP violation is the dominant source in quark flavour-changing processes. Existing measurements provide tests at the level of $\mathcal{O}(10\,\%)$, but improving the precision to search for smaller effects of NP is well motivated.

Several established methods to measure γ in tree decays exploit the $B^- \to D^{(*)}K^{(*)-}$ decays. They are based on the interference between the $b \to u$ and $b \to c$ tree amplitudes, which arises when the neutral D meson is reconstructed in a final state accessible to both D^0 and $\overline{D}^0$ decays. The interference between the amplitudes results in observables that depend on their relative weak phase γ. Besides γ they also depend on hadronic parameters, namely the ratio of magnitudes of amplitudes $r_B \equiv |A(b \to u)/A(b \to c)|$ and the relative strong phase δ_B between the two amplitudes. These hadronic parameters depend on the B

[26] By $B \to DK$ we include all related tree-dominated decay processes, including $B^+ \to DK^+$, $B^0 \to DK^{*0}$, $B_s^0 \to D\phi$, $B_s^0 \to D_s^{\mp}K^{\mp}$ and $B^0 \to D^{(*)\mp}\pi^{\pm}$. In these specific decay processes, the notation D refers to a neutral D meson that is an admixture of D^0 and $\overline{D}^0$ states.

decay under investigation. They can not be precisely calculated from theory (see, however, Ref. [286]), but can be extracted directly from data by simultaneously reconstructing several different D final states.

The various methods differ by the $D^{(*)}$ final state that is used. The three main categories of D decays considered so far by the B factories BaBar and Belle, and by CDF, are:

- *CP* eigenstates (the GLW method [287, 288]),
- doubly-Cabibbo-suppressed decays (the ADS method [289, 290]),
- three body, self-conjugate final states (the GGSZ or "Dalitz" method [291]).

An additional category has not been possible to pursue at previous experiments due to limited statistics:

- singly-Cabibbo-suppressed decays (the GLS method [292]).

In practise, apart from for two-body decays, there is often no clear distinction between the different methods.

The best sensitivity to γ obviously comes from combining the results of all different analyses. This not only improves the precision on γ, but provides additional constraints on the hadronic parameters. It also allows to overcome the fact that *CP* odd final states such as $K^0_S\pi^0$ are not easily accessible in LHCb's hadronic environment.

We briefly review the main ideas of the different methods. We write the amplitudes of the $B^- \to D^0 K^-$ and $B^- \to \overline{D}^0 K^-$ processes as:

$$\begin{aligned} A(B^- \to D^0 K^-) = &\quad A_c e^{i\delta_c}\,, \qquad A(D^0 \to f) = A_f e^{i\delta_f}\,, \\ A(B^- \to \overline{D}^0 K^-) = &\quad A_u e^{i(\delta_u - \gamma)}\,, \quad A(D^0 \to \bar{f}) = A_{\bar{f}} e^{i\delta_{\bar{f}}}\,, \end{aligned} \tag{49}$$

where A_c, A_u, A_f and $A_{\bar{f}}$ are real and positive (we have neglected *CP* violation in D^0 decays). The subscripts c and u refer to the $b \to c$ and $b \to u$ transitions, respectively. The amplitudes for the D^0 decay can generally include the case where the D^0 decays to a three-body final state. In this case, A_f, $A_{\bar{f}}$, δ_f and $\delta_{\bar{f}}$ are functions of the Dalitz plot coordinates. The amplitude of the process $B^- \to D[\to f]K^-$ can be written, neglecting D^0–$\overline{D}^0$ mixing, as

$$A(B^- \to D[\to f]K^-) = A_c A_f e^{i(\delta_c + \delta_f)} + A_u A_{\bar{f}} e^{i(\delta_u + \delta_{\bar{f}} - \gamma)}\,, \tag{50}$$

and the rate is given by

$$\begin{aligned} \Gamma(B^- \to D[\to f]K^-) &\propto A_c^2 A_f^2 + A_u^2 A_{\bar{f}}^2 + 2A_c A_f A_u A_{\bar{f}} \mathrm{Re}(e^{i(\delta_B + \delta_D - \gamma)}) \\ &\propto A_c^2 \left(A_f^2 + r_B^2 A_{\bar{f}}^2 + 2r_B A_f A_{\bar{f}} \mathrm{Re}(e^{i(\delta_B + \delta_D - \gamma)}) \right)\,, \end{aligned} \tag{51}$$

where $r_B = A_u/A_c$, $\delta_B = \delta_u - \delta_c$ and $\delta_D = \delta_{\bar{f}} - \delta_f$. The rate for the charge-conjugated mode (still neglecting *CP* violation in D^0 decays) is obtained by exchanging $\gamma \to -\gamma$. Taking

into account CKM factors and, in the case of charged B decays, colour suppression of the $b \to u$ amplitude, r_B is expected to be around 0.1 for B^- decays and around 0.3 for B^0 decays. From Eq. (51) all the relevant formulae of the GLW, ADS and GGSZ methods can be derived.

In the GLW analysis, the neutral D mesons are selected in CP eigenstates $f_{CP\pm}$ such as $D \to K^-K^+$ ($CP = +1$) or $D \to K^0_S\pi^0$ ($CP = -1$). We thus have $A_f/A_{\bar{f}} = 1$ and $\delta_D = 0, \pi$ for $CP = \pm 1$. Eq. (51) becomes:

$$\Gamma(B^- \to D[\to f_{CP\pm}]K^-) \propto A_c^2(1 + r_B^2 \pm 2r_B\cos(\delta_B - \gamma))\,. \tag{52}$$

The $B^- \to DK^-$ decays, where the D decays to Cabibbo-favoured final states (*e.g.* $D^0 \to K^-\pi^+$) can be used to normalise the rates in order to construct observables that minimise the systematic uncertainties. In their case we can write to a good approximation:

$$\Gamma(B^- \to D[\to K^-\pi^+]K^-) = \Gamma(B^+ \to D[\to K^+\pi^-]K^+) \propto A_c^2\,. \tag{53}$$

From Eqs. (52) and (53) and their CP conjugates the usual GLW observables follow:

$$R_{CP\pm} = \frac{2[\Gamma(B^- \to D_{CP\pm}K^-) + \Gamma(B^+ \to D_{CP\pm}K^+)]}{\Gamma(B^- \to D^0K^-) + \Gamma(B^+ \to \overline{D}^0K^+)} \tag{54}$$

$$A_{CP\pm} = \frac{\Gamma(B^- \to D_{CP\pm}K^-) - \Gamma(B^+ \to D_{CP\pm}K^+)}{\Gamma(B^- \to D_{CP\pm}K^-) + \Gamma(B^+ \to D_{CP\pm}K^+)}\,. \tag{55}$$

Eqs. (54) and (55) provide a set of four observables that are connected to the three unknowns γ, r_B and δ_B through

$$R_{CP\pm} = 1 + r_B^2 \pm 2r_B\cos\delta_B\cos\gamma \tag{56}$$

$$A_{CP\pm} = \frac{\pm 2r_B\sin\delta_B\sin\gamma}{R_{CP\pm}}\,. \tag{57}$$

However, only three of these equations are independent since, from Eq. (57), $R_{CP+}A_{CP+} = -R_{CP-}A_{CP-}$. Analogous relations hold for $B \to D^*_{CP}K$ and $B \to D_{CP}K^*$ decays, with different values of the hadronic parameters characterising the B decay. However, in the $B \to D^*_{CP}K$ case one has to take into account a CP flip due to the different charge conjugation quantum numbers of the π^0 and the photon from the D^* decay [293]: $D^*_{CP\pm} \to D_{CP\pm}\pi^0$, but $D^*_{CP\pm} \to D_{CP\mp}\gamma$. For analysis of $B \to D_{CP}K^*$ the finite width of the K^* resonance must be taken into account [294]. There are related important consequences for the ADS and GGSZ analyses of $B \to D^*K$ and $B \to DK^*$ decays.

In the ADS analysis, the neutral D mesons are selected in Cabibbo allowed and doubly Cabibbo suppressed decays, such as $D^0 \to K^-\pi^+$ and $D^0 \to \pi^-K^+$, respectively. The B decay rate is the result of the interference of the colour allowed $B^- \to D^0K^-$ decay followed by the doubly Cabibbo suppressed $D^0 \to \pi^-K^+$ decay and the colour suppressed $B^- \to \overline{D}^0K^-$ decay followed by the Cabibbo allowed $D^0 \to K^-\pi^+$ decay. As a consequence, the interfering amplitudes are of similar magnitude and hence large interference effects can occur. From Eq. (51) we have:

$$\Gamma(B^\mp \to D[\to K^\pm\pi^\mp]K^\mp) \propto r_B^2 + r_D^2 \pm 2r_Br_D\cos(\delta_B + \delta_D \mp \gamma) \tag{58}$$

where both $r_D = A_f/A_{\bar{f}} = |A(D^0 \to \pi^- K^+)/A(D^0 \to K^- \pi^+)|$ and the phase difference δ_D are measured in charm decays. The value of δ_D can be determined directly using data collected from e^+e^- collisions at the $\psi(3770)$ resonance, as has been done by CLEO [295], but the most precise value comes from a global fit including charm mixing parameters. The results provided by HFAG [63] from a combination with *CP* violation in charm allowed are $r_D = 0.0575 \pm 0.0007$, $\delta_D = \left(202\,^{+10}_{-11}\right)^\circ$. Defining $R_{\rm ADS}$ and $A_{\rm ADS}$ as:

$$R_{\rm ADS} = \frac{\Gamma(B^- \to D[\to \pi^- K^+]K^-) + \Gamma(B^+ \to D[\to \pi^+ K^-]K^+)}{\Gamma(B^- \to D[\to K^- \pi^+]K^-) + \Gamma(B^+ \to D[\to K^+ \pi^-]K^+)} \tag{59}$$

$$A_{\rm ADS} = \frac{\Gamma(B^- \to D[\to \pi^- K^+]K^-) - \Gamma(B^+ \to D[\to \pi^+ K^-]K^+)}{\Gamma(B^- \to D[\to \pi^- K^+]K^-) + \Gamma(B^+ \to D[\to \pi^+ K^-]K^+)} \tag{60}$$

we find, using Eq. (53) and (58):

$$R_{\rm ADS} = r_B^2 + r_D^2 + 2 r_B\, r_D \cos\gamma \cos(\delta_B + \delta_D) \tag{61}$$

$$A_{\rm ADS} = 2 r_B\, r_D \sin\gamma \sin(\delta_B + \delta_D)/R_{\rm ADS} \tag{62}$$

It has been noted that for the extraction of γ it can be more convenient to replace the pair of observables $R_{\rm ADS}, A_{\rm ADS}$ with a second pair, R_+, R_-, defined as:

$$R_\pm \equiv \frac{\Gamma(B^\pm \to [K^\mp \pi^\pm]_D K^\mp)}{\Gamma(B^\pm \to [K^\pm \pi^\mp]_D K^\pm)} = r_B^2 + r_D^2 + 2 r_B r_D \cos(\delta_B + \delta_D \pm \gamma) \tag{63}$$

Unlike $R_{\rm ADS}, A_{\rm ADS}$, the two quantities R_+, R_- are statistically independent. The ADS decay chain $B^\pm \to [\pi^\pm K^\mp]_D K^\pm$ has recently been observed for the first time by LHCb [43], confirming the evidence that had begun to accumulate in previous measurements [296–298].

In the GGSZ analysis, the neutral D mesons are selected in three-body self-conjugate final states. The channel that has been used most to date is $D \to K^0_{\rm S}\pi^+\pi^-$, though first results have also been presented with $D \to K^0_{\rm S} K^+ K^-$ and other channels are under consideration. For concreteness, we focus on $D \to K^0_{\rm S}\pi^+\pi^-$, with $A_f e^{i\delta_f} = f(m^2_-, m^2_+)$ and $A_{\bar{f}} e^{i\delta_{\bar{f}}} = f(m^2_+, m^2_-)$, where m^2_- and m^2_+ are the squared masses of the $K^0_{\rm S}\pi^-$ and $K^0_{\rm S}\pi^+$ combinations. The rate in Eq. (51) can be re-written as:

$$\begin{aligned}\Gamma(B^\mp \to & D[\to K^0_{\rm S}\pi^-\pi^+]K^\mp) \propto |f(m^2_\mp, m^2_\pm)|^2 + r_B^2 |f(m^2_\pm, m^2_\mp)|^2 \\ & + 2 r_B |f(m^2_\mp, m^2_\pm)||f(m^2_\pm, m^2_\mp)| \cos(\delta_B + \delta_D(m^2_\mp, m^2_\pm) \mp \gamma)\,,\end{aligned} \tag{64}$$

where $\delta_D(m^2_\mp, m^2_\pm)$ is the strong phase difference between $f(m^2_\pm, m^2_\mp)$ and $f(m^2_\mp, m^2_\pm)$. Due to the fact that r_B is bound to be positive, the direct extraction of r_B, δ_B and γ can be biased. To avoid these biases, the "Cartesian coordinates" have been introduced [299]

$$x_\pm = {\rm Re}[r_B e^{i(\delta_B \pm \gamma)}]\,, \quad y_\pm = {\rm Im}[r_B e^{i(\delta_B \pm \gamma)}]\,, \tag{65}$$

allowing to write Eq. (64) as

$$\Gamma(B^\mp \to D[\to K^0_{\rm S}\pi^+\pi^-]K^\mp) \propto |f_\mp|^2 + r_B^2 |f_\pm|^2 + 2\left[x_\mp {\rm Re}[f_\mp f^*_\pm] + y_\mp {\rm Im}[f_\mp f^*_\pm]\right]\,. \tag{66}$$

Here we have also simplified the notation using $f_\pm = f(m^2_\pm, m^2_\mp)$. This Dalitz plot-based method can be implemented in a model-dependent way by parametrising the amplitude as a function of the Dalitz plot of the three-body state, or in a model-independent way by dividing the Dalitz plot into bins and making use of external measurements of the D decay strong phase differences within these bins [291, 300, 301].[27]

Besides the established methods based on direct CP violation in $B \to DK$ decays, it is also possible to measure γ using time-dependent analyses of neutral B^0 and B^0_s tree decays [303–305]. The method still relies on the interference of $b \to u$ and $b \to c$ amplitudes, however interference is achieved through B^0 (B^0_s) mixing. Thus one measures the sum of γ and the mixing phase, namely $\gamma + 2\beta$ and $\gamma + \phi_s$ in the B^0 and B^0_s systems, respectively. Since both $\sin 2\beta$ and ϕ_s are now well measured, these measurements provide sensitivity to γ.

Pioneering time-dependent measurements using the $B^0 \to D^{(*)\mp}\pi^\pm$ decays have been performed by both BaBar [306, 307] and Belle [308, 309]. In these decays the amplitude ratios $r_{D\pi} = |A(B^0 \to D^{-(*)}\pi^+)/A(B^0 \to D^{+(*)}\pi^-)|$ are expected to be small, $r_{D\pi} \lesssim 0.02$, limiting the sensitivity. In the decays $B^0_s \to D^\mp_s K^\pm$, however, both $b \to c$ and $b \to u$ amplitudes are of same order in the Wolfenstein parameter λ, $\mathcal{O}(\lambda^3)$, so that the interference effects are expected to be large. In addition, the decay width difference in the B^0_s system, $\Delta\Gamma_s$, is non-zero, which adds sensitivity to the weak phase through the hyperbolic terms in the time evolution (see also Ref. [310]). The time-dependent decay rates of the initially produced flavour eigenstates are given by the decay equations

$$\begin{aligned}\frac{d\Gamma_{B^0_s(\bar{B}^0_s)\to f}(t)}{dt\, e^{-\Gamma_s t}} &= \frac{1}{2}|A_f|^2(1+|\lambda_f|^2) \\ &\times \left[\cosh\left(\frac{\Delta\Gamma_s t}{2}\right) + D_f \sinh\left(\frac{\Delta\Gamma_s t}{2}\right) \pm\ C_f \cos\left(\Delta m_s t\right) \mp S_f \sin\left(\Delta m_s t\right)\right],\end{aligned} \tag{67}$$

where Γ_s, $\Delta\Gamma_s$, Δm_s are the usual mixing parameters of the B^0_s system and we have assumed $|q/p| = 1$. A_f is the decay amplitude for a B^0_s meson to decay to a final state f, and λ_f is defined as

$$\lambda_f = \frac{q}{p}\frac{\overline{A}_f}{A_f}, \tag{68}$$

where $\overline{A}_f$ is the amplitude for a $\overline{B}^0_s$ to decay into f. Similar equations hold for the charge conjugate processes $\overline{B}^0_s(B^0_s) \to \bar{f}$, containing a separate set of coefficients $C_{\bar{f}}$, $S_{\bar{f}}$ and $D_{\bar{f}}$, and a separate λ parameter $\overline{\lambda}_{\bar{f}}$. As each decay is dominated by a single diagram, we have

[27] As for δ_D in the ADS method, the strong phase differences can be determined directly from $\psi(3770) \to D\bar{D}$ data, which has been done by CLEO [302]. In future, it is expected that the most precise value will comes from a global fit including results of time-dependent analyses of multibody charm decays.

$|\lambda_f| = |\bar{\lambda}_{\bar{f}}|$. The *CP* asymmetry observables are then given by

$$C_f = C_{\bar{f}} = \frac{1-|\lambda_f|^2}{1+|\lambda_f|^2}\,, \quad S_f = \frac{2\mathrm{Im}(\lambda_f)}{1+|\lambda_f|^2}\,, \quad D_f = \frac{2\mathrm{Re}(\lambda_f)}{1+|\lambda_f|^2}\,,$$
$$S_{\bar{f}} = \frac{2\mathrm{Im}(\overline{\lambda}_{\bar{f}})}{1+|\lambda_f|^2}\,, \quad D_{\bar{f}} = \frac{2\mathrm{Re}(\overline{\lambda}_{\bar{f}})}{1+|\lambda_f|^2}\,. \tag{69}$$

The term λ_f is connected to the weak phase by

$$\lambda_f = \Big(\frac{q}{p}\Big)\frac{\overline{A}_f}{A_f}\Big(\frac{V_{tb}^*V_{ts}}{V_{tb}V_{ts}^*}\Big)\Big(\frac{V_{ub}V_{cs}^*}{V_{cb}^*V_{us}}\Big)\Big|\frac{A_2}{A_1}\Big|e^{i\Delta} = |\lambda_f|e^{i(\Delta-(\gamma+\phi_s))}\,, \tag{70}$$

where $|A_2/A_1|$ is the ratio of the hadronic amplitudes between $B_s^0 \to D_s^- K^+$ and $B_s^0 \to D_s^+ K^-$, Δ is their strong phase difference, and $\gamma+\phi_s$ is the weak phase difference. An analogous relation exists for $\overline{\lambda}_{\bar{f}}$, $\overline{\lambda}_{\bar{f}} = |\lambda_f|e^{i(\Delta+(\gamma+\phi_s))}$. Thus one obtains five observables from Eq. (69) and solves for $|\lambda_f|$, Δ, and $(\gamma+\phi_s)$.

The LHCb experiment has the necessary decay time resolution, tagging power and access to large enough signal yields to perform this time dependent *CP* measurement. The signal yields can be seen from the measurement of $\mathcal{B}(B_s^0 \to D_s^\mp K^\pm)$ [311] (see Fig. 23 below). The identification of the initial flavour of the signal B_s^0 candidate can be done combining both the responses of opposite-side and same-side kaon tagging algorithms. The measured tagging power in the reference control channel $B_s^0 \to D_s^-\pi^+$ is $\varepsilon_{\mathrm{tag}}\mathcal{D}^2 = (4.1 \pm 0.5)\,\%$ [216], corresponding to a fraction of tagged events of $\sim 50\,\%$. In order to exploit the tagging at best, the mistag probability ω is evaluated event by event from the predicted mistag probability (η) that is calibrated using the control channel.

3.4.2 Theoretical cleanliness of γ from $B \to DK$ decays

We will now address the question: why it is interesting to measure γ precisely? The answer depends on the experimental precision that can be achieved. In the era of LHCb, the main motivation is the theoretically clean measurement of the SM CKM phase. The search for NP can thus be performed by comparing the extracted value of γ to other observables, for example in the CKM fit (see Sec. 3.2.4). However, one can also cross-check for the presence of NP in $B \to DK$ channels themselves. One way is to test that the values of γ determined from the many different $B \to DK$ type channels all coincide. Another is automatically built in to the method for γ extraction in the GGSZ analysis. Consider the case where the decay amplitudes get modified by an extra contribution with a new strong phase δ'_B and a weak phase γ'. Then instead of the decay amplitudes in Eq. (50) we have

$$A(B^\pm \to f_D K^\pm) \propto 1 + r_D e^{i\delta_D}(r_B e^{i(\delta_B \pm \gamma)} + r'_B e^{i(\delta'_B \pm \gamma')})\,. \tag{71}$$

This means that for B^+ and B^- decays the r_B ratios are different

$$r_{B^+} \to |r_B e^{i(\delta_B+\gamma)} + r'_B e^{i(\delta'_B+\gamma')}|\,, \quad r_{B^-} \to |r_B e^{i(\delta_B-\gamma)} + r'_B e^{i(\delta'_B-\gamma')}|\,. \tag{72}$$

Discovering that $r_{B^-} \neq r_{B^+}$ would signal a *CP* violating NP contribution to the $B \to DK$ amplitude. One signature of NP would then be $x_+^2 + y_+^2 \neq x_-^2 + y_-^2$, though it is also possible that the equality could be satisfied even in the presence of NP: in this case there can be a shift in the extracted value of γ.

It is hard, though maybe not impossible, to imagine that large tree-level NP effects, as could be discovered in near term measurements, would not have shown up in other observables. The situation could, however, be different in the far future. Since the extraction of γ is theoretically very clean, it can be used to search for high scale NP when a lot of statistics is available. Note that in principle NP with contributions of different chirality could give different shifts in γ, so that the above test is meaningful.

Let us thus turn to the following: what is the energy scale that we could probe in principle? To answer this we need to estimate how clean the determination of γ can be in principle. What is the theory error?

There are several sources that can induce a theory error in the determination of γ from $B \to DK$ decays. However, most of these can be avoided, either (i) with more statistics (for example, the Dalitz plot model uncertainty where a switch to a model-independent method is possible), or (ii) by modifying the equations used to determine γ (an example is to correct for effects of D^0–$\overline{D}^0$ mixing [312, 313]). The remaining, irreducible, theory uncertainties are then from the electroweak corrections.

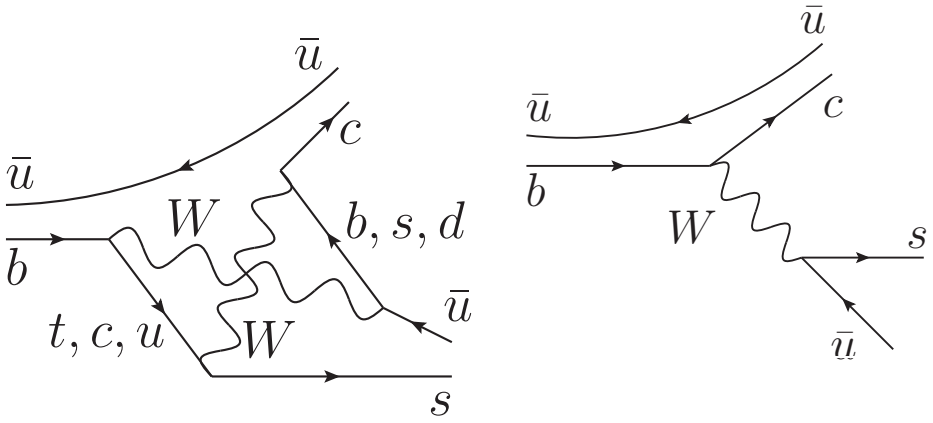

Figure 21: A $B^- \to D^0 K^-$ box diagram electroweak correction (left) with a different CKM structure than the leading weak decay amplitude (right).

The challenge to determine this uncertainty is that the hadronic elements can no longer be determined solely from the experiment. Not all electroweak corrections matter though – the important ones are the corrections that change the CKM structure. For instance, vertex corrections and Z exchanges do not affect γ, but corrections from box diagrams (Fig. 21) carry a different weak phase. The dominant contribution is effectively due to t and b running in the loop. For $b \to us\bar{c}$ transitions we have a tree level contribution with $\sim V_{ub}V_{cs}^*$ CKM structure, while the box diagram has $\sim (V_{tb}V_{ts}^*)(V_{ub}V_{cb}^*)$. Since this has

Table 6: The ultimate NP scales that can be probed using different observables listed in the first column. They are given by saturating the theoretical errors given respectively by 1) $\delta\gamma/\gamma = 10^{-6}$, 2) optimistically assuming no error on f_B, so that ultimate theoretical error just from electroweak corrections, 3) using SM predictions in Ref. [83], 4) optimistically assuming perturbative error estimates $\delta\beta/\beta$ 0.1 % [314], and 5) from bounds for $\mathrm{Re}\, C_1(\mathrm{Im}\, C_1)$ from UTfitter [249].

Probe	Λ_{NP} for (N)MFV NP	Λ_{NP} for gen. FV NP
γ from $B \to DK$[1)]	$\Lambda \sim \mathcal{O}(10^2$ TeV)	$\Lambda \sim \mathcal{O}(10^3$ TeV)
$B \to \tau\nu$[2)]	$\Lambda \sim \mathcal{O}(1$ TeV)	$\Lambda \sim \mathcal{O}(30$ TeV)
$b \to ss\bar{d}$[3)]	$\Lambda \sim \mathcal{O}(1$ TeV)	$\Lambda \sim \mathcal{O}(10^3$ TeV)
β from $B \to J/\psi\, K_S$[4)]	$\Lambda \sim \mathcal{O}(50$ TeV)	$\Lambda \sim \mathcal{O}(200$ TeV)
$K - \bar{K}$ mixing[5)]	$\Lambda > 0.4$ TeV (6 TeV)	$\Lambda > 10^{3(4)}$ TeV

the same weak phase, it does not introduce a shift in γ. For $b \to cs\bar{u}$ transitions, on the other hand, the tree level is $\sim V_{cb}V_{us}^*$, while the box diagram $\sim (V_{tb}V_{ts}^*)(V_{cb}V_{ub}^*)$. The two contributions have *different* weak phases, which means that the shift $\delta\gamma$ is non-zero.

We estimate the size of this effect by integrating over both t and b at the same time [315]. The electroweak corrections in the effective theory are then described by a local operator whose matrix elements are easier to estimate. The Wilson coefficient of the operator, however, contains large logarithms, $\log(m_b/m_W)$. Since we are only interested in $\mathcal{O}(1)$ estimates, the obtained precision suffices without resummation. If one resums $\log(m_b/m_W)$ then nonlocal contributions are also generated. As a rough estimate we can keep only the local contributions, which suffices for our purposes. The irreducible theory error on γ is conservatively estimated to be $\delta\gamma/\gamma < \mathcal{O}(10^{-6})$ (most likely it is even $\delta\gamma/\gamma \lesssim \mathcal{O}(10^{-7})$).

This is fantastically precise and it would be absolutely marvellous, if experiment could be pushed to this limit. Clearly the limiting factor in finding a small shift in γ will be how well it can be measured in different processes, but it is nonetheless interesting to consider would could be learnt in case such small deviations could be observed. How high NP scales can be probed using γ from $B \to DK$ in principle?

Assuming MFV one can probe $\Lambda_{\rm NP} \sim 10^2$ TeV, while assuming general flavour violating (FV) NP one can probe $\Lambda_{\rm NP} \sim 10^3$ TeV (where MFV and general FV NP scales are defined as in Ref. [249]). This is by far the most precise potential probe of (N)MFV, as shown in Table 6. The reason for such high scales is the small theoretical error on γ from $B \to DK$. The downside is the immense amount of data one would need: the ultimate precision will not be reached even by the LHCb upgrade (whereas for other observables the limitation will be reached by next generation experiments). For more realistic data-sets the NP scale reach is easily scaled, since Λ_{NP} one probes goes as fourth root of statistics, $L^{1/4}$. With the LHCb upgrade, an uncertainty of $< 1^\circ$ can be achieved (see Sec. 3.4.5), so that NP scales approaching $\Lambda_{\rm NP} \sim 5(50)$ TeV can be probed for NMFV (general FV) NP.

3.4.3 Current LHCb experimental situation

First results from LHCb in this area include a measurement using $B^- \to DK^-$ with the GLW and ADS final states [43]. GLW-type analyses have also been performed using $B^0 \to DK^{*0}$ [316] and $B^- \to D\pi^+\pi^-K^-$ [317]. A measurement of the branching ratio of $B_s^0 \to D_s^\mp K^\pm$ has also been performed [311]. Several other analyses, including studies of GGSZ-type final states, are in progress.

These measurements all share common selection strategies. They benefit greatly from boosted decision tree algorithms, which combine up to 20 kinematic variables to effectively suppress combinatorial backgrounds. Charmless backgrounds are suppressed by exploiting the large forward boost of the $D_{(s)}$ meson through a cut on its flight distance.

In the GLW/ADS analysis [43] of 1.0 fb^{-1} of $\sqrt{s} = 7$ TeV data collected in 2011, we use the *CP* eigenstates $D \to K^+K^-$, $\pi^+\pi^-$, and the flavour eigenstate $D \to \pi^-K^+$. We measure the *CP* asymmetries defined in Eq. 60, and the ratios $R_\pm$ defined in Eq. 63, for both the $B \to DK$ signal and the abundant $B \to D\pi$ control channel. The latter has limited sensitivity to γ but provides a large control sample from which probability density functions are shaped, and can be used to help reduce certain systematic uncertainties. We also use the control channel to measure three ratios of partial widths

$$R^f_{K/\pi} = \frac{\Gamma(B^- \to [f]_D K^-) + \Gamma(B^+ \to [f]_D K^+)}{\Gamma(B^- \to [f]_D \pi^-) + \Gamma(B^+ \to [f]_D \pi^+)}\,, \tag{73}$$

where f represents KK, $\pi\pi$ and the favoured $K\pi$ mode. The signal yields are estimated by a simultaneous fit to 16 independent subsamples, defined by the charges ($\times 2$), the D final states ($\times 4$), and the K or π nature of the bachelor hadron ($\times 2$). Figure 22 shows the projections of the suppressed $\pi^\pm K^\mp$ subsamples. It is crucial to control the cross feed of the abundant $B^- \to D\pi^-$ decays into the signal decays. For this we rely on the two RICH detectors, which allow to place particle identification (PID) cuts on the bachelor hadron. The systematic uncertainties are dominated by knowledge of the intrinsic charge asymmetry of the detector, and by the uncertainty on the PID. We find

$$\begin{aligned} R_{CP+} &= \quad 1.007 \pm 0.038 \pm 0.012\,, \\ A_{CP+} &= \quad 0.145 \pm 0.032 \pm 0.010\,, \\ R_- &= \quad 0.0073 \pm 0.0023 \pm 0.0004\,, \\ R_+ &= \quad 0.0232 \pm 0.0034 \pm 0.0007\,, \end{aligned}$$

where the first error is statistical and the second systematic; R_{CP+} is computed from $R_{CP+} \approx \langle R^{KK}_{K/\pi}, R^{\pi\pi}_{K/\pi}\rangle / R^{K\pi}_{K/\pi}$ with an additional 1 % systematic uncertainty assigned to account for the approximation; A_{CP+} is computed as $A_{CP+} = \langle A^{KK}_K, A^{\pi\pi}_K\rangle$. From the $R_\pm$ we also compute

$$\begin{aligned} R_{\rm ADS} &= \quad 0.0152 \pm 0.0020 \pm 0.0004\,, \\ A_{\rm ADS} &= -0.52 \pm 0.15 \pm 0.02\,, \end{aligned}$$

as $R_{\rm ADS} = (R_- + R_+)/2$ and $A_{\rm ADS} = (R_- - R_+)/(R_- + R_+)$. To summarise, the $B^\pm \to DK^\pm$ ADS mode is observed with $\approx 10\sigma$ statistical significance when comparing the maximum likelihood to that of the null hypothesis. This mode displays evidence (4.0σ) of a large negative asymmetry, consistent with previous experiments [296–298]. The combined asymmetry A_{CP+} is smaller than (but compatible with) previous measurements [318, 319]. It is 4.5σ significant. We compare the maximum likelihood with that under the null-hypothesis in all three D final states where the bachelor is a kaon, diluted by the non-negligible correlated systematic uncertainties. From this we observe, with a total significance of 5.8σ, direct CP violation in $B^\pm \to DK^\pm$ decays.

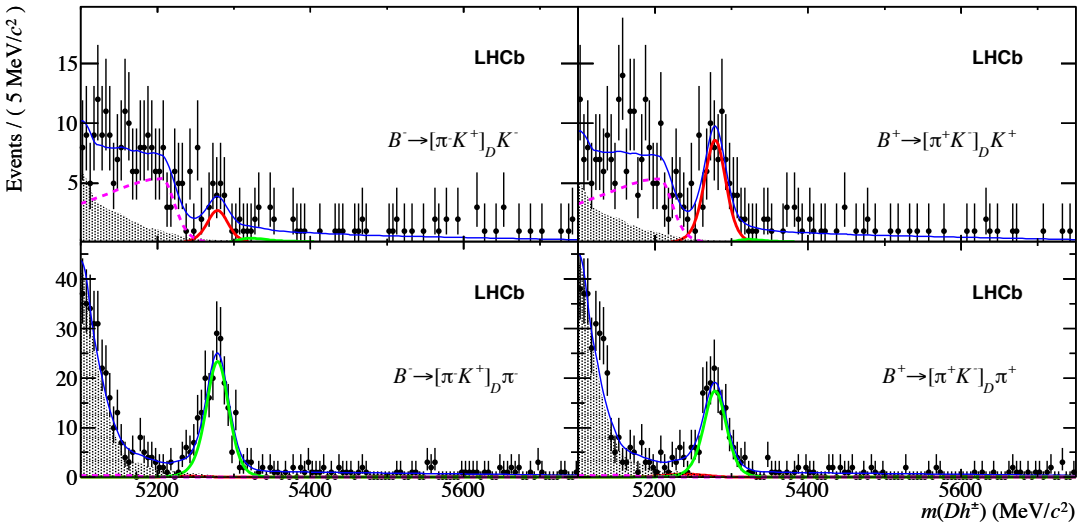

Figure 22: Invariant mass distributions of selected $B^\pm \to [\pi^\pm K^\pm]_D h^\pm$ candidates: (left) B^- candidates, (right) B^+ candidates. In the top plots, the bachelor track passes a kaon PID cut and the B candidates are reconstructed assigning this track the kaon mass. The remaining events are placed in the bottom row and are reconstructed with a pion mass hypothesis. The dark (red) curve represents the $B \to DK^\pm$ events, the light (green) curve is $B \to D\pi^\pm$. The shaded contribution are partially reconstructed events and the thin line shows the total PDF which also includes a linear combinatoric component. The broken line represents the partially reconstructed, but Cabibbo favoured, $\overline{B}{}^0_s \to D^0 K^+ \pi^-$ decays where the pion is lost.

The analysis of the $B^0_s \to D^\mp_s K^\pm$ decay mode [311] is based on a sample corresponding to an integrated luminosity of 0.37 fb^{-1}, collected in 2011 at a centre-of-mass energy of $\sqrt{s} = 7$ TeV. This decay mode has been observed by the CDF [320] and Belle [321] collaborations, who measured its branching fraction with an uncertainty around 23 % [193]. In addition to $B^0_s \to D^\mp_s K^\pm$, the channels $B^0 \to D^-\pi^+$and $B^0_s \to D^-_s \pi^+$are analysed. They are characterised by a similar topology and therefore are good control and normalisation channels. PID criteria are used to separate the Cabibbo favoured from the suppressed modes, and to suppress misidentified backgrounds.

The signal yields are obtained from extended maximum likelihood unbinned fits to the data. The fits include components for the combinatorial background and several

sources of background from b hadron decays. The most important is the misidentified $B_s^0 \to D_s^- \pi^+$ decay. Its shape is fixed from data using a reweighting procedure [322] while the yield is left free to float. A similar procedure is applied to a simulated data sample to extract the shape of the $B^0 \to D^- K^+$ misidentified background. The fit results are shown in Fig. 23.

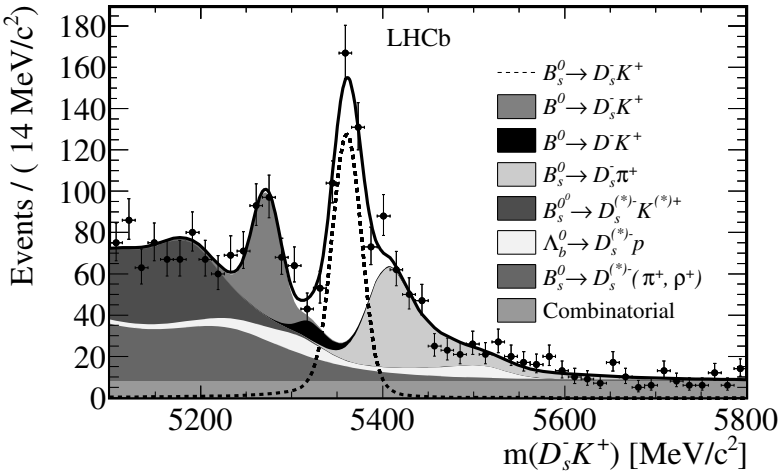

Figure 23: Mass distribution of the $B_s^0 \to D_s^\mp K^\pm$ candidates. The stacked background shapes follow the same top-to-bottom order in the legend and in the plot.

Correcting the raw signal yields for PID and selection efficiency differences the ratio

$$\frac{\mathcal{B}(B_s^0 \to D_s^\mp K^\pm)}{\mathcal{B}(B_s^0 \to D_s^- \pi^+)} = 0.0646 \pm 0.0043 \pm 0.0025\,, \tag{74}$$

is obtained, where the first uncertainty is statistical and the second is systematic. Using the measured relative yield of $B^0 \to D^- \pi^+$, the known $B^0 \to D^- \pi^+$ branching fraction [193], and the recent f_s/f_d measurement [69], the branching fractions

$$\mathcal{B}(B_s^0 \to D_s^- \pi^+) = (2.95 \pm 0.05 \pm 0.17\,^{+0.18}_{-0.22}) \times 10^{-3}\,, \tag{75}$$
$$\mathcal{B}(B_s^0 \to D_s^\mp K^\pm) = (1.90 \pm 0.12 \pm 0.13\,^{+0.12}_{-0.14}) \times 10^{-4}\,, \tag{76}$$

are obtained, where the first uncertainty is statistical, the second is the experimental systematic uncertainty, and the third is from the f_s/f_d measurement. Both measurements are significantly more precise than the previous world averages [193].

3.4.4 Measurements of γ using loop mediated decays

CP violation in $B_{d,s}$ decays plays a fundamental role in testing the consistency of the CKM paradigm in the SM and in probing virtual effects of heavy new particles.

With the advent of the B factories, the Gronau-London (GL) [323] isospin analysis of $B \to \pi\pi$ decays has been a precious source of information on the phase of the CKM matrix.

Although the method allows a full determination of the weak phase and of the relevant hadronic parameters, it suffers from discrete ambiguities that limit its constraining power. It is however possible to reduce the impact of discrete ambiguities by adding information on hadronic parameters [324, 325]. In particular, as noted in Refs. [45, 326, 327], the hadronic parameters entering the $B^0 \to \pi^+\pi^-$ and the $B_s^0 \to K^+K^-$ decays are connected by U-spin, so that experimental knowledge of $B_s^0 \to K^+K^-$ can improve the extraction of the CKM phase with the GL analysis. Indeed, in Ref. [325], the measurement of $\mathcal{B}(B_s^0 \to K^+K^-)$ was used to obtain an upper bound on one of the hadronic parameters.

LHCb recently measured [44] the time-dependent CP asymmetries using decays to CP eigenstates, namely $B^0 \to \pi^+\pi^-$ and $B_s^0 \to K^+K^-$, thereby permitting the use of the the U-spin strategy proposed by Fleischer (F) [45, 326, 327] to extract the CKM phase from a combined analysis of $B^0 \to \pi^+\pi^-$ and the $B_s^0 \to K^+K^-$ decays. However, as shown explicitly below, this strategy alone suffers from a sizable dependence on the breaking of U-spin symmetry. In Ref. [46] the authors propose to perform a combined analysis of the GL modes plus $B_s^0 \to K^+K^-$ to obtain an optimal determination of the CKM phase within the SM. They show that this combined strategy has a milder dependence on the magnitude of U-spin breaking, allowing for a more solid estimate of the theory error. The experimental data used for such a determination of γ are summarised in Table 7.

The time-dependent CP asymmetry for a CP eigenstate f can be written as

$$A_{CP}(t) = \frac{A_f^{\rm dir}\cos(\Delta m t) + A_f^{\rm mix}\sin(\Delta m t)}{\cosh\left(\frac{\Delta\Gamma}{2}t\right) - A_f^{\Delta\Gamma}\sinh\left(\frac{\Delta\Gamma}{2}t\right)}, \tag{77}$$

where $A_f^{\rm dir}$ and $A_f^{\rm mix}$ parametrise direct and mixing-induced CP violation respectively, and the quantity $A_f^{\Delta\Gamma}$ is constrained by the consistency relation

$$\left(A_f^{\rm dir}\right)^2 + \left(A_f^{\rm mix}\right)^2 + \left(A_f^{\Delta\Gamma}\right)^2 = 1. \tag{78}$$

The results of the first LHCb determination of direct and mixing-induced CP violation in $B^0 \to \pi^+\pi^-$ and $B_s^0 \to K^+K^-$ decays [44] are shown in Table 7. The measurements of $A_{\pi\pi}^{\rm dir}$ and $A_{\pi\pi}^{\rm mix}$ are compatible with those from the B factories and yield 3.2σ evidence of mixing-induced CP violation, whereas $A_{KK}^{\rm dir}$ and $A_{KK}^{\rm mix}$ are measured for the first time ever.

Beyond the SM, NP can affect both the $B_{(s)}^0$–$\bar{B}_{(s)}^0$ amplitudes and the $b \to d(s)$ penguin amplitudes. Taking the phase of the mixing amplitudes from other measurements, for example from $b \to c\bar{c}s$ decays, one can obtain a constraint on NP in $b \to s$ (or $b \to d$) penguins. Alternatively, assuming no NP in the penguin amplitudes, one can obtain a constraint on NP in mixing.

The authors study the determination of γ in a simplified framework, neglecting SM correlations with other observables and using as input values $\sin 2\beta = 0.679 \pm 0.024$ [63] and $2\beta_s = (0 \pm 5)^\circ$ [30], obtained from $b \to c\bar{c}s$ decays. Clearly, the optimal strategy will be to include the combined analysis of the GL and F modes in a global fit of the CKM matrix plus possible NP contributions.

Table 7: Experimental data used in the analysis. The correlation column refers to the $A^{\rm mix}$ and $A^{\rm dir}$ measurements. Except for the results in Ref. [44], all other measurements have been averaged by HFAG [63]. The CP asymmetry of $B^+ \to \pi^+\pi^0$ has been reported for completeness, although it has not been used in the analysis.

Channel	$\mathcal{B} \times 10^6$	$A^{\rm mix}(\%)$	$A^{\rm dir}(\%)$	Corr.	Ref.
$B^0 \to \pi^+\pi^-$	5.11 ± 0.22	-65 ± 7	38 ± 6	0.08	[328–333]
$B^0 \to \pi^+\pi^-$	–	$-56 \pm 17 \pm 3$	$11 \pm 21 \pm 3$	-0.34	[44]
$B^0 \to \pi^0\pi^0$	1.91 ± 0.23	–	43 ± 24	–	[328, 332, 334]
$B^+ \to \pi^+\pi^0$	5.48 ± 0.35	–	2.6 ± 3.9	–	[331, 332, 335]
$B_s^0 \to K^+K^-$	25.4 ± 3.7	$17 \pm 18 \pm 5$	$2 \pm 18 \pm 4$	-0.1	[44, 333, 336]

The GL and F analyses were formulated with different parametrisations of the decay amplitudes. In order to use the constraints in a global fit one can write the amplitudes as follows:

$$\begin{aligned}
&A(B^0 \to \pi^+\pi^-) = C(e^{i\gamma} - de^{i\theta})\,, && A(\bar{B}^0 \to \pi^+\pi^-) = C(e^{-i\gamma} - de^{i\theta})\,,\\
&A(B^0 \to \pi^0\pi^0) = \tfrac{C}{\sqrt{2}}(Te^{i\theta_T}e^{i\gamma} + de^{i\theta})\,, && A(\bar{B}^0 \to \pi^0\pi^0) = \tfrac{C}{\sqrt{2}}(Te^{i\theta_T}e^{-i\gamma} + de^{i\theta})\,,\\
&A(B^+ \to \pi^+\pi^0) = \tfrac{A(B^0\to\pi^+\pi^-)}{\sqrt{2}} + A(B^0 \to \pi^0\pi^0)\,, && A(B^- \to \pi^-\pi^0) = \tfrac{A(\bar{B}^0\to\pi^+\pi^-)}{\sqrt{2}} + A(\bar{B}^0 \to \pi^0\pi^0)\,,\\
&A(B_s^0 \to K^+K^-) = C'\tfrac{\lambda}{1-\lambda^2/2}(e^{i\gamma} + \tfrac{1-\lambda^2}{\lambda^2}d'e^{i\theta'})\,, && A(\bar{B}_s^0 \to K^+K^-) = C'\tfrac{\lambda}{1-\lambda^2/2}(e^{-i\gamma} + \tfrac{1-\lambda^2}{\lambda^2}d'e^{i\theta'})\,,
\end{aligned} \tag{79}$$

where the magnitude of $V_{ub}V_{ud}^*$ has been reabsorbed in C, and the magnitude of $V_{cb}V_{cd}^*/(V_{ub}V_{ud}^*)$ has been reabsorbed in d. In the exact U-spin limit, one has $C = C'$, $d = d'$ and $\theta = \theta'$. The authors neglected isospin breaking in $B^0 \to \pi\pi$, since its impact on the extraction of the weak phase is at the level of 1° [337–340]. The physical observables entering the analysis are:

$$\mathcal{B}(B \to MM) = F(B)\frac{|A(B \to MM)|^2 + |A(\bar{B} \to MM)|^2}{2}\,, \tag{80}$$

$$A^{\rm dir} = \frac{|A(\bar{B} \to MM)|^2 - |A(B \to MM)|^2}{|A(\bar{B} \to MM)|^2 + |A(B \to MM)|^2}\,, \qquad A^{\rm mix} = \frac{2{\rm Im}\left(e^{-i\phi_M(B)}\frac{A(\bar{B}\to MM)}{A(B\to MM)}\right)}{1 + \left|\frac{A(\bar{B}\to MM)}{A(B\to MM)}\right|^2}\,,$$

where $\phi_M(B^0) = 2\beta$, $\phi_M(B_s^0) = -2\beta_s$ in the SM, and $F(B^0) = 1$, $F(B^+) = \tau_{B^+}/\tau_{B^0} = 1.08$, $F(B_s^0) = \tau_{B_s^0}/\tau_{B^0}(m_{B^0}^2/m_{B_s^0}^2)\sqrt{(M_{B_s^0}^2 - 4M_{K^+}^2)/(M_{B^0}^2 - 4M_{\pi^+}^2)} = 0.9112$.

In the GL approach, one extracts the PDF for the angle $\alpha = \pi - \beta - \gamma$ of the Unitarity Triangle (UT) from the measurements of the three $\mathcal{B}(B \to \pi\pi)$, $A^{\rm mix}_{\pi^+\pi^-}$, $A^{\rm mix}_{\pi^+\pi^-}$, $A^{\rm dir}_{\pi^+\pi^0}$ and $A^{\rm dir}_{\pi^0\pi^0}$. Using the unitarity of the CKM matrix, it is possible to write the $B \to \pi\pi$ decay amplitudes and observables in terms of α instead of γ and β. However, for the purpose of connecting $B \to \pi\pi$ to $B_s^0 \to KK$ it is more convenient to use the parametrisation in Eq. (79). In this way, α (or, equivalently, γ), is determined up to discrete ambiguities, that correspond however to different values of the hadronic parameters. As discussed in detail in Ref. [325], the shape of the PDF obtained in a Bayesian analysis depends on the allowed range for the hadronic parameters. For example, using the data in Table 7, solving for C and choosing flat *a priori* distributions for $d \in [0, 2]$, $\theta \in [-\pi, \pi]$, $T \in [0, 1.5]$ and $\theta_T \in [-\pi, \pi]$ the PDF for γ in Fig. 24 is obtained, corresponding to $\gamma = (68 \pm 15)^\circ$

($\gamma \in [25, 87]^\circ$ at 95 % probability). Using instead the F method, one can obtain a PDF for γ given a range for the U-spin breaking effects. In this method it was originally suggested to parametrise the U-spin breaking in C'/C using the result one would obtain in factorisation, namely

$$r_{\rm fact} = \left|\frac{C'}{C}\right|_{\rm fact} = 1.46 \pm 0.15\,, \tag{81}$$

where the error obtained using light-cone QCD sum rule calculations [341] has been symmetrised. However, this can only serve as a reference value, since there are non-factorisable contributions to C and C' that could affect this estimate. In this analysis, the non-factorisable U-spin breaking is parametrised as follows:

$$C' = r_{\rm fact} r_C C\,, \qquad {\rm Re}(d'e^{i\theta'}) = r_r {\rm Re}(de^{i\theta})\,, \qquad {\rm Im}(d'e^{i\theta'}) = r_i {\rm Im}(de^{i\theta})\,, \tag{82}$$

with r_C, r_r and r_i uniformly distributed in the range $[1-\kappa, 1+\kappa]$.

In Fig. 24 the PDF for γ obtained with the F method for three different values of U-spin breaking parameter $\kappa = 0.1, 0.3, 0.5$ is shown. The method is very precise for small amount of U-spin breaking ($\kappa = 0.1$), is comparable to the GL method for $\kappa = 0.3$, and becomes clearly worse for $\kappa = 0.5$. Thus, a determination of γ from the F method alone is subject to uncertainty on the size of U-spin breaking.

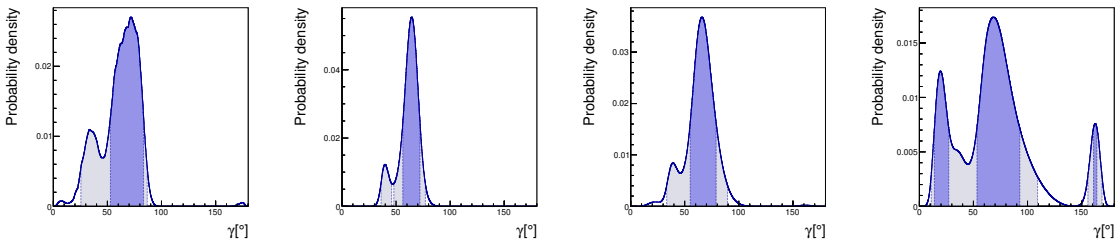

Figure 24: From left to right: PDF for γ obtained using the GL method as described in the text; PDF for γ obtained using the F method for $\kappa = 0.1, 0.3, 0.5$. Here and in the following, dark (light) areas correspond to 68 % (95 %) probability regions.

The result of the combined GL+F analysis it is reported in Fig. 25, where the PDF for γ for $\kappa = 0.1$, 0.3 and 0.5 is shown. The result of the combined analysis is much more stable against the allowed amount of U-spin breaking. In Fig. 25 the 68 % probability region for γ obtained using the combined method as a function of κ is also shown, and compared to the GL result. The combined method shows a considerable gain in precision even for very large values of κ. Actually, as can be seen in Fig. 26, where the posteriors for hadronic parameters and the U-spin breaking parameter r_C are reported, the 68 % probability range for r_C is between 0.4 and 0.9. The fact that the r_C posterior is not centred around 1, but the product $r_C r_{\rm fact}$ is close to 1, may signal a failure of factorisation and/or of the QCD sum rule estimate of $r_{\rm fact}$. On the other hand, the posterior for d' and θ' are well compatible with small U-spin breaking. In any case, the lesson to be learnt

from Fig. 26 is that values of κ up to 0.6 or 0.7 cannot be excluded, but nevertheless the combined method remains useful. This happens because the peak around $\gamma \sim 30°$ in the GL result corresponds to values of θ that are different from the ones needed in the F analysis to obtain similar values of γ, while the peak at $\gamma \sim 70°$ is obtained for the same values of hadronic parameters in both the GL and F analyses.

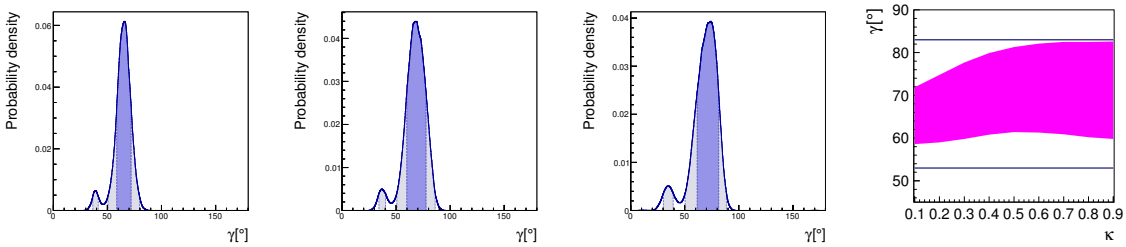

Figure 25: From left to right: PDF for γ obtained using the combined method for $\kappa = 0.1$, 0.3, 0.5; 68 % probability region for γ obtained using the combined method (filled area) or the GL method (horizontal lines) as a function of κ.

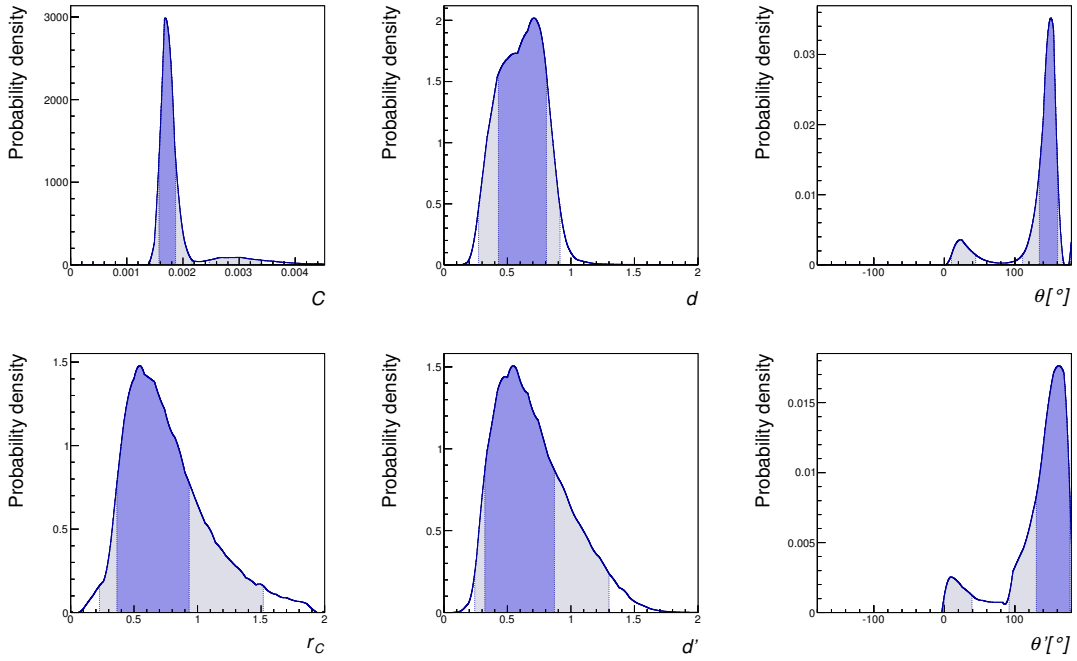

Figure 26: From left to right and from top to bottom: PDF for C, d, θ, r_C, d', θ' obtained using the combined method for $\kappa = 0.9$.

NP could affect the determination of γ in the combined method by giving (electroweak) penguin contributions with a new CP-violating phase. If one assumes that the isospin

analysis of the GL channels is still valid, barring order-of-magnitude enhancements of electroweak penguins in $B \to \pi\pi$, and if one assume for concreteness that NP enters only $b \to s$ penguins, in the framework of a global fit, one can simultaneously determine γ and the NP contribution to $b \to s$ penguins. For the purpose of illustration, the value of γ from tree-level processes, $\gamma_{\rm tree} = (76 \pm 9)^\circ$ is used as input [249],[28] and we look at the posterior for γ and for the NP penguin amplitude. Writing

$$\begin{aligned} A(B_s^0 \to K^+K^-) &= C' \frac{\lambda}{1-\lambda^2/2}(e^{i\gamma} + \frac{1-\lambda^2}{\lambda^2}\left(d' e^{i\theta'} + e^{i\phi_{\rm NP}} d'_{\rm NP} e^{i\theta'_{\rm NP}}\right)), \\ A(\bar{B}_s^0 \to K^+K^-) &= C' \frac{\lambda}{1-\lambda^2/2}(e^{-i\gamma} + \frac{1-\lambda^2}{\lambda^2}\left(d' e^{i\theta'} + e^{-i\phi_{\rm NP}} d'_{\rm NP} e^{i\theta'_{\rm NP}}\right)), \end{aligned} \tag{83}$$

and taking uniformly distributed $d'_{\rm NP} \in [0,2]$ and $\phi_{\rm NP}, \theta'_{\rm NP} \in [-\pi, \pi]$ the PDF reported in Fig. 27 is obtained for $\kappa = 0.5$. This yields $\gamma = (74 \pm 7)^\circ$, and a 95 % probability upper bound on $d'_{\rm NP}$ around 1. Clearly, the bound is stronger for large values of $\phi_{\rm NP}$.

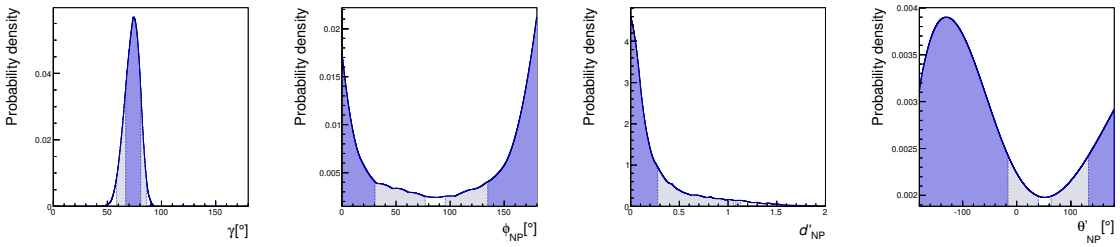

Figure 27: From left to right: PDF for γ, $\phi_{\rm NP}$, $d'_{\rm NP}$ and $\theta'_{\rm NP}$ obtained using the combined method for $\kappa = 0.5$.

Finally, $B_s^0 \to KK$ decays can also be used to extract $2\beta_s$ in the SM. The optimal choice in this respect is represented by $B_s^0 \to K^{(*)0}\bar{K}^{(*)0}$ (with $B^0 \to K^{(*)0}\bar{K}^{(*)0}$ as U-spin related control channel to constrain subleading contributions), since in this channel there is no tree contribution proportional to $e^{i\gamma}$ [48,284]. However, the combined analysis described above, in the framework of a global SM fit, can serve for the same purpose. To illustrate this point, the GL+F analysis is performed, taking as input the SM fit result $\gamma = (69.7 \pm 3.1)^\circ$ [249] and not using the measurement of $2\beta_s$ from $b \to c\bar{c}s$ decays. In this way, $2\beta_s = (3 \pm 14)^\circ$ is obtained for $\kappa = 0.5$. The analysis can be also performed not using the measurement of γ, in this case the result is $2\beta_s = (6 \pm 14)^\circ$. With improved experimental accuracy, this determination could become competitive with that from $b \to c\bar{c}s$ decays. Once results of time-dependent analyses of the $B_{(s)} \to K^{(*)0}\bar{K}^{(*)0}$ channels are available these may also provide useful constraints.[29]

[28] Note that the value of γ quoted here differs from that obtained from the full CKM fit (given in Table 3) due to the different inputs used.

[29] The proposal of Ref. [48] has been recently critically reexamined in Ref. [342]. The present analysis shows no particular enhancement of the contribution proportional to $e^{i\gamma}$ in $B_s^0 \to K^+K^-$, in agreement with the expectation that $B_s^0 \to K^{(*)0}\bar{K}^{(*)0}$ should be penguin-dominated to a very good accuracy.

To conclude, the usual GL analysis to extract α from $B^0 \to \pi\pi$ can be supplemented with the inclusion of the $B_s^0 \to K^+K^-$ modes, in the framework of a global CKM fit. The method optimises the constraining power of these decays and allows to derive constraints on NP contributions to penguin amplitudes or on the B_s^0 mixing phase and illustrates these capabilities with a simplified analysis, neglecting correlations with other SM observables.

3.4.5 Prospects of future LHCb measurements

In addition to the modes discussed above, any channel that involves the interference of $b \to c\bar{u}s$ and $b \to u\bar{c}s$ transitions is potentially sensitive to γ. Many of these modes can be analysed in the upgraded phase of LHCb. Such modes are:

1. $B^+ \to DK^+\pi^-\pi^+$ where, similarly to the $B \to DK$ mode, the neutral D can be reconstructed either in the two-body (ADS and GLW-like measurement) or multibody (GGSZ-like measurement) final state. The observation of the Cabibbo favoured mode in LHCb data [343] indicates a yield only twice lower than that for the $B \to DK$ mode, which makes it competitive for the measurement of γ. First results of a GLW analysis of this channel was presented at ICHEP 2012 [317]. However, two unknown factors affect the expected γ sensitivity. First, since this is a multibody decay, the overlap between the interfering amplitudes is in general less than 100 %; this is accounted for by the coherence factor $0 < \kappa < 1$ which enters the interference term in Eqs. (56), (57), (61), (62) as an unknown parameter. Second, the value of r_B can be different from that in $B \to DK$ and is unmeasured yet, although it is expected [294] that it can be larger in this decay than in $B \to DK$.

2. $B^0 \to DK^+\pi^-$. Although the rate of these decays is smaller that that of $B^+ \to DK^+$, both interfering amplitudes are colour-suppressed, therefore the expected value of r_B is larger, $r_B \simeq 0.3$. As a result, the sensitivity to γ should be similar to that in the $B \to DK$ modes. First results on a GLW analysis of $B^0 \to DK^{*0}$ were presented at ICHEP 2012 [316]. Depending on the content of $B^0 \to D^0K^+\pi^-$ and $B^0 \to \overline{D}^0K^+\pi^-$ amplitudes, the optimal strategy may involve Dalitz plot analysis of the B^0 decay [344, 345]. In this case, control of amplitude model uncertainty will become essential for a precision measurement; it can be eliminated by studying the decays $B^0 \to DK^+\pi^-$ with $D \to K^0_S\pi^+\pi^-$ [346].

3. $B_s^0 \to D\phi$. This mode is not self-tagging (the flavor of initial B_s^0 cannot be determined from the decay products), but sensitivity to γ can be obtained from untagged time-integrated measurements using several different neutral D decay modes [347, 348]. The first evidence for the three-body decay $B_s^0 \to \overline{D}^0K^+K^-$ has just been reported by LHCb [349], and investigation of its resonant structure is in progress.

4. $B_c^+ \to DD_s^+$. B_c^+ production in pp collisions is significantly suppressed, however, in this mode the magnitude of CP violation is expected to be $\mathcal{O}(100\,\%)$: the two

interfering amplitudes are of the same magnitude because the $b \to u\bar{c}s$ amplitude is colour allowed, while the $b \to c\bar{u}s$ amplitude is colour suppressed [350–353].

5. $\Lambda_b^0 \to D\Lambda^0$ and $\Lambda_b^0 \to DpK^-$. Measurement of γ from analysis of $\Lambda_b^0 \to D\Lambda^0$ mode was proposed in Ref. [354]. This method allows one to measure γ is a model-independent way by comparing the S- and P-wave amplitudes. However, this mode is problematic to reconstruct at LHCb because of the poorly defined Λ_b vertex (both particles from its decay are long-lived) and low efficiency of Λ^0 reconstruction. Alternatively, one can consider a similar measurement with the decay $\Lambda_b \to DpK^-$. This mode has been observed in early LHCb data [355].

Table 8 shows the expected sensitivity to γ from tree level decays in the upgrade scenario. The LHCb upgrade is the only proposed experiment which will be able to reach sub-degree precision on γ.

Table 8: Estimated precision of γ measurements with $50\,\text{fb}^{-1}$ for various charmed B decay modes.

Decay mode	γ sensitivity
$B \to DK$ with $D \to hh'$, $D \to K\pi\pi\pi$	1.3°
$B \to DK$ with $D \to K^0_S\pi\pi$	1.9°
$B \to DK$ with $D \to 4\pi$	1.7°
$B^0 \to DK\pi$ with $D \to hh'$, $D \to K^0_S\pi\pi$	1.5°
$B \to DK\pi\pi$ with $D \to hh'$	$\sim 3^\circ$
Time-dependent $B_s \to D_sK$	2.0°
Combined	$\sim 0.9^\circ$

Measurement of γ and ϕ_s by means of the CP-violating observables from loop mediated decays $B^0 \to \pi^+\pi^-$ and $B_s^0 \to K^+K^-$ was discussed in Sec. 3.4.4. Extrapolating the current sensitivity on A^{dir} and A^{mix} to the upgrade scenario, when 50 fb^{-1} of integrated luminosity will be collected, LHCb will be able to reach a statistical sensitivity $\sigma_{\text{stat}}(A^{\text{dir}}) \approx \sigma_{\text{stat}}(A^{\text{mix}}) \simeq 0.008$ in both $B^0 \to \pi^+\pi^-$ and $B_s^0 \to K^+K^-$. This corresponds to a precision on γ of 1.4°, and on ϕ_s of 0.01 rad, assuming perfect U-spin symmetry.

4 Mixing and *CP* violation in the charm sector

4.1 Introduction

The study of D mesons offers a unique opportunity to access up-type quarks in flavour changing neutral current (FCNC) processes. It probes scenarios where up-type quarks play a special role, such as supersymmetric models with alignment [356, 357] and more generally models in which quark mixing is generated in the up sector. It offers complementary constraints on possible NP contributions to those arising from the measurements of FCNC processes of down-type quarks (B or K mesons).

The neutral D system is the latest and last system of neutral mesons where mixing between particles and anti-particles has been established. The mixing rate is consistent with, but at the upper end of, SM expectations [358] and constrains many NP models [359]. More precise D^0-$\overline{D}^0$ mixing measurements will provide even stronger constraints. However, increasingly the focus has been shifting to *CP* violation observables, which provide cleaner tests of the SM. First evidence for direct *CP* violation in the charm sector has been reported by the LHCb collaboration in the study of the difference of the time-integrated asymmetries of $D^0 \to K^+K^-$ and $D^0 \to \pi^+\pi^-$ decay rates through the parameter $\Delta\mathcal{A}_{CP}$ [8]. No evidence of indirect *CP* violation has yet been found. As discussed in detail below, these results on *CP* violation in the charm sector appear marginally compatible with the SM but contributions from NP are not excluded.

The mass eigenstates of neutral D mesons, $|D_{1,2}\rangle$, with masses $m_{1,2}$ and widths $\Gamma_{1,2}$ can be written as linear combinations of the flavour eigenstates $|D_{1,2}\rangle = p|D^0\rangle \pm q|\overline{D}^0\rangle$, with complex coefficients p and q which satisfy $|p|^2 + |q|^2 = 1$. The average mass and width are defined as $m \equiv (m_1+m_2)/2$ and $\Gamma \equiv (\Gamma_1+\Gamma_2)/2$. The D mixing parameters are defined using the mass and width difference as $x_D \equiv (m_2-m_1)/\Gamma$ and $y_D \equiv (\Gamma_2-\Gamma_1)/2\Gamma$. The phase convention of p and q is chosen such that $CP|D^0\rangle = -|\overline{D}^0\rangle$. First evidence for mixing of neutral D^0 mesons was discovered in 2007 by Belle and BaBar [360, 361] and is now well established [63]: the no-mixing hypothesis is excluded at more than $10\,\sigma$ for the world average ($x_D = 0.63\,^{+0.19}_{-0.20}\,\%$, $y_D = 0.75 \pm 0.12\,\%$).

It is convenient to group hadronic charm decays into three categories. Cabibbo-favoured (CS) decays, such as $D^0 \to K^-\pi^+$, are mediated by tree amplitudes, and therefore no direct *CP* violation effects are expected. The same is true for doubly-Cabibbo-suppressed (DCS) decays, such as $D^0 \to K^+\pi^-$, even though these are much rarer. Singly-Cabibbo-suppressed (SCS) decays, on the other hand, can also have contributions from penguin amplitudes, and therefore direct *CP* violation is possible, even though the penguin contributions are expected to be small. Within this classification, it should be noted that some decays to final states containing K^0_S mesons, *e.g.* $D^0 \to K^0_S\rho^0$, have both CS and DCS contributions which can interfere [362]. Within the SM, however, *CP* violation effects are expected to be negligible.

LHCb is ideally placed to carry out a wide physics programme in the charm sector, thanks to the high production rate of open charm, with cross-section 6.10 ± 0.93 mb [72]: one tenth of LHC interactions produce charm hadrons. Its PID system provides excellent

separation between pions and kaons in the momentum range between 2 and 100 GeV/c, and also provides clean identification of muons, electrons and protons. This allows high purity samples to be obtained both for hadronic and muonic decays. The large boost of the D hadrons produced at LHCb is beneficial for time-dependent studies. LHCb has the potential to improve the precision on all the key observables in the charm sector in the next years.

In the remainder of this section the key observables in the charm sector are described, and the current status and near term prospects of the measurements at LHCb are reviewed. A discussion of the implications of the LHCb results to date follows, motivating improved measurements and studies of additional channels. The potential of the LHCb upgrade to make the precise measurements needed to challenge the theory is then described.

4.1.1 Key observables

Currently the most precise individual measurements of mixing parameters are those of the relative effective lifetime difference between D^0 and $\overline{D}^0$ decays to CP eigenstates ($\hat{\Gamma}$ and $\hat{\bar{\Gamma}}$) and flavour specific final states (Γ), y_{CP}, which is defined as

$$y_{CP} = \frac{\hat{\Gamma} + \hat{\bar{\Gamma}}}{2\Gamma} - 1 \approx \eta_{CP} \left[\left(1 - \frac{1}{8} A_m^2 \right) y_D \cos\phi - \frac{1}{2} (A_m) x_D \sin\phi \right], \tag{84}$$

where terms below order 10^{-4} have been ignored [363], η_{CP} is the CP eigenvalue of the final state, ϕ is the CP violating relative phase between q/p and $\bar{A}_f/A_f$ where $\overset{(-)}{A}_f$ are the decay amplitudes, and A_m represents a CP violation contribution from mixing ($|q/p|^{\pm 2} \approx 1 \pm A_m$).[30] In the limit of CP conservation y_{CP} is equal to the mixing parameter y. The resulting world average value for y_{CP} is $0.87 \pm 0.16\,\%$ [364][31] and is consistent with the value of y within the current accuracy.

The CP violating observable A_Γ quantifies the difference in decay rates of D^0 and $\overline{D}^0$ to a CP eigenstate and is defined as

$$A_\Gamma = \frac{\hat{\Gamma} - \hat{\bar{\Gamma}}}{\hat{\Gamma} + \hat{\bar{\Gamma}}} \approx \eta_{CP} \left[\frac{1}{2} (A_m + A_d) y_D \cos\phi - x_D \sin\phi \right], \tag{85}$$

where terms below order 10^{-4} have been ignored [363] and both mixing and direct CP contributions are assumed to be small. A_d is the contribution from direct CP violation ($|\bar{A}_f/A_f|^{\pm 2} \approx 1 \pm A_d$). The current world average of A_Γ is $0.02 \pm 0.16\,\%$ [63], consistent with the no CP violation hypothesis. Due to the smallness of x_D and y_D, A_Γ provides essentially the same information as a full time-dependent CP violation analysis of $D^0 \to K^+K^-$ decays.

[30] A_m can be determined from asymmetries in semileptonic charm decays, with the assumption of vanishing direct CP violation.

[31] New results presented by Belle at ICHEP 2012 [365] are not included in this average.

An alternative way to search for *CP* violation in charm mixing is with a time-dependent Dalitz plot analysis of D^0 and $\overline{D}^0$ decays to $K^0_S\pi^+\pi^-$ or $K^0_S K^+K^-$. Such analyses have been carried out at the B factories [366, 367]. Also in these cases no *CP* violation was observed.

In time-integrated analyses the measured rate asymmetry is

$$\mathcal{A}_{CP} \equiv \frac{\Gamma(D^0 \to f) - \Gamma(\overline{D}^0 \to f)}{\Gamma(D^0 \to f) + \Gamma(\overline{D}^0 \to f)} \approx a^{\rm dir}_{CP} - A_\Gamma \frac{\langle t \rangle}{\tau}, \tag{86}$$

where the direct *CP* asymmetry contribution is defined as

$$a^{\rm dir}_{CP} \equiv \frac{|A_f|^2 - |\bar{A}_f|^2}{|A_f|^2 + |\bar{A}_f|^2} \approx -\frac{1}{2} A_d \tag{87}$$

and $\langle t \rangle$ denotes the average decay time of the observed candidates.

A powerful way to reduce experimental systematic uncertainties is to measure the difference in time-integrated asymmetries in related final states. For the two-body final states K^+K^- and $\pi^+\pi^-$, this difference is given by

$$\begin{aligned} \Delta\mathcal{A}_{CP} \;&\equiv A_{CP}(K^+K^-) - A_{CP}(\pi^+\pi^-) \;=\; a^{\rm dir}_{CP}(K^+K^-) - a^{\rm dir}_{CP}(\pi^+\pi^-) \\ &\approx \Delta a^{\rm dir}_{CP} \left(1 + y\cos\phi \tfrac{\overline{\langle t \rangle}}{\tau}\right) + \left(a^{\rm ind}_{CP} + \overline{a^{\rm dir}_{CP}} y \cos\phi\right) \tfrac{\Delta\langle t \rangle}{\tau} \end{aligned} \tag{88}$$

where the *CP* violating phase ϕ is assumed to be universal [368], $\Delta X \equiv X(K^+K^-) - X(\pi^+\pi^-)$, $\overline{X} \equiv (X(K^+K^-) + X(\pi^+\pi^-))/2$ and the indirect *CP* asymmetry parameter is defined as $a^{\rm ind}_{CP} = -(A_m/2) y_D \cos\phi + x_D \sin\phi$. The ratio $\Delta\langle t \rangle/\tau$ is equal to zero for the lifetime-unbiased B factory measurements [369,370] and is 0.098 ± 0.003 for LHCb [8] and 0.25 ± 0.04 for CDF [371], therefore $\Delta\mathcal{A}_{CP}$ is largely a measure of direct *CP* violation.

The current most accurate measurements of $\Delta\mathcal{A}_{CP}$ from the LHCb collaboration and the CDF collaboration giving $(-0.82 \pm 0.21 \pm 0.11)\,\%$ [8] and $(-0.62 \pm 0.21 \pm 0.10)\,\%$ [372], respectively.[32] These results show first evidence of *CP* violation in the charm sector: the world average is consistent with no *CP* violation at only 0.006 % C.L. [63].

4.1.2 Status and near-term future of LHCb measurements

LHCb has a broad programme of charm physics, including searches for rare charm decays (see Sec. 2), spectroscopy and measurements of production cross-sections and asymmetries (see Sec. 5). In this section we will discuss only studies of mixing and *CP* violation. For reviews of the formalism, the reader is referred to Refs. [363, 374] and the references therein, and for an overview of new physics implications to Ref. [368].

Mixing and indirect *CP* violation occur only in neutral mesons. These are probed in a number of different decay modes, predominantly—but not exclusively—time-dependent ratio measurements. In most cases, the same analysis yields measurements of both mixing

[32] At ICHEP 2012, Belle also presented new results on $\Delta\mathcal{A}_{CP}$ [373], that are consistent with, but less precise than, those from LHCb and CDF.

and *CP* violation parameters, so we consider them together. By contrast, direct *CP* violation may occur in decays of both neutral and charged hadrons, and our primary sensitivity to it comes from time-integrated measurements—though it may affect certain time-dependent asymmetries as well, as discussed in Section 4.7.1.

We consider first mixing and indirect *CP* violation. Several classes of measurement are possible at LHCb, particularly:

- Measurements of the ratios of the effective D^0 lifetimes in decays to quasi-flavour-specific states (*e.g.* $D^0 \to K^-\pi^+$) and *CP* eigenstates f_{CP} (*e.g.* $D^0 \to K^-K^+$). These yield y_{CP}. Comparing the lifetime of $D^0 \to f_{CP}$ and $\overline{D}^0 \to f_{CP}$ yields the *CP* violation parameter A_Γ.

- Measurements of the time-dependence of the ratio of wrong-sign to right-sign hadronic decays (*e.g.* $D^0 \to K^+\pi^-$ *vs.* $D^0 \to K^-\pi^+$). These yield x'^2_D and y'_D, where

$$x'_D = x_D \cos\delta + y_D \sin\delta$$
$$y'_D = y_D \cos\delta - x_D \sin\delta$$

  and δ is the mode-dependent strong phase between the Cabibbo-favoured and doubly-Cabibbo-suppressed amplitudes. The mixing parameters can be measured independently for D^0 and $\overline{D}^0$ to constrain indirect *CP* violation, and the overall asymmetry in wrong-sign decay rates for D^0 and $\overline{D}^0$ gives the direct *CP* violation parameter A_d.

- Time-dependent Dalitz plot fits to self-conjugate final states (*e.g.* $D^0 \to K^0_S\pi^-\pi^+$). These combine features of the two methods above, along with simultaneous extraction of the strong phases relative to *CP* eigenstate final states. Consequently they yield measurements of x_D and y_D directly. Likewise, the indirect *CP* violation parameters $|q/p|$ and ϕ may be extracted, along with the asymmetry in phase and magnitude of each contributing amplitude (in a model-dependent analysis).

- Measurements of the ratio of time-integrated rates of wrong-sign to right-sign semileptonic decays (*e.g.* $D^0 \to \overline{D}^0 \to K^+l^-\bar{\nu}_l$ *vs.* $D^0 \to K^-l^+\nu_l$). These yield $(x^2_D + y^2_D)$ and A_m.

Within LHCb, analyses are planned or in progress for each of these methods, but are at quite different stages. The only publication to date is a measurement of y_{CP} and A_Γ from the 2010 data sample [53]. In addition, a preliminary result on the time-integrated wrong-sign rate in $D^0 \to K\pi$ from the 2010 sample is available [375]; this is a validation of the method rather than a measurement of mixing and *CP* violation parameters. A summary of what can be achieved with the 2010–2012 prompt charm samples is given in Table 9. Note that the observables are generally related to several physics parameters, such that the combined constraints are much more powerful than individual measurements. After analysing 2.5 fb^{-1} of data, we expect the mixing parameters x_D and y_D to be determined

at the level of $\mathcal{O}(\text{few} \times 10^{-4})$, and A_Γ to be measured with a similar uncertainty. This will represent a great improvement over the current world averages, which have $\sigma_{x_D} = 0.19\,\%$, $\sigma_{y_D} = 0.12\,\%$, and $\sigma_{A_\Gamma} = 0.23\,\%$.

Table 9: Projected statistical uncertainties with 1.0 and 2.5 fb^{-1} of LHCb data. Yields are extrapolated based on samples used in analyses of 2011 data; sensitivities are projected from these yields assuming $1/\sqrt{N}$ scaling based on reported yields and statistical uncertainties in published analyses from LHCb, BaBar, Belle, and CDF. The projected *CP*-violation sensitivities may vary depending on the values of the mixing parameters.

Sample	Observable	Sensitivity (1.0 fb^{-1})	Sensitivity (2.5 fb^{-1})
Tagged KK	y_{CP}	6×10^{-4}	4×10^{-4}
Tagged $\pi\pi$	y_{CP}	11×10^{-4}	7×10^{-4}
Tagged KK	A_Γ	6×10^{-4}	4×10^{-4}
Tagged $\pi\pi$	A_Γ	11×10^{-4}	7×10^{-4}
Tagged WS/RS $K\pi$	x'^2_D	7×10^{-5}	4×10^{-5}
Tagged WS/RS $K\pi$	y'_D	13×10^{-4}	8×10^{-4}
Tagged $K^0_S\pi\pi$	x_D	4×10^{-3}	3×10^{-3}
Tagged $K^0_S\pi\pi$	y_D	3×10^{-3}	2×10^{-3}
Tagged $K^0_S\pi\pi$	$\lvert q/p \rvert$	0.4	0.3
Tagged $K^0_S\pi\pi$	ϕ	25°	15°

For direct *CP* violation, control of systematic uncertainties associated with production and efficiency asymmetries is key. To date, we have used two techniques to mitigate these effects:

- Measurement of differences in asymmetry between two related final states, such that systematic effects largely cancel—for example, $A_{CP}(D^0 \to K^-K^+) - A_{CP}(D^0 \to \pi^-\pi^+)$ [8]. This is simplest with two-body or quasi-two-body decays. This is discussed in more detail in Sec. 4.1.3.

- Looking for asymmetries in the distributions of multi-body decays, such that differences in overall normalisation can be neglected and effects related to lab-frame kinematics are largely washed out — for example, in the Dalitz plot distribution of $D^+ \to K^-K^+\pi^+$ [376].

In the longer term, the goal is to extract the *CP* asymmetries for $D^0 \to K^+K^-$ and $D^0 \to \pi^+\pi^-$ separately, along with those for many other decay modes. To achieve this, it will be necessary to determine the production and detector efficiencies from data. Some progress has been made in this area, notably in the D_s^+ production asymmetry measurement [377], which involves an elegant determination of the pion reconstruction efficiency from $D^{*+} \to D^0\pi^+, D^0 \to K^-\pi^-\pi^+\pi^+$ decays in which one of the D^0 daughter pions is not used in the reconstruction. The detector asymmetries need to be determined

as functions of the relevant variables, and similarly, the production asymmetries can vary as functions of transverse momentum and pseudorapidity. Calibration with the level of precision and granularity needed for *CP* asymmetry measurements is difficult and we do not assume that it will be solved in a short time scale. Moreover, production asymmetries can be determined only with the assumption of vanishing *CP* asymmetry in a particular (usually CF) control mode. Therefore ultimately the resulting measurements of *CP* asymmetries for individual decay modes are not essentially different to $\Delta\mathcal{A}_{CP}$ measurements relative to CF decays.

A summary of analyses that are in progress or planned with the 2011–2012 data is given below:

$D^0 \to K^-K^+$, $\pi^-\pi^+$: Updates to the 0.6 fb^{-1} ΔA_{CP} analysis [8] are in progress, using both prompt charm and charm from semileptonic B decays. See Sec. 4.1.3.

$D^+_{(s)} \to K^0_S h^+$, ϕh^+: A ΔA_{CP}-style analysis is possible by comparing asymmetries in a CF control mode (*e.g.* $D^+ \to K^0_S\pi^+$) and the associated SCS mode (*e.g.* $D^+ \to \phi\pi^+$), taking advantage of the inherent symmetry of the $K^0_S \to \pi^-\pi^+$ and $\phi \to K^-K^+$ decays.[33] There are two points to take into account: the different kinematic distributions of the bachelor tracks (requiring binning or reweighting) and the *CP* asymmetry in the K^0_S decay.

$D^+ \to \pi^+\pi^-\pi^+$, $K^+K^-\pi^+$: A search for *CP* violation in $D^+ \to K^+K^-\pi^+$ with the model-independent (so-called "Miranda") technique [378] was published with the 2010 data sample [376], comprising 0.04 fb^{-1}. At this level of statistics, detector effects are negligible. However, from studies of control modes such as $D^+_s \to K^-K^+\pi^+$ we find that this is no longer the case with 1.0 fb^{-1} of data or more, so an update will require careful control of systematic effects. The $\pi^+\pi^-\pi^+$ final state should be more tractable, since the $\pi^\pm$ interaction asymmetry is a very weak function of momentum.

$D^0 \to \pi^-\pi^+\pi^-\pi^+$, $K^-K^+\pi^-\pi^+$: Previous high-statistics publications have focused mainly on T-odd moments [379], but there is further information in the distribution of final-state particles. A Miranda-style binned analysis or a comparable unbinned method [380] can be used. First results on the $D^0 \to \pi^-\pi^+\pi^-\pi^+$ decay were presented at ICHEP 2012 [381].

Baryonic decays: LHCb will also collect large samples of charmed baryons. Triggering presents a challenge, but trigger lines for several Λ^+_c decay modes of the form Λh^+ or $ph^-h'^+$ are already incorporated, allowing large samples to be recorded. In addition to the considerations outlined above for D meson decays, the large proton-antiproton interaction asymmetry and the possibility of polarisation in the initial state must also be taken into account.

[33] A small difference in kinematic distributions can occur in $\phi \to K^-K^+$ due to crossing resonances.

4.1.3 Experimental aspects of ΔA_{CP} and related measurements

The raw asymmetry measured for D^{*+}-tagged D^0 decays to a final state f is defined as:

$$A_{\rm raw}(f) \equiv \frac{N(D^{*+} \to D^0(f)\pi_s^+) \; - \; N(D^{*-} \to \overline{D}^0(f)\pi_s^-)}{N(D^{*+} \to D^0(f)\pi_s^+) \; + \; N(D^{*-} \to \overline{D}^0(f)\pi_s^-)}, \tag{89}$$

where $N(X)$ refers to the number of reconstructed events of decay X after background subtraction. This raw asymmetry arises from several sources: the D^{*+} production asymmetry $A_{\rm P}$) the asymmetry in selecting the tagging slow pion $A_{\rm D}(\pi_{\rm s}^+)$, the asymmetry in selecting the D^0 decay into the final state $A_{\rm D}(f)$, and the *CP* asymmetry in the decay $A_{CP}(f)$.

Consider the general case of a measured rate $n_\pm$, an efficiency (or other correction) $\varepsilon_\pm$, and the corrected rate $N_\pm$, where the subscript refers to D^0 or $\overline{D}^0$. Then:

$$\frac{N_+}{N_-} = \frac{n_+/\varepsilon_+}{n_-/\varepsilon_-} = \frac{n_+}{n_-}\frac{\varepsilon_-}{\varepsilon_+}. \tag{90}$$

Defining a generic asymmetry A_x as

$$A_x \equiv \frac{x_+ - x_-}{x_+ + x_-},$$

we have the identity

$$\frac{x_+}{x_-} = \frac{1 + A_x}{1 - A_x}.$$

Then applying this to Eq. 90:

$$\frac{1 + A_n}{1 - A_n} = \left(\frac{1 + A_N}{1 - A_N}\right)\left(\frac{1 + A_\varepsilon}{1 - A_\varepsilon}\right). \tag{91}$$

Applying the Taylor series expansion to Eq. 91, we find:

$$\left(1 + 2A_n + 2A_n^2 + ...\right) = \left(1 + 2A_N + 2A_N^2 + ...\right) + \left(1 + 2A_\varepsilon + 2A_\varepsilon^2 + ...\right)$$

and thus:

$$A_n = A_N + A_\varepsilon + (\text{terms of order } A^2). \tag{92}$$

Generalising this to include multiple asymmetries, we obtain the first-order formula used in the published analysis [8]:

$$A_{\rm raw}(f) = A_{CP}(f) + A_P + A_{\rm D}(\pi_{\rm s}^+) + A_{\rm D}(f)\,, \tag{93}$$

which is correct up to terms of second order in the asymmetries. In practise, for $D^0 \to h^+h^-$, we find $A_P \sim 1\,\%$, $A_{\rm D}(\pi_{\rm s}^+) \sim 1$–$2\,\%$, and $A_D(f) = 0$ by construction. Thus, the second-order correction is $\mathcal{O}(\text{few} \times 10^{-4})$.[34] Further, A_D and A_P are the same for

[34] Note that the LHCb dipole magnet creates regions of parameter space with large $A_{\rm D}(\pi_{\rm s}^+)$, particularly at the left and right edges of the acceptance. We exclude these regions with fiducial cuts.

$f = K^+K^-$ and $f = \pi^+\pi^-$ (leaving aside differences in kinematic distribution, considered below) and so many terms cancel in the difference:[35]

$$\Delta A_{CP} = A_{\rm raw}(K^+K^-) - A_{\rm raw}(\pi^+\pi^-) \approx A_{CP}(K^+K^-) - A_{CP}(\pi^+\pi^-)\,.$$

At the present level of precision, with a statistical uncertainty of around 0.2 %, this approximation is perfectly adequate. However, as we take more data—and certainly in the upgrade—it will be necessary to change the analysis to take second-order terms into account. This can be done by via the ratio formulation of Eq. (90), *i.e.*

$$\frac{N_{KK,+}}{N_{KK,-}} = \left(\frac{n_{KK,+}}{n_{KK,-}}\right)\left(\frac{\varepsilon_-}{\varepsilon_+}\right)\,, \quad \frac{N_{\pi\pi,+}}{N_{\pi\pi,-}} = \left(\frac{n_{\pi\pi,+}}{n_{\pi\pi,-}}\right)\left(\frac{\varepsilon_-}{\varepsilon_+}\right)$$
$$\Rightarrow \frac{N_{KK,+}/N_{KK,-}}{N_{\pi\pi,+}/N_{\pi\pi,+}} = \frac{n_{KK,+}/n_{KK,-}}{n_{\pi\pi,+}/n_{\pi\pi,-}}$$

The nuisance asymmetries A_P and $A_{\rm D}(\pi_{\rm s}^+)$ cancel between the K^+K^- and $\pi^+\pi^-$ final states because these are properties of the D^{*+} and of the tagging slow pion, respectively, which do not depend on the decay of the D^0. However, an artificial correlation between these asymmetries and the decay mode can arise if the asymmetry varies as a function of some variable[36] (*e.g.* the momentum of the D^{*+}) *and* the reconstructed distributions in this variable are different for the K^+K^- and $\pi^+\pi^-$ final states (*e.g.* due to detector acceptance of the daughter tracks). In such a scenario, the two modes would populate regions with different raw asymmetries and so the nuisance asymmetries would not cancel fully. Two techniques have been used to address this:

- the data can be partitioned into smaller kinematic regions such that within each region the raw asymmetries are constant and/or the K^+K^- and $\pi^+\pi^-$ kinematic distributions are equal;
- the data can be reweighted such that the K^+K^- and $\pi^+\pi^-$ kinematic distributions are equalised.

The first approach was used in the published LHCb result, and the second in the CDF result [371].

There is another way in which the formalism could be broken: through the presence of peaking backgrounds which (a) fake the signal, (b) occur at different levels for the K^+K^- and $\pi^+\pi^-$ final states, *and* (c) have a different raw asymmetry from the signal. The signal extraction procedure used in the published LHCb analysis is a fit to the mass difference from threshold $\delta m \equiv m(D^{*+}) - m(D^0) - m(\pi^+)$. This is vulnerable to a class of background in which a real D^{*+} decay occurs and the correct slow pion is found but the D^0 decay is partly misreconstructed, *e.g.* $D^0 \to K^-\pi^+\pi^0$ misidentified as $D^0 \to K^-K^+$. This typically creates a background which peaks in δm but is broadly distributed in

[35] Note in particular that if $A_{CP}(K^+K^-) = A_{CP}(\pi^+\pi^-) = 0$, the approximation becomes exact at all orders.

[36] We will frame the discussion in terms of kinematic variables, since there are clear mechanisms that could cause problems there, but the same logic can be applied to magnet polarity, trigger conditions, *etc.*

Table 10: Summary of absolute systematic uncertainties for ΔA_{CP}.

Source	Uncertainty
Fiducial requirement	0.01%
Peaking background asymmetry	0.04%
Fit procedure	0.08%
Multiple candidates	0.06%
Kinematic binning	0.02%
Total	0.11%

$m(D^0)$. Only cases which lie within the narrow $m(D^0)$ signal window will survive. This is more common for the K^+K^- final state than for $\pi^+\pi^-$: the energy of a missing particle can be made up by misidentifying a pion as a kaon, but apart from $D^0 \to \pi^- e^+ \nu_e$ there is little that can fake the kinematics of $D^0 \to \pi^+\pi^-$. In practise, the excellent charged hadron ID at LHCb suppresses these background greatly, and their raw asymmetries are not expected to be very different from the signal. In the published LHCb analysis, the impact of these backgrounds on the asymmetry was estimated by measuring their size and asymmetry in the D^0 mass sidebands and computing the effect of such a background on the signal with a toy Monte Carlo study. The alternative approach would be to use a full 2D fit to $m(D^0)$ and δm, which would distinguish this class of peaking background from the signal by its $m(D^0)$ distribution.

The three issues discussed above—terms entering at second order in the asymmetries, non-cancellation due to kinematic correlations, and peaking backgrounds—are particular to this analysis and will require some changes to the procedure as we scale to larger data samples. In addition, there are more generic systematic uncertainties associated with the fit procedure and with the handling of events with more than one candidate. These are summarised in Table 10.

4.2 Theory status of mixing and indirect *CP* violation

4.2.1 Theoretical predictions for $\Delta\Gamma_D$, Δm_D and indirect *CP* violation in the standard model

As discussed in Sec. 4.1, mixing of charmed mesons provides outstanding opportunities to search for physics beyond the Standard Model (SM). New flavour-violating interactions at some high-energy scale may, together with the SM interactions, mix the flavour eigenstates giving mixing parameters that differ from their SM expectations. It is known experimentally that D^0-$\overline{D}^0$ mixing proceeds extremely slowly, which in the SM is usually attributed to the absence of super-heavy quarks.

Both SM and NP contributions to mass and width differences can be summarised as

$$x_D = \frac{1}{2M_D\Gamma_D}\,\mathrm{Re}\left[2\langle\overline{D}^0|H^{|\Delta C|=2}\,|D^0\rangle + \langle\overline{D}^0|\,i\int \mathrm{d}^4x\,T\Big\{\mathcal{H}_w^{|\Delta C|=1}(x)\,\mathcal{H}_w^{|\Delta C|=1}(0)\Big\}|D^0\rangle\right],$$
$$y_D = \frac{1}{2M_D\Gamma_D}\,\mathrm{Im}\,\langle\overline{D}^0|\,i\int \mathrm{d}^4x\,T\Big\{\mathcal{H}_w^{|\Delta C|=1}(x)\,\mathcal{H}_w^{|\Delta C|=1}(0)\Big\}|D^0\rangle. \tag{94}$$

These formulae serve as the initial point of calculations of the mass and lifetime differences. They include contributions from local (at charm mass scale) $\Delta C = 2$ interactions generated by the b-quark [382–386] or NP particles and from SM-dominated time-ordered products of two $\Delta C = 1$ interaction Hamiltonians (see, however, Ref. [387]).

A simple examination of Eq. (94) reveals that the local $\Delta C = 2$ interactions only affect x_D, thus one can conclude that it is x_D that is most likely to receive large new physics contributions. Hence, it was believed that an experimental observation of $x_D \gg y_D$ would unambiguously reveal NP contributions to charm mixing. Clearly, this simple signal for NP did not materialise, but it is interesting that the reverse relation, $x_D < y_D$ with y_D expected to be determined by the SM processes, might nevertheless significantly affect the sensitivity to NP of experimental analyses of D mixing [388]. Also, it is important to point out that, contrary to the calculations of the SM contribution to mixing, the contributions of NP models can be calculated relatively unambiguously [359, 389, 390].

The calculation of the SM contribution to the mixing amplitudes is rather sophisticated. In the SM x_D and y_D are generated only at second order in flavour $\mathrm{SU}(3)_F$ breaking,

$$x_D\,,\; y_D \sim \sin^2\theta_C \times [SU(3)_F \text{ breaking}]^2\,, \tag{95}$$

where θ_C is the Cabibbo angle. Therefore, predicting the SM values of x_D and y_D depends crucially on estimating the size of $\mathrm{SU}(3)_F$ breaking [358, 391].

There are currently two approaches, neither of which give very reliable results because m_c is in some sense intermediate between heavy and light. The "inclusive" approach is based on the operator product expansion (OPE). In the $m_c \gg \Lambda_{\mathrm{QCD}}$ limit, where Λ_{QCD} is a scale characteristic of the strong interactions, Δm_D and $\Delta\Gamma_D$ can be expanded in terms of matrix elements of local operators [383–386]. Such calculations typically yield $x_D, y_D < 10^{-3}$. The use of the OPE relies on local quark-hadron duality, and on $\Lambda_{\mathrm{QCD}}/E_{\mathrm{released}}$ (with $E_{\mathrm{released}} \sim m_c$) being small enough to allow a truncation of the series. Moreover, a careful reorganisation of the OPE series is needed, as terms with smaller powers of m_s are numerically more important despite being more suppressed by powers of $1/m_c$ [383–386]. The numerically dominant contribution is composed of over twenty unknown matrix elements of dimension-12 operators, which are very hard to estimate. As a possible improvement of this approach, it would be important to perform lattice calculations of those matrix elements, as well as make perturbative QCD corrections to Wilson coefficients of those operators.

The "exclusive" approach sums over intermediate hadronic states, which may be modelled or fit to experimental data [392–397]. Since there are cancellations between states

within a given $SU(3)_F$ multiplet, one needs to know the contribution of each state with high precision. However, the D meson is not light enough that its decays are dominated by a few final states. In the absence of sufficiently precise data on many decay rates and on strong phases, one is forced to use some assumptions. While most studies find $x_D, y_D < 10^{-3}$, Refs. [392–397] obtain x_D and y_D at the 10^{-2} level by arguing that $\mathrm{SU}(3)_F$ violation is of order unity. Particular care should be taken if experimental data are used to estimate the mixing parameters, as the large cancellations expected in the calculation make the final result sensitive to uncertainties in the experimental inputs. It was shown that phase space effects alone provide enough $\mathrm{SU}(3)_F$ violation to induce $x_D, y_D \sim 10^{-2}$ [391]. Large effects in y_D appear for decays close to threshold, where an analytic expansion in $\mathrm{SU}(3)_F$ violation is no longer possible; a dispersion relation can then be used to show that x_D would receive contributions of similar order of magnitude. The dispersion calculation suffers from uncertainties associated with unknown (off-shell) q^2-dependences of non-leptonic transition amplitudes and thus cannot be regarded as a precision calculation. But it provides a realistic estimate of x_D. As a possible improvement of this approach, an estimate of $\mathrm{SU}(3)_F$ breaking in matrix elements should be performed. In addition, a calculation with $V_{ub} \neq 0$ should also be done, which is important for understanding of the size of *CP*-violation in charm mixing.

Based on the above discussion, it can be seen that it is difficult to find a clear indication of physics beyond the SM in D^0-$\overline{D}^0$ mixing measurements alone. However, an observation of large *CP* violation in charm mixing would be a robust signal of NP.

CP violation in D decays and mixing can be searched for by a variety of methods. Most of the techniques that are sensitive to *CP* violation make use of the decay asymmetry [368, 374],

$$\mathcal{A}_{CP}(f) = \frac{\Gamma(D \to f) - \Gamma(\overline{D} \to \overline{f})}{\Gamma(D \to f) + \Gamma(\overline{D} \to \overline{f})}. \tag{96}$$

For instance, time-dependent decay widths for $D \to K\pi$ are sensitive to *CP* violation in mixing. In particular, a combined analysis of $D \to K\pi$ and $D \to KK$ can yield interesting constraints on *CP*-violating parameters y_{CP} and A_Γ, as discussed in Sec. 4.1.1.

With the D^0-$\overline{D}^0$ transition amplitudes defined as follows:

$$\langle D^0|\mathcal{H}|\overline{D}^0\rangle = M_{12} - \frac{i}{2}\Gamma_{12}\,, \qquad \langle \overline{D}^0|\mathcal{H}|D^0\rangle = M_{12}^* - \frac{i}{2}\Gamma_{12}^*\,, \tag{97}$$

then in the limit where direct *CP*-violation is neglected, one can measure [368, 374] four quantities, x_D, y_D, A_m, and ϕ, which are described by three physical variables,[37]

$$x_{12} = \frac{2|M_{12}|}{\Gamma}\,,\ y_{12} = \frac{|\Gamma_{12}|}{\Gamma}\,,\ \phi_{12} = \arg(M_{12}/\Gamma_{12})\,. \tag{98}$$

This implies that there is a model-independent relation among experimental quantities [374, 398],

$$\frac{x_D}{y_D} = -\frac{1}{2}\frac{A_M}{\tan\phi}\,. \tag{99}$$

[37] Among various possible phase definitions, only ϕ_{12}, the relative phase between M_{12} and Γ_{12}, is convention-independent and so has physical consequences.

4.2.2 New physics in indirect *CP* violation

Indirect *CP* violation in charm mixing and decays is a unique probe for NP, since within the SM the relevant processes are described by the physics of the first two generations to an excellent approximation. Hence, observation of *CP* violation in D^0-$\overline{D}^0$ mixing at a level higher than $\mathcal{O}(10^{-3})$ (which is the SM contribution) would constitute an unambiguous signal of NP.

The commonly used theoretical parameters x_{12} and ϕ_{12} defined in Eq. (98) can be expressed in terms of x_D, y_D and $|q/p|$ as:

$$\begin{aligned} x_{12}^2 &= x_D^2 \frac{(1+|q/p|^2)^2}{4|q/p|^2} + y_D^2 \frac{(1-|q/p|^2)^2}{4|q/p|^2}\,, \\ \sin^2\phi_{12} &= \frac{(x_D^2+y_D^2)^2(1-|q/p|^4)^2}{16x_D^2y_D^2|q/p|^4 + (x_D^2+y_D^2)^2(1-|q/p|^4)^2}\,. \end{aligned} \tag{100}$$

The latest fit yields the following ranges [63]

$$x_D \in [0.24, 0.99]\,\%\,, \qquad y_D \in [0.51, 0.98]\,\%\,, \qquad |q/p| \in [0.59, 1.26]\,, \tag{101}$$

all at 95 % CL. The fit also provides 95% CL ranges also for the theoretical parameters from Eq. (98):

$$x_{12} \in [0.25, 0.99]\,\%\,, \qquad y_{12} \in [0.51, 0.98]\,\%\,, \qquad \phi_{12} \in [-8.4^\circ, 24.6^\circ]\,. \tag{102}$$

It should be noted that the experimental precision on the *CP* violation parameters is more than two orders of magnitude away from their SM predictions.

It is reasonable to assume that there are no accidental strong cancellations between the SM and the NP contributions to M_{12}. Useful bounds can thus be obtained by taking the NP contribution to saturate the upper limits in Eq. (102). The resulting constraints are presented in the $x_{12}^{\rm NP}/x_{12} - \phi_{12}^{\rm NP}$ plane in Fig. 28. One can also translate the data into model-independent bounds on four-quark operators, as performed *e.g.* in Refs. [389, 390].

The generic NP analysis can also be applied to models that exhibit a minimal flavour violation (MFV) structure, where new contributions to FCNCs originate only from the Yukawa matrices $Y_{u,d}$. The relevant basis is then the up mass basis, where Y_u is diagonal, so that flavour violation comes from powers of $Y_d Y_d^\dagger$. The leading contribution is to the operator $(u_L^\alpha \gamma_\mu c_L^\alpha)^2$ (α is a colour index), and it is given in terms of its Wilson coefficient C_1 by

$$C_1 \propto [y_s^2 (V_{cs}^* V_{us}) + (1 + r_{\rm GMFV}) \times y_b^2 (V_{cb}^* V_{ub})]^2. \tag{103}$$

Here $r_{\rm GMFV}$ parameterizes the effect of resummation of higher powers of the Yukawa matrices when these are important, namely in general MFV (GMFV) models [399].

The contribution to x_{12} in the linear MFV case ($r_{\rm GMFV} = 0$) is orders of magnitude below the current experimental sensitivity, assuming $\mathcal{O}(1)$ proportionality coefficient in Eq. (103). Yet in the context of GMFV with two Higgs doublets and large $\tan\beta$, such that $y_b \sim 1$, observable signals can be obtained, as shown in Fig. 28 for $r_{\rm GMFV}$ in the

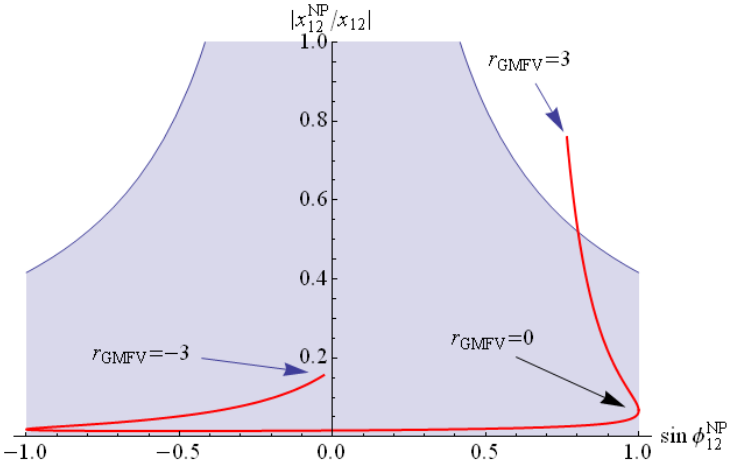

Figure 28: Allowed region (shaded) in the $x_{12}^{\rm NP}/x_{12} - \sin\phi_{12}^{\rm NP}$ plane. The red line corresponds to a GMFV prediction (see text for details) with $r_{\rm GMFV} \in [-3, 3]$.

range $[-3, 3]$. Note that strictly speaking $r_{\rm GMFV}$ (and thus the resulting signal) is not bounded, but higher absolute values than those considered here are much less likely in realistic models. Indeed in the current example $r_{\rm GMFV} \gtrsim 2$ is excluded, as shown in the figure.

The available data on D^0-$\overline{D}^0$ mixing can also be used to constrain the parameter space of specific theories, such as supersymmetry and warped extra dimensions. This is done *e.g.* in Refs. [389,390] (see also Refs. [400,401] where the interplay between the constraints from the K and D systems is presented). Here we wish to demonstrate the influence of improving the current bounds.

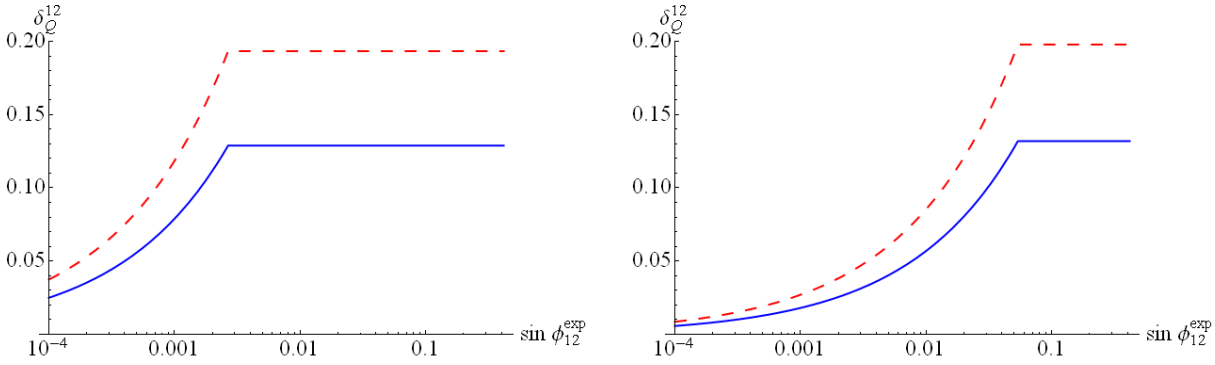

Figure 29: Bound on the squark mass degeneracy δ_Q^{12}, defined in Eq. (104), as a function of the experimental constraint on CP violation in D^0–$\overline{D}^0$ mixing, parametrised by $\sin\phi_{12}^{\rm exp}$. The alignment angle from the down sector is $\lambda_{\rm C}^5$ (left panel) or $\lambda_{\rm C}^3$ (right panel). The solid blue line in each panel is for $\bar{m}_{\tilde{Q}} = m_{\tilde{g}} = 1$ TeV and the dashed red line is for $\bar{m}_{\tilde{Q}} = m_{\tilde{g}} = 1.5$ TeV.

We consider a SUSY framework and focus on the first two generations of the left-

handed squark mass-squared matrix, $\tilde{m}^2_Q$, as the source of flavour violation. We further assume that it is aligned with the down sector, where the constraints are generically stronger. As in realistic alignment models (see *e.g.* Refs. [356, 402]), the off-diagonal element of $\tilde{m}^2_Q$ in the down mass basis (which induces $s \leftrightarrow d$ FCNCs) is taken to be small but not zero, with comparable real and imaginary parts. For concreteness, we examine values of either λ_C^5 or λ_C^3 (with λ_C as the Cabibbo angle), where in both cases the dominant bounds still arise from D^0-$\overline{D}^0$ mixing and not from the K system [401]. The constrained parameter is the squark mass degeneracy, defined by

$$\delta_Q^{12} \equiv \frac{m_{\tilde{Q}_2} - m_{\tilde{Q}_1}}{m_{\tilde{Q}_2} + m_{\tilde{Q}_1}}\,. \tag{104}$$

In order to analyze the effect of improving the experimental constraints on indirect *CP* violation in charm (assuming that no such violation is actually observed), we keep for simplicity the bound on x_{12} fixed as in Eq. (102) and vary that on ϕ_{12}. This is shown in Fig. 29 for the two alignment angles mentioned above and for two points in the SUSY parameter space $\bar{m}_{\tilde{Q}} = m_{\tilde{g}} = 1, 1.5$ TeV, where $\bar{m}_{\tilde{Q}}$ is the average squark mass and $m_{\tilde{g}}$ is the gluino mass. The right edge of each of the four lines in the plots marks the current situation, where the dominant constraint is from Δm_D. It is evident that after a certain level of improvement, the bound from *CP* violation becomes the important one, and this happens more quickly for a weaker alignment model (λ_C^3) than for λ_C^5 alignment. The reason is the larger phase in the former case.

To conclude, the experimental search for indirect *CP* violation in charm is one of the most promising channels for discovering NP or obtaining strong constraints. This is not negated by the large hadronic uncertainties in the D system, because of the very small SM short distance contribution to *CP* violation in D^0-$\overline{D}^0$ mixing.

4.3 The status of $\Delta\mathcal{A}_{CP}$ in the standard model

As discussed above, the LHCb collaboration has measured a surprisingly large time-integrated *CP* asymmetry difference [8],

$$\Delta\mathcal{A}_{CP} \equiv \mathcal{A}_{CP}(D^0 \to K^-K^+) - \mathcal{A}_{CP}(D^0 \to \pi^-\pi^+) = (-0.82 \pm 0.21 \pm 0.11)\%, \tag{105}$$

which has recently been supported by a preliminary result from the CDF collaboration [372].[38] Inclusion of the BaBar and Belle measurements of the individual K^-K^+ and $\pi^-\pi^+$ time-integrated *CP* asymmetries [369, 370] and the BaBar, Belle, and LHCb measurements of the indirect *CP* asymmetry A_Γ [53, 361, 403] yields the world average for the direct *CP* asymmetry difference [63]

$$\Delta a_{CP}^{\rm dir} \equiv a_{CP}^{\rm dir}(D^0 \to K^-K^+) - a_{CP}^{\rm dir}(D^0 \to \pi^-\pi^+) = (-0.67 \pm 0.16)\,\%. \tag{106}$$

[38] New results presented at ICHEP 2012, including a new result from Belle on $\Delta\mathcal{A}_{CP}$ [373], are not included in the averages discussed here.

The naive penguin-to-tree amplitude ratio is of $\mathcal{O}([V_{cb}V_{ub}/V_{cs}V_{us}]\alpha_S/\pi) \sim 10^{-4}$, yielding $\Delta a_{CP}^{\rm dir} < 0.1\%$ in the SM. This has led to extensive speculation in the literature that the measurement of $\Delta a_{CP}^{\rm dir}$ is a signal for NP. This is a particularly exciting possibility, given that reasonable NP models can be constructed in which all related flavour changing neutral current (FCNC) constraints, *e.g.*, from D^0-$\overline{D}^0$ mixing, are satisfied. A summary of work done on the NP interpretation is given in Section 4.4.1. We begin with a discussion of $\Delta a_{CP}^{\rm dir}$ in the SM.

The naive expectation for the SM penguin-to-tree ratio is based on estimates of the "short-distance" penguins with b-quarks in the loops. In fact, there is consensus that a SM explanation for $\Delta a_{CP}^{\rm dir}$ would have to proceed via dynamical enhancement of the long-distance "penguin contraction" contributions to the penguin amplitudes, *i.e.*, penguins with s and d quarks inside the "loops". Research addressing the direct *CP* asymmetry in the SM has largely fallen into one of two categories: (i) flavour $SU(3)_F$ or U-spin fits to the D decay rates, to check that an enhanced penguin amplitude can be accommodated [52, 404–408] (this, by itself, would not mean that $\Delta\mathcal{A}_{CP}^{\rm dir}$ is due to SM dynamics); (ii) rough estimates of the magnitudes of certain contributions to the long-distance penguin contractions [407, 409–411], to check if, in fact, it is reasonable that SM dynamics could yield the enhanced penguin amplitudes returned by the $SU(3)_F$ or U-spin fits.

We first summarize the results obtained using the flavour symmetry decompositions. An $SU(3)_F$ analysis of the $D \to PP$ decay amplitudes that incorporates *CP* violation (CPV) effects was first carried out about 20 years ago [393,404,412]. Already in this study the possibility of large direct *CP* asymmetries was anticipated, *e.g.*, as large as the percent level assuming that the penguins receive a large enhancement akin to the $\Delta I = 1/2$ rule in kaon decays. An updated $SU(3)_F$ analysis, working to first order in $SU(3)_F$ breaking, has been presented [405], making use of branching ratio measurements for the $D \to K\pi, \pi\pi$ and $D^0 \to K^-K^+, \overline{K}^0\eta$ decay modes. The authors concluded that $\Delta a_{CP}^{\rm dir}$ can be easily reconciled with the measured branching ratios. This was also the conclusion of a study based on a diagrammatic $SU(3)_F$ amplitude decomposition [406], which considered a larger set of $D \to PP$ decay modes. Again, this is only a statement about the possibility of accommodating the required amplitudes in the flavour decomposition, not about their realisation via long distance QCD dynamics. Both studies observe that a SM explanation of $\Delta a_{CP}^{\rm dir}$ could be combined with precise measurements of the individual asymmetries $a_{CP}^{\rm dir}(D^0 \to K^-K^+)$ and $a_{CP}^{\rm dir}(D^0 \to \pi^-\pi^+)$ to obtain predictions for $a_{CP}^{\rm dir}(D^0 \to \pi^0\pi^0)$. The conclusion, based on current data, is that percent level asymmetries for the latter could be realised. Ref. [406] also discusses implications for $a_{CP}^{\rm dir}(D^+ \to K^+\overline{K}^0)$.

Studies employing U-spin [52, 407] necessarily focus on amplitude fits to the smaller set of decay modes $D^0 \to K^-\pi^+, \pi^-K^+, \pi^-\pi^+, K^-K^+$, as the D^0 is a U-spin singlet, while the four final states and the operators mediating these decays in the SM $\Delta C = 1$ effective Hamiltonian each consist of a U-spin triplet and a singlet. Working to first order in U-spin

breaking, we can write the four decay amplitudes as

$$A(\overline{D}^0 \to K^+\pi^-) = V_{cs}V_{ud}^*\left(T - \tfrac{1}{2}\delta T\right), \quad A(\overline{D}^0 \to \pi^+K^-) = V_{cd}V_{us}^*\left(T + \tfrac{1}{2}\delta T\right)$$
$$A(\overline{D}^0 \to \pi^+\pi^-,\, K^+K^-) = \mp\tfrac{1}{2}\left(V_{cs}V_{us}^* - V_{cd}V_{ud}^*\right)(T \pm \delta S) - V_{cb}V_{ub}^*\left(P \mp \tfrac{1}{2}\delta P\right), \tag{107}$$

where the U-spin triplet "tree" amplitude T and the singlet "penguin" amplitude P arise at 0^{th} order in U-spin breaking, and δT, δS and δP are the first order U-spin breaking corrections, which transform in turn as a triplet, singlet, and singlet under U-spin. The singlet amplitude δS accounts for the large rate difference $\Gamma(D^0 \to K^-K^+)/\Gamma(D^0 \to \pi^-\pi^+) = 2.8$ (after accounting for phase space). A ratio $\delta S/T \sim 0.5$ is found in Refs. [52, 407], and in the $SU(3)_F$ study of Ref. [405] which effectively contains the above U-spin decomposition. Realisation of Eq. (106) requires $|P/T| \sim 3$, for $\mathcal{O}(1)$ strong phases and $a_{CP}^{\text{dir}}(D^0 \to K^-K^+) \sim -a_{CP}^{\text{dir}}(D^0 \to \pi^-\pi^+)$, where the last relation becomes an equality in the U-spin limit. This amounts to an order of magnitude enhancement of the penguin amplitude beyond the naive estimate.

The U-spin analysis in Ref. [407] begins with the observation that the *CP* averaged experimental "sum-rule" relation for the above amplitudes,

$$\Sigma_{\text{sum-rule}} = \frac{|A(D^0 \to K^-K^+)\,/\,V_{cs}V_{us}| + |A(D^0 \to \pi^-\pi^+)\,/\,V_{cd}V_{ud}|}{|A(D^0 \to \pi^-K^+)\,/\,V_{cd}V_{us}| + |A(D^0 \to K^-\pi^+)\,/\,V_{cs}V_{ud}|} - 1 = (4.0 \pm 1.6)\%., \tag{108}$$

together with the observation of small ($\approx 15\,\%$) U-spin breaking in $A(D^0 \to \pi^-K^+)$ *vs.* $A(D^0 \to K^-\pi^+)$ suggests that U-spin is a good symmetry in these decays. They therefore assume that $SU(3)_F$ breaking is of nominal size in these decays, *i.e.*, characterized by the small parameter $\epsilon \sim (f_K/f_\pi - 1) \sim \mathcal{O}(0.2)$. This helps to explain the above sum-rule with minimal tuning of strong phases. Other authors take the large difference between $\Gamma(D^0 \to K^-K^+)$ and $\Gamma(D^0 \to \pi^-\pi^+)$ or $\delta S/T \sim 0.5$ as evidence for large U-spin breaking in the singly Cabbibo suppressed (SCS) decays. In Ref. [407], rather than interpreting the amount of U-spin breaking implied by δS by comparing it to T, as in other works, δS is compared to P. It is observed that whereas $\Delta a_{CP}^{\text{dir}}$ implies that P must be dominated by the sum of the long distance s- and d- quark penguin contractions, nominal U-spin breaking would imply that δS must be dominated by their difference, denoted as P_{break}, with P and P_{break} satisfying the relation $P_{\text{break}} \sim \epsilon P$. A consistent picture emerges in which the magnitude of P_{break} is determined by the large difference between the $D^0 \to K^-K^+$ and $D^0 \to \pi^-\pi^+$ rates, yielding $P_{\text{break}} \sim T/2$, which in turn implies that $P \sim T/2\epsilon$, which is of the correct magnitude to explain $\Delta a_{CP}^{\text{dir}}$. Thus, large direct *CP* asymmetries of order a few per mille are not surprising given the size of $\Gamma(D^0 \to K^-K^+)/\Gamma(D^0 \to \pi^-\pi^+)$. However, as always in the flavour decomposition approach, accommodation need not translate to realisation by QCD dynamics. One consequence of this picture is that large $a_{CP}^{\text{dir}}(D^0 \to K_S^0K_S^0) \sim 0.6\,\%$ could be realised for $\mathcal{O}(1)$ strong phases.

Finally, we review the estimates for the long-distance penguin contractions [411,413] to see if the required enhancement can be realised. Ref. [413] employs the one-gluon exchange approximation. The essential ingredients are: (i) $1/N_c$ counting; (ii) D branching ratio

data which shows that certain formally $1/m_c$ power-suppressed amplitudes are of same order as their leading $(1/m_c)^0$ counterparts; (iii) translation of this breakdown of the $1/m_c$ expansion to the penguin contraction amplitudes, in the approximation of a hard gluon exchange; (iv) use of a partonic quantity as a rough estimator of the hadronic interactions, *e.g.*, final state interactions, underlying the penguin contraction "loops". This results in a rough estimate for $\Delta a_{CP}^{\rm dir}$ at the few per mille level. The authors of Ref. [413] thus conclude that a SM explanation is plausible, given that their estimate suffers from large uncertainties. In Ref. [411] the penguin contractions are estimated using isospin and information from $\pi\pi$ scattering and unitarity. The authors have performed a fit of the *CP* conserving contributions from the *CP*-averaged branching ratios, obtaining information on the isospin amplitudes and the underlying renormalisation group invariant amplitude contributions. Allowing for three coupled channel contributions to $\pi\pi, KK$ scattering (and finding essentially no difference in their results if allowing for more channels), they conclude that the observed asymmetries are marginally compatible with the SM.

To summarise, flavour $SU(3)$ or U-spin fits to the $D \to PP$ data can accommodate the enhanced penguin amplitudes required to reproduce $\Delta a_{CP}^{\rm dir}$. There is consensus that in this case $a_{CP}^{\rm dir}(D^0 \to \pi^0\pi^0)$ could lie at the percent level, while $a_{CP}^{\rm dir}(D^+ \to K^+\overline{K}^0)$ could certainly lie at the few per mille level. Experimentally, the latter asymmetry requires *CP* violation in the kaon system to be accounted for. Under the assumption of nominal $SU(3)_F$ breaking in $D \to PP$ decays, the enhancement of the long-distance penguin contractions required to realise $\Delta a_{CP}^{\rm dir}$ is not surprising, given the large difference between the $D^0 \to K^-K^+$ and $D^0 \to \pi^-\pi^+$ decay rates. It would of course be of interest to extend the above *CP* violation studies to the SCS $D \to VP$ and $D \to VV$ decay modes. Finally, among the works which have attempted to directly estimate the magnitudes of the long distance penguin contractions, there is no consensus on whether they can be enhanced by an order of magnitude beyond the naive penguin amplitude estimates, as would be required in order to explain $\Delta a_{CP}^{\rm dir}$. Ultimately this question will have to be answered directly via lattice studies. In the following section, future prospects are discussed. In subsequent sections, several definitive CPV signals for NP in SCS D decays will be discussed.

4.4 $\Delta\mathcal{A}_{CP}$ in the light of physics beyond the standard model

4.4.1 Implications of $\Delta\mathcal{A}_{CP}$ for physics beyond the standard model

General considerations

Potential NP contributions to $\Delta\mathcal{A}_{CP}$ can be parametrized in terms of an effective Hamiltonian valid below the W and top mass scales

$$\mathcal{H}_{|\Delta c|=1}^{\rm eff-NP} = \frac{G_F}{\sqrt{2}} \sum_i C_i^{{\rm NP}(\prime)} \mathcal{Q}_i^{(\prime)} \,, \tag{109}$$

where the relevant operators $\mathcal{Q}_i^{(\prime)}$ are defined in Ref. [51]. Introducing the ratios $R_{K,\pi}^{{\rm NP},i}$ as the relevant NP hadronic amplitudes (matrix elements $\langle K^-K^+, \pi^-\pi^+|\mathcal{Q}_i^{(\prime)}|D\rangle$) normalised

to the leading *CP* conserving SM contributions and writing $C_i^{\rm NP} = v_{\rm EW}^2/\Lambda^2$, the relevant NP scale Λ is given by

$$\frac{(10\ \text{TeV})^2}{\Lambda^2} = \frac{(0.61 \pm 0.17) - 0.12\,\text{Im}(\Delta R^{\rm SM})}{\text{Im}(\Delta R^{{\rm NP},i})}\,, \tag{110}$$

where $\Delta R^i = R_K^i + R_\pi^i$ and $R_{K,\pi}^{\rm SM}$ parametrize the unknown hadronic amplitude ratios associated with the *CP* violating SM contributions. Comparing this estimate to the much higher effective scales probed by *CP* violating observables in D mixing and also in the kaon sector, one first needs to verify, if such large contributions can still be allowed by other flavour constraints. Within the effective theory approach, this can be estimated via so-called "weak mixing" of the effective operators. In particular, time-ordered correlators of $\mathcal{H}^{\rm eff-NP}_{|\Delta c|=1}$ with the SM effective weak Hamiltonian can, at the one weak loop order, induce important contributions to *CP* violation in both D meson mixing and kaon decays (ϵ'/ϵ). On the other hand, analogue correlators quadratic in $\mathcal{H}^{\rm eff-NP}_{|\Delta c|=1}$ turn out to be either chirally suppressed and thus negligible, or yield quadratically divergent contributions, which are thus highly sensitive to particular UV completions of the effective theory [51].

Universality of *CP* violation in $\Delta F = 1$ processes

The strongest bounds can be derived for a particular class of operators, which transform non-trivially only under the $SU(3)_Q$ subgroup of the global SM quark flavour symmetry $\mathcal{G}_F = SU(3)_Q \times SU(3)_U \times SU(3)_D$, respected by the SM gauge interactions. In particular one can prove that their *CP* violating contributions to $\Delta F = 1$ processes have to be approximately universal between the up and down sectors [401]. Within the SM one can identify two unique sources of $SU(3)_Q$ breaking given by $\mathcal{A}_u \equiv (Y_u Y_u^\dagger)_{\not{\rm tr}}$ and $\mathcal{A}_d \equiv (Y_d Y_d^\dagger)_{\not{\rm tr}}$, where $\not{\rm tr}$ denotes the traceless part. Then in the two generation limit, one can construct a single source of *CP* violation, given by $J \equiv i[\mathcal{A}_u, \mathcal{A}_d]$ [414, 415]. The crucial observation is that J is invariant under $SO(2)$ rotations between the $\mathcal{A}_u$ and $\mathcal{A}_d$ eigenbases. Introducing now $SU(2)_Q$ breaking NP effective operator contributions of the form $\mathcal{Q}_L = \Big[(X_L)^{ij}\,\overline{Q}_i \gamma^\mu Q_j\Big] L_\mu$, where L_μ denotes a flavour singlet current, it follows that their *CP* violating contributions have to be proportional to J and thus invariant under flavour rotations. The universality of *CP* violation induced by $\mathcal{Q}_L$ can be expressed explicitly as [401]

$$\text{Im}(X_L^u)_{12} = \text{Im}(X_L^d)_{12} \propto \text{Tr}\,(X_L \cdot J)\ . \tag{111}$$

The above identity holds to a very good approximation even in the three-generation framework. In the SM, large values of $Y_{b,t}$ induce a $SU(3)/SU(2)$ flavour symmetry breaking pattern [399] which allows to decompose X_L under the residual $SU(2)$ in a well defined way. Finally, residual SM $SU(2)_Q$ breaking is necessarily suppressed by small mass ratios $m_{c,s}/m_{t,b}$, and small CKM mixing angles. The most relevant implication of Eq. (111) is that it predicts a direct correspondence between $SU(3)_Q$ breaking NP contributions to $\Delta\mathcal{A}_{CP}$ and ϵ'/ϵ [401]. It follows immediately that stringent limits on possible NP contributions to the latter require $SU(3)_Q$ breaking contributions to the former to be below the per mille level (for $\Delta R^{{\rm NP},i} = \mathcal{O}(1)$). As a corollary, one can show that within NP scenarios

which only break $SU(3)_Q$, existing stringent experimental bounds on new contributions to *CP* violating rare semileptonic kaon decays $K_{\rm L}^0 \to \pi^0(\nu\overline{\nu}, \ell^+\ell^-)$ put robust constraints on *CP* asymmetries of corresponding rare charm decays $D \to \pi(\nu\overline{\nu}, \ell^+\ell^-)$. In particular $|a_{CP}^{\cancel{SU(3)_Q}}(\pi e^+e^-)| \lesssim 2\,\%$ [401].

The viability of the remaining 4-quark operators in $\mathcal{H}^{\rm eff-NP}_{|\Delta c|=1}$ as explanations of the experimental $\Delta\mathcal{A}_{CP}$ value, depends crucially on their flavour and chiral structure (a full list can be found in Ref. [51]). In particular, operators involving purely right-handed quarks are unconstrained in the effective theory analysis but may be subject to severe constraints from their UV sensitive contributions to D mixing observables. On the other hand, QED and QCD dipole operators are at present only weakly constrained by nuclear EDMs and thus present the best candidates to address the $\Delta\mathcal{A}_{CP}$ puzzle [51].

Finally, we note that it was shown that the impact of universality of *CP* within the alignment framework is to limit the amount of CPV in D^0-$\overline{D}^0$ mixing to below $\sim 20\%$, which is interestingly near the current bound. The expected progress in this measurement with the LHCb detector is therefore going to start probing this framework.

Explanations of $\Delta\mathcal{A}_{CP}$ within new physics models

Since the announcement of the LHCb result, several prospective explanations of $\Delta\mathcal{A}_{CP}$ within various NP frameworks have appeared. In the following we briefly discuss $\Delta\mathcal{A}_{CP}$ within some of the well-motivated beyond SM contexts.

In the Minimal Supersymmetric SM (MSSM), the right size of the QCD dipole operator contributions can be generated with non-zero left-right up-type squark mixing contributions $(\delta^u_{12})_{LR}$ [368, 416, 417]. Parametrically, such effects in $\Delta\mathcal{A}_{CP}$ can be written as [416]

$$|\Delta a_{CP}^{\rm SUSY}| \approx 0.6\% \left(\frac{|{\rm Im}(\delta^u_{12})_{LR}|}{10^{-3}}\right)\left(\frac{\rm TeV}{\tilde{m}}\right), \tag{112}$$

where $\tilde{m}$ denotes a common squark and gluino mass scale. At the same time dangerous contributions to D mixing observables are chirally suppressed. It turns out however that even the apparently small $(\delta^u_{12})_{LR}$ value required implies a highly nontrivial flavour structure of the UV theory; in particular, large trilinear (A) terms and sizable mixing among the first two generation squarks (θ_{12}) are required [416].

$$\begin{aligned} {\rm Im}(\delta^u_{12})_{LR} &\approx \frac{{\rm Im}(A)\theta_{12} m_c}{\tilde{m}} \\ &\approx \left(\frac{{\rm Im}(A)}{3}\right)\left(\frac{\theta_{12}}{0.3}\right)\left(\frac{\rm TeV}{\tilde{m}}\right) 0.5\times 10^{-3}\,. \end{aligned} \tag{113}$$

Similarly, warped extra dimensional models [418] that explain the quark spectrum through flavour anarchy [418–421] can naturally give rise to QCD dipole contributions affecting $\Delta\mathcal{A}_{CP}$ as [422]

$$|\Delta a_{CP}^{\rm RS}| \approx 0.6\% \left(\frac{Y_5}{6}\right)^2 \left(\frac{3\,{\rm TeV}}{m_{\rm KK}}\right)^2, \tag{114}$$

where $m_{\rm KK}$ is the KK scale and Y_5 is the 5D Yukawa coupling in appropriate units of the AdS curvature. Reproducing the experimental value of $\Delta\mathcal{A}_{CP}$ requires near-maximal 5D Yukawa coupling, close to its perturbative bound [423, 424] of $4\pi/\sqrt{N_{\rm KK}} \simeq 7$ for $N_{\rm KK} = 3$ perturbative KK states. In turn, this helps to suppress dangerous tree-level contributions to *CP* violation in D^0-$\overline{D}^0$ mixing [389, 390]. This scenario can also be interpreted within the framework of partial compositeness in four dimensions, but generic composite models typically require smaller Yukawas to explain Δa_{CP} and consequently predict sizable contributions to CP violation in $\Delta F = 2$ processes [425].

On the other hand, in the SM extension with a fourth family of chiral fermions $\Delta\mathcal{A}_{CP}$ can be affected by 3×3 CKM non-unitarity and b' penguin operators

$$|\Delta a_{CP}^{\rm 4th\,gen}| \propto {\rm Im}\left(\frac{\lambda_{b'}}{\lambda_d - \lambda_s}\right) . \tag{115}$$

However, due to the existing stringent constraints on the new *CP* violating phases entering $\lambda_{b'}$ [383, 426], only moderate effects comparable to the SM estimates are allowed [52].

Finally, it is possible to relate $\Delta\mathcal{A}_{CP}$ to the anomalously large forward-backward asymmetry in the $t\bar{t}$ system measured at the Tevatron [427] through a minimal model. Among the single scalar mediated mechanisms that can explain the top data, only the t-channel exchange of a colour-singlet weak-doublet, with a very special flavour structure, is consistent with the total and differential $t\bar{t}$ cross-section, flavour constraints and electroweak precision measurements [428]. The required flavour structure implies that the scalar *unavoidably* contributes at tree level to $\Delta\mathcal{A}_{CP}$ [54]. The relevant electroweak parameters are either directly measured, or fixed by the top-related data, implying that, for a plausible range of the hadronic parameters, the scalar mediated contribution is of the right size.

4.4.2 Shedding light on direct *CP* violation via $D \to V\gamma$ decays

The theoretical interpretation of $\Delta\mathcal{A}_{CP}$ is puzzling: it is above its naive estimate in the SM and it could well be a signal of NP, but it is not large enough to rule out a possible SM explanation. It is then important to identify possible future experimental tests able to distinguish standard *vs.* non-standard explanations of $\Delta\mathcal{A}_{CP}$. Among the NP explanations of $\Delta\mathcal{A}_{CP}$, the most interesting ones are those based on a new *CP* violating phase in the $\Delta C = 1$ chromomagnetic operator. A general prediction of this class of models, that could be used to test this hypothesis from data, are enhanced direct *CP* violation (DCPV) asymmetries in radiative decay modes [55].

1. The first key observation to estimate DCPV asymmetries in radiative decay modes is the strong link between the $\Delta C = 1$ chromomagnetic operator ($Q_8 \sim \bar{u}_L \sigma_{\mu\nu} T^a g_s G_a^{\mu\nu} c_R$) and the $\Delta C = 1$ electromagnetic-dipole operator ($Q_7 \sim \bar{u}_L \sigma_{\mu\nu} Q_u e F^{\mu\nu} c_R$). In most explicit new-physics models the short-distance Wilson coefficients of these two operators ($C_{7,8}$) are expected to be similar. Moreover, even assuming that only a non-vanishing C_8 is generated at some high scale, the mixing of the two operators from strong interactions implies $C_{7,8}$ of comparable size at the

charm scale. Thus if $\Delta\mathcal{A}_{CP}$ is dominated by NP contribution generated by Q_8, we can infer that $|\mathrm{Im}[C_7^{\mathrm{NP}}(m_c)]| \approx |\mathrm{Im}[C_8^{\mathrm{NP}}(m_c)]| = (0.2 - 0.8) \times 10^{-2}$.

2. The second important ingredient is the observation that in the Cabibbo-suppressed $D \to V\gamma$ decays, where V is a light vector meson with $u\overline{u}$ valence quarks ($V = \rho^0, \omega$), Q_7 has a sizable hadronic matrix element. More explicitly, the short-distance contribution induced by Q_7, relative to the total (long-distance) amplitude, is substantially larger with respect to the corresponding relative weight of Q_8 in $D \to P^+P^-$ decays. Estimating the SM long-distance contributions from data, and evaluating the short-distance *CP* violating contributions under the hypothesis that $\Delta\mathcal{A}_{CP}$ is dominated by (dipole-type) NP, leads to the following estimate for the maximal direct *CP* asymmetries in the $D \to (\rho, \omega)\gamma$ modes [55]:

$$|a_{CP}^{\mathrm{dir}}(D \to (\rho,\omega)\gamma)|^{\mathrm{max}} = 0.04 \left|\frac{\mathrm{Im}[C_7(m_c)]}{0.4 \times 10^{-2}}\right| \times \left[\frac{10^{-5}}{\mathcal{B}(D \to (\rho,\omega)\gamma)}\right]^{1/2} \lesssim 10\% \ . \tag{116}$$

The case of the ϕ resonance, or better the $K^+K^-\gamma$ final state with M_{KK} close to the ϕ peak, is more involved since the matrix element of Q_7 vanishes in the large m_c limit for a pure $s\overline{s}$ state. However, a non-negligible *CP* asymmetry can be expected also in this case since: 1) the matrix element of Q_7 is not expected to be identically zero because of sizable $\mathcal{O}(\Lambda_{\mathrm{QCD}}/m_c)$ corrections; 2) non-resonant contributions due to (off-shell) ρ and ω exchange can also contribute to the $K^+K^-\gamma$ final state. Taking into account these effects, the following estimates for the maximal direct *CP* asymmetries are obtained [55]:

$$\begin{aligned} &|a_{CP}^{\mathrm{dir}}(D \to K^+K^-\gamma)|^{\mathrm{max}} \approx 2\% \ , \quad 2m_K < \sqrt{s} < 1.05 \ \mathrm{GeV} \ , \\ &|a_{CP}^{\mathrm{dir}}(D \to K^+K^-\gamma)|^{\mathrm{max}} \approx 6\% \ , \quad 1.05 \ \mathrm{GeV} < \sqrt{s} < 1.20 \ \mathrm{GeV} \ . \end{aligned} \tag{117}$$

In the first bin, close to the ϕ peak, the leading contribution is due to the ϕ-exchange amplitude. The contribution due to the non-resonant amplitudes plays a significant role far enough from the ϕ peak, where the *CP* asymmetry can become larger.

3. In order to establish the significance of these results, two important issues have to be clarified: 1) the size of the *CP* asymmetries within the SM, 2) the role of the strong phases.

As far as the SM contribution is concerned, we first notice that short-distance contributions generated by the operator Q_7 are safely negligible. Using the result in Ref. [429] we find asymmetries below the 0.1% level. The dominant SM contribution is expected from the leading non-leptonic four-quark operators, for which we can apply the general arguments discussed in Ref. [51]. The *CP* asymmetries can be decomposed as $|a_{CP}^{\mathrm{SM}}(f)| \approx 2\xi \ \mathrm{Im}(R_f^{\mathrm{SM}}) \approx 0.13\% \times \mathrm{Im}(R_f^{\mathrm{SM}})$, where $\xi \equiv |V_{cb}V_{ub}|/|V_{cs}V_{us}| \approx 0.0007$ and R_f^{SM} is a ratio of suppressed over leading hadronic amplitudes, naturally expected to be smaller than one. This decomposition holds both for $f = \pi\pi, KK$ and for $f = V\gamma$ channels. The SM model explanations of Δa_{CP}

require $R^{\rm SM}_{\pi\pi,KK} \sim 3$. While we cannot exclude this possibility from first principles, a further enhancement of one order of magnitude in the $D \to V\gamma$ mode is beyond any reasonable explanation in QCD. As a result, an observation of $|a^{\rm dir}_{CP}(D \to V\gamma)| \gtrsim 3\%$ would be a clear signal of physics beyond the SM, and a clean indication of new *CP*-violating dynamics associated to dipole operators.

Having clarified that large values of $|a^{\rm dir}_{CP}(D \to V\gamma)|$ would be a clear footprint of non-standard dipole operators, we can ask the question if potential tight limits on $|a^{\rm dir}_{CP}(D \to V\gamma)|$ could exclude this non-standard framework. Unfortunately, uncertainty on the strong phases does not allow to draw this conclusion. Indeed the maximal values for the DCPV asymmetries presented above are obtained in the limit of maximal constructive interference of the various strong phases involved. In principle, this problem could be overcome via time-dependent studies of $D(\overline{D}) \to V\gamma$ decays or using photon polarisation, accessible via lepton pair conversion in $D \to V(\gamma^* \to \ell^+\ell^-)$; however, these types of measurements are certainly more challenging from the experimental point of view.

4.4.3 Testing for *CP* violating new physics in the $\Delta I = 3/2$ amplitudes

It is possible to at least in principle distinguish between NP and the SM origin of $\Delta\mathcal{A}_{CP}$. If $\Delta\mathcal{A}_{CP}$ is due to a chromomagnetic operator, *i.e.* due to $\Delta I = 1/2$ contributions, one can measure *CP* violation in radiative D decays, as explained in the previous section. Examples of NP models that can be tested in this way are, *e.g.*, flavour violating supersymmetric squark-gluino loops that mediate the $c \to ug$ transition [368, 416, 417]. On the other hand, if $\Delta\mathcal{A}_{CP}$ is due to $\Delta I = 3/2$ NP one can use isospin symmetry to write down sum rules for direct *CP* asymmetries in D decays [430]. If the sum rules are violated, then NP would be found. An example of a NP model that can be tested in this way is an addition of a single new scalar field with nontrivial flavour couplings [54].

The basic idea behind the $\Delta I = 3/2$ NP tests [430] is that in the SM the *CP* violation in singly Cabibbo suppressed (SCS) D decays arises from penguin amplitudes which are $\Delta I = 1/2$ transitions. On the other hand, $\Delta I = 3/2$ amplitudes are *CP* conserving in the SM. Observing any *CP* violation effects in the $\Delta I = 3/2$ amplitudes would therefore be a clear signal of NP.

In the derivation of the sum rules it is important to pay attention to the potentially important effects of the isospin breaking. Isospin symmetry is broken at $\mathcal{O}(10^{-2})$, which is also the size of the *CP* asymmetries we are interested in. There are two qualitatively different sources of isospin breaking—due to electromagnetic interactions, u and d quark masses, which are all *CP* conserving effects, and due to electroweak penguin operators that are a *CP* violating source of isospin breaking. The *CP* conserving isospin breaking is easy to cancel in the sum rules. As long as the *CP* conserving amplitudes completely cancel in the sum rules, which is the case in Ref. [430], the isospin breaking will only enter suppressed by the small *CP* violation amplitude and is therefore negligible. The electroweak penguin operators, on the other hand, are suppressed by $\alpha/\alpha_s \sim \mathcal{O}(10^{-2})$ compared to the leading *CP* violating but isospin conserving penguin contractions of the $Q_{1,2}$ operators, and can thus also be safely neglected.

Among the SCS decays, the $D\to\pi\pi$, $D\to\rho\pi$, $D\to\rho\rho$, $D\to\overline{K}K\pi$, and $D_s^+\to K^*\pi$ modes carry enough information to construct tests of $\Delta I=3/2$ NP. We discuss each of them in turn. Before proceeding, a word of caution. Below, we keep the final states K^0 and $\overline{K}^0$ mesons explicit in the notation. When measurements are performed they will be part of the $K^0_{\rm S}$ meson. In checking for the presence of $\Delta I=3/2$ NP one thus needs to keep track of the CP violation in the neutral kaon system. This effect cannot be neglected as it generates CP asymmetries of order ϵ_K. However, this effect can be taken into account explicitly by appropriately modifying the sum rule equations and also by correcting for the time dependence efficiency for detecting the $K^0_{\rm S}$ decay [431].

Let us start with sum rules for $D\to\pi\pi$ decays, which have a nice feature that the charged decay $D^+\to\pi^+\pi^0$ is purely $\Delta I=3/2$. In the SM therefore

$$a_{CP}^{\rm dir}(D^+\to\pi^+\pi^0)=0. \tag{118}$$

If it is measured to be nonzero this would be a signal of $\Delta I=3/2$ NP. Even, if it is found experimentally to be very small, it is still possible that this is only because the strong phase between the SM and NP amplitudes is accidentally small.

This possibility can be checked with more data if time-dependent $D(t)\to\pi^-\pi^+$ and $D(t)\to\pi^0\pi^0$ measurements become available, or if there is additional information on relative phases from a charm factory running on the $\psi(3770)$. It amounts to measuring the weak phase of the $\Delta I=3/2$ amplitude A_3 via generalised triangle constructions that also take isospin breaking into account [430]. If

$$\frac{1}{\sqrt{2}}A_{\pi^-\pi^+}+A_{\pi^0\pi^0}-\frac{1}{\sqrt{2}}\overline{A}_{\pi^+\pi^-}-\overline{A}_{\pi^0\pi^0}=3\big(A_3-\overline{A}_3\big) \tag{119}$$

is found to be nonzero, this would mean there is CP violating NP in the $\Delta I=3/2$ amplitude.

The above results apply also to $D\to\rho\rho$ decays, but for each polarisation amplitude separately. The corrections due to finite ρ width can be controlled experimentally in the same way as in $B\to\rho\rho$ decays [432]. As long as the polarisations of the ρ resonances are measured (or if the longitudinal decay modes dominate, as is the case in $B\to\rho\rho$ decays), the search for $\Delta I=3/2$ NP could be easier experimentally in $D\to\rho\rho$ decays since there are more charged tracks in the final state. The most promising observable where polarisation measurement is not needed, is $\mathcal{A}_{CP}(D^+\to\rho^+\rho^0)$, which if found nonzero (after the correction for the effect of finite ρ decay widths) would signal $\Delta I=3/2$ NP.

Another experimentally favourable probe is the isospin analysis of the $D^0\to\pi^+\pi^-\pi^0$ Dalitz plot in terms of the $D\to\rho\pi$ decays. There are two combinations of measured amplitudes that are proportional to $\Delta I=3/2$ amplitudes

$$\begin{aligned} A_{\rho^+\pi^0}+A_{\rho^0\pi^+}&=3\sqrt{2}A_3,\\ A_{\rho^+\pi^-}+2A_{\rho^0\pi^0}+A_{\rho^-\pi^+}&=6A_3. \end{aligned} \tag{120}$$

A measurement of the second sum can be obtained from the $D^0\to\pi^+\pi^-\pi^0$ Dalitz plot.

If the related *CP* asymmetry

$$\begin{aligned}|A_{\rho^+\pi^-}+2A_{\rho^0\pi^0}+A_{\rho^-\pi^+}|^2-|\overline{A}_{\rho^-\pi^+}+2\overline{A}_{\rho^0\pi^0}+\overline{A}_{\rho^+\pi^-}|^2\\ =36\big(|A_3|^2-|\overline{A}_3|^2\big),\end{aligned} \tag{121}$$

is found to be nonzero, this would mean that the $\Delta I = 3/2$ NP contribution is nonzero. If it is found to vanish, it could still be that this is due to the strong phase difference being vanishingly small.

A definitive answer can be provided by another test that is directly sensitive to the weak phase of A_3. This test is possible if the time-dependent $D(t)\to\pi^+\pi^-\pi^0$ Dalitz plot is measured. In this case the relative phases between the $D^0\to\rho\pi$ and $\overline{D}^0\to\rho\pi$ amplitudes can be obtained (alternatively one could use time integrated entangled decays of $\psi(3770)$ at the charm factory). The presence of a weak phase in A_3 can then be determined from the following sum-rule

$$\big(A_{\rho^+\pi^-}+A_{\rho^-\pi^+}+2A_{\rho^0\pi^0}\big)-\big(\overline{A}_{\rho^-\pi^-}+\overline{A}_{\rho^+\pi^-}+2\overline{A}_{\rho^0\pi^0}\big)=6\big(A_3-\overline{A}_3\big). \tag{122}$$

A non-vanishing result for Eq. (122) would provide a definitive proof for $\Delta I = 3/2$ NP. A similar sum rule for the *CP* asymmetries rather than the amplitudes was given in Eq. (121). In that case the time-integrated Dalitz plot suffices to determine the sum rule inputs.

The sum rules involving $D\to K\overline{K}\pi$ decays are somewhat more complex because there are three particles in the final state. There are three $\Delta I = 3/2$ reduced matrix elements, $\mathcal{B}_3, \mathcal{B}'_3, \mathcal{C}_3$. In the case of D^+ decays it is possible to construct a purely $\Delta I = 3/2$ matrix element by summing only three decay amplitudes, while in the case of D^0 decays four amplitudes are needed. For this reason let us consider only the D^+ decays. For instance, for D^+ decays to $K^*\overline{K}^*$ resonances we have for each polarisation (suppressing polarisations in the notation)

$$\sqrt{2}A_{K^{*+}\overline{K}^{*0}\pi^0}+A_{K^{*+}K^{*-}\pi^+}+A_{K^{*0}\overline{K}^{*0}\pi^+}=6\,\mathcal{C}_3. \tag{123}$$

Thus, if the *CP* violating difference

$$\begin{aligned}&|\sqrt{2}A_{K^{*+}\overline{K}^{*0}\pi^0}+A_{K^{*+}K^{*-}\pi^+}+A_{K^{*0}\overline{K}^{*0}\pi^+}|^2\\ &-|\sqrt{2}\overline{A}_{K^{*-}K^{*0}\pi^0}+\overline{A}_{K^{*-}K^{*+}\pi^-}+\overline{A}_{\overline{K}^{*0}K^{*0}\pi^-}|^2,\end{aligned} \tag{124}$$

is found to be nonzero, this would mean that there is $\Delta I = 3/2$ NP. The relative phases of the three amplitudes can be measured in the five-body decay $D^+\to K^0K^-\pi^0\pi^+\pi^+$ and its *CP* conjugate. All three resonant decays, $D^+\to K^{*+}\overline{K}^{*0}\pi^0$, $D^+\to K^{*+}K^{*-}\pi^+$, and $D^+\to K^{*0}\overline{K}^{*0}\pi^+$ are part of this final state. The relative phases between the amplitudes can then be obtained from the overlaps of the resonances in the five body final state phase space.

A somewhat more complicated possibility is represented by the $D\to K\overline{K}^*\pi$ and $D\to K^*\overline{K}\pi$. A test that is similar to Eq. (124) can be devised for each of the two sets of

decays. If either one of the *CP* violating differences

$$\begin{aligned}&|\sqrt{2}A_{K^+\overline{K}^{*0}\pi^0} + A_{K^+K^{*-}\pi^+} + A_{K^0\overline{K}^{*0}\pi^+}|^2 \\ &- |\sqrt{2}\overline{A}_{K^-K^{*0}\pi^0} + \overline{A}_{K^-K^{*+}\pi^-} + \overline{A}_{\overline{K}^0K^{*0}\pi^-}|^2,\end{aligned} \tag{125}$$

and

$$\begin{aligned}&|\sqrt{2}A_{K^{*+}\overline{K}^0\pi^0} + A_{K^{*+}K^-\pi^+} + A_{K^{*0}\overline{K}^0\pi^+}|^2 \\ &- |\sqrt{2}\overline{A}_{K^{*-}K^0\pi^0} + \overline{A}_{K^{*-}K^+\pi^-} + \overline{A}_{K^{*-}K^+\pi^-}|^2,\end{aligned} \tag{126}$$

is found to be nonzero, this would mean that there is $\Delta I = 3/2$ NP.

In order to experimentally construct Eq. (125) or Eq. (126), the magnitudes of the amplitudes and their relative phases need to be measured. To determine the relative phase differences a number of four body decays and their *CP* conjugates need to be measured. The phase difference between $A_{K^{*+}K^-\pi^+}$ and $A_{K^0\overline{K}^{*0}\pi^+}$ can be measured from the decay $D^+ \to K^0K^-\pi^+\pi^+$. The phase difference between $A_{K^+K^{*-}\pi^+}$ and $A_{K^{*0}\overline{K}^0\pi^+}$ can be measured from the decay $D^+ \to K^+\overline{K}^0\pi^-\pi^+$. In order to completely fix all of the required phase differences, the decay $D^+ \to K^0\overline{K}^0\pi^0\pi^+$ or the decay $D^+ \to K^+K^-\pi^0\pi^+$ also needs to be measured (as well as the *CP* conjugated decays of all the above mentioned modes). From the resonance overlaps in the decay $D^+ \to K^0\overline{K}^0\pi^0\pi^+$, the relative phases of $A_{K^{*0}\overline{K}^0\pi^+}$, $A_{K^{*+}\overline{K}^0\pi^0}$, and $A_{K^0\overline{K}^{*0}\pi^+}$ can be obtained, so that Eq. (126) is fully determined. Similarly, from the decay $D^+ \to K^+K^-\pi^0\pi^+$ the relative phases of $A_{K^+\overline{K}^{*0}\pi^0}$, $A_{K^{*+}K^-\pi^+}$, and $A_{K^+K^{*-}\pi^+}$ can be obtained so that, Eq. (125) is fully determined.

It is also possible to search for *CP* violation in $\Delta I = 3/2$ amplitudes using $D_s^+ \to K^*\pi$ decays. The sum

$$\sqrt{2}A(D_s^+ \to \pi^0K^{*+}) + A(D_s^+ \to \pi^+K^{*0}) = 3A_3, \tag{127}$$

is $\Delta I = 3/2$ and can be measured from the common Dalitz plot for $D_s^+ \to K^0_{\rm S}\pi^+\pi^0$ decay. Direct *CP* violation in this sum, *i.e.*,

$$\begin{aligned}&|\sqrt{2}A(D_s^+ \to \pi^0K^{*+}) + A(D_s^+ \to \pi^+K^{*0})|^2 - \\ &|\sqrt{2}A(D_s^- \to \pi^0K^{*-}) + A(D_s^- \to \pi^-\overline{K}^{*0})|^2 \neq 0,\end{aligned} \tag{128}$$

would necessarily be due to $\Delta I = 3/2$ NP contributions. Additional information on the absolute value of $|A(D_s^+ \to \pi^+K^{*0})|$ can be obtained from the $D_s^+ \to \pi^+K^+\pi^-$ three body decay.

An analogous test using $D_s^+ \to \rho K^*$ decays also exists, with expressions obtained from the above via the replacement $\pi \to \rho$ and valid for each polarisation separately. The relative phase between $A(D_s^+ \to \rho^0K^{*+})$ and $A(D_s^+ \to \rho^+K^{*0})$ can be measured from the four body decay $D_s^+ \to \pi^+\pi^-K^+\pi^0$. The absolute magnitude $|A(D_s^+ \to \rho^0K^{*+})|$ can be obtained from the more easily measured decay $D_s^+ \to \pi^+\pi^-K^0_{\rm S}\pi^+$, and can be used as a further constraint.

4.5 Potential for lattice computations of direct CP violation and mixing in the D^0–$\overline{D}^0$ system

In searches for NP using charmed mesons, it is obviously crucial to determine accurately the size of SM contributions. In the next few paragraphs we discuss the prospects for such a determination in the future using the methods of lattice QCD.

Lattice QCD provides a first-principles method for determining the strong-interaction contributions to weak decay and mixing processes. It has developed into a precision tool, allowing determinations of the light hadron spectrum, decay constants, and matrix elements such as B_K and B_B with percent-level accuracy. For reviews and collections of recent results, see Refs. [141, 433]. The results provide confirmation that QCD indeed describes the strong interactions in the non-perturbative regime, as well as providing predictions that play an important role in searching for new physics by looking for inconsistencies in unitarity triangle analyses.

Results with high precision are, however, only available for processes involving single hadrons and a single insertion of a weak operator. For the D^0 system, the "high-precision" quantities are thus the matrix elements describing the short-distance parts of D^0-$\overline{D}^0$ mixing and the matrix elements of four-fermion operators arising after integrating out NP. The methodology for such calculations is in place (and has been applied successfully to the K and B meson systems), and we expect results to be forthcoming in the next 1-2 years.

More challenging, and of course more interesting, are calculations of the decay amplitudes to $\pi\pi$ and $K\overline{K}$. For kaon physics, this is the present frontier of lattice calculations. One must deal with two technical challenges: (i) the fact that one necessarily works in finite volume so the states are not asymptotic two-particle states and (ii) the need to calculate Wick contractions (such as the penguin-type contractions) which involve gluonic intermediate states in some channels. The former challenge has been solved in principle by the work of Lüscher [434, 435] and Lellouch and Lüscher [436] for the $K \to \pi\pi$ case, while advances in lattice algorithms and computational power have allowed the numerical aspects of both challenges to be overcome. There are now well controlled results for the $K \to (\pi\pi)_{I=2}$ amplitude [437] and preliminary results for the $K \to (\pi\pi)_{I=0}$ amplitude [438]. It is likely that results to $\sim 10\%$ accuracy for all amplitudes will be available in a few years. We note that, once a lattice calculation is feasible, it will be of roughly equal difficulty to obtain results for the CP conserving and violating parts.

To extend these results to the charm case, one must face a further challenge. This is that, even when one has fixed the strong-interaction quantum numbers of a final state, say to $I = S = 0$, the strong interactions necessarily bring in multiple final states when $E = m_D$. For example, $\pi\pi$ and $K\overline{K}$ states mix with $\eta\eta$, 4π, 6π, *etc.* The finite-volume states that are used by lattice QCD are inevitably mixtures of all these possibilities, and one must learn how, in principle and in practise, to disentangle these states so as to obtain the desired matrix element. Recently, in Ref. [439], a first step towards developing a complete method has been taken, in which the problem has been solved in principle for any number of two-particle channels, and assuming that the scattering is dominantly

S-wave. This is encouraging, and it may be that this method will allow one to obtain semi-quantitative results for the amplitudes of interest. We expect that turning this method into practise will take 3–5 years due to a number of numerical challenges (in particular the need to calculate several energy levels with good accuracy). We also expect that it will be possible to generalise the methodology to include four particle states; several groups are actively working on the theoretical issues. It is unclear at this stage, however, what time scale one should assign to this endeavour.

Finally, we comment briefly on the possibility of calculating long-distance contributions to D^0-$\overline{D}^0$ mixing using lattice methods. Here the challenge is that there are two insertions of the weak Hamiltonian, with many allowed states propagating between them. Some progress has been made recently on the corresponding problem for kaons [440, 441] but the D^0 system is much more challenging. The main problem is that, as for the decay amplitudes, there are many strong-interaction channels with $E < m_D$. Further theoretical work is needed to develop a practical method.

4.6 Interplay of $\Delta\mathcal{A}_{CP}$ with non-flavour observables

4.6.1 Direct *CP* violation in charm *vs.* hadronic EDMs

Models in which the primary source of flavour violation is linked to the breaking of chiral symmetry (left-right flavour mixing) are natural candidates to explain direct *CP* violation in singly-Cabibbo-suppressed D meson decays, via enhanced $\Delta C = 1$ chromomagnetic operators. Interestingly, the chromomagnetic operator generates contributions to D^0-$\overline{D}^0$ mixing and ϵ'/ϵ that are always suppressed by at least the square of the charm Yukawa couplings, thus naturally explaining why they have remained undetected.

On the other hand, the dominant constraints are posed by the neutron and nuclear electric dipole moments (EDMs), which are expected to be close to their experimental bounds. This result is fairly robust because the Feynman diagram contributing to quark EDMs has essentially the same structure as that contributing to the chromomagnetic operator.

In the following we analyse the connection between $\Delta a_{CP}^{\rm dir}$ and hadronic EDMs in concrete NP scenarios, following the analyses of Refs. [416, 417].

Supersymmetry

The leading SUSY contribution to $\Delta a_{CP}^{\rm dir}$ stems from loops involving up-squarks and gluinos and off-diagonal terms in the squark squared-mass matrix in the left-right up sector, the so-called $(\delta^u_{12})_{LR}$ mass-insertion. In the mass-insertion approximation it reads

$$\left|\Delta a_{CP}^{\rm SUSY}\right| \approx 0.6\% \left(\frac{|{\rm Im}\,(\delta^u_{12})_{LR}|}{10^{-3}}\right)\left(\frac{\rm TeV}{\tilde{m}}\right) \ . \tag{129}$$

In a general supersymmetric framework, we expect the parametric relation

$${\rm Im}\,(\delta^u_{12})_{LR} \approx \frac{{\rm Im}(A)\ \theta_{12}\ m_c}{\tilde{m}} \approx \left(\frac{{\rm Im}(A)}{3}\right)\left(\frac{\theta_{12}}{0.3}\right)\left(\frac{\rm TeV}{\tilde{m}}\right) 0.5\times 10^{-3} \ , \tag{130}$$

where A is the trilinear coupling and θ_{12} is a mixing angle between the first two generations of squarks. Taking into account the large uncertainties involved in the evaluation of the matrix element, we conclude that a supersymmetric theory with left-right up-squark mixing can potentially explain the LHCb result.

Among the hadronic EDMs, the best constraints come from mercury and neutron EDMs. Their current experimental bounds are $|d_n| < 2.9 \times 10^{-26}\ e\,\text{cm}$ (90% CL) and $|d_{\text{Hg}}| < 3.1 \times 10^{-29}\ e\,\text{cm}$ (95% CL). In the mass-insertion approximation one can find

$$|d_n| \approx 3 \times 10^{-26} \left(\frac{|\text{Im}\,(\delta^u_{11})_{LR}|}{10^{-6}}\right) \left(\frac{\text{TeV}}{\tilde{m}}\right)\ e\,\text{cm}\ . \tag{131}$$

and therefore it has to be seen whether a concrete SUSY scenario can naturally account for the required level of suppression $|\text{Im}(\delta^u_{11})_{LR}| \lesssim 10^{-6}$.

Disoriented A terms

While we can envisage scenarios in which flavour violation is restricted to the trilinear terms, it is natural to generalise the structure of Eq. (130) to all squarks and take

$$(\delta^q_{ij})_{LR} \sim \frac{A\,\theta^q_{ij}\,m_{q_j}}{\tilde{m}} \qquad q = u, d\ , \tag{132}$$

where θ^q_{ij} are generic mixing angles. This pattern can be obtained when the matrices of the up and down trilinear coupling constants follow the same hierarchical pattern as the corresponding Yukawa matrices but they do not respect exact proportionality.

It is found that θ^q_{ij} can all be of order unity not only in the up, but also in the down sector, thanks to the smallness of the down-type quark masses entering $(\delta^d_{ij})_{LR}$. The only slightly problematic bounds are those on $|\theta^{u,d}_{11}|$ coming from the neutron EDM.

Split families

The severe suppression of $(\delta^u_{21})^{\text{eff}}_{RL}$ stemming from the charm mass can be partially avoided in a framework with split families, where the first two generations of squarks are substantially heavier than $\tilde{t}_{1,2}$ and $\tilde{b}_L$, the only squarks required to be close to the electroweak scale by naturalness arguments. In this case we can decompose the effective couplings relevant to $\Delta a_{CP}^{\text{SUSY}}$ as follows

$$(\delta^u_{12})^{\text{eff}}_{RL} = (\delta^u_{13})_{RR}\,(\delta^u_{33})_{RL}\,(\delta^u_{32})_{LL}\ , \qquad (\delta^u_{12})^{\text{eff}}_{LR} = (\delta^u_{13})_{LL}\,(\delta^u_{33})_{RL}\,(\delta^u_{32})_{RR}\ . \tag{133}$$

Notice that in this scenario we take advantage of the large $(\delta^u_{33})_{LR} \sim Am_t/\tilde{m}$ which we assume to be of order one. We can consider the following two options to explain the LHCb results:

$$\begin{aligned} (\delta^u_{32})_{LL} = O(\lambda^2),\quad (\delta^u_{13})_{RR} = O(\lambda^2) \quad &\to \quad (\delta^u_{12})^{\text{eff}}_{RL} = O(\lambda^4) = O(10^{-3})\ , \\ (\delta^u_{13})_{LL} = O(\lambda^3),\quad (\delta^u_{32})_{RR} = O(\lambda) \quad &\to \quad (\delta^u_{12})^{\text{eff}}_{LR} = O(\lambda^4) = O(10^{-3})\ . \end{aligned} \tag{134}$$

Gluino-squark loops yield an EDM (d_u) and a chromo-EDM (d^c_u) for the up quark proportional to $d^{(c)}_u \sim \text{Im}\,[(\delta^u_{13})_{LL}(\delta^u_{31})_{RR}]$ and it turns out that

$$\left|\Delta\mathcal{A}_{CP}^{\text{SUSY}}\right| \approx 10^{-3} \times \left|\frac{d_n}{3\times 10^{-26}}\right| \left|\frac{\text{Im}\,(\delta^u_{32})_{RR}}{0.2}\right| \left|\frac{10^{-3}}{\text{Im}\,(\delta^u_{31})_{RR}}\right|\ . \tag{135}$$

In conclusion, the EDM bounds require a strong hierarchical structure in the off-diagonal terms of the RR up-squark mass matrix, as happens in models predicting $(\delta^u_{ij})_{RR} \sim (m_{u_i}/m_{u_j})/|V_{ij}|$.

Supersymmetric flavour models

In models where the flavour structure of the soft breaking terms is dictated by an approximate flavour symmetry, $(\delta^u_{LR})_{12}$ is generically flavour-suppressed by $(m_c\,|V_{us}|\,/\tilde{m})$, which is of order a few times 10^{-4}. There is however additional dependence on the ratio between flavour-diagonal parameters, $A/\tilde{m}$, and on unknown coefficients of order one, that can provide enhancement by a factor of a few. In most such models, the selection rules that set the flavour structure of the soft breaking terms, relate $(\delta^u_{LR})_{12}$ to $(\delta^d_{LR})_{12}$ and to $(\delta^{u,d}_{LR})_{11}$, which are bounded from above by, respectively, ϵ'/ϵ and EDM constraints. Since both ϵ'/ϵ and EDMs suffer from hadronic uncertainties, small enhancements due to the flavour-diagonal supersymmetric parameters cannot be ruled out. It is thus possible to accommodate $\Delta\mathcal{A}_{CP} \sim 0.006$ in supersymmetric models that are non-minimally flavour violating, but – barring hadronic enhancements in charm decays – it takes a fortuitous accident to lift the supersymmetric contribution above the permille level [417].

New-physics scenarios with Z-mediated FCNC

Effective FCNC couplings of the Z boson to SM quarks can appear in the SM with non-sequential generations of quarks, models with an extra $U(1)$ symmetry or models with extra vector-like doublets and singlets. The effective FCNC Lagrangian can be written as

$$\mathcal{L}^{Z-\mathrm{FCNC}}_{\mathrm{eff}} = -\frac{g}{2\cos\theta_W}\bar{q}_i\gamma^\mu\left[(g^Z_L)_{ij}\,P_L + (g^Z_R)_{ij}\,P_R\right]q_j\;Z_\mu + \;\mathrm{h.c.}\,, \tag{136}$$

The chromomagnetic operator is generated at the one-loop level, with leading contribution from Z–top exchange diagrams leading to

$$\left|\Delta\mathcal{A}^{Z-\mathrm{FCNC}}_{CP}\right| \approx 0.6\% \;\left|\frac{\mathrm{Im}\left[(g^Z_L)^*_{ut}(g^Z_R)_{ct}\right]}{2\times10^{-4}}\right|\,. \tag{137}$$

The presence of new CP violating phases in the couplings $(g^Z_{L,R})_{ij}$ are also expected to generate hadronic EDMs, In particular, one can find

$$|d_n| \approx 3\times10^{-26}\;\left|\frac{\mathrm{Im}\left[(g^Z_L)^*_{ut}(g^Z_R)_{ut}\right]}{2\times10^{-7}}\right|\;e\,\mathrm{cm}\,, \tag{138}$$

and therefore $\Delta\mathcal{A}^{Z-\mathrm{FCNC}}_{CP} = O(10^{-2})$ only provided $\mathrm{Im}(g^Z_R)_{ut}/\mathrm{Im}(g^Z_R)_{ct} \lesssim 10^{-3}$.

In the NP scenarios with Z-mediated FCNCs, the most interesting FCNC processes in the top sector are $t\to cZ$ and $t\to uZ$, which arise at the tree level. In particular, we have

$$\mathcal{B}(t\to cZ) \approx 0.7\times10^{-2}\left|\frac{(g^Z_R)_{tc}}{10^{-1}}\right|^2\,, \tag{139}$$

which is within the reach of the LHC for the values of $(g^Z_R)_{tc}$ relevant to $\Delta\mathcal{A}^{Z-\mathrm{FCNC}}_{CP}$.

New-physics scenarios with scalar-mediated FCNC

Finally, we analyse a new-physics framework with effective FCNC couplings to SM quarks of a scalar particle h. The effective Lagrangian reads

$$\mathcal{L}_{\text{eff}}^{h-\text{FCNC}} = -\bar{q}_i \left[(g_L^h)_{ij} \, P_L + (g_R^h)_{ij} \, P_R \right] q_j \; h + \text{ h.c.} \tag{140}$$

Also in this case the chromomagnetic operator is generated at the one-loop level, with a leading contribution from h–top exchange diagrams. This leads to

$$\left| \Delta a_{CP}^{\text{FCNC}} \right| \approx 0.6\% \left| \frac{\text{Im} \left[(g_L^h)_{ut}^* (g_R^h)_{tc} \right]}{2 \times 10^{-4}} \right| . \tag{141}$$

As in all the other frameworks, the most severe constraints are posed by the hadronic EDMs

$$|d_n| \approx 3 \times 10^{-26} \left| \frac{\text{Im} \left[(g_L^h)_{ut}^* (g_R^h)_{tu} \right]}{2 \times 10^{-7}} \right| e \, \text{cm} \, . \tag{142}$$

With scalar-mediated FCNCs, the potentially most interesting signals are the rare top decays $t \to ch$ or $t \to uh$, if kinematically allowed. In particular, we find that

$$\mathcal{B}(t \to qh) \approx 0.4 \times 10^{-2} \left| \frac{(g_R^h)^{tq}}{10^{-1}} \right|^2 , \tag{143}$$

which could be within the reach of the LHC.

4.6.2 Interplay of collider physics and a new physics origin for $\Delta\mathcal{A}_{CP}$

The first observation of direct CP violation in singly Cabibbo suppressed D decays may have interesting implications for NP searches around the TeV scale at the LHC. The NP contribution to $\Delta a_{CP}^{\text{dir}}$ can be fully parametrised by a complete set of $\Delta C = 1$ effective operators at the charm scale. As shown by the authors of Ref. [51] only a few of these operators can accommodate the LHCb result without conflicting with present bounds from D^0-$\overline{D}^0$ mixing and ϵ'/ϵ. In particular four fermion operators of the form $\mathcal{O}^q = (\bar{u}_R \gamma^\mu c_R)(\bar{q}_R \gamma_\mu q_R)$ with $q = u, d, s$ are promising since they do not lead to flavour violation in the down-type quark sector. We define the corresponding Wilson coefficients as $1/\Lambda_q^2$. Assuming the SM expectation for $\Delta a_{CP}^{\text{dir}}$ is largely subdominant, the LHCb measurement suggests a scale of $\Lambda_q \simeq 15$ TeV [51].

There is an immediate interplay between charm decay and flavour (and CP) conserving observables at much higher energies provided $\mathcal{O}^q$ arises from a heavy NP state exchanged in the s-channel. Under this mild assumption $\mathcal{O}^q$ factorises as the product of two quark currents and the same NP induces D^0-$\overline{D}^0$ mixing and quark compositeness through the $(\bar{u}_R \gamma_\mu c_R)^2$ and $(\bar{q}_R \gamma_\mu q_R)^2$ operators, respectively. Denoting their respective Wilson coefficients by $\Lambda_{\bar{u}c}$ and $\Lambda_{\bar{q}q}$, the relation $\Lambda_q = \sqrt{\Lambda_{\bar{u}c} \Lambda_{\bar{q}q}}$ is predicted. The D^0-$\overline{D}^0$ mixing bound on NP implies $\Lambda_{\bar{u}c} \gtrsim 1200$ TeV [390]. Combining this stringent $\Delta C = 2$ bound with the

$\Delta C = 1$ scale suggested by $\Delta a_{CP}^{\rm dir}$ thus generically requires $\Lambda_{\bar{q}q} \lesssim 200$ GeV, which a rather low compositeness scale for the light quark flavours.

Quark compositeness can be probed at the LHC through dijet searches. Actually for the up or the down quark the low scale suggested by $\Delta a_{CP}^{\rm dir}$ is already excluded by the Tevatron [442, 443]. On the other hand dijet searches are less sensitive to contact interactions involving only the strange quark since the latter, being a sea quark, has a suppressed parton distribution function in a proton. The authors of Ref. [444] showed that a first estimation at the partonic level of the extra dijet production from a $(\bar{s}_R \gamma_\mu s_R)^2$ operator with a scale of $\Lambda_{\bar{s}s} \sim 200$ GeV is marginally consistent, given the $\mathcal{O}(1)$ uncertainty of the problem, with the present bounds from the ATLAS and CMS experiments [445, 446].

One concludes that an $\mathcal{O}^s$ operator induced by a s-channel exchanged NP can accommodate the $\Delta a_{CP}^{\rm dir}$ measurement without conflicting with $\Delta C = 2$, ϵ'/ϵ and dijet searches. Furthermore such a NP scenario makes several generic predictions both for charm and high $p_{\rm T}$ physics: 1) most of the *CP* asymmetry is predicted to be in the $K^+ K^-$ channel, 2) *CP* violation in D^0-$\overline{D}^0$ mixing should be observed in the near future, and 3) an excess of dijets at the LHC is expected at a level which should be visible in the 2012 data.

4.7 Future potential of LHCb measurements

4.7.1 Requirements on experimental precision

The ultimate goal of mixing and *CP* violation measurements in the charm sector is to reach the precision of the SM predictions (or better). In some cases this requires measurements in several decay modes in order to distinguish enhanced contributions of higher order SM diagrams from effects caused by new particles.

Indirect *CP* violation measurements at LHCb are mostly constrained by the observable A_Γ (see Eq. 85). The *CP* violating parameters in this observable are multiplied by the mixing parameters x_D and y_D, respectively. Hence, the relative precision on the *CP* violating parameters is limited by the relative precision of the mixing parameters. Therefore, aiming at a relative precision below 10% and taking into account the current mixing parameter world averages, the target precision would be $2 - 3 \times 10^{-4}$. With Standard Model indirect *CP* violation expected to be of the order of 10^{-4}, the direct *CP* violation parameter contributing to A_Γ has to be measured to a precision of 10^{-3} in order to distinguish the two types of *CP* violation in A_Γ.

Direct *CP* violation is not expected to be as large as the current world average of ΔA_{CP} in most other decay modes. However, a few large *CP* violation signatures are expected. Using flavour-SU(3) and U-spin estimations lead to expectations of $a_{CP}^{\rm dir}(D^+ \to K^+ \overline{K}^0) \gtrsim 0.1\%$ and $a_{CP}^{\rm dir}(D^0 \to K^0_{\rm S} K^0_{\rm S}) \sim 0.6\%$. Considerations assuming universality of $\Delta F = 1$ transitions lead to a limit of $a_{CP}^{\rm dir}(D \to \pi e^+ e^-) \lesssim 2\%$. Enhanced electro-magnetic dipole operators can lead to $a_{CP}^{\rm dir}(D \to V\gamma)$ of a few %, equivalent to the influence of chromo-magnetic dipole operators on $\Delta \mathcal{A}_{CP}$. Additional information can be obtained from time-dependent studies of $D \to V\gamma$ decays or from angular analyses of $D \to V l^+ l^-$ decays.

Analyses of $\Delta I = \frac{3}{2}$ transitions involve asymmetry measurements of several related decay modes. Examples are the decays $D \to \pi\pi$, $D \to \rho\pi$, $D \to \rho\rho$, $D \to \overline{K}K\pi$, and $D_s^+ \to K^*\pi$. The number of final state particles in these decays varies from two to six (counting the pions from K_S^0 decays) and many of these modes contain neutral pions in their final state. The precision for modes involving neutral pions or photons will be limited by the ability of the calorimeter of identifying these particles in the dense hadronic environment. An upgraded calorimeter with smaller Molière radius would greatly extend the physics reach in this area.[39]

In general, a precision of 5×10^4 or better for asymmetry differences as well as individual asymmetries is needed for measurements of other singly-Cabibbo-suppressed charm decays. While measurements of time-integrated raw asymmetries at this level should be well within reach, the challenge lies in the control of production and detection asymmetries in order to extract the physics asymmetries of individual decay modes. This can be achieved by assuming that there is no significant *CP* violation in Cabibbo-allowed decay modes.

4.7.2 Prospects of future LHCb measurements

We project the numbers of events in various channels directly from the numbers reconstructed in the 2011 data set, in most cases. We assume the prompt charm cross-section will increase by a factor of 1.8 in moving from $\sqrt{s} = 7$ TeV to $\sqrt{s} = 14$ TeV, that the integrated luminosity will increase from $1\,\text{fb}^{-1}$ to $50\,\text{fb}^{-1}$, and that trigger efficiency for charm will increase by a factor of 2 as the current hardware trigger requirement is effectively removed (or substantially relaxed). We additionally project a factor of 3.5 times greater efficiency in channels with $K_S^0 \to \pi^-\pi^+$ daughters based on progress made in the trigger software between 2011 and 2012. This primarily results from reconstructing candidates which decay downstream of the VELO. The results of this exercise are summarised in Table 11 for D^0 decays and in Table 12 for D^+ and D_s^+ decays.

Estimating the physics reach possible with the projected data sets requires a number of assumptions. The statistical precision generally improves as $1/\sqrt{n}$. Estimating the systematic error, and therefore ultimate physics reach, is more of an art. It is often the case that data can be used to control systematic uncertainties at the level of the statistical error, but for the moment we make no estimates of what will be possible. In some cases controlling systematics will require sacrificing some of the statistics to work with cleaner signals or with signals which populate only parts of the detector where the performance is very well understood. Estimates of sensitivity to CPV in mixing generally depend on the values of the mixing parameters – the larger the number of mixed events, the larger the effective statistics contributing to the corresponding CPV measurement.

The estimated statistical precisions for mixing parameters and CPV in D^0 measurements are presented in Table 13. The precision for measuring $(x'^2_D,\, y'_D)$ using the time-dependence of the wrong-sign (WS) to right-sign (RS) $K\pi$ rate comes from extrapolating the BaBar [360] and Belle [447] sensitivities. The precision for measuring r_M using the

[39] Such an upgrade to the calorimeter system is not in the baseline plan for the LHCb upgrade [60,61].

Table 11: Numbers of D^0 and $D^{*+} \to D^0\pi^+$ signal events observed in the 2011 data in a variety of channels and those projected for $50\,\text{fb}^{-1}$. These channels can be used for mixing studies, for indirect *CP* violation studies, and for direct *CP* violation studies. As discussed in the text, the numbers of events in any one channel can vary from one analysis to another, depending on the level of cleanliness required. Hence, all numbers should be understood to have an inherent variation of a factor of 2. To control systematics with the very high level of precision that will be required at the end of the upgrade, it may be necessary to sacrifice some of the statistics.

Mode	2011 yield (kilo events)	$50\,\text{fb}^{-1}$ yield (mega events)
untagged $D^0 \to K^-\pi^+$	230 000	40 000
$D^{*+} \to D^0\pi^+;\ D^0 \to K^-\pi^+$	40 000	7 000
$D^{*+} \to D^0\pi^+;\ D^0 \to K^+\pi^-$	130	20
$D^0 \to K^-K^+$	25 000	4 600
$D^0 \to \pi^-\pi^+$	6 500	1 200
$D^{*+} \to D^0\pi^+;\ D^0 \to K^-K^+$	4 300	775
$D^{*+} \to D^0\pi^+;\ D^0 \to \pi^-\pi^+$	1 100	200
$D^{*+} \to D^0\pi^+;\ D^0 \to K^0_S\pi^-\pi^+$	300	180
$D^{*+} \to D^0\pi^+;\ D^0 \to K^0_S K^-K^+$	45	30
$D^{*+} \to D^0\pi^+;\ D^0 \to K^-\pi^+\pi^-\pi^+$	7 800	1 400
$D^{*+} \to D^0\pi^+;\ D^0 \to K^-K^+\pi^-\pi^+$	120	20
$D^{*+} \to D^0\pi^+;\ D^0 \to \pi^-\pi^+\pi^-\pi^+$	470	85
$D^{*+} \to D^0\pi^+;\ D^0 \to K^-\mu^+X$	–	4 000
$D^{*+} \to D^0\pi^+;\ D^0 \to K^+\mu^-X$	–	0.1

ratio of WS to RS $K\mu\nu$ events assumes the central value to be 2.5×10^{-5}. The S:B ratio is assumed to be 30 times better than reported by BaBar [448] for their similar $Ke\nu$ analysis. Background can be reduced by a factor of 10 using LHCb's excellent vertex resolution to remove candidates with decay time less than 2 D^0 lifetimes – a requirement which reduces the WS signal by relatively little as its decay time distribution has the form $dN/dt \propto t^2\, e^{-\Gamma t}$. In addition, the excellent vertex resolution and the decay time requirement allow the neutrino momentum, and hence the D^{*+}-D^0 mass difference to be measured with better resolution than was possible in the e^+e^- experiments. BaBar demonstrated that using a doubly-tagged sample of semileptonic decay candidates provides the same mixing sensitivity as the more traditional singly-tagged sample [449]. By combining singly- and doubly-tagged samples, it should be possible to effectively double the statistics.

The projected sensitivities for the two-body direct CPV measurements are relatively solid: the 2011 $\Delta\mathcal{A}_{CP}$ measurements provide benchmark samples with full analysis cuts including fiducial cuts necessary to control systematics for measuring $\Delta\mathcal{A}_{CP}$. The systematics for the separate $\mathcal{A}_{CP}(K^-K^+)$ and $\mathcal{A}_{CP}(\pi^-\pi^+)$ measurements will be more challenging and may require sacrificing statistical precision. The projections for measuring

Table 12: Numbers of D^+ and D_s^+ signal events observed in the 2011 data in a variety of channels and those projected for $50\,\text{fb}^{-1}$. These channels can be used for direct *CP* violation studies. As discussed in the text, the numbers of events in any one channel can vary from one analysis to another, depending on the level of cleanliness required. To control systematics with the very high level of precision that will be required at the end of the upgrade, it may be necessary to sacrifice some of the statistics.

Mode	2011 yield (kilo events)	50 fb^{-1} yield (mega events)
$D^+ \to K^-\pi^+\pi^+$	60 000	11 000
$D^+ \to K^+\pi^+\pi^-$	200	40
$D^+ \to K^-K^+\pi^+$	6 500	1 200
$D^+ \to \phi\pi^+$	2 800	500
$D^+ \to \pi^-\pi^+\pi^+$	3 200	575
$D^+ \to K^0_S\pi^+$	1 500	1 000
$D^+ \to K^0_S K^+$	525	330
$D^+ \to K^-K^+K^+$	60	10
$D_s^+ \to K^-K^+\pi^+$	8 900	1 600
$D_s^+ \to \phi\pi^+$, $(\phi \to K^-K^+)$	5 350	1 000
$D_s^+ \to \pi^-\pi^+\pi^+$	2 000	360
$D_s^+ \to K^-\pi^+\pi^+$		
$D_s^+ \to \pi^-K^+\pi^+$	555	100
$D_s^+ \to K^-K^+K^+$	50	10
$D_s^+ \to K^0_S K^+$	410	260
$D_s^+ \to K^0_S\pi^+$	33	20

y_{CP} and A_Γ using K^-K^+ and $\pi^-\pi^+$ should also be robust as the same samples will be used for these analyses as for the $\mathcal{A}_{CP}$ measurements.

The projected precision for measuring (x_D, y_D) from $D^0 \to K^0_S\pi^-\pi^+$ comes from scaling the Belle [366] and BaBar [450] sensitivities. The statistical precisions could be even better as LHCb's prompt sample will be enhanced at higher decay times where the mixing effects are greater. By constrast, D^0 mesons from semileptonic B decays should be unbiased in terms of decay, providing a useful sample at lower decay times.

The estimated statistical precisions for direct CPV in D^+ measurements are presented in Table 14. The estimates for the phase-space integrated CPV rates are $1/\sqrt{n}$ rounded up by a factor of order 2 to allow for using tighter cuts to control systematic uncertainties. The estimates for measuring CPV in the magnitudes and phases of quasi-two-body amplitudes contributing to three-body final states come from scaling the BaBar sensitivities for time-integrated CPV in $D^0 \to \pi^-\pi^+\pi^0$ and $D^0 \to K^-K^+\pi^0$ by $1/\sqrt{n}$. The angular moments of the cosine of the helicity angle of the D decay products reflect the spin and mass structure of the intermediate resonant and nonresonant amplitudes with no explicit

Table 13: Estimated statistical uncertainties for mixing and *CP* violation measurements which can be made with the projected samples for $50\,\text{fb}^{-1}$ described in Table 11.

Sample	Parameter(s)	Precision
WS/RS $K\pi$	(x'^2, y')	$\mathcal{O}[(10^{-5}, 10^{-4})]$
WS/RS $K\mu\nu$	r_M	$\mathcal{O}(5 \times 10^{-7})$
WS/RS $K\mu\nu$	$\lvert p/q \rvert$	$\mathcal{O}(1\%)$
$D^{*+} \to D^0\pi^+;\ D^0 \to K^-K^+, \pi^-\pi^+$	$\Delta\mathcal{A}_{CP}$	0.015%
$D^{*+} \to D^0\pi^+;\ D^0 \to K^-K^+$	$\mathcal{A}_{CP}$	0.010%
$D^{*+} \to D^0\pi^+;\ D^0 \to \pi^-\pi^+$	$\mathcal{A}_{CP}$	0.015%
$D^{*+} \to D^0\pi^+;\ D^0 \to K^0_S\pi^-\pi^+$	(x, y)	$(0.015\%, 0.010\%)$
$D^{*+} \to D^0\pi^+;\ D^0 \to K^-K^+, (\pi^-\pi^+)$	y_{CP}	0.004% (0.008%)
$D^{*+} \to D^0\pi^+;\ D^0 \to K^-K^+, (\pi^-\pi^+)$	A_Γ	0.004% (0.008%)
$D^{*+} \to D^0\pi^+;\ D^0 \to K^-K^+\pi^-\pi^+$	$\mathcal{A}_\text{T}$	2.5×10^{-4}

Table 14: Estimated statistical uncertainties for *CP* violation measurements which can be made with the projected D^+ samples for $50\,\text{fb}^{-1}$ described in Table 12.

Sample	Parameter(s)	Precision
$D^+ \to K^0_S K^+$	PSP-integrated CPV	10^{-4}
$D^+ \to K^-K^+\pi^+$	PSP-integrated CPV	5×10^{-5}
$D^+ \to \pi^-\pi^+\pi^+$	PSP-integrated CPV	8×10^{-5}
$D^+ \to K^-K^+\pi^+$	CPV in phases, amplitude model	$(0.01 - 0.10)^\circ$
$D^+ \to K^-K^+\pi^+$	CPV in fraction differences, amplitude model	$(0.01 - 0.10)\%$
$D^+ \to \pi^-\pi^+\pi^+$	CPV in phases, amplitude model	$(0.01 - 0.10)^\circ$
$D^+ \to \pi^-\pi^+\pi^+$	CPV in fraction differences, amplitude model	$(0.01 - 0.10)\%$
$D^+ \to K^-K^+\pi^+$	CPV in phases, model independent	$(0.01 - 0.10)^\circ$
$D^+ \to K^-K^+\pi^+$	CPV in fraction differences, model independent	$(0.01 - 0.10)\%$
$D^+ \to \pi^-\pi^+\pi^+$	CPV in phases, model independent	$(0.01 - 0.10)^\circ$
$D^+ \to \pi^-\pi^+\pi^+$	CPV in fraction differences, model independent	$(0.01 - 0.10)\%$

model dependence. The difference between the angular moment distributions observed in D^0 and $\overline{D}^0$ decays provides sensitivity to CPV in the magnitudes (or fractions) and phases of amplitudes about equal to that of model-dependent fits. The angular moment differences are robust, in the sense that they are model-independent, but they are less specific compared to the results from model-dependent analyses: they indicate only the spins and mass ranges where particle and antiparticle amplitudes differ, but do not identify a specific *CP*-violating intermediate state or how much it varies. The sensitivity to CPV in any contributing amplitude depends on how much it contributes to the three-body decay, and also on the other amplitudes with which it interferes. For this reason, ranges of sensitivity are indicated rather than single values. No sensitivities for CPV measurements in

three-body D_s^+ decay channels are estimated explicitly. They can be estimated roughly by extrapolating from the numbers for D^+ decays using $1/\sqrt{n}$. These estimates should be degraded slightly as the lifetime of the D^+ is much greater than that of the D_s^+, making it easier to select clean D^+ samples.

4.8 Conclusion

LHCb has proven its capability of performing high-precision charm physics measurements. The experiment is ideally suited for *CP* violation searches and for measurements of decay-time-dependent processes such as mixing.

Finding evidence for a non-zero value of ΔA_{CP} has raised the question of whether or not this may be interpreted as the first hint of physics beyond the SM at the LHC. Within the SM the central value can only be explained by significantly enhanced penguin amplitudes. This enhancement is conceivable when estimating flavour $SU(3)$ or U-spin breaking effects from fits to $D \to PP$ data. However, attempts at estimating the long distance penguin contractions directly have failed to yield conclusive results to explain the enhancement.

Lattice QCD has the potential of assessing the penguin enhancement directly. However, several challenges arise which make these calculations impossible at the moment. Following promising results on $K \to \pi\pi$ decays, additional challenges arise in the charm sector as $\pi\pi$ and KK states mix with $\eta\eta$, 4π, 6π and other states. Possible methods have been proposed and results may be expected in three to five years time.

General considerations on the possibility of interpreting ΔA_{CP} in models beyond the SM have led to the conclusion that an enhanced chromomagnetic dipole operator is required. These operators can be accommodated in minimal supersymmetric models with non-zero left-right up-type squark mixing contributions or, similarly, in warped extra dimensional models. Tests of these interpretations beyond the SM are needed. One promising group of channels are radiative charm decays where the link between the chromomagnetic and the electromagnetic dipole operator leads to predictions of enhanced *CP* asymmetries of several percent. These can be measured to sufficient precision at the LHCb upgrade.

Another complementary test is to search for contributions beyond the SM in $\Delta I = 3/2$ amplitudes. This class of amplitudes leads to several isospin relations which can be tested in a range of decay modes, *e.g.* $D \to \pi\pi$, $D \to \rho\pi$, $D \to K\bar{K}$, *etc.* Several of these measurements, such as the Dalitz plot analysis of the decay $D^0 \to \pi^+\pi^-\pi^0$, can be performed at LHCb.

Beyond charm physics, the chromomagnetic dipole operators would affect the neutron and nuclear EDMs, which are expected to be close to the current experimental bound. Similarly, rare FCNC top decays are expected to be enhanced, if kinematically allowed. Furthermore, quark compositeness can be related to the ΔA_{CP} measurement and tested in dijet searches. Current results favour the new physics contribution to be located in the $D^0 \to K^-K^+$ decay as the strange quark compositeness scale is less well constrained. Measurements of the individual asymmetries of sufficient precision will be possible at the

LHCb upgrade.

The charm mixing parameters have not yet been precisely calculated in the SM. An inclusive approach based on an operator product expansion relies on the expansion scale being small enough to allow convergence and furthermore involves the calculation of a large number of unknown matrix elements. An exclusive approach sums over intermediate hadronic states and requires very precise branching ratio determinations of these final states which are currently not available. Contrary to the SM, contributions beyond the SM can be calculated reliably. With the SM contribution to indirect *CP* violation being $< 10^{-4}$, the LHCb upgrade is ideally suited to cover the parameter space available for enhanced asymmetries beyond the SM. Measurements in several complementary modes will permit the extraction of the underlying theory parameters with high precision.

The LHCb upgrade will allow to constrain *CP* asymmetries and mixing observables to a level of precision which, in most of the key modes, cannot be matched by any other experiment foreseen on a similar timescale. This level of precision will permit us not only to discover *CP* violation in charm decays but also to unambiguously understand its origin.

5 The LHCb upgrade as a general purpose detector in the forward region

5.1 Quarkonia and multi-parton scattering

The mechanism of heavy quarkonium production is a long-standing problem in QCD. An effective field theory, non-relativistic QCD (NRQCD), provides the foundation for much of the current theoretical work. According to NRQCD, the production of heavy quarkonium factorizes into two steps: a heavy quark-antiquark pair is first created perturbatively at short distances and subsequently evolves non-perturbatively into quarkonium at long distances. The NRQCD calculations depend on the colour-singlet (CS) and colour-octet (CO) matrix elements, which account for the probability of a heavy quark-antiquark pair in a particular colour state to evolve into heavy quarkonium. The CS model [451,452], which provides a leading-order (LO) description of quarkonia production, was first used to describe experimental data. However, it underestimates the observed cross-section for single J/ψ production at high $p_{\rm T}$ at the Tevatron [453]. To resolve this discrepancy the CO mechanism was introduced [454]. The corresponding matrix elements were determined from the large-$p_{\rm T}$ data as the CO cross-section falls more slowly than that for CS. More recent higher-order calculations [455–458] close the gap between the CS predictions and the experimental data [459] reducing the need for large CO contributions.

Traditionally, quarkonia production studies at hadron colliders have focussed on the study of J/ψ, $\psi(2S)$ and $\Upsilon(nS)$ decays to di-muon or di-electron pairs [459]. The LHCb program so far has followed this pattern with measurement of many cross-sections already published [460–464]. As an example of the quality of the data Fig. 30 shows the Υ mass distribution observed in the data. By the time of the upgrade in 2019, data samples corresponding to several fb^{-1} will have been collected at $\sqrt{s} = 7, 8$ and 14 TeV and the results will be dominated by systematic uncertainties. Therefore, new probes of quarkonia production will be pursued. Two possibilities are detailed here: multiple quarkonia production and probing quarkonia production via hadronic decay modes. These studies will profit from the higher integrated luminosity and improved trigger. These modes provide clear signals in the detector and will be relatively uneffected by the increased pile-up. As the cross-sections for charmonium [462] production at the LHC are large, the question of multiple production of these states in a single proton-proton collision naturally arises. Recently, studies of double hidden charm and hidden and associated open charm production have been proposed as probes of the quarkonium production mechanism [465]. In proton-proton collisions contributions from other mechanisms, such as Double Parton Scattering (DPS) [466–468] or the intrinsic charm content of the proton [469], are possible. First studies of both processes have been carried out with the current LHCb data; more details can be found in Refs. [49, 57].

Leading order (LO) colour singlet calculations for the $gg \to J/\psi\, J/\psi$ process in perturbative QCD, exist and give consistent results with the data [470–472]. In the LHCb fiducial region ($2 < y_{J/\psi} < 4.5$, $p^{\rm T}_{J/\psi} < 10$ GeV/c, where $y_{J/\psi}$ and $p^{\rm T}_{J/\psi}$ stand for rapidity and transverse momentum of the J/ψ, respectively) these calculations give that the

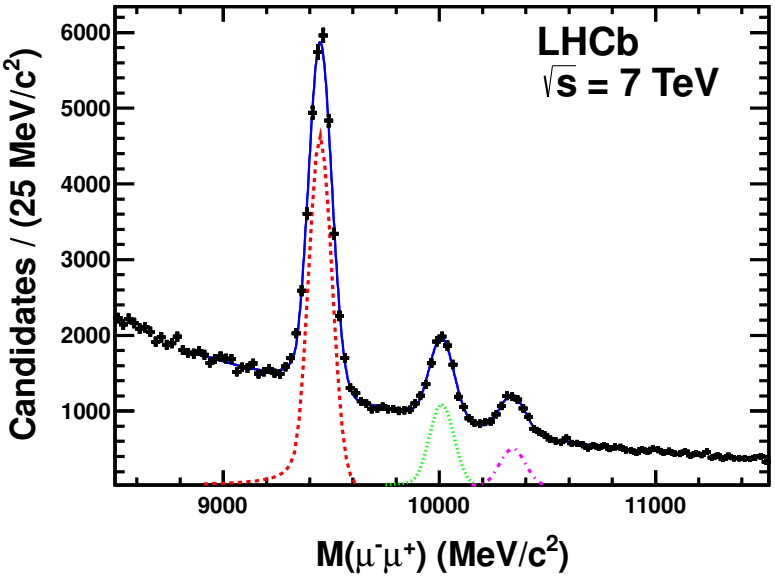

Figure 30: Invariant mass distribution of selected Υ candidates taken from Ref. [463]. The study uses 25 pb^{-1} of data collected in 2010. The $\Upsilon(1S)$, $\Upsilon(2S)$ and $\Upsilon(3S)$ states are clearly resolved. The results of a maximum likelihood fit are superimposed.

$J/\psi\, J/\psi$ production cross-section is 4.1 ± 1.2 nb [472] in agreement with the measured value of 5.1 ± 1.0 nb [57]. Similar calculations exist for the case of double $\Upsilon(1S)$ production. For the case of J/ψ plus $\Upsilon(1S)$ production no leading order diagrams contribute and hence the rate is expected to be suppressed in SPS. This leads to an 'unnatural' ordering of the cross-section values: $\sigma_{gg}^{J/\psi\, J/\psi} > \sigma_{gg}^{\Upsilon(1S)\Upsilon(1S)} > \sigma_{gg}^{\Upsilon(1S)J/\psi}$.

The DPS contributions to all these double onia production modes can be estimated, neglecting partonic correlations in the proton, as the product of the measured cross-sections of the sub-processes involved divided by an effective cross-section [466–468, 473]. The value of the latter is determined from multi-jet events at the Tevatron to be $\sigma_{\rm eff}^{\rm DPS} = 14.5 \pm 1.7\,^{+1.7}_{-2.3}$ mb [474]. At $\sqrt{s} = 7$ TeV the contribution from this source to the total cross-section is similar in size to the LO contribution from Single Parton Scattering (SPS). For DPS the ordering of the cross-section values is: $\sigma_{\rm DPS}^{J/\psi\, J/\psi} > \sigma_{\rm DPS}^{\Upsilon(1S)J/\psi} > \sigma_{\rm DPS}^{\Upsilon(1S)\Upsilon(1S)}$.

The expected cross-sections for a few double quarkonia processes, together with their yields, are summarized in Table 15. Measurements of the cross-section and properties in these modes will allow to disentangle the importance of the two contributions.

As well as probing the production mechanism these studies are sensitive to a potential first observation of tetraquark states [472] and of χ_b and η_b states decaying in the double J/ψ mode. Based on the cross-sections and branching ratios given in Ref. [475], 500 (1500) fully reconstructed $\chi_{b0}(1P)$ ($\chi_{b2}(1P)$) are expected with the upgraded detector and these decays will be visible at LHCb. In the case of the η_b, several estimates exist, based on

Table 15: Expected cross-sections in the LHCb acceptance and yields for double quarkonia production with 50 fb^{-1} at $\sqrt{s} = 14$ TeV.

Mode	σ_{gg} [nb]	Yield [SPS]	$\sigma_{\rm DPS}$ [nb]	Yield [DPS]
$J/\psi\ J/\psi$	7.2	270,000	11	430, 000
$J/\psi\ \psi(2S)$	3.2	14,000	4.0	19,000
$\psi(2S)\ \psi(2S)$	0.4	180	0.6	300
$J/\psi\ \chi_{c0}$	-	-	4.3	200
$J/\psi\ \chi_{c1}$	-	-	6.6	14000
$J/\psi\ \chi_{c2}$	-	-	8.6	11000
$J/\psi\ \Upsilon(1S)$	0.0036	360	0.27	20,000
$J/\psi\ \Upsilon(2S)$	0.0011	90	0.07	5300
$J/\psi\ \Upsilon(3S)$	0.0005	50	0.035	2000
$\Upsilon(1S)\ \Upsilon(1S)$	0.014	1100	0.0027	200

values of the branching ratio $\eta_b \to J/\psi\, J/\psi$ ranging from 10^{-6} to 10^{-8} [476], corresponding to yields of 0.02 to 5 events.

The upgraded detector is expected to have excellent hadron identification capabilities both offline and at the trigger level. As discussed in Ref. [477], this allows charmonium studies to be performed in hadronic decay modes. A particularly convenient mode is the $p\overline{p}$ final state. This is accessible for the J/ψ, η_c, χ_{cJ}, h_c and $\psi(2S)$ mesons. Extrapolating from studies with the current detector large inclusive samples of these decays will be collected. For example around 0.5 million $\eta_c \to p\overline{p}$ will be collected.

Hadronic decays of heavy bottomonium have received less attention in the literature [476]. The high mass implies a large phase space for innumerable decay modes, but with the price that the branching ratio for each individual mode is greatly diluted. In Ref [476] it is estimated that the $\eta_b \to D^*\overline{D}$ branching fraction is 10^{-5} and the $\eta_b \to D\overline{D}\pi$ rate maybe a factor of ten higher. Though no specific studies have been performed, based on the studies of double open charm production given in Ref. [49] it is plausible that an η_b signal will be detected in this mode with the upgraded detector.

5.2 Exotic meson spectroscopy

The spectroscopy of bound states formed by heavy quark-antiquark pairs (c or b quarks), has been intensively studied from both theoretical and experimental points of view since the discovery of the $J/\psi\,(cc)$ state in 1974 [478] and the discovery of the $\Upsilon(1S)\,(b\bar{b})$ state in 1977 [479]. Until recently, all experimentally observed charmonium ($c\bar{c}$) and bottomonium ($b\bar{b}$) states matched well with expectations.

However, in 2003, a new and unexpected charmonium state was observed by the Belle experiment [480] and then confirmed independently by the BaBar [481], CDF [482] and D0 [483] experiments. This new particle, referred to as the $X(3872)$, was reconstructed in $B \to J/\psi\, K$ decays, in the decay mode $X(3872) \to J/\psi\pi^+\pi^-$ and has a mass indistin-

guishable (within uncertainties) from the $D^{*0}\overline{D}^{0}$ threshold [459]. Several of the $X(3872)$ parameters are unknown (such as its spin) or have large uncertainties, but this state does not match any predicted charmonium state [459]. The discovery of the $X(3872)$ has led to a resurgence of interest in exotic spectroscopy and subsequently many new states have been claimed. For example: the Y family, $Y(4260), Y(4320)$ and $Y(4660)$, of spin parity 1^-, or the puzzling charged Z family, $Z(4050)^+, Z(4250)^+$ and $Z(4430)^+$, so far observed only by the Belle experiment [484]. The nature of these states has drawn much theoretical attention and many models have been proposed. One possible explanation is that they are bound molecular states of open charm mesons [485]. Another is that these are tetraquarks [486] states formed of four quarks (*e.g.* $c, \bar{c}$, one light quark and one light anti-quark). Other interpretations have been postulated such as quark-gluon hybrid [486] or hadrocharmonium models [487], but experimental data is still lacking to be able to conclude definitely. The bottomonium system should exhibit similar exotic states to the charmonium case. The Belle experiment recently reported the observation of exotic bottomonium charged particles $Z_b(10610)^+$ and $Z_b(10650)^+$ in the decays $Z_b \to \Upsilon(nS)\pi^+$ and $Z_b \to h_b(nP)\pi^+$ [488]. These states appear similar to the $Z(4430)^+$ observed in the charmonium case. In addition, neutral states analogous to the $X(3872)$ and the Y states are expected in the bottomonium system.

Studies of the $X(3872)$ have already been performed with the current detector [58]. The 50 fb^{-1} of integrated luminosity collected with the upgraded detector will contain over one million $X(3872) \to J/\psi\pi\pi$ candidates, by far the largest sample ever collected and allow study of this meson with high precision. Around 10% of these events will originate in the decays of B-mesons allowing the quantum numbers and other properties to be determined. With such a large sample the missing $^3D_2$ state of the charmonium system [489] will be also be observed and studied with high precision.

Another study being pursued with the current detector is to confirm the existence of the $Z(4430)^+$ state. If confirmed, the $Z(4430)^+$ will be copiously produced at $\sqrt{s} = 14$ TeV and the larger dataset will allow detailed study of its properties in different B decay modes, thus setting the basis for all future searches for exotic charged states.

Similar to the charmonium-like states, exotic bottomonium states will mainly be searched for in the $\Upsilon(nS)\pi^+\pi^-$ channel, with $\Upsilon(nS) \to \mu^+\mu^-$. The excellent resolution observed in the $\Upsilon(nS)$ analysis [463] allows efficient separation of the three states, which is crucial in searching for exotic bottomonium states in these channels.

All these studies, and searches for other exotica such as pentaquarks will profit from the increased integrated luminosity.

5.3 Precision measurements of b- and c-hadron properties

A major focus of activity with the current LHCb detector is the study of the properties of beauty and charm hadrons. This is a wide ranging field including studies of properties such as mass and lifetime, observation of excited b-states and the measurements of branching ratios. These studies provide important input to perturbative QCD models. Three topics are considered here: b decays to charmonia, B_c^+, and b-baryon decays.

One important field being studied with the current detector is exclusive b decays to charmonia. Studies of these modes are important for understanding the shape of the momentum spectrum of J/ψ produced in b-decays measured by the B-factories [490, 491]. To explain the observed shape new contributions to the total $b \to J/\psi X$ rate are needed. Several sources have been proposed in the literature: intrinsic charm [492], baryonium formation [493] and as yet unobserved exotic states [494]. One of the first proposed explanations for the excess was a contribution from an intrinsic charm component to the b-hadron wave-function [492]. This would lead to an enhancement of b-hadron decays to J/ψ in association with open charm. The B-factories have set limits on such decays at the level of 10^{-5} [193], which considerably restricts, but does not exclude, contributions from intrinsic charm models. The branching ratios of these decays have been estimated in pQCD [495]. In the case of $B^0 \to J/\psi D^0$ the branching ratio has been estimated to be 7×10^{-7}. If this value is correct, several hundred fully reconstructed events will be collected with the upgraded detector. Similar decay modes are possible for B_s and B_c mesons though no limits (or predictions) exist.

Another possibility discussed to explain the shape of the J/ψ spectrum is contributions from exotic strange baryonia formed in decays such as $B^+ \to J/\psi \overline{\Lambda}^0 p$. This decay has been observed by BaBar [496], with a branching ratio of $(1.18 \pm 0.31) \times 10^{-5}$. The related decay $B_d \to J/\psi p\overline{p}$ is unobserved, with an upper limit on the branching ratio of 8.3×10^7 at 90 % confidence level [497]. At present, these decays are experimentally challenging due to the low Q-values involved. The larger data samples available at the time of the upgrade, together with improved proton identification at low momentum, may lead to their observation.

Compared to the case of B^0 and B^+, the B_s^0 sector is less well explored both experimentally and theoretically. Decays such as $B_s^0 \to J/\psi K^{*0}\overline{K}^{*0}$, $B_s^0 \to J/\psi \phi\rho$ should be observable with the present detector. With the upgraded apparatus, the decay modes $B_s^0 \to J/\psi K_s^0 K_s^0$ and $B_s^0 \to J/\psi \phi\phi$ will also become accessible. The latter channel is interesting as the low Q-value will allow a precision determination of the B_s^0 mass.

As the lowest bound state of two heavy quarks $\overline{b}$ and c, the B_c^+ meson forms a unique flavoured, weakly decaying quarkonium system. Studies of the properties of B_c^+ mesons such as the mass, lifetime and two-body non-leptonic decay modes are being performed with the current detector. As an example, Fig. 31 shows the signals observed for B_c^+ decays in to $B_c^+ \to J/\psi \pi^+$ and $B_c^+ \to J/\psi 3\pi^+$. The large dataset collected with the upgraded detector will allow these studies to be pursued with higher precision together with first studies of CP and triple-product asymmetries in the B_c^+ system. In Table 16 the expected yields of selected decay modes are estimated extrapolating from the yields of $B_c^+ \to J/\psi \pi^+$ and $B_c^+ \to J/\psi 3\pi^+$ observed with the current detector. As well as studies of the branching ratios and searches for new physics, these modes will allow precision measurements of the B_c^+ mass and lifetime to be made. Based on ongoing studies with the current detector, a statistical precision of 0.1 MeV/c^2 on the mass will be achieved. The uncertainty on the mass will most likely be dominated by systematics related to the momentum scale. A 10^{-4} precision on this variable would translate to an uncertainty of 0.3 MeV/c^2 on the mass. Measurements of the B_c lifetime in the same mode are ongoing.

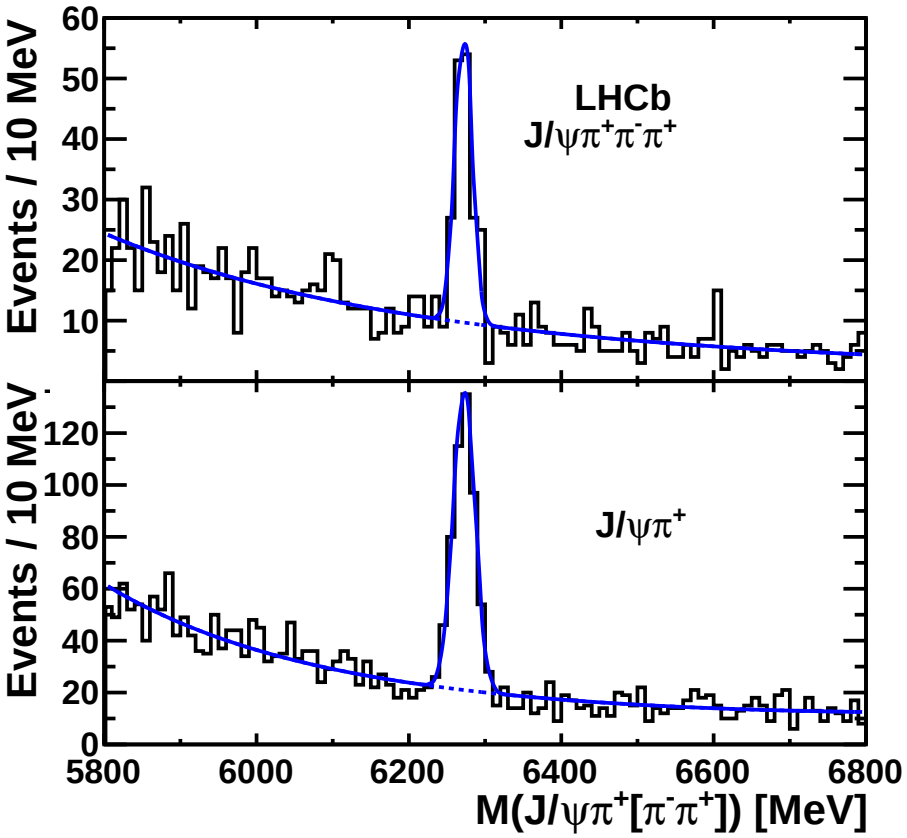

Figure 31: Invariant mass distribution of $B_c^+ \to J/\psi 3\pi^+$ (top) and $B_c^+ \to J/\psi\,\pi^+$ (bottom) candidates using 0.8 fb^{-1} of integrated luminosity collected in 2011. The figures are taken from Ref. [498]. The results of maximum likelihood fits of B_c^+ signals are superimposed.

Extrapolating these results to 50 fb^{-1}, a statistical precision of 0.004 ps will be achieved.

The large B_c dataset will open possibilities for many other studies. Decay modes of the B_c^+ meson to a B_s^0 or B^0 meson together with a pion or kaon will also be accessible. Studies of the $B_c^+ \to B_s^0\pi^+$ decay have been started with the data collected in 2011 where a handful of events are expected. As discussed in Ref. [499], semi-leptonic B_c^+ decays to B_s^+ can be used to provide a clean tagged decay source for CP violation studies. Finally, we expect to observe signals of the currently unexplored excited B_c^+ meson states [502–505]. As discussed in Ref. [501] observation of the B_c^{*+} decay is extremely challenging due to the soft photon produced in the decay to to the ground state. The prospects for observation of the first P-wave multiplet decays decaying radiatively to the ground state are more promising.

Large samples of b-baryons decaying to final states containing charmonia will also be collected. For the already known states, precision measurements of properties such as

Table 16: Branching ratios and expected yields of selected B_c^+ decay modes containing a J/ψ or $\psi(2S)$ meson. The branching ratios for the J/ψ are taken from Ref. [499], with the additional constraint of the ratio of the $B_c^+ \to J/\psi 3\pi^+$ to $B_c^+ \to J/\psi \pi^+$ reported in Ref. [498]. The $\psi(2S)$ branching ratios are estimated assuming that they are 0.5 of the J/ψ values, as observed in many modes (see for example Ref. [500]). Only di-muon modes are considered for the J/ψ and $\psi(2S)$, and only the $K^+K^-\pi^+$ ($K^+\pi^-\pi^+$) modes are considered for the D_s^+ (D^+) modes. The $B_c^+ \to K^+K^{*0}$ numbers are taken from Ref. [501].

Mode	Branching ratio	Expected yield [50 fb^{-1}]
$B_c^+ \to J/\psi \pi^+$	2×10^{-3}	52,000
$B_c^+ \to J/\psi 3\pi^+$	5×10^{-3}	17,000
$B_c^+ \to J/\psi K^+$	$(1-2) \times 10^{-4}$	3000 -4000
$B_c^+ \to J/\psi K_1^+$	3×10^{-5}	1000
$B_c^+ \to \psi(2S)\pi^+$	1×10^{-3}	3000
$B_c^+ \to \psi(2S)3\pi^+$	2.5×10^{-3}	1000
$B_c^+ \to J/\psi D_s^+$	$(2-3) \times 10^{-3}$	1400 - 1900
$B_c^+ \to J/\psi D^+$	$(5-13) \times 10^{-4}$	8-100
$B_c^+ \to K^+K^{*0}$	10^{-6}	500

lifetimes and mass can be made. For example extrapolating the studies with 0.3 fb^{-1} discussed in Ref. [506] 10 000 $\Xi_b \to J/\psi\Xi$ and 2000 $\Omega_b \to J/\psi\Omega$ events will be collected. This will allow the Ξ_b (Ω_b) mass to be measured to a precision of 0.1 MeV/c^2 (0.5 MeV/c^2). Precision studies of the Λ_b^* baryons, for example determination of the quantum numbers, that have recently been observed by LHCb (Fig. 32) will also be made.

Baryonic states containing two heavy quarks will also be observable. The lightest of these, the Ξ_{cc} isodoublet, have an estimated cross-section of $\mathcal{O}(10^2)$ nb [507, 508] and so should be visible with the 5 fb^{-1} collected with the current detector . However, the statistics may be marginal for follow-on analyses: measurement of the lifetime, ratios of branching fractions, searches for low-lying excited states, and so forth. They will certainly be insufficient for angular analyses aimed at confirming the quark model predictions for the spin-parity of these states. These studies will require the statistics and improved triggering of the LHCb upgrade. Heavier states such as the Ω_{cc}, Ξ_{bc}, and Ξ_{bb} have still smaller production cross-sections [508]. First studies of the Ξ_{bc} are ongoing with the current detector and indicate that at best a handful of events can be expected in 5 fb^{-1}. This state (at least) should be should also be observable with the upgrade.

5.4 Measurements with electroweak gauge bosons

Two of the most important quantities in electroweak physics are the sine of the effective electroweak mixing angle for leptons, $\sin^2\theta_{\rm eff}^{\rm lept}$, and the mass of the W-boson, m_W. Until the ILC or CLIC is operational, responsibility for improving our knowledge of these pa-

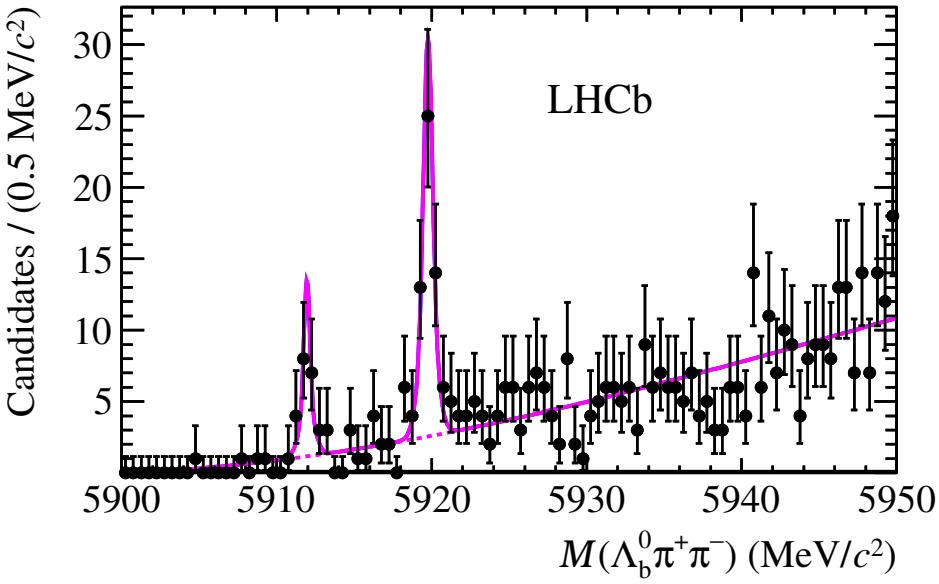

Figure 32: Invariant mass spectrum of $\Lambda_b^*\pi^+\pi^-$ taken from Ref [12]. The points with error bars are the data, the solid line is the result of a fit to this distribution, the dashed line is the fitted background contribution.

rameters rests with the LHC. Thanks to its unique forward coverage, an upgraded LHCb can make important contributions to this programme. The forward coverage of LHCb also allows a probe of electroweak production in a different regime to ATLAS and CMS, and the range of accessible physics topics is not limited to electroweak bosons. For example, $t\bar{t}$ production proceeds predominantly by gluon gluon fusion in the central region, but has a significant contribution from quark antiquark annihilation in the forward region, giving a similar production regime to that studied at the Tevatron.

5.4.1 $\sin^2\theta_{\rm eff}^{\rm lept}$

The value of $\sin^2\theta_{\rm eff}^{\rm lept}$ can be extracted from $A_{\rm FB}$, the forward-backward asymmetry of leptons produced in Z decays. The raw value of $A_{\rm FB}$ measured in dimuon final states at the LHC is about five times larger than at an e^+e^- collider, due to the initial state couplings, and so, in principle, it can be measured with a better relative precision, given equal amounts of data. The measurement however requires knowledge of the direction of the matter and antimatter partons that created the Z boson, and any uncertainty in this quantity results in a dilution of the observed value of $A_{\rm FB}$. This dilution is very significant in the central region, as there is an approximately equal probability for each proton to contain the quark or anti-quark that is involved in the creation of the Z, leading to an ambiguity in the definition of the axis required in the measurement. However, the more forward the Z boson is produced, the more likely it is that it follows the quark

direction; for rapidities $y > 3$, the Z follows the quark direction around 95% of the time. Furthermore, in the forward region, the partonic collisions that produce the Z are nearly always between u-valence and $\bar{u}$-sea quark or d-valence and $\bar{d}$-sea quark. The $s\bar{s}$ contribution, with a less well known parton density function (PDF), is smaller than in the central region. Consequently, the forward region is the optimum environment in which to measure $A_{\rm FB}$ at the LHC. Preliminary studies [509] have shown that with a 50 fb^{-1} data sample collected by the LHCb upgrade, $A_{\rm FB}$ could be measured with a statistical precision of around 0.0004. This would give a statistical uncertainty on $\sin^2\theta^{\rm lept}_{\rm eff}$ of better than 0.0001, which is a significant improvement in precision on the current world average value. It is also worth remarking that the two most precise values entering this world average at present, the forward-backward $b\bar{b}$ asymmetry measured at LEP ($\sin^2\theta^{\rm lept}_{\rm eff} = 0.23221 \pm 0.00029$), and the left-right asymmetries measured at SLD with polarised beams ($\sin^2\theta^{\rm lept}_{\rm eff} = 0.23098 \pm 0.00026$), are over three sigma discrepant with each other [510]. LHCb will be able to bring clarity to this unsatisfactory situation.

More work is needed to identify the important systematic uncertainties on the $A_{\rm FB}$ measurement. One source of error is the uncertainty in the PDFs. With current knowledge this contribution would lead to an uncertainty of almost double the statistical precision estimated above, but this will reduce when the differential cross-section measurements of the W and Z bosons and Drell-Yan lower mass di-muon production measured at the LHC are included in the PDF global fits. LHCb has already embarked on this measurement programme. Fig. 33 (left) shows the $Z \to \mu^+\mu^-$ peak obtained with 37 pb^{-1} of data [10]. Figure 33 (right) shows the measured asymmetry between W^+ and W^- production as a function of lepton pseudorapidity. This measurement is already approaching the accuracy of the theoretical uncertainties. The W and Z measurements described in [10] are already being used to constrain parton density functions by some groups [511]. A measurement of lower mass Drell Yan production [512] will extend these constraints to lower Q^2 (masses above 5 GeV/c^2 are currently considered) and Bjorken x. The range of the ATLAS and CMS experiments only extends up to lepton pseudorapidities of 2.5.

5.4.2 m_W

Decreasing the uncertainty on m_W from its present error of 15 MeV is one of the most challenging tasks for the LHC (it may also be reduced further at the Tevatron). Although no studies have yet been made of determining m_W with LHCb itself, it is evident that the experiment can give important input to the measurements being made at the GPDs [513]. A significant and potentially limiting external uncertainty on m_W will again come from the knowledge of the PDFs. The PDFs are less constrained in the kinematic range accessible to LHCb, and high statistics, precise measurements of W^+, W^-, Z and low-mass Drell-Yan production in this region, in particular the shapes of the differential cross-sections, can be used to improve the global picture. One specific area of concern arises from the knowledge of the heavy quarks in the proton. Around $20-30\%$ of W production in the central region is expected to involve s and c quarks, making the understanding of this component very important for the m_W measurement. LHCb can make a

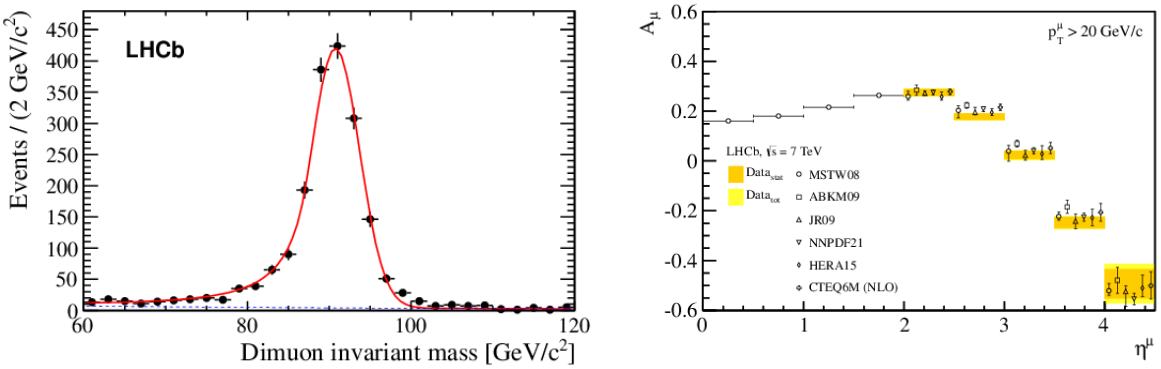

Figure 33: LHCb Z and W results for 37 pb^{-1} at $\sqrt{s} = 7$ TeV. Left: $Z \to \mu^+\mu^-$ peak. Right: $W^+ - W^-$ production asymmetry, where the points with error bars are the data and the boxes are the theoretical predictions with their uncertainties (only indicated within the LHCb acceptance).

unique contribution to improving the knowledge of the heavy-quark PDFs by exploiting its vertexing and particle identification capabilities to tag the relatively low-p_T final-state quarks produced in processes such as $gs \to Wc$, $gc \to Zc$, $gb \to Zb$, $gc \to \gamma c$ and $gb \to \gamma b$. These processes provide direct probes of the strange, charm and bottom partons, and can be probed at high and low values of Bjorken x inside the LHCb acceptance.

5.4.3 $t\bar{t}$ production

Understanding the nature of top production, and in particular the asymmetry in $t\bar{t}$ events reported by Fermilab [514–518], is of prime concern. As for the measurement of $\sin^2\theta^{\rm lept}_{\rm eff}$, identifying the forward direction of events is crucial. Although the LHCb acceptance for identifying the two leptons from $t\bar{t}$ decay is far smaller than that of the GPDs (typically 2% rather than 70%, according to `PYTHIA` generator level studies), the higher $q\bar{q}$ production fraction and better identified forward direction within LHCb combine to suggest that the overall efficiency multiplied by dilution squared performance is similar for all experiments. With the integrated luminosity offered by the upgrade, statistical precision will no longer be an issue, and LHCb measurements of the $t\bar{t}$ asymmetry will offer a competitive and complementary test of Tevatron observations.

5.5 Searches for exotic particles with displaced vertices

Different theoretical paradigms have been proposed to solve the so-called 'hierarchy problem', the most discussed being Supersymmetry. There are, however, many other ideas including Extra Dimensions (large, warped, Higgsless), Technicolour and Little Higgs. These models focus on a strong dynamics type solution to the problem [519].

A growing subset of models features new massive long-lived particles with a macro-

scopic distance of flight. They can be produced by the decay of a single-produced resonance, such as a Higgs boson or a Z' [520, 521], from the decay chain of Supersymmetric particles [522], or by a 'hadronisation' mechanism in models where the long-lived particle is a bound state of quarks from a new confining gauge group, as discussed in Ref. [520]. In the last case, the multiplicity of long-lived particles in an event can be large, while only one long-lived particle is expected to be produced in other models. The decay modes may also vary depending on the nature of the particle, from several jets in the final state [521] to several leptons [523] or lepton plus jets [524]. A comprehensive review of the experimental signatures is given in [525].

The common feature amongst these models is the presence of vertices displaced from the interaction region. Such signatures are well suited to LHCb, and in particular to the upgraded experiment, which will be able to select events with displaced vertices at the earliest trigger level.

We focus in the following on the Hidden Valley model already discussed in Ref. [60]. In this model the hidden sector, or v-sector, contains two new heavy quarks: U and C. Strassler and Zurek [522] suggest that an exotic Higgs boson could decay with a significant branching fraction to a pair of π_v^0 particles, where the π_v^0 is the 'neutral' member of the isotriplet of v-isospin 1 hadrons formed by U and C quarks. The π_v^0 can decay in SM particles and if the mass of the spinless π_v^0 is below the ZZ threshold it will decay dominantly into $b\bar{b}$ pairs due to helicity conservation. Here the π_v^0 widths are determined by their lifetime which could be very long, resulting in narrow states. The final state would consist of four b-jets, each pair being produced from a displaced vertex corresponding to the π_v^0 decay as illustrated in Fig. 34. If these decays exist, the lower limit on the Higgs mass set by LEP would be misleading, as it assumes the prompt decay of the Higgs to $b\bar{b}$ to be dominant.

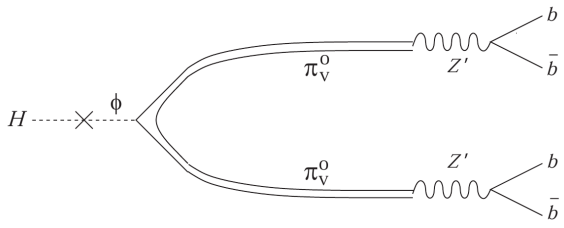

Figure 34: Decay of a Higgs via a scalar field ϕ into two π_v^0 particles, with π_v^0 charge equal to zero, which subsequently decay into $b\bar{b}$ jets. (Adapted from Ref. [522].)

The potential of LHCb to search for such exotic Higgs decays at $\sqrt{s} = 14\,\text{TeV}$ has been discussed in Ref. [60], and is briefly summarised here. The benchmark model uses $m_H = 120\ \text{GeV}/c^2$, $m_{\pi_v^0} = 35\ \text{GeV}/c^2$ and $\tau_{\pi_v^0} = 10$ ps. By combining vertex and jet reconstruction, the capacity to reconstruct this final state was shown using full simulation of the detector, assuming 0.4 interaction per crossing. Backgrounds to this signal from other processes, such as the production of two pairs of $b\bar{b}$ quarks, have been considered and found to be negligible.

During 2010 and 2011 data taking, an inclusive displaced vertex trigger has been introduced in the second level of the software trigger. Preliminary studies [16] have demonstrated that for an output rate below 1% of the overall trigger bandwidth, the efficiency of the whole trigger chain on events with two offline reconstructible π_v^0 vertices with a minimum mass of 6 GeV and good vertex quality is of the order of 80%. This strategy has been tested up to on average two visible interaction per crossing which is what is expected for the upgraded experiment.

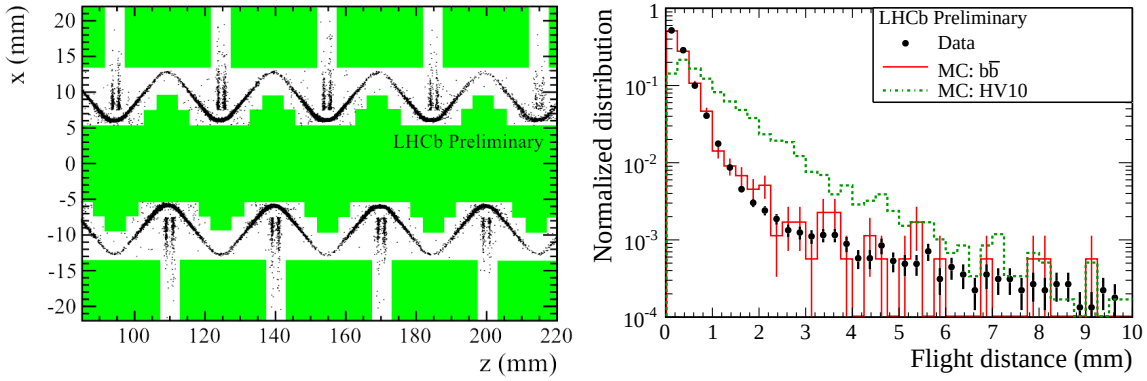

Figure 35: Left: Distribution in x and z, for $|y| < 1$ mm, of the reconstructed vertices. The visible structures reflect the geometry of the VELO detector, with the pairs of silicon sensors appearing as pairs of vertical bands and the RF foil as the two wave shapes. The green shaded region represents the fiducial vacuum volume in which candidates are accepted. Right: Flight distance of offline reconstructed vertices in events outside the matter region. Data are compatible with $b\bar{b}$ background. The black points are for data in 36 pb^{-1}, the red line is a full simulation of $b\bar{b}$ production and the green dashed line is a full simulation of the Hidden Valley benchmark channel.

The analysis of the trigger output showed that once vertices arising from hadronic interactions with material are rejected, the dominant background is compatible with b hadron decay vertices as shown in Fig. 35. Those b hadron vertices are reconstructed with large masses because of the presence of fakes or cloned tracks. With the present detector, it is difficult to keep the trigger rate down for single candidate events without using tight cuts on the mass and the displacement of the candidates. In the previous model, the trigger efficiency for events with a single long-lived particle reconstructible in LHCb is only about 20%. This efficiency is expected to decrease for models where the mass of the long-lived particle is smaller. In addition, the number of events with at least on π_v^0 in the acceptance is three times higher than the number of events with two π_v^0. Improving the single candidate efficiency would increase sensitivity to this model. It would also gives a better coverage for the models where only one long-lived particle is produced.

In an upgraded detector, with the VELO pixel detector option, the VELO track fake rate is expected to be below one percent [61]. It is to be compared to 6% in the

present detector. The upgraded TT will also reduce the fake rate due to mis-combination between VELO tracks and Tracker-station track segments. Moreover the use of a GDML description for the complex RF foil shape will give a better control on the background arising from hadronic interactions. It will enable the use of the true shape of the RF foil, rather than the loose fiducial volume cut used at present, which depending on the considered lifetime, rejects 10−30% of the long-lived particles. Those improvements would allow to decrease the thresholds on the single candidates trigger and therefore increase the reach of such searches.

As discussed in Ref. [60] the coupling of vertex information to jet reconstruction will allow to reduce the physical backgrounds. Studies are on-going on this matter. Assuming a Higgs production cross-section at 14 TeV of 50 pb, an integrated luminosity of 50 fb^{-1} and a geometric efficiency of 10%, 250 000 Higgs bosons will be produced in LHCb. If $H^0 \to \pi_v^0\pi_v^0$ is a dominant decay mode, then LHCb will be in an excellent position to observe this signal, taking advantage of the software trigger's ability to select high multiplicity events with good efficiency.

5.6 Central exclusive production

Central exclusive production (CEP) processes provide a promising and novel way to study QCD and the nature of new particles, from low mass glueball candidates up to the Higgs boson itself. The CEP of an object X in a pp collider may be written as follows

$$pp \to p \,+\, X \,+\, p\,,$$

where the '+' signs denote the presence of large rapidity gaps. At high energies the t-channel exchanges giving rise to these processes can only be zero-charge colour singlets. Known exchanges include the photon and the pomeron. Another possibility, allowed in QCD, but not yet observed, is the odderon, a negative C-parity partner to the pomeron with at least three gluons. The most attractive aspect of CEP reactions is that they offer a very clean environment in which to measure the nature and quantum numbers of the centrally produced state X.

Central exclusive $\gamma\gamma$ [526], dijet [527, 528] and χ_c [529] production has been observed at the Tevatron. LHCb has also collected candidate di-muon events compatible with CEP [530]. In Fig. 36 is shown the invariant mass of CEP χ_c candidates. These are events in which only a $J/\psi \to \mu^+\mu^-$ decay and γ candidate are reconstructed, with no other activity (inconsistent with noise) seen elsewhere in the detector. An important observable in CEP is the relative production rates of χ_{c0}, χ_{c1} and χ_{c2}. As is evident from Fig. 36, the invariant mass resolution of LHCb is sufficient for this measurement to be made.

These early results make clear the promise of CEP measurements at LHCb. Additional instrumentation can be considered which will help in these studies. For example, the inclusion of Forward Shower Counters (FSCs) on both sides of the interaction point, as proposed in [532], would be able to detect showers from very forward particles interacting in the beam pipe and surrounding material. The absence of a shower would

Figure 36: Preliminary LHCb results on central exclusive χ_c production. Also shown is the expectation of the `SuperCHIC` Monte Carlo generator [531], which has been normalised to the number events observed in the data. The relative proportions of χ_{c0}, χ_{c1} and χ_{c2} are 12%, 36% and 52% respectively.

indicate a rapidity gap and be helpful in increasing the purity of a CEP sample. More ambitiously, the deployment of semi-conductor detectors very close to the beam, within Roman pots, several 100 m away from the interaction point, as proposed for the GPD experiments [533] would also be beneficial for LHCb. The ability to measure the directions of the deflected protons in the CEP interaction provides invaluable information in determining the quantum numbers of the centrally produced state.

Several important physics goals may already by identified for the LHCb CEP programme:

- To accumulate and characterise large samples of exclusive $c\bar{c}$ and $b\bar{b}$ events. A full measurement programme of these 'standard candles' will be essential to understand better the QCD mechanism of CEP [534], and may provide vital input if CEP is used for studies of Higgs and other new particles [535].

- Searches for structure in the mass spectra of decay states such as K^+K^-, $2\pi^+2\pi^-$, $K^+K^-\pi^+\pi^-$ and $p\bar{p}$. A particular interest of this study would be the hunt for glueballs, which are a key prediction of QCD.

- Observation and study of exotic particles in CEP processes would be extremely illuminating as to their nature. By way of example, a detailed study of the CEP process $pp \to p + X(3872) + p$ would provide a valuable new tool to test the quantum numbers of this state. This and other states could also be searched for in, for example, decays containing $D\bar{D}$, which if observed would shed light onto the nature of the parent particle [534].

There are several reasons which make LHCb a suitable detector for realising these goals, particularly with the upgraded experiment:

- Even when running at a luminosity of $10^{33}\,\mathrm{cm}^{-2}\,\mathrm{s}^{-1}$ LHCb will have much less pileup

than the GPDs, which will be operating in a much more severe regime. This will be advantageous in triggering and reconstructing low mass CEP states.

- The higher integrated luminosity that will be collected by the upgraded detector will allow studies to be performed on states that are inaccessible with only a few fb^{-1}. This is true, for example, of central exclusive χ_b production, which is expected to be a factor of ~ 1000 less than that of χ_c mesons [534].

- The particle identification capabilities of the LHCb RICH system allow centrally produced states to be cleanly separated into decays involving pions, kaons and protons.

- The low p_{T} acceptance of LHCb, and high bandwidth trigger, will allow samples of relatively low mass states to be collected and analysed.

6 Summary

The previous chapters have described the impact of the first measurements from LHCb, and the strong physics motivation to upgrade the experiment in order to exploit fully the potential of the LHC in the forward region. The programme includes not only flavour physics observables with high sensitivity to theories of physics beyond the Standard Model, but a wide range of measurements covering many physics topics. For most of the observables discussed in the text, and summarised in Tab. 1, the sensitivity of the LHCb upgrade exceeds by far that of any other experiment. Other flavour physics experiments do have better sensitivity to some channels that cannot be well measured at LHCb: $K \to \pi\nu\bar{\nu}$ requires dedicated experiments, while B decays with large missing energy, such as $B^+ \to \tau\nu$, channels involving multiple neutral particles, such as $B^0 \to \pi^0\pi^0$, and rare τ lepton decays such as $\tau \to e\gamma$ require an e^+e^- facility. On the other hand, LHCb will have no serious competition in its study of B_s^0 decays, b-baryon decays and CP violation. Similarly the yields in charmed-particle decays to final states consisting of only charged tracks cannot be matched by any other experiment.

6.1 Importance of the LHCb upgrade

The study of deviations from the SM in quark flavour physics provides key information about any extension of the SM. We already know that the NP needed to stabilize the electroweak sector must have a non-generic flavour structure in order to be compatible with the tight constraints of flavour-changing processes, even if the precise form of this structure is still unknown. Hopefully, ATLAS and CMS will detect new particles belonging to these models, but the couplings of the theory and, in particular, its flavour structure, cannot be determined only using high-$p_{\rm T}$ data.

Therefore, the LHCb upgrade will play a vital role in any of these scenarios, including the possibility of covering NP phase space, which *a priori* cannot be exploited by high energy searches. Future plans for full exploitation of the LHC should be consistent with a co-extensive LHCb programme.

Acknowledgements

We express our gratitude to our colleagues in the CERN accelerator departments for the excellent performance of the LHC. We thank the technical and administrative staff at CERN and at the LHCb institutes, and acknowledge support from the National Agencies: CAPES, CNPq, FAPERJ and FINEP (Brazil); CERN; NSFC (China); CNRS/IN2P3 (France); BMBF, DFG, HGF and MPG (Germany); SFI (Ireland); INFN (Italy); FOM and NWO (The Netherlands); SCSR (Poland); ANCS (Romania); MinES of Russia and Rosatom (Russia); MICINN, XuntaGal and GENCAT (Spain); SNSF and SER (Switzerland); NAS Ukraine (Ukraine); STFC (United Kingdom); NSF (USA). We also acknowledge the support received from the ERC under FP7 and the Region Auvergne.

References

[1] LHCb collaboration, *Implications of LHCb measurements and future prospects – Summary for input to the European Strategy Preparatory Group*, LHCb-PUB-2012-009.

[2] N. Cabibbo, *Unitary symmetry and leptonic decays*, Phys. Rev. Lett. **10** (1963) 531; M. Kobayashi and T. Maskawa, *CP Violation in the Renormalizable Theory of Weak Interaction*, Prog. Theor. Phys. **49** (1973) 652.

[3] J. Christenson, J. Cronin, V. Fitch, and R. Turlay, *Evidence for the 2π decay of the K_2^0 meson*, Phys. Rev. Lett. **13** (1964) 138.

[4] LHCb collaboration, R. Aaij *et al.*, *Strong constraints on the rare decays $B_s^0 \to \mu^+\mu^-$ and $B^0 \to \mu^+\mu^-$*, Phys. Rev. Lett. **108** (2012) 231801, arXiv:1203.4493.

[5] LHCb collaboration, R. Aaij *et al.*, *Differential branching fraction and angular analysis of the decay $B^0 \to K^{*0}\mu^+\mu^-$*, Phys. Rev. Lett. **108** (2012) 181806, arXiv:1112.3515.

[6] LHCb collaboration, R. Aaij *et al.*, *Measurement of the CP-violating phase ϕ_s in the decay $B_s^0 \to J/\psi\phi$*, Phys. Rev. Lett. **108** (2012) 101803, arXiv:1112.3183.

[7] LHCb collaboration, *Flavour specific CP asymmetry using semileptonic B_s^0 decays*, LHCb-CONF-2012-022.

[8] LHCb collaboration, R. Aaij *et al.*, *Evidence for CP violation in time-integrated $D^0 \to h^-h^+$ decay rates*, Phys. Rev. Lett. **108** (2012) 111602, arXiv:1112.0938.

[9] LHCb collaboration, R. Aaij *et al.*, *Measurement of the isospin asymmetry in $B \to K^{(*)}\mu^+\mu^-$ decays*, arXiv:1205.3422.

[10] LHCb collaboration, R. Aaij *et al.*, *Inclusive W and Z production in the forward region at $\sqrt{s} = 7$ TeV*, JHEP **1206** (2012) 058, arXiv:1204.1620.

[11] LHCb collaboration, R. Aaij *et al.*, *Observation of double charm production involving open charm in pp collisions at $\sqrt{s} = 7$ TeV*, JHEP **1206** (2012) 141, arXiv:1205.0975.

[12] LHCb collaboration, R. Aaij *et al.*, *Observation of excited Λ_b baryons*, arXiv:1205.3452.

[13] LHCb collaboration, R. Aaij *et al.*, *Search for the $X(4140)$ in $B^+ \to J/\psi\phi K^+$*, Phys. Rev. **D85** (2012) 091103, arXiv:1202.5087.

[14] LHCb collaboration, R. Aaij *et al.*, *Searches for Majorana neutrinos in B^- decays*, Phys. Rev. **D85** (2012) 112004, arXiv:1201.5600.

[15] LHCb collaboration, *Search for the Lepton Flavor Violating decay* $\tau^- \to \mu^+\mu^-\mu^-$, LHCb-CONF-2012-015.

[16] LHCb collaboration, *Search for (Higgs-like) bosons decaying into long-lived exotic particles*, LHCb-CONF-2012-014.

[17] A. J. Buras and J. Girrbach, *BSM models facing the recent LHCb data: A First look*, arXiv:1204.5064.

[18] K. de Bruyn *et al.*, *A New Window for New Physics in* $B_s^0 \to \mu^+\mu^-$, arXiv:1204.1737.

[19] F. Mahmoudi, *Direct and indirect searches for New Physics*, arXiv:1205.3099, Proceedings of Moriond QCD 2012.

[20] O. Buchmueller *et al.*, *Supersymmetry in Light of 1/fb of LHC Data*, Eur. Phys. J. **C72** (2012) 1878, arXiv:1110.3568.

[21] D. M. Straub, *Overview of constraints on new physics in rare B decays*, arXiv:1205.6094, Proceedings of Moriond EW 2012.

[22] U. Egede *et al.*, *New observables in the decay mode* $\bar{B}_d \to \bar{K}^{*0}\ell^+\ell^-$, JHEP **0811** (2008) 032, arXiv:0807.2589.

[23] U. Egede *et al.*, *New physics reach of the decay mode* $\bar{B} \to \bar{K}^{*0}\ell^+\ell^-$, JHEP **1010** (2010) 056, arXiv:1005.0571.

[24] LHCb collaboration, *Measurement of the ratio of branching fractions for* $B_s^0 \to \phi\mu\mu$ *and* $B_s^0 \to J/\psi\phi$, LHCb-CONF-2012-003.

[25] W. Altmannshofer and D. M. Straub, *Cornering New Physics in* $b \to s$ *Transitions*, arXiv:1206.0273.

[26] T. Hurth and F. Mahmoudi, *The Minimal Flavour Violation benchmark in view of the latest LHCb data*, arXiv:1207.0688.

[27] LHCb collaboration, R. Aaij *et al.*, *Measurement of the ratio of branching fractions* $\mathcal{B}(B^0 \to K^{*0}\gamma)/\mathcal{B}(B_s^0 \to \phi\gamma)$, Phys. Rev. **D85** (2012) 112013, arXiv:1202.6267.

[28] LHCb collaboration, *Measurement of the direct* CP *asymmetry in the* $B_d^0 \to K^{*0}\gamma$ *decay*, LHCb-CONF-2012-004.

[29] LHCb collaboration, *First observation of* $B^+ \to \pi^+\mu^+\mu^-$, LHCb-CONF-2012-006.

[30] LHCb collaboration, *Tagged time-dependent angular analysis of* $B_s^0 \to J/\psi\phi$ *decays at LHCb*, LHCb-CONF-2012-002.

[31] LHCb collaboration, R. Aaij *et al.*, *Determination of the sign of the decay width difference in the* B_s *system*, Phys. Rev. Lett. **108** (2012) 241801, arXiv:1202.4717.

[32] LHCb collaboration, R. Aaij *et al.*, *Measurement of the CP-violating phase ϕ_s in $\overline{B}_s \to J/\psi\pi^+\pi^-$ decays*, Phys. Lett. **B713** (2012) 378, arXiv:1204.5675.

[33] A. Lenz and U. Nierste, *Theoretical update of B_s^0–$\overline{B}_s^0$ mixing*, JHEP **06** (2007) 072, arXiv:hep-ph/0612167.

[34] J. Charles *et al.*, *Predictions of selected flavour observables within the Standard Model*, Phys. Rev. **D84** (2011) 033005, arXiv:1106.4041.

[35] R. Barbieri *et al.*, *U(2) and Minimal Flavour Violation in Supersymmetry*, Eur. Phys. J. **C71** (2011) 1725, arXiv:1105.2296.

[36] D0 collaboration, V. M. Abazov *et al.*, *Measurement of the anomalous like-sign dimuon charge asymmetry with 9 fb^{-1} of p pbar collisions*, Phys. Rev. **D84** (2011) 052007, arXiv:1106.6308.

[37] A. Dighe, A. Kundu, and S. Nandi, *Enhanced $B_s - \bar{B}_s$ lifetime difference and anomalous like-sign dimuon charge asymmetry from new physics in $B_s \to \tau^+\tau^-$*, Phys. Rev. **D82** (2010) 031502, arXiv:1005.4051.

[38] C. Bobeth and U. Haisch, *New Physics in Γ_{12}^s: $(\bar{s}b)$ $(\bar{\tau}\tau)$ Operators*, arXiv:1109.1826.

[39] A. Lenz *et al.*, *New Physics in B-Bbar mixing in the light of recent LHCb data*, arXiv:1203.0238.

[40] CKMfitter group, J. Charles *et al.*, *CP violation and the CKM matrix: Assessing the impact of the asymmetric B factories*, Eur. Phys. J. **C41** (2005) 1, arXiv:hep-ph/0406184, updated results and plots available at: http://ckmfitter.in2p3.fr.

[41] UTfit collaboration, M. Bona *et al.*, *The 2004 UTfit collaboration report on the status of the unitarity triangle in the standard model*, JHEP **0507** (2005) 028, arXiv:hep-ph/0501199, updated results and plots available at: http://www.utfit.org/UTfit/.

[42] E. Lunghi and A. Soni, *Possible evidence for the breakdown of the CKM-paradigm of CP-violation*, Phys. Lett. **B697** (2011) 323, arXiv:1010.6069.

[43] LHCb collaboration, R. Aaij *et al.*, *Observation of CP violation in $B^+ \to DK^+$ decays*, Phys. Lett. **B712** (2012) 203, arXiv:1203.3662.

[44] LHCb collaboration, *Measurement of time-dependent CP violation in charmless two-body B decays*, LHCb-CONF-2012-007.

[45] R. Fleischer and R. Knegjens, *In Pursuit of New Physics with $B_s^0 \to K^+K^-$*, Eur. Phys. J. **C71** (2011) 1532, arXiv:1011.1096.

[46] M. Ciuchini, E. Franco, S. Mishima, and L. Silvestrini, *Testing the Standard Model and searching for New Physics with $B_d \to \pi\pi$ and $B_s \to KK$ decays*, arXiv:1205.4948.

[47] LHCb collaboration, R. Aaij *et al.*, *First observation of the decay $B_s^0 \to K^{*0}\overline{K}^{*0}$*, Phys. Lett. **B709** (2012) 50, arXiv:1111.4183.

[48] M. Ciuchini, M. Pierini, and L. Silvestrini, *$B_s^0 \to K^{*0}\bar{K}^{*0}$ decays: The Golden channels for new physics searches*, Phys. Rev. Lett. **100** (2008) 031802, arXiv:hep-ph/0703137.

[49] LHCb collaboration, R. Aaij *et al.*, *Measurement of the polarization amplitudes and triple product asymmetries in the $B_s^0 \to \phi\phi$ decay*, Phys. Lett. **B713** (2012) 369, arXiv:1204.2813.

[50] LHCb collaboration, *Evidence for CP violation in $B \to K\pi\pi$ and $B \to KKK$ decays*, LHCb-CONF-2012-018.

[51] G. Isidori, J. F. Kamenik, Z. Ligeti, and G. Perez, *Implications of the LHCb Evidence for Charm CP Violation*, Phys. Lett. **B711** (2012) 46, arXiv:1111.4987.

[52] T. Feldmann, S. Nandi, and A. Soni, *Repercussions of Flavour Symmetry Breaking on CP Violation in D-Meson Decays*, JHEP **1206** (2012) 007, arXiv:1202.3795.

[53] LHCb collaboration, R. Aaij *et al.*, *Measurement of mixing and CP violation parameters in two-body charm decays*, JHEP **04** (2012) 129, arXiv:1112.4698.

[54] Y. Hochberg and Y. Nir, *Relating direct CP violation in D decays and the forward-backward asymmetry in $t\bar{t}$ production*, Phys. Rev. Lett. **108** (2012) 261601, arXiv:1112.5268.

[55] G. Isidori and J. F. Kamenik, *Shedding light on CP violation in the charm system via $D \to V\gamma$ decays*, arXiv:1205.3164.

[56] LHCb collaboration, *Search for the $D^0 \to \mu^+\mu^-$ decay with 0.9 fb^1 at LHCb*, LHCb-CONF-2012-005.

[57] LHCb collaboration, R. Aaij *et al.*, *Observation of J/ψ pair production in pp collisions at $\sqrt{s} = 7$ TeV*, Phys. Lett. **B707** (2012) 52, arXiv:1109.0963.

[58] LHCb collaboration, R. Aaij *et al.*, *Observation of $X(3872)$ production in pp collisions at $\sqrt{s} = 7$ TeV*, Eur. Phys. J. **C72** (2011) 1972, arXiv:1112.5310.

[59] LHCb collaboration, *Measurement of jet production in $Z^0/\gamma^* \to \mu^+\mu^-$ events at LHCb in $\sqrt{s} = 7\,TeV$ pp collisions*, LHCb-CONF-2012-016.

[60] LHCb collaboration, *Letter of Intent for the LHCb Upgrade*, CERN-LHCC-2011-001. LHCC-I-018.

[61] LHCb collaboration, *Framework TDR for the LHCb Upgrade*, CERN-LHCC-2012-007. LHCB-TDR-012.

[62] LHCb collaboration, *The LHCb upgrade*, LHCb-PUB-2012-010.

[63] Heavy Flavor Averaging Group, Y. Amhis *et al.*, *Averages of b-hadron, c-hadron, and τ-lepton properties as of early 2012*, arXiv:1207.1158, updated results and plots available at: http://www.slac.stanford.edu/xorg/hfag/.

[64] LHCb collaboration, *Differential branching fraction and angular analysis of the $B^0 \to K^{*0}\mu^+\mu^-$ decay*, LHCb-CONF-2012-008.

[65] S. Faller, R. Fleischer, and T. Mannel, *Precision physics with $B_s^0 \to J/\psi\phi$ at the LHC: the quest for New Physics*, Phys. Rev. **D79** (2009) 014005, arXiv:0810.4248.

[66] C.-W. Chiang *et al.*, *New Physics in $B_s^0 \to J/\psi\phi$: a General Analysis*, JHEP **04** (2010) 031, arXiv:0910.2929.

[67] W. Altmannshofer *et al.*, *Symmetries and Asymmetries of $B \to K^*\mu^+\mu^-$ Decays in the Standard Model and Beyond*, JHEP **0901** (2009) 019, arXiv:0811.1214.

[68] F. Kruger and J. Matias, *Probing new physics via the transverse amplitudes of $B^0 \to K^{*0}(\to K^-\pi^+)\ell^+\ell^-$ at large recoil*, Phys. Rev. **D71** (2005) 094009, arXiv:hep-ph/0502060.

[69] LHCb collaboration, R. Aaij *et al.*, *Measurement of b hadron production fractions in 7 TeV pp collisions*, Phys. Rev. **D85** (2012) 032008, arXiv:1111.2357.

[70] LHCb collaboration, A. A. Alves Jr. *et al.*, *The LHCb detector at the LHC*, JINST **3** (2008) S08005.

[71] LHCb collaboration, R. Aaij *et al.*, *Measurement of $\sigma(pp \to b\bar{b}X)$ at $\sqrt{s} = 7$ TeV in the forward region*, Phys. Lett. **B694** (2010) 209, arXiv:1009.2731.

[72] LHCb collaboration, *Prompt charm production in pp collisions at $\sqrt{s} = 7$ TeV*, LHCb-CONF-2010-013.

[73] LHCb collaboration, B. Adeva *et al.*, *Roadmap for selected key measurements of LHCb*, arXiv:0912.4179.

[74] LHCb collaboration, R. Aaij *et al.*, *First evidence of direct CP violation in charmless two-body decays of B_s^0 mesons*, Phys. Rev. Lett. **108** (2012) 201601, arXiv:1202.6251.

[75] LHCb collaboration, R. Aaij *et al.*, *Search for the rare decays $B_s^0 \to \mu^+\mu^-$ and $B^0 \to \mu^+\mu^-$*, Phys. Lett. **B699** (2011) 330, arXiv:1103.2465.

[76] LHCb collaboration, R. Aaij *et al.*, *Searches for the rare decays $B_s^0 \to \mu^+\mu^-$ and $B^0 \to \mu^+\mu^-$*, Phys. Lett. **B708** (2012) 55, arXiv:1112.1600.

[77] V. Gligorov, C. Thomas, and M. Williams, *The HLT inclusive B triggers*, LHCb-PUB-2011-016.

[78] HyperCP collaboration, H. Park *et al.*, *Evidence for the decay $\Sigma^+ \to p\mu^+\mu^-$*, Phys. Rev. Lett. **94** (2005) 021801, arXiv:hep-ex/0501014.

[79] E. Majorana, *Teoria simmetrica dell'elettrone e del positrone*, Nuovo Cim. **14** (1937) 171.

[80] A. Atre, T. Han, S. Pascoli, and B. Zhang, *The Search for Heavy Majorana Neutrinos*, JHEP **0905** (2009) 030, arXiv:0901.3589.

[81] G. Cvetic, C. Dib, S. K. Kang, and C. Kim, *Probing Majorana neutrinos in rare K and D, D_s, B, B_c meson decays*, Phys. Rev. **D82** (2010) 053010, arXiv:1005.4282.

[82] S. Fajfer, J. F. Kamenik, and N. Kosnik, *$b \to dd\bar{s}$ transition and constraints on new physics in B-decays*, Phys. Rev. **D74** (2006) 034027, arXiv:hep-ph/0605260.

[83] D. Pirjol and J. Zupan, *Predictions for $b \to ss\bar{d}$, and $b \to dd\bar{s}$ decays in the SM and with new physics*, JHEP **1002** (2010) 028, arXiv:0908.3150.

[84] L. Hofer, D. Scherer, and L. Vernazza, *$B_s^0 \to \phi\rho^0$ and $B_s^0 \to \phi\pi^0$ as a handle on isospin-violating New Physics*, JHEP **1102** (2011) 080, arXiv:1011.6319.

[85] A. Buras *et al.*, *Universal unitarity triangle and physics beyond the standard model*, Phys. Lett. **B500** (2001) 161, arXiv:hep-ph/0007085.

[86] G. D'Ambrosio, G. Giudice, G. Isidori, and A. Strumia, *Minimal flavor violation: An Effective field theory approach*, Nucl. Phys. **B645** (2002) 155, arXiv:hep-ph/0207036.

[87] S. Descotes-Genon, D. Ghosh, J. Matias, and M. Ramon, *Exploring New Physics in the $C_7 - C_7'$ plane*, JHEP **1106** (2011) 099, arXiv:1104.3342.

[88] W. Altmannshofer, P. Paradisi, and D. M. Straub, *Model-Independent Constraints on New Physics in $b \to s$ Transitions*, JHEP **1204** (2012) 008, arXiv:1111.1257.

[89] C. Bobeth, G. Hiller, D. van Dyk, and C. Wacker, *The Decay $B \to K\ell^+\ell^-$ at Low Hadronic Recoil and Model-Independent Delta B = 1 Constraints*, JHEP **1201** (2012) 107, arXiv:1111.2558.

[90] F. Beaujean, C. Bobeth, D. van Dyk, and C. Wacker, *Bayesian Fit of Exclusive $b \to s\bar{\ell}\ell$ Decays: The Standard Model Operator Basis*, arXiv:1205.1838.

[91] M. Misiak *et al.*, *Estimate of $\mathcal{B}(\bar{B} \to X_s\gamma)$ at $\mathcal{O}(\alpha_s^2)$*, Phys. Rev. Lett. **98** (2007) 022002, arXiv:hep-ph/0609232.

[92] M. Beneke, T. Feldmann, and D. Seidel, *Systematic approach to exclusive $B \to V\ell^+\ell^-$, $V\gamma$ decays*, Nucl. Phys. **B612** (2001) 25, arXiv:hep-ph/0106067.

[93] M. Beneke, T. Feldmann, and D. Seidel, *Exclusive radiative and electroweak $b \to d$ and $b \to s$ penguin decays at NLO*, Eur. Phys. J. **C41** (2005) 173, arXiv:hep-ph/0412400, 29 pages, LaTeX Report-no: PITHA 04/19.

[94] J. Charles *et al.*, *Heavy to light form-factors in the heavy mass to large energy limit of QCD*, Phys. Rev. **D60** (1999) 014001, arXiv:hep-ph/9812358.

[95] J. Matias, F. Mescia, M. Ramon, and J. Virto, *Complete Anatomy of $\bar{B}_d \to \bar{K}^{*0}(\to K\pi)\ell^+\ell^-$ and its angular distribution*, JHEP **1204** (2012) 104, arXiv:1202.4266.

[96] A. Khodjamirian, T. Mannel, A. Pivovarov, and Y.-M. Wang, *Charm-loop effect in $B \to K^{(*)}\ell^+\ell^-$ and $B \to K^*\gamma$*, JHEP **1009** (2010) 089, arXiv:1006.4945.

[97] B. Grinstein and D. Pirjol, *Exclusive rare $B \to K^*\ell^+\ell^-$ decays at low recoil: Controlling the long-distance effects*, Phys. Rev. **D70** (2004) 114005, arXiv:hep-ph/0404250.

[98] M. Beylich, G. Buchalla, and T. Feldmann, *Theory of $B \to K^{(*)}\ell + \ell^-$ decays at high q^2: OPE and quark-hadron duality*, Eur. Phys. J. **C71** (2011) 1635, arXiv:1101.5118.

[99] N. Isgur and M. B. Wise, *Weak transition form-factors between heavy measons*, Phys. Lett. **B237** (1990) 527.

[100] Z. Liu *et al.*, *A Lattice calculation of $B \to K^{(*)}$ form factors*, arXiv:1101.2726, Proceedings of CKM2010, the 6th International Workshop on the CKM Unitarity Triangle, University of Warwick, UK, 6-10 September 2010.

[101] F. Kruger, L. M. Sehgal, N. Sinha, and R. Sinha, *Angular distribution and CP asymmetries in the decays $\bar{B} \to K^-\pi^+e^-e^+$ and $\bar{B} \to \pi^-\pi^+e^-e^+$*, Phys. Rev. **D61** (2000) 114028, arXiv:hep-ph/9907386.

[102] C. Bobeth, G. Hiller, and G. Piranishvili, *CP Asymmetries in bar $B \to \bar{K}^*(\to \bar{K}\pi)\bar{\ell}\ell$ and Untagged $\bar{B}_s$, $B_s \to \phi(\to K^+K^-)\bar{\ell}\ell$ Decays at NLO*, JHEP **0807** (2008) 106, arXiv:0805.2525.

[103] C. Bobeth, G. Hiller, and D. van Dyk, *The Benefits of $\bar{B} \to \bar{K}^*\ell^+\ell^-$ Decays at Low Recoil*, JHEP **1007** (2010) 098, arXiv:1006.5013.

[104] C. Bobeth, G. Hiller, and D. van Dyk, *More Benefits of Semileptonic Rare B Decays at Low Recoil: CP Violation*, JHEP **1107** (2011) 067, arXiv:1105.0376.

[105] M. Benzke, S. J. Lee, M. Neubert, and G. Paz, *Long-Distance Dominance of the CP Asymmetry in $B \to X_{s,d}\gamma$ Decays*, Phys. Rev. Lett. **106** (2011) 141801, arXiv:1012.3167.

[106] CDF collaboration, T. Aaltonen *et al.*, *Measurements of the Angular Distributions in the Decays $B \to K^{(*)}\mu^+\mu^-$ at CDF*, Phys. Rev. Lett. **108** (2012) 081807, arXiv:1108.0695.

[107] Belle, J.-T. Wei *et al.*, *Measurement of the Differential Branching Fraction and Forward-Backword Asymmetry for $B \to K^{(*)}\ell^+\ell^-$*, Phys. Rev. Lett. **103** (2009) 171801, arXiv:0904.0770.

[108] S. Descotes-Genon, J. Matias, M. Ramon, and J. Virto, *Implications from clean observables for the binned analysis of $B \to K^*ll$ at large recoil*, arXiv:1207.2753.

[109] A. Bharucha and W. Reece, *Constraining new physics with $B \to K^*\mu^+\mu^-$ in the early LHC era*, Eur. Phys. J. **C69** (2010) 623, arXiv:1002.4310.

[110] C. Hambrock and G. Hiller, *Extracting $B \to K^*$ Form Factors from Data*, arXiv:1204.4444.

[111] CDF collaboration, T. Aaltonen *et al.*, *Observation of the Baryonic Flavor-Changing Neutral Current Decay $\Lambda_b \to \Lambda\mu^+\mu^-$*, Phys. Rev. Lett. **107** (2011) 201802, arXiv:1107.3753.

[112] BaBar collaboration, J. P. Lees *et al.*, *Measurement of Branching Fractions and Rate Asymmetries in the Rare Decays $B \to K^{(*)}\ell + \ell-$*, arXiv:1204.3933.

[113] C. Bobeth, G. Hiller, and G. Piranishvili, *Angular distributions of $B \to K^*\ell^+\ell^-$ decays*, JHEP **0712** (2007) 040, arXiv:0709.4174.

[114] D. Becirevic, N. Kosnik, F. Mescia, and E. Schneider, *Complementarity of the constraints on New Physics from $B_s^0 \to \mu^+\mu^-$ and from $B \to Kl^+l^-$ decays*, arXiv:1205.5811.

[115] BaBar collaboration, J. Lees *et al.*, *Evidence for an excess of $\bar{B} \to D^{(*)}\tau^-\bar{\nu}_\tau$ decays*, arXiv:1205.5442.

[116] Belle collaboration, A. Matyja *et al.*, *Observation of $B^0 \to D^{*-}\tau^+\nu_\tau$ decay at Belle*, Phys. Rev. Lett. **99** (2007) 191807, arXiv:0706.4429.

[117] Belle collaboration, A. Bozek *et al.*, *Observation of $B^+- \to \bar{D}^{*0}\tau^+\nu_\tau$ and evidence for $B^+ \to \bar{D}^0\tau^+\nu_\tau$ at Belle*, Phys. Rev. **D82** (2010) 072005, arXiv:1005.2302.

[118] G. Hiller and F. Kruger, *More model independent analysis of $b \to s$ processes*, Phys. Rev. **D69** (2004) 074020, arXiv:hep-ph/0310219.

[119] BaBar collaboration, P. del Amo Sanchez *et al.*, *Study of $B \to X\gamma$ decays and determination of $|V_{td}/V_{ts}|$*, Phys. Rev. **D82** (2010) 051101, arXiv:1005.4087.

[120] T. Feldmann and J. Matias, *Forward backward and isospin asymmetry for $B \to K^*\ell^+\ell^-$ decay in the standard model and in supersymmetry*, JHEP **0301** (2003) 074, arXiv:hep-ph/0212158.

[121] D. Atwood, M. Gronau, and A. Soni, *Mixing induced CP asymmetries in radiative B decays in and beyond the standard model*, Phys. Rev. Lett. **79** (1997) 185, arXiv:hep-ph/9704272.

[122] D. Atwood, T. Gershon, M. Hazumi, and A. Soni, *Mixing-induced CP violation in $B \to P_1P_2\gamma$ in search of clean new physics signals*, Phys. Rev. **D71** (2005) 076003, arXiv:hep-ph/0410036.

[123] F. Muheim, Y. Xie, and R. Zwicky, *Exploiting the width difference in $B_s \to \phi\gamma$*, Phys. Lett. **B664** (2008) 174, arXiv:0802.0876.

[124] F. Legger and T. Schietinger, *Polarized radiative Λ_b decays at LHCb*, CERN-LHCB-2006-013.

[125] G. Hiller, M. Knecht, F. Legger, and T. Schietinger, *Photon polarization from helicity suppression in radiative decays of polarized Λ_b to spin-3/2 baryons*, Phys. Lett. **B649** (2007) 152, arXiv:hep-ph/0702191.

[126] Y.-m. Wang, Y. Li, and C.-D. Lu, *Rare Decays of $\Lambda_b^0 \to \Lambda\gamma$ and $\Lambda_b^0 \to \Lambda l^+l^-$ in the Light-cone Sum Rules*, Eur. Phys. J. **C59** (2009) 861, arXiv:0804.0648.

[127] T. Mannel and Y.-M. Wang, *Heavy-to-light baryonic form factors at large recoil*, JHEP **1112** (2011) 067, arXiv:1111.1849.

[128] T. Feldmann and M. W. Yip, *Form Factors for $\Lambda \to \Lambda$ Transitions in SCET*, Phys. Rev. **D85** (2012) 014035, arXiv:1111.1844.

[129] M. Gronau, Y. Grossman, D. Pirjol, and A. Ryd, *Measuring the photon polarization in $B \to K\pi\pi\gamma$*, Phys. Rev. Lett. **88** (2002) 051802, arXiv:hep-ph/0107254.

[130] M. Gronau and D. Pirjol, *Photon polarization in radiative B decays*, Phys. Rev. **D66** (2002) 054008, arXiv:hep-ph/0205065.

[131] D. Atwood, T. Gershon, M. Hazumi, and A. Soni, *Clean Signals of CP-violating and CP-conserving New Physics in $B \to P\ V\ \gamma$ Decays at B Factories and Hadron Colliders*, arXiv:hep-ph/0701021.

[132] E. Kou, A. Le Yaouanc, and A. Tayduganov, *Determining the photon polarization of the $b \to s\gamma$ using the $B \to K_1(1270)\gamma \to (K\pi\pi)\gamma$ decay*, Phys. Rev. **D83** (2011) 094007, arXiv:1011.6593.

[133] BaBar collaboration, B. Aubert *et al.*, *Measurement of B Decays to $\phi K\gamma$*, Phys. Rev. **D75** (2007) 051102, arXiv:hep-ex/0611037.

[134] Belle collaboration, H. Yang *et al.*, *Observation of $B^+ \to K_1(1270)^+\gamma$*, Phys. Rev. Lett. **94** (2005) 111802, arXiv:hep-ex/0412039.

[135] C. Bobeth, T. Ewerth, F. Kruger, and J. Urban, *Analysis of neutral Higgs boson contributions to the decays $\bar{B}_{(}s) \to \ell^+\ell^-$ and $\bar{B} \to K\ell^+\ell^-$*, Phys. Rev. **D64** (2001) 074014, arXiv:hep-ph/0104284.

[136] C. Bobeth, A. J. Buras, F. Kruger, and J. Urban, *QCD corrections to $\bar{B} \to X_{d,s}\nu\bar{\nu}$, $\bar{B}_{d,s} \to \ell^+\ell^-$, $K \to \pi\nu\bar{\nu}$ and $K_L \to \mu^+\mu^-$ in the MSSM*, Nucl. Phys. **B630** (2002) 87, arXiv:hep-ph/0112305.

[137] A. J. Buras, P. H. Chankowski, J. Rosiek, and L. Slawianowska, *$\Delta M_{d,s}, B^0_{d,s} \to \mu^+\mu^-$ and $B \to X_s\gamma$ in supersymmetry at large* $\tan\beta$, Nucl. Phys. **B659** (2003) 3, arXiv:hep-ph/0210145.

[138] F. Mahmoudi, *SuperIso v2.3: A Program for calculating flavor physics observables in Supersymmetry*, Comput. Phys. Commun. **180** (2009) 1579, arXiv:0808.3144.

[139] HPQCD collaboration, E. Gamiz *et al.*, *Neutral B Meson Mixing in Unquenched Lattice QCD*, Phys. Rev. **D80** (2009) 014503, arXiv:0902.1815.

[140] C. Bernard *et al.*, *B and D Meson Decay Constants*, PoS **LATTICE2008** (2008) 278, arXiv:0904.1895.

[141] J. Laiho, E. Lunghi, and R. S. Van de Water, *Lattice QCD inputs to the CKM unitarity triangle analysis*, Phys. Rev. **D81** (2010) 034503, arXiv:0910.2928, updated results and plots available at: http://www.latticeaverages.org/.

[142] Fermilab Lattice and MILC collaborations, J. Simone *et al.*, *The decay constants f_{D_s}, f_{D^+}, f_{B_s} and f_B from lattice QCD*, PoS **LATTICE2010** (2010) 317.

[143] ETM collaboration, P. Dimopoulos *et al.*, *Lattice QCD determination of m_b, f_B and f_{B_s} with twisted mass Wilson fermions*, JHEP **1201** (2012) 046, arXiv:1107.1441.

[144] Fermilab Lattice and MILC collaborations, A. Bazavov *et al.*, *B- and D-meson decay constants from three-flavor lattice QCD*, Phys. Rev. **D85** (2012) 114506, arXiv:1112.3051.

[145] Fermilab Lattice collaboration, MILC collaboration, E. Neil *et al.*, *B and D meson decay constants from $2+1$ flavor improved staggered simulations*, PoS **LATTICE2011** (2011) 320, arXiv:1112.3978.

[146] H. Na *et al.*, *The B and B_s Meson Decay Constants from Lattice QCD*, arXiv:1202.4914.

[147] C. McNeile *et al.*, *High-Precision f_{B_s} and HQET from Relativistic Lattice QCD*, Phys. Rev. **D85** (2012) 031503, arXiv:1110.4510.

[148] F. Mahmoudi, S. Neshatpour, and J. Orloff, *Supersymmetric constraints from $B_s \to \mu^+\mu^-$ and $B \to K^*\mu^+\mu^-$ observables*, arXiv:1205.1845.

[149] A. J. Buras, J. Girrbach, D. Guadagnoli, and G. Isidori, *On the Standard Model prediction for $\mathcal{B}(B_{s,d} \to \mu^+\mu^-)$*, arXiv:1208.0934.

[150] A. J. Buras, M. V. Carlucci, S. Gori, and G. Isidori, *Higgs-mediated FCNCs: Natural Flavour Conservation vs. Minimal Flavour Violation*, JHEP **1010** (2010) 009, arXiv:1005.5310.

[151] S. R. Choudhury and N. Gaur, *Dileptonic decay of $B_{(s)}$ meson in SUSY models with large* $\tan\beta$, Phys. Lett. **B451** (1999) 86, arXiv:hep-ph/9810307.

[152] K. Babu and C. F. Kolda, *Higgs mediated $B^0 \to \mu^+\mu^-$ in minimal supersymmetry*, Phys. Rev. Lett. **84** (2000) 228, arXiv:hep-ph/9909476.

[153] J. R. Ellis, K. A. Olive, and V. C. Spanos, *On the interpretation of $B_s \to \mu^+\mu^-$ in the CMSSM*, Phys. Lett. **B624** (2005) 47, arXiv:hep-ph/0504196.

[154] M. S. Carena *et al.*, *Constraints on B and Higgs physics in minimal low energy supersymmetric models*, Phys. Rev. **D74** (2006) 015009, arXiv:hep-ph/0603106.

[155] J. R. Ellis, S. Heinemeyer, K. Olive, and G. Weiglein, *Light Heavy MSSM Higgs Bosons at Large tan beta*, Phys. Lett. **B653** (2007) 292, arXiv:0706.0977.

[156] F. Mahmoudi, *New constraints on supersymmetric models from btosgamma*, JHEP **0712** (2007) 026, arXiv:0710.3791.

[157] E. Golowich *et al.*, *Relating B_s Mixing and $B_s \to \mu^+\mu^-$ with New Physics*, Phys. Rev. **D83** (2011) 114017, arXiv:1102.0009.

[158] A. Akeroyd, F. Mahmoudi, and D. Martinez Santos, *The decay $B_s \to \mu^+\mu^-$: updated SUSY constraints and prospects*, JHEP **1112** (2011) 088, arXiv:1108.3018.

[159] M. Blanke *et al.*, *Rare and CP-Violating K and B Decays in the Littlest Higgs Model with T-Parity*, JHEP **0701** (2007) 066, arXiv:hep-ph/0610298.

[160] M. Blanke *et al.*, *Rare K and B Decays in a Warped Extra Dimension with Custodial Protection*, JHEP **0903** (2009) 108, arXiv:0812.3803.

[161] W. Liu, C.-X. Yue, and H.-D. Yang, *Rare decays $B_s \to \ell^+\ell^-$ and $B \to K\ell^+\ell^-$ in the topcolor-assisted technicolor model*, Phys. Rev. **D79** (2009) 034008, arXiv:0901.3463.

[162] M. Bauer, S. Casagrande, U. Haisch, and M. Neubert, *Flavor Physics in the Randall-Sundrum Model: II. Tree-Level Weak-Interaction Processes*, JHEP **1009** (2010) 017, arXiv:0912.1625.

[163] A. J. Buras *et al.*, *Lepton Flavour Violation in the Presence of a Fourth Generation of Quarks and Leptons*, JHEP **1009** (2010) 104, arXiv:1006.5356.

[164] K. de Bruyn *et al.*, *On Branching Ratio Measurements of B_s Decays*, Phys. Rev. Lett. **109** (2012) 041801, arXiv:1204.1735.

[165] S. Descotes-Genon, J. Matias, and J. Virto, *An analysis of $B_{d,s}$ mixing angles in presence of New Physics and an update of $B_s^0 \to K^{*0}\bar{K}^{*0}$*, Phys. Rev. **D85** (2012) 034010, arXiv:1111.4882.

[166] CLEO collaboration, J. Alexander *et al.*, *Absolute Measurement of Hadronic Branching Fractions of the D(s)+ Meson*, Phys. Rev. Lett. **100** (2008) 161804, arXiv:0801.0680.

[167] Belle collaboration, M. Wang, *Charm decays at Belle*, , talk given at ICHEP 2012, Melbourne, July 5$^{\text{th}}$ 2012.

[168] CMS collaboration, S. Chatrchyan *et al.*, *Search for $B_s^0 to \mu^+\mu^-$ and $B^0 to \mu^+\mu^-$ decays*, JHEP **1204** (2012) 033, arXiv:1203.3976.

[169] ATLAS collaboration, G. Aad *et al.*, *Search for the decay $B_s^0 \to \mu^+\mu^-$ with the ATLAS detector*, Phys. Lett. **B713** (2012) 387, arXiv:1204.0735.

[170] CDF collaboration, T. Aaltonen *et al.*, *Search for $B_s \to \mu^+\mu^-$ and $B_d \to \mu^+\mu^-$ Decays with CDF II*, Phys. Rev. Lett. **107** (2011) 239903, arXiv:1107.2304.

[171] C. W. Bauer and N. D. Dunn, *Comment on new physics contributions to Γ_{12}^s*, Phys. Lett. **B696** (2011) 362, arXiv:1006.1629.

[172] A. Dighe, A. Kundu, and S. Nandi, *Possibility of large lifetime differences in neutral B meson systems*, Phys. Rev. **D76** (2007) 054005, arXiv:0705.4547.

[173] A. K. Alok, S. Baek, and D. London, *Neutral gauge boson contributions to the dimuon charge asymmetry in B decays*, JHEP **1107** (2011) 111, arXiv:1010.1333.

[174] J. E. Kim, M.-S. Seo, and S. Shin, *The D0 same-charge dimuon asymmetry and possibile new CP violation sources in the $B_s - \bar{B}_s$ system*, Phys. Rev. **D83** (2011) 036003, arXiv:1010.5123.

[175] H. D. Kim, S.-G. Kim, and S. Shin, *D0 dimuon charge asymmetry from B_s system with Z' couplings and the recent LHCb result*, arXiv:1205.6481.

[176] F. Mahmoudi, *SuperIso: A Program for calculating the isospin asymmetry of $B \to K^*\gamma$ in the MSSM*, Comput. Phys. Commun. **178** (2008) 745, arXiv:0710.2067.

[177] CMS collaboration, S. Chatrchyan *et al.*, *Search for Supersymmetry at the LHC in Events with Jets and Missing Transverse Energy*, Phys. Rev. Lett. **107** (2011) 221804, arXiv:1109.2352.

[178] CMS collaboration, *Search for supersymmetry with the razor variables at CMS*, Tech. Rep. CMS-PAS-SUS-12-005, 2012.

[179] A. Behring, C. Gross, G. Hiller, and S. Schacht, *Squark Flavor Implications from* $B \to K^* l^+ l^-$, arXiv:1205.1500.

[180] O. Buchmueller *et al.*, *Higgs and Supersymmetry*, arXiv:1112.3564.

[181] A. Crivellin and U. Nierste, *Supersymmetric renormalisation of the CKM matrix and new constraints on the squark mass matrices*, Phys. Rev. **D79** (2009) 035018, arXiv:0810.1613.

[182] MSSM Working Group, A. Djouadi *et al.*, *The Minimal supersymmetric standard model: Group summary report*, arXiv:hep-ph/9901246.

[183] A. Arbey, M. Battaglia, and F. Mahmoudi, *Constraints on the MSSM from the Higgs Sector: A pMSSM Study of Higgs Searches,* $B_s^0 \to \mu^+\mu^-$ *and Dark Matter Direct Detection*, Eur. Phys. J. **C72** (2012) 1906, arXiv:1112.3032.

[184] ATLAS collaboration, G. Aad *et al.*, *Observation of a new particle in the search for the Standard Model Higgs boson with the ATLAS detector at the LHC*, arXiv:1207.7214.

[185] CMS collaboration, S. Chatrchyan *et al.*, *Observation of a new boson at a mass of 125 GeV with the CMS experiment at the LHC*, arXiv:1207.7235.

[186] G. Burdman, E. Golowich, J. L. Hewett, and S. Pakvasa, *Rare charm decays in the standard model and beyond*, Phys. Rev. **D66** (2002) 014009, arXiv:hep-ph/0112235.

[187] E. Golowich, J. Hewett, S. Pakvasa, and A. A. Petrov, *Relating* D^0–$\bar{D}^0$ *mixing and* $D^0 \to l^+ l^-$ *with New Physics*, Phys. Rev. **D79** (2009) 114030, arXiv:0903.2830.

[188] M. Artuso *et al.*, *B, D and K decays*, Eur. Phys. J. **C57** (2008) 309, arXiv:0801.1833.

[189] S. Fajfer, N. Kosnik, and S. Prelovsek, *Updated constraints on new physics in rare charm decays*, Phys. Rev. **D76** (2007) 074010, arXiv:0706.1133.

[190] D0 collaboration, V. Abazov *et al.*, *Search for flavor-changing-neutral-current D meson decays*, Phys. Rev. Lett. **100** (2008) 101801, arXiv:0708.2094.

[191] I. I. Bigi and A. Paul, *On CP Asymmetries in Two-, Three- and Four-Body D Decays*, JHEP **1203** (2012) 021, arXiv:1110.2862.

[192] W. J. Marciano, T. Mori, and J. M. Roney, *Charged Lepton Flavour Violation Experiments*, Ann. Rev. Nucl. Part. Sci **58** (2008) 315.

[193] Particle Data Group, K. Nakamura *et al.*, *Review of particle physics*, J. Phys. **G37** (2010) 075021, and 2011 partial update for the 2012 edition.

[194] J. C. Pati and A. Salam, *Lepton Number as the Fourth Color*, Phys. Rev. **D10** (1974) 275, Erratum-ibid. **D11** (1975) 703.

[195] L. Landsberg, *Is it still worth searching for lepton flavor violation in rare kaon decays?*, Phys. Atom. Nucl. **68** (2005) 1190, arXiv:hep-ph/0410261.

[196] M. Shaposhnikov, *The nuMSM, leptonic asymmetries, and properties of singlet fermions*, JHEP **0808** (2008) 008, arXiv:0804.4542.

[197] R. Aaij *et al.*, *Search for the lepton number violating decays* $B^+ \to \pi^-\mu^+\mu^+$ *and* $B^+ \to K^-\mu^+\mu^+$, Phys. Rev. Lett. **108** (2012) 101601, arXiv:1110.0730.

[198] G. Ecker and A. Pich, *The Longitudinal muon polarization in* $K_L \to \mu^+\mu^-$, Nucl. Phys. **B366** (1991) 189.

[199] G. Isidori and R. Unterdorfer, *On the short distance constraints from* $K_{L,S} \to \mu^+\mu^-$, JHEP **0401** (2004) 009, arXiv:hep-ph/0311084.

[200] S. Gjesdal *et al.*, *Search for the decay* $K_S^0 \to \mu\mu$, Phys. Lett. **B44** (1973) 217.

[201] Y. Kahn, M. Schmitt, and T. M. Tait, *Enhanced rare pion decays from a model of MeV dark matter*, Phys. Rev. **D78** (2008) 115002, arXiv:0712.0007; R. Dermisek and J. F. Gunion, *Consistency of LEP event excesses with an* $h \to aa$ *decay scenario and low-fine-tuning NMSSM models*, Phys. Rev. **D73** (2006) 111701, arXiv:hep-ph/0510322; C. Bouchiat and P. Fayet, *Constraints on the parity-violating couplings of a new gauge boson*, Phys. Lett. **B608** (2005) 87, arXiv:hep-ph/0410260; C. Boehm *et al.*, *MeV dark matter: Has it been detected?*, Phys. Rev. Lett. **92** (2004) 101301, arXiv:astro-ph/0309686; D. Gorbunov and V. Rubakov, *Kaon physics with light sgoldstinos and parity conservation*, Phys. Rev. **D64** (2001) 054008, arXiv:hep-ph/0012033.

[202] PAMELA collaboration, O. Adriani *et al.*, *An anomalous positron abundance in cosmic rays with energies 1.5-100 GeV*, Nature **458** (2009) 607, arXiv:0810.4995.

[203] J. Chang *et al.*, *An excess of cosmic ray electrons at energies of 300-800 GeV*, Nature **456** (2008) 362.

[204] X.-G. He, J. Tandean, and G. Valencia, *Implications of a new particle from the hyperCP data on* $\Sigma^+ \to p\mu^+\mu^-$, Phys. Lett. **B631** (2005) 100, arXiv:hep-ph/0509041.

[205] C. Geng and Y. Hsiao, *Constraints on the new particle in $\Sigma^+ \to p\mu^+\mu^-$*, Phys. Lett. **B632** (2006) 215, arXiv:hep-ph/0509175.

[206] J. R. Ellis, K. Enqvist, and D. V. Nanopoulos, *A Very Light Gravitino in a No Scale Model*, Phys. Lett. **B147** (1984) 99; T. Bhattacharya and P. Roy, *Role of chiral scalar and psuedoscalar in two photon production of a superlight gravitino*, Phys. Rev. **D38** (1988) 2284; G. Giudice and R. Rattazzi, *Theories with gauge mediated supersymmetry breaking*, Phys. Rept. **322** (1999) 419, arXiv:hep-ph/9801271.

[207] X.-G. He, J. Tandean, and G. Valencia, *Does the HyperCP Evidence for the Decay $\Sigma \to p\mu^+\mu^-$ Indicate a Light Pseudoscalar Higgs Boson?*, Phys. Rev. Lett. **98** (2007) 081802, arXiv:hep-ph/0610362.

[208] Belle collaboration, H. Hyun *et al.*, *Search for a Low Mass Particle Decaying into mu^+mu^- in $B^0 \to K^{*0}X$ and $B^0 \to \rho^0 X$ at Belle*, Phys. Rev. Lett. **105** (2010) 091801, arXiv:1005.1450.

[209] M. Freytsis, Z. Ligeti, and J. Thaler, *Constraining the Axion Portal with $B \to Kl^+l^-$*, Phys. Rev. **D81** (2010) 034001, arXiv:0911.5355.

[210] A. Sakharov, *Violation of CP Invariance, C Asymmetry, and Baryon Asymmetry of the Universe*, Pisma Zh. Eksp. Teor. Fiz. **5** (1967) 32.

[211] A. Lenz, *Theoretical update of B-Mixing and Lifetimes*, arXiv:1205.1444.

[212] A. Lenz, *Theoretical status of B_s-mixing and lifetimes of heavy hadrons*, Nucl. Phys. Proc. Suppl. **177-178** (2008) 81, arXiv:0705.3802.

[213] LHCb collaboration, R. Aaij *et al.*, *Measurement of the CP violating phase ϕ_s in $\overline{B}^0_s \to J/\psi f_0(980)$*, Phys. Lett. **B707** (2012) 497, arXiv:1112.3056.

[214] A. Lenz and U. Nierste, *Numerical updates of lifetimes and mixing parameters of B mesons*, arXiv:1102.4274.

[215] M. Beneke *et al.*, *Next-to-leading order QCD corrections to the lifetime difference of B^0_s mesons*, Phys. Lett. **B459** (1999) 631, arXiv:hep-ph/9808385; M. Ciuchini *et al.*, *Lifetime differences and CP violation parameters of neutral B mesons at the next-to-leading order in QCD*, JHEP **0308** (2003) 031, arXiv:hep-ph/0308029; M. Beneke, G. Buchalla, and I. Dunietz, *Width Difference in the B^0_s–$\overline{B}^0_s$ System*, Phys. Rev. **D54** (1996) 4419, arXiv:hep-ph/9605259; M. Beneke, G. Buchalla, A. Lenz, and U. Nierste, *CP asymmetry in flavor specific B decays beyond leading logarithms*, Phys. Lett. **B576** (2003) 173, arXiv:hep-ph/0307344.

[216] LHCb collaboration, *Measurement of Δm_s in the decay $B^0_s \to D^-_s(K^+K^-\pi^-)\pi^+$ using opposite-side and same-side flavour tagging algorithms*, LHCb-CONF-2011-050.

[217] D0 collaboration, V. Abazov *et al.*, *Search for CP violation in semileptonic B_s decays*, Phys. Rev. **D82** (2010) 012003, arXiv:0904.3907.

[218] CDF collaboration, A. Abulencia *et al.*, *Observation of B0(s) - anti-B0(s) Oscillations*, Phys. Rev. Lett. **97** (2006) 242003, arXiv:hep-ex/0609040.

[219] LHCb collaboration, R. Aaij *et al.*, *Measurement of the $B_s^0-\overline{B}_s^0$ oscillation frequency Δm_s in $B_s^0 \to D_s(3)\pi$ decays*, Phys. Lett. **B709** (2012) 177, arXiv:1112.4311.

[220] A. S. Dighe, I. Dunietz, and R. Fleischer, *Extracting CKM phases and B_s^0–$\overline{B}_s^0$ mixing parameters from angular distributions of nonleptonic B decays*, Eur. Phys. J. **C6** (1999) 647, arXiv:hep-ph/9804253.

[221] I. Dunietz, R. Fleischer, and U. Nierste, *In pursuit of new physics with B_s^0 decays*, Phys. Rev. **D63** (2001) 114015, arXiv:hep-ph/0012219.

[222] Y. Xie, P. Clarke, G. Cowan, and F. Muheim, *Determination of $2\beta_s$ in $B_s^0 \to J/\psi\, K^+K^-$ Decays in the Presence of a K^+K^- S-Wave Contribution*, JHEP **0909** (2009) 074, arXiv:0908.3627.

[223] LHCb collaboration, R. Aaij *et al.*, *Analysis of the resonant components in $\overline{B}_s^0 \to J/\psi\pi^+\pi^-$*, arXiv:1204.5643.

[224] R. Fleischer, R. Knegjens, and G. Ricciardi, *Anatomy of $B_{s,d}^0 \to J/\psi f_0(980)$*, Eur. Phys. J. **C71** (2011) 1832, arXiv:1109.1112.

[225] LHCb collaboration, R. Aaij *et al.*, *Measurement of the $\bar{B}_s^0$ effective lifetime in the $J/\psi f_0(980)$ final state*, arXiv:1207.0878.

[226] CDF collaboration, T. Aaltonen *et al.*, *Measurement of the CP-Violating Phase $\beta_s^{J/\Psi\phi}$ in $B_s^0 \to J/\Psi\phi$ Decays with the CDF II Detector*, Phys. Rev. **D85** (2012) 072002, arXiv:1112.1726.

[227] D0 collaboration, V. M. Abazov *et al.*, *Measurement of the CP-violating phase $\phi_s^{J/\psi\phi}$ using the flavor-tagged decay $B_s^0 \to J/\psi\phi$ in 8 fb^{-1} of $p\bar{p}$ collisions*, Phys. Rev. **D85** (2012) 032006, arXiv:1109.3166.

[228] LHCb collaboration, R. Aaij *et al.*, *Opposite-side flavour tagging of B mesons at the LHCb experiment*, Eur. Phys. J. **C72** (2012) 2022, arXiv:1202.4979.

[229] LHCb collaboration, *Performance of flavor tagging algorithms optimised for the analysis of $B_s^0 \to J/\psi\phi$*, LHCb-CONF-2012-026.

[230] R. Fleischer, R. Knegjens, and G. Ricciardi, *Exploring CP violation and η-η' mixing with the $B_{s,d}^0 \to J/\psi\eta^{(\prime)}$ systems*, Eur. Phys. J. **C71** (2011) 1798, arXiv:1110.5490.

[231] R. Fleischer, *Exploring CP violation and penguin effects through $B_d^0 \to D^+D^-$ and $B_s^0 \to D_s^+D_s^-$*, Eur. Phys. J. **C51** (2007) 849, arXiv:0705.4421.

[232] LHCb collaboration, *First observations and branching fraction measurements of $\bar{B}^0_s$ to double-charm final states*, LHCb-CONF-2012-009.

[233] D0 collaboration, V. Abazov, *Measurement of the semileptonic charge asymmetry using $B^0_s \to D_s \mu X$ decays*, arXiv:1207.1769.

[234] Belle collaboration, K. Hara *et al.*, *Evidence for $B^- \to \tau^- \bar{\nu}$ with a Semileptonic Tagging Method*, Phys. Rev. **D82** (2010) 071101, arXiv:1006.4201.

[235] BaBar collaboration, J. Lees *et al.*, *Evidence of $B \to \tau\nu$ decays with hadronic B tags*, arXiv:1207.0698.

[236] Belle collaboration, Y. Yook, *Leptonic & semileptonic B decays at Belle*, , talk given at ICHEP 2012, Melbourne, July 5$^{\text{th}}$ 2012.

[237] LHCb collaboration, *Search for CP violation in $B^0 \to J/\psi K^0_S$ decays with first LHCb data*, LHCb-CONF-2011-004.

[238] T. Gershon, *$\Delta\Gamma_d$: A Forgotten Null Test of the Standard Model*, J. Phys. G **G38** (2011) 015007, arXiv:1007.5135.

[239] A. J. Lenz, *A simple relation for B^0_s mixing*, Phys. Rev. **D84** (2011) 031501, arXiv:1106.3200.

[240] Y. Grossman, *The B_s width difference beyond the standard model*, Phys. Lett. **B380** (1996) 99, arXiv:hep-ph/9603244.

[241] A. Lenz *et al.*, *Anatomy of New Physics in $B - \bar{B}$ mixing*, Phys. Rev. **D83** (2011) 036004, arXiv:1008.1593.

[242] A. Badin, F. Gabbiani, and A. A. Petrov, *Lifetime difference in B_s mixing: Standard model and beyond*, Phys. Lett. **B653** (2007) 230, arXiv:0707.0294.

[243] B. A. Dobrescu, P. J. Fox, and A. Martin, *CP violation in B_s mixing from heavy Higgs exchange*, Phys. Rev. Lett. **105** (2010) 041801, arXiv:1005.4238.

[244] Z. Ligeti, M. Papucci, G. Perez, and J. Zupan, *Implications of the dimuon CP asymmetry in $B_{d,s}$ decays*, Phys. Rev. Lett. **105** (2010) 131601, arXiv:1006.0432.

[245] BaBar collaboration, K. Flood, *New results in radiative electroweak penguin decays at BaBar*, PoS **ICHEP2010** (2010) 234.

[246] Y. Bai and A. E. Nelson, *CP Violating Contribution to $\Delta\Gamma$ in the B_s System from Mixing with a Hidden Pseudoscalar*, Phys. Rev. **D82** (2010) 114027, arXiv:1007.0596.

[247] S. Oh and J. Tandean, *Anomalous CP-Violation in $B_s - \bar{B}_s$ Mixing Due to a Light Spin-One Particle*, Phys. Lett. **B697** (2011) 41, arXiv:1008.2153.

[248] UTfit Collaboration, M. Bona *et al.*, *An improved Standard Model prediction Of $\mathcal{B}(B \to \tau nu)$ and its implications for New Physics*, Phys. Lett. **B687** (2010) 61, arXiv:0908.3470.

[249] UTfit collaboration, M. Bona *et al.*, *Model-independent constraints on Δ F=2 operators and the scale of new physics*, JHEP **0803** (2008) 049, arXiv:0707.0636.

[250] I. I. Bigi and A. Sanda, *Notes on the observability of CP violations in B decays*, Nucl. Phys. **B193** (1981) 85.

[251] H. Boos, T. Mannel, and J. Reuter, *The gold plated mode revisited:* $\sin(2\beta)$ *and* $B0 \to J/\psi K^0_{\rm S}$ *in the standard model*, Phys. Rev. **D70** (2004) 036006, arXiv:hep-ph/0403085.

[252] H.-n. Li and S. Mishima, *Penguin pollution in the $B^0 \to J/\psi K^0_{\rm S}$ decay*, JHEP **0703** (2007) 009, arXiv:hep-ph/0610120.

[253] M. Gronau and J. L. Rosner, *Doubly CKM-suppressed corrections to CP asymmetries in $B^0 \to J/\psi K^0$*, Phys. Lett. **B672** (2009) 349, arXiv:0812.4796.

[254] R. Fleischer, *Extracting γ from $B_{s(d)} \to J/\psi K^0_{\rm S}$ and $B_{d(s)} \to D^+_{d(s)} D^-_{(d(s)}$*, Eur. Phys. J. **C10** (1999) 299, arXiv:hep-ph/9903455.

[255] M. Ciuchini, M. Pierini, and L. Silvestrini, *The effect of penguins in the $B^0 \to J/\psi K^0_{\rm S}$ CP asymmetry*, Phys. Rev. Lett. **95** (2005) 221804, arXiv:hep-ph/0507290.

[256] S. Faller, M. Jung, R. Fleischer, and T. Mannel, *The golden modes $B^0 \to J/\psi K_{S,L}$ in the era of precision flavour physics*, Phys. Rev. **D79** (2009) 014030, arXiv:0809.0842.

[257] M. Jung and T. Mannel, *General analysis of U-Spin breaking in B decays*, Phys. Rev. **D80** (2009) 116002, arXiv:0907.0117.

[258] K. De Bruyn, R. Fleischer, and P. Koppenburg, *Extracting gamma and penguin topologies through CP violation in $B^0_s \to J/\psi K^0_{\rm S}$*, Eur. Phys. J. **C70** (2010) 1025, arXiv:1010.0089.

[259] M. Ciuchini, M. Pierini, and L. Silvestrini, *Theoretical uncertainty in sin 2β: An Update*, arXiv:1102.0392.

[260] CDF collaboration, T. Aaltonen *et al.*, *Observation of $B^0_s \to J/\psi K^{*0}(892)$ and $B^0_s \to J/\psi K^0_S$ Decays*, Phys. Rev. **D83** (2011) 052012, arXiv:1102.1961.

[261] LHCb collaboration, *Evidence for the decay $B^0_s \to J/\psi \overline{K}^{*0}$*, LHCb-CONF-2011-025.

[262] M. Jung, *Determining weak phases from $B \to J/\psi P$ decays*, arXiv:1206.2050.

[263] LHCb collaboration, R. Aaij *et al.*, *Measurements of the branching fractions and CP asymmetries of $B^+ \to J/\psi\,\pi^+$ and $B^+ \to \psi(2S)\pi^+$ decays*, Phys. Rev. (2012) 091105, arXiv:1203.3592.

[264] LHCb collaboration, R. Aaij *et al.*, *Measurement of the $B_s^0 \to J/\psi K_{\rm S}^0$ branching fraction*, Phys. Lett. **B713** (2012) 172, arXiv:1205.0934.

[265] LHCb collaboration, R. Aaij *et al.*, *Measurement of $B_s \to J/\psi \bar{K}^{*0}$ branching fraction and angular amplitudes*, arXiv:1208.0738.

[266] R. Fleischer, *A closer look at $B_{d,s} \to D f_r$ decays and novel avenues to determine gamma*, Nucl. Phys. **B659** (2003) 321, arXiv:hep-ph/0301256.

[267] S. Nandi and D. London, *$B_s^0(\overline{B}_s^0) \to D_{CP}^0 K\bar{K}$: detecting and discriminating New Physics in B_s^0–$\overline{B}_s^0$ mixing*, Phys. Rev. **D85** (2012) 114015, arXiv:1108.5769.

[268] J. Charles *et al.*, *$B^0(t) \to$ time-dependent Dalitz plots, CP violating angles 2β, $2\beta+\gamma$, and discrete ambiguities*, Phys. Lett. **B425** (1998) 375, arXiv:hep-ph/9801363.

[269] T. Latham and T. Gershon, *A method to measure $\cos(2\beta)$ using time-dependent Dalitz plot analysis of $B^0 \to D_{CP}\pi^+\pi^-$*, J. Phys. G **G36** (2009) 025006, arXiv:0809.0872.

[270] Belle collaboration, Y. Nakahama *et al.*, *Measurement of CP violating asymmetries in $B^0 \to K^+K^-K_S^0$ decays with a time-dependent Dalitz approach*, Phys. Rev. **D82** (2010) 073011, arXiv:1007.3848.

[271] BaBar collaboration, J. Lees *et al.*, *Study of CP violation in Dalitz-plot analyses of $B^0 \to K^+K^-K_{\rm S}^0$, $B^+ \to K^+K^-K^+$, and $B^+ \to K_{\rm S}^0K_{\rm S}^0K^+$*, Phys. Rev. **D85** (2012) 112010, arXiv:1201.5897.

[272] R. Fleischer and R. Knegjens, *Effective Lifetimes of B_s Decays and their Constraints on the B_s^0-$\bar{B}_s^0$ Mixing Parameters*, Eur. Phys. J. **C71** (2011) 1789, arXiv:1109.5115.

[273] A. Dighe, T. Hurth, C. Kim, and T. Yoshikawa, *Measurement of the lifetime difference of B^0 mesons: Possible and worthwhile?*, Nucl. Phys. **B624** (2002) 377, arXiv:hep-ph/0109088.

[274] V. A. Kostelecky and R. J. Van Kooten, *Bounding CPT violation in the neutral B system*, Phys. Rev. **D54** (1996) 5585, arXiv:hep-ph/9607449.

[275] B. Kayser, *Cascade mixing and the CP violating angle β*, arXiv:hep-ph/9709382, Proceedings of the Moriond Electroweak 1997.

[276] D.-S. Du and Z.-T. Wei, *Test of CPT symmetry in cascade decays*, Eur. Phys. J. **C14** (2000) 479, arXiv:hep-ph/9904403.

[277] M. Gronau and J. L. Rosner, *Triple product asymmetries in K, $D(s)$ and $B(s)$ decays*, Phys. Rev. **D84** (2011) 096013, arXiv:1107.1232.

[278] M. Beneke, *Corrections to $\sin(2\beta)$ from CP asymmetries in $B^0 \to (\pi^0, \rho^0, \eta, \eta', \omega, \phi)K^0_S$ decays*, Phys. Lett. **B620** (2005) 143, arXiv:hep-ph/0505075.

[279] H.-Y. Cheng, C.-K. Chua, and A. Soni, *Effects of final-state interactions on mixing-induced CP violation in penguin-dominated B decays*, Phys. Rev. **D72** (2005) 014006, arXiv:hep-ph/0502235.

[280] S. Descotes-Genon, J. Matias, and J. Virto, *Exploring $B_{d,s} \to KK$ decays through flavour symmetries and QCD-factorisation*, Phys. Rev. Lett. **97** (2006) 061801, arXiv:hep-ph/0603239.

[281] S. Descotes-Genon, J. Matias, and J. Virto, *Penguin-mediated $B_{d,s} \to VV$ decays and the B^0_s–$\overline{B}^0_s$ mixing angle*, Phys. Rev. **D76** (2007) 074005, arXiv:0705.0477.

[282] CDF collaboration, T. Aaltonen *et al.*, *Measurement of Polarization and Search for CP-Violation in $B^0_s \to \phi\phi$ Decays*, Phys. Rev. Lett. **107** (2011) 261802, arXiv:1107.4999.

[283] M. Bartsch, G. Buchalla, and C. Kraus, *$B \to V_L V_L$ Decays at Next-to-Leading Order in QCD*, arXiv:0810.0249.

[284] R. Fleischer, *Extracting CKM phases from angular distributions of $B_{d,s}$ decays into admixtures of CP eigenstates*, Phys. Rev. **D60** (1999) 073008, arXiv:hep-ph/9903540.

[285] A. Datta and D. London, *Triple-product correlations in $B \to V_1 V_2$ decays and new physics*, Int. J. Mod. Phys. **A19** (2004) 2505, arXiv:hep-ph/0303159.

[286] C. Aubin, C. D. Lin, and A. Soni, *Possible lattice approach to $B \to D\pi(K)$ matrix elements*, Phys. Lett. **B710** (2012) 164, arXiv:1111.4686.

[287] M. Gronau and D. London, *How to determine all the angles of the unitarity triangle from $B^0 \to DK^0_{\rm S}$ and $B^0_s \to D\phi$*, Phys. Lett. **B253** (1991) 483.

[288] M. Gronau and D. Wyler, *On determining a weak phase from CP asymmetries in charged B decays*, Phys. Lett. **B265** (1991) 172.

[289] D. Atwood, I. Dunietz, and A. Soni, *Enhanced CP violation with $B \to KD^0$ ($\overline{D}^0$) modes and extraction of the CKM angle γ*, Phys. Rev. Lett. **78** (1997) 3257, arXiv:hep-ph/9612433.

[290] D. Atwood, I. Dunietz, and A. Soni, *Improved methods for observing CP violation in $B^\pm \to KD$ and measuring the CKM phase γ*, Phys. Rev. **D63** (2001) 036005, arXiv:hep-ph/0008090.

[291] A. Giri, Y. Grossman, A. Soffer, and J. Zupan, *Determining γ using $B^{\pm} \to DK^{\pm}$ with multibody D decays*, Phys. Rev. **D68** (2003) 054018, arXiv:hep-ph/0303187.

[292] Y. Grossman, Z. Ligeti, and A. Soffer, *Measuring gamma in $B^{\pm} \to K^{\pm}(KK^*)_D$ decays*, Phys. Rev. **D67** (2003) 071301, arXiv:hep-ph/0210433.

[293] A. Bondar and T. Gershon, *On ϕ_3 measurements using $B^- \to D^*K^-$ decays*, Phys. Rev. **D70** (2004) 091503, arXiv:hep-ph/0409281.

[294] M. Gronau, *Improving bounds on gamma in $B^{\pm} \to DK^{\pm}$ and $B^{\pm,0} \to DX_s^{\pm,0}$*, Phys. Lett. **B557** (2003) 198, arXiv:hep-ph/0211282.

[295] CLEO collaboration, D. M. Asner *et al.*, *Determination of the $D^0 \to K^+\pi^-$ Relative Strong Phase Using Quantum-Correlated Measurements in $e^+e^- \to D^0D^0$ bar at CLEO*, Phys. Rev. **D78** (2008) 012001, arXiv:0802.2268.

[296] Belle collaboration, Y. Horii *et al.*, *Evidence for the Suppressed Decay $B^- \to DK^-$, $D \to K^+\pi^-$*, Phys. Rev. Lett. **106** (2011) 231803, arXiv:1103.5951.

[297] BaBar collaboration, P. del Amo Sanchez *et al.*, *Search for $b \to u$ transitions in $B^- \to DK^-$ and D^*K^- Decays*, Phys. Rev. **D82** (2010) 072006, arXiv:1006.4241.

[298] CDF collaboration, T. Aaltonen *et al.*, *Measurements of branching fraction ratios and CP-asymmetries in suppressed $B^- \to D(\to K^+\pi^-)K^-$ and $B^- \to D(\to K^+\pi^-)\pi^-$ decays*, Phys. Rev. **D84** (2011) 091504, arXiv:1108.5765.

[299] BaBar collaboration, B. Aubert *et al.*, *Measurement of γ in $B^{\mp} \to D^{(*)}K^{\mp}$ decays with a Dalitz analysis of $D \to K^0_S\pi^-\pi^+$*, Phys. Rev. Lett. **95** (2005) 121802, arXiv:hep-ex/0504039.

[300] A. Bondar and A. Poluektov, *Feasibility study of model-independent approach to phi(3) measurement using Dalitz plot analysis*, Eur. Phys. J. **C47** (2006) 347, arXiv:hep-ph/0510246.

[301] A. Bondar and A. Poluektov, *The Use of quantum-correlated D0 decays for phi3 measurement*, Eur. Phys. J. **C55** (2008) 51, arXiv:0801.0840.

[302] CLEO collaboration, J. Libby *et al.*, *Model-independent determination of the strong-phase difference between D^0 and $\bar{D}^0 \to K^0_{S,L}h^+h^-$ ($h = \pi, K$) and its impact on the measurement of the CKM angle γ/ϕ_3*, Phys. Rev. **D82** (2010) 112006, arXiv:1010.2817.

[303] I. Dunietz and R. G. Sachs, *Asymmetry between inclusive charmed and anticharmed mopdes in B^0, $\bar{B}^0$ decay as a measure of CP violation*, Phys. Rev. **D37** (1988) 3186.

[304] R. Aleksan, I. Dunietz, and B. Kayser, *Determining the CP violating phase γ*, Z. Phys. **C54** (1992) 653.

[305] R. Fleischer, *New strategies to obtain insights into CP violation through $B_s^0 \to D_s^\pm K^\mp$, $D_s^{*\pm} K^\mp$, ... and $B^0 \to D^\pm \pi^\mp$, $D_s^\pm \pi^\mp$, ... decays*, Nucl. Phys. **B671** (2003) 459, arXiv:hep-ph/0304027.

[306] BaBar collaboration, B. Aubert *et al.*, *Measurement of time-dependent CP-violating asymmetries and constraints on* $\sin(2\beta+\gamma)$ *with partial reconstruction of* $B \to D^{*\mp}\pi^\pm$ *decays*, Phys. Rev. **D71** (2005) 112003, arXiv:hep-ex/0504035.

[307] BaBar collaboration, B. Aubert *et al.*, *Measurement of time-dependent CP asymmetries in* $B^0 \to D^{(*)\pm}\pi^\mp$ *and* $B^0 \to D^\pm \rho^\mp$ *decays*, Phys. Rev. **D73** (2006) 111101, arXiv:hep-ex/0602049.

[308] Belle collaboration, F. Ronga *et al.*, *Measurements of CP violation in* $B^0 \to D^{*-}\pi^+$ *and* $B^0 \to D^-\pi^+$ *decays*, Phys. Rev. **D73** (2006) 092003, arXiv:hep-ex/0604013.

[309] Belle collaboration, S. Bahinipati *et al.*, *Measurements of time-dependent CP asymmetries in* $B \to D^{*\mp}\pi^\pm$ *decays using a partial reconstruction technique*, Phys. Rev. **D84** (2011) 021101, arXiv:1102.0888.

[310] S. Nandi and U. Nierste, *Resolving the sign ambiguity in* $\Delta\Gamma_s$ *with* $B_s \to D_s K$, Phys. Rev. **D77** (2008) 054010, arXiv:0801.0143.

[311] LHCb collaboration, R. Aaij *et al.*, *Measurements of the branching fractions of the decays* $B_s^0 \to D_s^\mp K^\pm$ *and* $B_s^0 \to D_s^- \pi^+$, JHEP **1206** (2012) 115, arXiv:1204.1237.

[312] Y. Grossman, A. Soffer, and J. Zupan, *The effect of* D^0–$\overline{D}^0$ *mixing on the measurement of* γ *in* $B \to DK$ *decays*, Phys. Rev. **D72** (2005) 031501, arXiv:hep-ph/0505270.

[313] A. Bondar, A. Poluektov, and V. Vorobiev, *Charm mixing in the model-independent analysis of correlated* D^0–$\overline{D}^0$ *decays*, Phys. Rev. **D82** (2010) 034033, arXiv:1004.2350.

[314] Y. Grossman, A. L. Kagan, and Z. Ligeti, *Can the CP asymmetries in* $B \to \psi K^0_{\rm S}$ *and* $B \to \psi K^0_{\rm L}$ *differ?*, Phys. Lett. **B538** (2002) 327, arXiv:hep-ph/0204212.

[315] D. Pirjol and J. Zupan, in preparation.

[316] LHCb collaboration, *Measurement of CP observables in* $B^0 \to DK^{*0}$ *with* $D \to K^+K^-$, LHCb-CONF-2012-024.

[317] LHCb collaboration, *Study of the* $B^- \to D^0 K^-\pi^+\pi^-$ *and* $B^- \to D^0\pi^-\pi^+\pi^-$ *decays*, LHCb-CONF-2012-021.

[318] BaBar collaboration, P. del Amo Sanchez *et al.*, *Measurement of CP observables in* $B^\pm \to D_{CP} K^\pm$ *decays and constraints on the CKM angle* γ, Phys. Rev. **D82** (2010) 072004, arXiv:1007.0504.

[319] CDF collaboration, T. Aaltonen *et al.*, *Measurements of branching fraction ratios and CP asymmetries in $B^{\pm} \to D_{CP}K^{\pm}$ decays in hadron collisions*, Phys. Rev. **D81** (2010) 031105, arXiv:0911.0425.

[320] CDF collaboration, T. Aaltonen *et al.*, *First observation of $\bar{B}_s^0 \to D_s^{\pm}K^{\mp}$ and measurement of the ratio of branching fractions $\mathcal{B}(\bar{B}_s^0 \to D_s^{\pm}K^{\mp})/\mathcal{B}(\bar{B}_s^0 \to D_s^{+}\pi^{-})$*, Phys. Rev. Lett. **103** (2009) 191802, arXiv:0809.0080.

[321] Belle collaboration, R. Louvot *et al.*, *Measurement of the Decay $B_s^0 \to D_s^-\pi^+$ and Evidence for $B_s^0 \to D_s^{\pm}K^{\pm}$ in e^+e^- Annihilation at $\sqrt{s}$ = 10.87 GeV*, Phys. Rev. Lett. **102** (2009) 021801, arXiv:0809.2526.

[322] LHCb collaboration, R. Aaij *et al.*, *Determination of f_s/f_d for 7*TeV *pp collisions and a measurement of the branching fraction of the decay $B_d \to D^-K^+$*, Phys. Rev. Lett. **107** (2011) 211801, arXiv:1106.4435.

[323] M. Gronau and D. London, *Isospin analysis of CP asymmetries in B decays*, Phys. Rev. Lett. **65** (1990) 3381.

[324] J. Charles, *Taming the penguin in the $B_d^0(t) \to \pi^+\pi^-$ CP asymmetry: Observables and minimal theoretical input*, Phys. Rev. **D59** (1999) 054007, arXiv:hep-ph/9806468.

[325] UTfit collaboration, M. Bona *et al.*, *Improved determination of the CKM angle α from $B \to \pi\pi$ decays*, Phys. Rev. **D76** (2007) 014015, arXiv:hep-ph/0701204.

[326] R. Fleischer, *New strategies to extract β and γ from $B_d \to \pi^+\pi^-$and$B_s \to K^+K^-$*, Phys. Lett. **B459** (1999) 306, arXiv:hep-ph/9903456.

[327] R. Fleischer, *$B_{s,d} \to \pi\pi, \pi K, KK$: Status and Prospects*, Eur. Phys. J. **C52** (2007) 267, arXiv:0705.1121.

[328] BaBar collaboration, J. Lees, *Measurement of CP asymmetries and branching fractions in charmless two-body B-meson decays to pions and kaons*, arXiv:1206.3525.

[329] Belle collaboration, H. Ishino *et al.*, *Observation of direct CP-violation in $B^0 \to \pi^+\pi^-$ decays and model-independent constraints on ϕ_2*, Phys. Rev. Lett. **98** (2007) 211801, arXiv:hep-ex/0608035.

[330] BaBar collaboration, B. Aubert *et al.*, *Improved Measurements of the Branching Fractions for $B^0 \to \pi^+\pi^-$ and $B^0 \to K^+\pi^-$, and a Search for $B^0 \to K^+K^-$*, Phys. Rev. **D75** (2007) 012008, arXiv:hep-ex/0608003.

[331] Belle collaboration, P. Chang, talk presented at EPS-HEP 2011.

[332] CLEO collaboration, A. Bornheim *et al.*, *Measurements of charmless hadronic two body B meson decays and the ratio $\mathcal{B}(B \to DK)/\mathcal{B}(B \to D\pi)$*, Phys. Rev. **D68** (2003) 052002, arXiv:hep-ex/0302026.

[333] CDF collaboration, T. Aaltonen *et al.*, *Measurements of Direct CP Violating Asymmetries in Charmless Decays of Strange Bottom Mesons and Bottom Baryons*, Phys. Rev. Lett. **106** (2011) 181802, arXiv:1103.5762.

[334] Belle collaboration, K. Abe *et al.*, *Observation of $B^0 \to \pi^0\pi^0$*, Phys. Rev. Lett. **94** (2005) 181803, arXiv:hep-ex/0408101.

[335] BaBar collaboration, B. Aubert *et al.*, *Study of $B^0 \to \pi^0\pi^0$, $B^\pm \to \pi^\pm\pi^0$, and $B^\pm \to K^\pm\pi^0$ decays, and isospin analysis of $B \to \pi\pi$ decays*, Phys. Rev. **D76** (2007) 091102, arXiv:0707.2798.

[336] Belle collaboration, C.-C. Peng *et al.*, *Search for $B^0_s \to hh$ Decays at the $\Upsilon(5S)$ resonance*, Phys. Rev. **D82** (2010) 072007, arXiv:1006.5115.

[337] M. Gronau, D. Pirjol, and T.-M. Yan, *Model independent electroweak penguins in B decays to two pseudoscalars*, Phys. Rev. **D60** (1999) 034021, arXiv:hep-ph/9810482.

[338] J. Zupan, *Penguin pollution estimates relevant for ϕ_2/α extraction*, Nucl. Phys. Proc. Suppl. **170** (2007) 33, arXiv:hep-ph/0701004.

[339] S. Gardner, *Towards a precision determination of α in $B \to \pi\pi$ decays*, Phys. Rev. **D72** (2005) 034015, arXiv:hep-ph/0505071.

[340] F. Botella, D. London, and J. P. Silva, *Looking for $\Delta I = 5/2$ amplitude components in $B \to \pi\pi$ and $B \to \rho\rho$ experiments*, Phys. Rev. **D73** (2006) 071501, arXiv:hep-ph/0602060.

[341] G. Duplancic and B. Melic, *B, $B_s \to K$ form factors: an update of light-cone sum rule results*, Phys. Rev. **D78** (2008) 054015, arXiv:0805.4170.

[342] B. Bhattacharya, A. Datta, M. Imbeault, and D. London, *Measuring β_s with $B_s \to K^{0(*)}\bar{K}^{0(*)}$ – a reappraisal*, arXiv:1203.3435.

[343] LHCb collaboration, R. Aaij *et al.*, *First observation of the decays $\overline{B}^0 \to D^+K^-\pi^+\pi^-$ and $B^- \to D\ K^-\pi^+\pi^-$*, Phys. Rev. Lett. **108** (2012) 161801, arXiv:1201.4402.

[344] T. Gershon, *On the measurement of the Unitarity Triangle angle γ from $B^0 \to DK^{*0}$ decays*, Phys. Rev. **D79** (2009) 051301, arXiv:0810.2706.

[345] T. Gershon and M. Williams, *Prospects for the measurement of the Unitarity Triangle angle γ from $B^0 \to DK^+\pi^-$ decays*, Phys. Rev. **D80** (2009) 092002, arXiv:0909.1495.

[346] T. Gershon and A. Poluektov, *Double Dalitz plot analysis of the decay $B^0 \to DK^+\pi^-$, $D \to K^0_S\pi^+\pi^-$*, Phys. Rev. **D81** (2010) 014025, arXiv:0910.5437.

[347] M. Gronau, Y. Grossman, Z. Surujon, and J. Zupan, *Enhanced effects on extracting gamma from untagged B^0 and B_s^0 decays*, Phys. Lett. **B649** (2007) 61, arXiv:hep-ph/0702011.

[348] S. Ricciardi, *Measuring the CKM angle γ at LHCb using untagged $B_s^0 \to D\phi$ decays*, LHCb-PUB-2010-005.

[349] LHCb collaboration, R. Aaij *et al.*, *Observation of the decay $B^0 \to \bar{D}^0 K^+ K^-$ and evidence of $B_s^0 \to \bar{D}^0 K^+ K^-$*, arXiv:1207.5991.

[350] M. Masetti, *CP violation in B_c^+ decays*, Phys. Lett. **B286** (1992) 160.

[351] R. Fleischer and D. Wyler, *Exploring CP violation with B_c^+ decays*, Phys. Rev. **D62** (2000) 057503, arXiv:hep-ph/0004010.

[352] A. Giri, R. Mohanta, and M. Khanna, *Determination of the angle γ from nonleptonic $B_c^+ \to D_s^+ D^0$ decays*, Phys. Rev. **D65** (2002) 034016, arXiv:hep-ph/0104009.

[353] A. Giri, B. Mawlong, and R. Mohanta, *Determining the CKM angle γ with B_c^+ decays*, Phys. Rev. **D75** (2007) 097304, arXiv:hep-ph/0611212.

[354] A. Giri, R. Mohanta, and M. Khanna, *Possibility of extracting the weak phase γ from $\Lambda_b \to \Lambda D^0$ decays*, Phys. Rev. **D65** (2002) 073029, arXiv:hep-ph/0112220.

[355] LHCb collaboration, *Studies of beauty baryons decaying to $D^0 p\pi^-$ and $D^0 pK^-$*, LHCb-CONF-2011-036.

[356] Y. Nir and N. Seiberg, *Should squarks be degenerate?*, Phys. Lett. **B309** (1993) 337, arXiv:hep-ph/9304307.

[357] M. Leurer, Y. Nir, and N. Seiberg, *Mass matrix models: the sequel*, Nucl. Phys. **B420** (1994) 468, arXiv:hep-ph/9310320.

[358] A. F. Falk *et al.*, *The D^0-$\overline{D}^0$ mass difference from a dispersion relation*, Phys. Rev. **D69** (2004) 114021, arXiv:hep-ph/0402204.

[359] E. Golowich, J. Hewett, S. Pakvasa, and A. A. Petrov, *Implications of D^0-$\overline{D}^0$ Mixing for New Physics*, Phys. Rev. **D76** (2007) 095009, arXiv:0705.3650.

[360] BaBar collaboration, B. Aubert *et al.*, *Evidence for D^0-$\overline{D}^0$ Mixing*, Phys. Rev. Lett. **98** (2007) 211802, arXiv:hep-ex/0703020.

[361] Belle collaboration, M. Staric *et al.*, *Evidence for D^0-$\overline{D}^0$ Mixing*, Phys. Rev. Lett. **98** (2007) 211803, arXiv:hep-ex/0703036.

[362] I. I. Bigi and H. Yamamoto, *Interference between Cabibbo allowed and doubly forbidden transitions in $D \to K^0_{\rm S}, K^0_{\rm L} + \pi$s decays*, Phys. Lett. **B349** (1995) 363, arXiv:hep-ph/9502238.

[363] M. Gersabeck *et al.*, *On the interplay of direct and indirect CP violation in the charm sector*, J. Phys. G **G39** (2012) 045005, arXiv:1111.6515.

[364] N. Neri, *D^0-$\overline{D}^0$ mixing CP violation results and HFAG averages*, in *5th International Workshop on Charm Physics*, (Honolulu, Hawaii, US), May, 2012.

[365] Belle collaboration, T. Peng, *D^0–$\overline{D}^0$ mixing results from Belle*, , talk given at ICHEP 2012, Melbourne, July 5th 2012.

[366] Belle collaboration, L. M. Zhang *et al.*, *Measurement of D^0-$\overline{D}^0$ mixing in $D^0 \to K^0_S\pi^+\pi^-$ decays*, Phys. Rev. Lett. **99** (2007) 131803, arXiv:0704.1000.

[367] BaBar collaboration, P. del Amo Sanchez *et al.*, *Measurement of D^0-$\overline{D}^0$ mixing parameters using $D^0 \to K^0_S\pi^+\pi^-$ and $D^0 \to K^0_S K^+K^-$ decays*, Phys. Rev. Lett. **105** (2010) 081803, arXiv:1004.5053.

[368] Y. Grossman, A. L. Kagan, and Y. Nir, *New physics and CP violation in singly Cabibbo suppressed D decays*, Phys. Rev. **D75** (2007) 036008, arXiv:hep-ph/0609178.

[369] BaBar collaboration, B. Aubert *et al.*, *Search for CP violation in the decays $D^0 \to K^-K^+$ and $D^0 \to \pi^-\pi^+$*, Phys. Rev. Lett. **100** (2008) 061803, arXiv:0709.2715.

[370] Belle collaboration, M. Staric *et al.*, *Measurement of CP asymmetry in Cabibbo suppressed D^0 decays*, Phys. Lett. **B670** (2008) 190, arXiv:0807.0148.

[371] CDF collaboration, T. Aaltonen *et al.*, *Measurement of CP–violating asymmetries in $D^0 \to \pi^+\pi^-$ and $D^0 \to K^+K^-$ decays at CDF*, Phys. Rev. **D85** (2012) 012009, arXiv:1111.5023.

[372] CDF collaboration, *Measurement of the difference in CP violating asymmetry between $D^0 \to KK$ and $D^0 \to \pi\pi$*, CDF Public Note 10784, Feb, 2012.

[373] Belle collaboration, B. R. Ko, *Direct CP violation in charm at Belle*, , talk given at ICHEP 2012, Melbourne, July 5th 2012.

[374] A. L. Kagan and M. D. Sokoloff, *On Indirect CP Violation and Implications for D^0-$\overline{D}^0$ and B^0_s-$\overline{B}^0_s$ mixing*, Phys. Rev. **D80** (2009) 076008, arXiv:0907.3917.

[375] LHCb collaboration, *Time integrated ratio of wrong-sign to right-sign $D^0 \to K\pi$ decays in 2010 data at LHCb*, LHCb-CONF-2011-029.

[376] LHCb collaboration, R. Aaij *et al.*, *Search for CP violation in $D^+ \to K^-K^+\pi^+$ decays*, Phys. Rev. **D84** (2011) 112008, arXiv:1110.3970.

[377] LHCb collaboration, R. Aaij *et al.*, *Measurement of the D^+_s–D^-_s production asymmetry in 7 TeV pp collisions*, Phys. Lett. **713** (2012) 186, arXiv:1205.0897.

[378] I. Bediaga *et al.*, *On a CP anisotropy measurement in the Dalitz plot*, Phys. Rev. **D80** (2009) 096006, arXiv:0905.4233.

[379] BABAR collaboration, P. del Amo Sanchez *et al.*, *Search for CP violation using T-odd correlations in $D^0 \to K^+K^-\pi^+\pi^-$ decays*, Phys. Rev. **D81** (2010) 111103, arXiv:1003.3397.

[380] M. Williams, *Observing CP Violation in Many-Body Decays*, Phys. Rev. **D84** (2011) 054015, arXiv:1105.5338.

[381] LHCb collaboration, *Search for CP violation in $D^0 \to \pi^-\pi^+\pi^+\pi^-$ decays*, LHCb-CONF-2012-019.

[382] E. Golowich and A. A. Petrov, *Short distance analysis of D^0-$\overline{D}^0$ mixing*, Phys. Lett. **B625** (2005) 53, arXiv:hep-ph/0506185.

[383] M. Bobrowski, A. Lenz, J. Riedl, and J. Rohrwild, *How Large Can the SM Contribution to CP Violation in D^0-$\overline{D}^0$ Mixing Be?*, JHEP **1003** (2010) 009, arXiv:1002.4794.

[384] H. Georgi, *D-$\overline{D}$ mixing in heavy quark effective field theory*, Phys. Lett. **B297** (1992) 353, arXiv:hep-ph/9209291.

[385] T. Ohl, G. Ricciardi, and E. H. Simmons, *D-$\overline{D}$ mixing in heavy quark effective field theory: the sequel*, Nucl. Phys. **B403** (1993) 605, arXiv:hep-ph/9301212.

[386] I. I. Bigi and N. G. Uraltsev, *D^0-$\overline{D}^0$ oscillations as a probe of quark hadron duality*, Nucl. Phys. **B592** (2001) 92, arXiv:hep-ph/0005089.

[387] E. Golowich, S. Pakvasa, and A. A. Petrov, *New Physics contributions to the lifetime difference in D^0-$\overline{D}^0$ mixing*, Phys. Rev. Lett. **98** (2007) 181801, arXiv:hep-ph/0610039.

[388] S. Bergmann *et al.*, *Lessons from CLEO and FOCUS measurements of D^0-$\overline{D}^0$ mixing parameters*, Phys. Lett. **B486** (2000) 418, arXiv:hep-ph/0005181.

[389] O. Gedalia, Y. Grossman, Y. Nir, and G. Perez, *Lessons from Recent Measurements of D^0-$\overline{D}^0$ Mixing*, Phys. Rev. **D80** (2009) 055024, arXiv:0906.1879.

[390] G. Isidori, Y. Nir, and G. Perez, *Flavor physics constraints for physics Beyond the Standard Model*, Ann. Rev. Nucl. Part. Sci. **60** (2010) 355, arXiv:1002.0900.

[391] A. F. Falk, Y. Grossman, Z. Ligeti, and A. A. Petrov, *SU(3) breaking and D^0-$\overline{D}^0$ mixing*, Phys. Rev. **D65** (2002) 054034, arXiv:hep-ph/0110317.

[392] J. F. Donoghue, E. Golowich, B. R. Holstein, and J. Trampetic, *Dispersive Effects in D^0-$\overline{D}^0$ Mixing*, Phys. Rev. **D33** (1986) 179.

[393] L. Wolfenstein, *D^0-$\overline{D}^0$ Mixing*, Phys. Lett. **B164** (1985) 170.

[394] P. Colangelo, G. Nardulli, and N. Paver, *On D^0-$\overline{D}^0$ Mixing in the Standard Model*, Phys. Lett. **B242** (1990) 71.

[395] T. A. Kaeding, *D meson mixing in broken SU(3)*, Phys. Lett. **B357** (1995) 151, arXiv:hep-ph/9505393.

[396] A. Anselm and Y. I. Azimov, *CP violating effects in e^+e^- annihilation*, Phys. Lett. **B85** (1979) 72.

[397] H.-Y. Cheng and C.-W. Chiang, *Long-distance contributions to D^0-$\overline{D}^0$ mixing parameters*, Phys. Rev. **D81** (2010) 114020, arXiv:1005.1106.

[398] Y. Grossman, Y. Nir, and G. Perez, *Testing mew indirect CP violation*, Phys. Rev. Lett. **103** (2009) 071602, arXiv:0904.0305.

[399] A. L. Kagan, G. Perez, T. Volansky, and J. Zupan, *General Minimal Flavor Violation*, Phys. Rev. **D80** (2009) 076002, arXiv:0903.1794.

[400] K. Blum, Y. Grossman, Y. Nir, and G. Perez, *Combining K^0-$\overline{K}^0$ mixing and D^0-$\overline{D}^0$ mixing to constrain the flavor structure of new physics*, Phys. Rev. Lett. **102** (2009) 211802, arXiv:0903.2118.

[401] O. Gedalia, J. F. Kamenik, Z. Ligeti, and G. Perez, *On the Universality of CP Violation in $\Delta F = 1$ Processes*, arXiv:1202.5038.

[402] Y. Nir and G. Raz, *Quark squark alignment revisited*, Phys. Rev. **D66** (2002) 035007, arXiv:hep-ph/0206064.

[403] BaBar collaboration, B. Aubert *et al.*, *Measurement of D^0-$\overline{D}^0$ mixing using the ratio of lifetimes for the decays $D^0 \to K^-\pi^+$, K^-K^+, and $\pi^-\pi^+$*, Phys. Rev. **D78** (2008) 011105, arXiv:0712.2249.

[404] M. Golden and B. Grinstein, *Enhanced CP Violations in Hadronic Charm Decays*, Phys. Lett. **B222** (1989) 501.

[405] D. Pirtskhalava and P. Uttayarat, *CP Violation and flavor SU(3) breaking in D-meson decays*, Phys. Lett. **B712** (2012) 81, arXiv:1112.5451.

[406] B. Bhattacharya, M. Gronau, and J. L. Rosner, *CP asymmetries in singly-Cabibbo-suppressed D decays to two pseudoscalar mesons*, Phys. Rev. **D85** (2012) 054014, arXiv:1201.2351.

[407] J. Brod, Y. Grossman, A. L. Kagan, and J. Zupan, *A consistent picture for large penguins in $D \to \pi^+\pi^-$, K^+K^-*, arXiv:1203.6659.

[408] H.-Y. Cheng and C.-W. Chiang, *SU(3) symmetry breaking and CP violation in D $\to$ P P decays*, arXiv:1205.0580.

[409] F. Buccella *et al.*, *Nonleptonic weak decays of charmed mesons*, Phys. Rev. **D51** (1995) 3478, arXiv:hep-ph/9411286.

[410] H.-n. Li, C.-D. Lu, and F.-S. Yu, *Branching ratios and direct CP asymmetries in $D \to PP$ decays*, arXiv:1203.3120.

[411] E. Franco, S. Mishima, and L. Silvestrini, *The Standard Model confronts CP violation in $D^0 \to \pi^+\pi^-$ and $D^0 \to K^+K^-$*, JHEP **1205** (2012) 140, arXiv:1203.3131.

[412] L. Wolfenstein, *CP Violation in D^0- $\overline{D}^0$ Mixing*, Phys. Rev. Lett. **75** (1995) 2460.

[413] J. Brod, A. L. Kagan, and J. Zupan, *On the size of direct CP violation in singly Cabibbo-suppressed D decays*, arXiv:1111.5000.

[414] O. Gedalia, L. Mannelli, and G. Perez, *Covariant Description of Flavor Violation at the LHC*, Phys. Lett. **B693** (2010) 301, arXiv:1002.0778.

[415] O. Gedalia, L. Mannelli, and G. Perez, *Covariant Description of Flavor Conversion at the LHC Era*, JHEP **1010** (2010) 046, arXiv:1003.3869.

[416] G. F. Giudice, G. Isidori, and P. Paradisi, *Direct CP violation in charm and flavor mixing beyond the SM*, JHEP **1204** (2012) 060, arXiv:1201.6204.

[417] G. Hiller, Y. Hochberg, and Y. Nir, *Supersymmetric $\Delta\mathcal{A}_{CP}$*, Phys. Rev. **D85** (2012) 116008, arXiv:1204.1046.

[418] L. Randall and R. Sundrum, *A Large mass hierarchy from a small extra dimension*, Phys. Rev. Lett. **83** (1999) 3370, arXiv:hep-ph/9905221.

[419] W. D. Goldberger and M. B. Wise, *Modulus stabilization with bulk fields*, Phys. Rev. Lett. **83** (1999) 4922, arXiv:hep-ph/9907447.

[420] S. J. Huber and Q. Shafi, *Fermion masses, mixings and proton decay in a Randall-Sundrum model*, Phys. Lett. **B498** (2001) 256, arXiv:hep-ph/0010195.

[421] T. Gherghetta and A. Pomarol, *Bulk fields and supersymmetry in a slice of AdS*, Nucl. Phys. **B586** (2000) 141, arXiv:hep-ph/0003129.

[422] C. Delaunay, J. F. Kamenik, G. Perez, and L. Randall, *Charming CP Violation and Dipole Operators from RS Flavor Anarchy*, arXiv:1207.0474.

[423] K. Agashe, A. Azatov, and L. Zhu, *Flavor Violation Tests of Warped/Composite SM in the Two-Site Approach*, Phys. Rev. **D79** (2009) 056006, arXiv:0810.1016.

[424] C. Csaki, G. Perez, Z. Surujon, and A. Weiler, *Flavor Alignment via Shining in RS*, Phys. Rev. **D81** (2010) 075025, arXiv:0907.0474.

[425] B. Keren-Zur *et al.*, *On Partial Compositeness and the CP asymmetry in charm decays*, arXiv:1205.5803.

[426] S. Nandi and A. Soni, *Constraining the mixing matrix for Standard Model with four generations: time dependent and semi-leptonic CP asymmetries in B^0_d, B^0_s and D^0*, Phys. Rev. **D83** (2011) 114510, arXiv:1011.6091.

[427] CDF collaboration, *Study of the top quark production asymmetry and its mass and rapidity dependence in the full run II Tevatron dataset*, CDF Public Note 10807, March, 2012.

[428] K. Blum, Y. Hochberg, and Y. Nir, *Scalar-mediated $t\bar{t}$ forward-backward asymmetry*, JHEP **1110** (2011) 124, arXiv:1107.4350.

[429] C. Greub, T. Hurth, M. Misiak, and D. Wyler, *The $c \to u\gamma$ contribution to weak radiative charm decay*, Phys. Lett. **B382** (1996) 415, arXiv:hep-ph/9603417.

[430] Y. Grossman, A. L. Kagan, and J. Zupan, *Testing for new physics in singly Cabibbo suppressed D decays*, arXiv:1204.3557.

[431] Y. Grossman and Y. Nir, *CP violation in $\tau \to \nu\pi K^0_S$ and $D \to \pi K^0_S$: the importance of K^0_S-K^0_L interference*, JHEP **1204** (2012) 002, arXiv:1110.3790.

[432] A. F. Falk, Z. Ligeti, Y. Nir, and H. Quinn, *Comment on extracting α from $B \to \rho\rho$*, Phys. Rev. **D69** (2004) 011502, arXiv:hep-ph/0310242.

[433] G. Colangelo *et al.*, *Review of lattice results concerning low energy particle physics*, Eur. Phys. J. **C71** (2011) 1695, arXiv:1011.4408.

[434] M. Luscher, *Volume Dependence of the Energy Spectrum in Massive Quantum Field Theories. 2. Scattering States*, Commun. Math. Phys. **105** (1986) 153.

[435] M. Luscher, *Two particle states on a torus and their relation to the scattering matrix*, Nucl. Phys. **B354** (1991) 531.

[436] L. Lellouch and M. Luscher, *Weak transition matrix elements from finite volume correlation functions*, Commun. Math. Phys. **219** (2001) 31, arXiv:hep-lat/0003023.

[437] T. Blum *et al.*, *The $K \to (\pi\pi)_{I=2}$ Decay Amplitude from Lattice QCD*, Phys. Rev. Lett. **108** (2012) 141601, arXiv:1111.1699.

[438] T. Blum *et al.*, *K to $\pi\pi$ Decay amplitudes from Lattice QCD*, Phys. Rev. **D84** (2011) 114503, arXiv:1106.2714.

[439] M. T. Hansen and S. R. Sharpe, *Multiple-channel generalization of Lellouch-Luscher formula*, arXiv:1204.0826.

[440] RBC and UKQCD collaborations, N. H. Christ, *Computing the long-distance contribution to second order weak amplitudes*, PoS **LATTICE2010** (2010) 300.

[441] J. Yu, *Long distance contribution to K_L^0-K_S^0 mass difference*, PoS **LATTICE2011** (2011) 297, arXiv:1111.6953.

[442] CDF collaboration, *Search for Quark Substructure in the angular distribution of dijets produced in p $\bar{p}$ collisions at $\sqrt{s} = 1.96\,\text{TeV}$*, CDF Public Note 9609, Nov, 2008.

[443] D0 collaboration, V. Abazov *et al.*, *Measurement of dijet angular distributions at $\sqrt{s} = 1.96\,\text{TeV}$ and searches for quark compositeness and extra spatial dimensions*, Phys. Rev. Lett. **103** (2009) 191803, arXiv:0906.4819.

[444] L. Da Rold, C. Delaunay, C. Grojean, and G. Perez, *Up Asymmetries From Exhilarated Composite Flavor Structures*, arXiv:1208.1499.

[445] ATLAS collaboration, *Search for New Physics in Dijet Mass and Angular Distributions using $4.8\,fb^{-1}$ of pp Collisions at $\sqrt{s} = 7\,\text{TeV}$ collected by the ATLAS Detector*, Tech. Rep. ATLAS-CONF-2012-038, Mar, 2012.

[446] CMS collaboration, S. Chatrchyan *et al.*, *Search for quark compositeness in dijet angular distributions from p p collisions at $\sqrt{s} = 7\,\text{TeV}$*, JHEP **1205** (2012) 055, arXiv:1202.5535.

[447] Belle collaboration, L. M. Zhang *et al.*, *Improved constraints on D^0-$\overline{D}^0$ mixing in $D^0 \to K^+\pi^-$ decays at Belle*, Phys. Rev. Lett. **96** (2006) 151801, arXiv:hep-ex/0601029.

[448] BaBar collaboration, B. Aubert *et al.*, *Search for D^0-$\overline{D}^0$ mixing using semileptonic decay modes*, Phys. Rev. **D70** (2004) 091102, arXiv:hep-ex/0408066.

[449] BaBar collaboration, B. Aubert *et al.*, *Search for D^0-$\overline{D}^0$ mixing using doubly flavor tagged semileptonic decay modes*, Phys. Rev. **D76** (2007) 014018, arXiv:0705.0704.

[450] BaBar collaboration, B. Aubert *et al.*, *Measurement of D^0-$\overline{D}^0$ mixing from a time-dependent amplitude analysis of $D^0 \to K^+\pi^-\pi^0$ decays*, Phys. Rev. Lett. **103** (2009) 211801, arXiv:0807.4544.

[451] V. Kartvelishvili, A. Likhoded, and S. Slabospitsky, *D meson and ψ meson production in hadronic interactions*, Sov. J. Nucl. Phys. **28** (1978) 678.

[452] R. Baier and R. Ruckl, *Hadronic production of J/ψ and Υ: transverse momentum distribution*, Phys. Lett. **B102** (1981) 364.

[453] CDF collaboration, F. Abe *et al.*, *Inclusive J/ψ, $\psi(2S)$ and b quark production in $\bar{p}p$ collisions at $\sqrt{s} = 1.8$ TeV*, Phys. Rev. Lett. **69** (1992) 3704.

[454] E. Braaten and S. Fleming, *Color octet fragmentation and the ψ'-surplus at the Tevatron*, Phys. Rev. Lett **74** (1995) 3327, arXiv:hep-ph/9411365.

[455] J. M. Campbell, F. Maltoni, and F. Tramontano, *QCD corrections to J/ψ and Υ production at hadron colliders*, Phys. Rev. Lett. **98** (2007) 252002, arXiv:hep-ph/0703113.

[456] B. Gong and J. Wang, *Next-to-leading-order QCD corrections to J/ψ polarization at Tevatron*, Phys. Rev. Lett. **100** (2008) 232001, arXiv:0802.3727.

[457] P. Artoisenet *et al.*, Υ *Production at Fermilab Tevatron and LHC Energies*, Phys. Rev. Lett. **101** (2008) 152001, arXiv:0806.3282.

[458] J. Lansberg, *On the mechanisms of heavy-quarkonium hadroproduction*, Eur. Phys. J. **C61** (2009) 693, arXiv:0811.4005.

[459] N. Brambilla *et al.*, *Heavy quarkonium: progress, puzzles, and opportunities*, Eur. Phys. J. **C71** (2011) 1534, arXiv:1010.5827.

[460] LHCb collaboration, R. Aaij *et al.*, *Measurement of J/ψ production in pp collisions at $\sqrt{s} = 7$ TeV*, Eur. Phys. J. **C71** (2011) 1645, arXiv:1103.0423.

[461] LHCb collaboration, R. Aaij *et al.*, *Measurement of the cross-section ratio $\sigma(\chi_{c2})/\sigma(\chi_{c1})$ for prompt χ_c production at $\sqrt{s} = 7$ TeV*, arXiv:1202.1080.

[462] LHCb collaboration, R. Aaij *et al.*, *Measurement of the ratio of prompt χ_c to J/ψ production in pp collisions at $\sqrt{s} = 7$ TeV*, arXiv:1204.1462.

[463] LHCb collaboration, R. Aaij *et al.*, *Measurement of Υ production in pp collisions at $\sqrt{s} = 7$ TeV*, Eur. Phys. J. **C72** (2012) 2025, arXiv:1202.6579.

[464] LHCb collaboration, R. Aaij *et al.*, *Measurement of $\psi(2S)$ meson production in pp collisions at $\sqrt{s} = 7$ TeV*, arXiv:1204.1258.

[465] S. J. Brodsky and J.-P. Lansberg, *Heavy-Quarkonium Production in High Energy Proton-Proton Collisions at RHIC*, Phys. Rev. **D81** (2010) 051502, arXiv:0908.0754.

[466] C. H. Kom, A. Kulesza, and W. J. Stirling, *Pair production of J/ψ as a probe of double parton scattering at LHCb*, Phys. Rev. Lett. **107** (2011) 082002, arXiv:1105.4186.

[467] S. P. Baranov, A. M. Snigirev, and N. P. Zotov, *Double heavy meson production through double parton scattering in hadronic collisions*, Phys. Lett. **B705** (2011) 116, arXiv:1105.6276.

[468] A. Novoselov, *Double parton scattering as a source of quarkonia pairs in LHCb*, arXiv:1106.2184.

[469] S. Brodsky, P. Hoyer, C. Peterson, and N. Sakai, *The intrinsic charm of the proton*, Phys. Lett. **B93** (1980) 451.

[470] V. G. Kartvelishvili and S. M. Esakiya, *On hadron induced production of J/ψ meson pairs*, Yad. Fiz. **38** (1983) 722.

[471] B. Humpert and P. Mery, *$\psi\psi$ production at collider energies*, Z. Phys. **C20** (1983) 83.

[472] A. V. Berezhnoy, A. K. Likhoded, A. V. Luchinsky, and A. A. Novoselov, *Double J/ψ meson Production at LHC and 4c-tetraquark state*, Phys. Rev. **D84** (2011) 094023, arXiv:1101.5881.

[473] M. Luszczak, R. Maciula, and A. Szczurek, *Production of two $c\bar{c}$ pairs in double-parton scattering*, Phys. Rev. **D85** (2011) 094034, arXiv:1111.3255.

[474] CDF collaboration, F. Abe *et al.*, *Double parton scattering in $\bar{p}p$ collisions at $\sqrt{s} =$ 1.8 TeV*, Phys. Rev. **D56** (1997) 3811.

[475] V. V. Braguta, A. K. Likhoded, and A. V. Luchinsky, *Double charmonium production in exclusive bottomonia decays*, Phys. Rev. D **80** (2009) 094008, arXiv:hep-ph/0902.0459.

[476] Y. Jia, *Which hadronic decay modes are good for η_b searching: Double J/ψ or something else?*, Phys. Rev. D **78** (2008) 054003, arXiv:0611140v2.

[477] S. Barsuk, J. He, E. Kou, and B. Viaud, *Investigating charmonium production at LHC with the p pbar final state*, arXiv:1202.2273.

[478] E598 collaboration, J. J. Aubert *et al.*, *Experimental Observation of a Heavy Particle J*, Phys. Rev. Lett. **33** (1974) 1404.

[479] SLAC-SP-017 collaboration, J. E. Augustin *et al.*, *Discovery of a Narrow Resonance in e+ e- Annihilation*, Phys. Rev. Lett. **33** (1974) 1406.

[480] Belle collaboration, S. K. Choi *et al.*, *Observation of a new narrow charmonium state in exclusive $B^+ \to K^{\pm}\pi^+\pi^- J/\psi$ decays*, Phys. Rev. Lett. **91** (2003) 262001, arXiv:hep-ex/0309032.

[481] BaBar collaboration, B. Aubert *et al.*, *A Study of $B \to X(3872)K$, with $X(3872) \to J/\psi\pi^+\pi^-$*, Phys. Rev. **D77** (2008) 111101, arXiv:0803.2838.

[482] CDF collaboration, D. Acosta *et al.*, *Observation of the narrow state $X(3872) \to J/\psi\pi^+\pi^-$ in $\overline{p}p$ collisions at $\sqrt{s} = 1.96 - TeV$*, Phys. Rev. Lett. **93** (2004) 072001, arXiv:hep-ex/0312021.

[483] D0 collaboration, V. Abazov *et al.*, *Observation and properties of the $X(3872)$ decaying to $J/\psi\pi^+\pi^-$ in $p\bar{p}$ collisions at $\sqrt{s} = 1.96$ TeV*, Phys. Rev. Lett. **93** (2004) 162002, arXiv:hep-ex/0405004.

[484] Belle collaboration, S. K. Choi *et al.*, *Observation of a resonance-like structure in the $\pi^\pm\psi'$ mass distribution in exclusive $B \to K\pi^\pm\psi'$ decays*, Phys. Rev. Lett. **100** (2008) 142001, arXiv:0708.1790.

[485] E. S. Swanson, *The new heavy mesons: A Status report*, Phys. Rept. **429** (2006) 243, arXiv:hep-ph/0601110.

[486] N. V. Drenska, R. Faccini, and A. D. Polosa, *Exotic hadrons with hidden charm and strangeness*, Phys. Rev. **D79** (2009) 077502, arXiv:0902.2803.

[487] M. B. Voloshin, *Charmonium*, Prog. Part. Nucl. Phys. **61** (2008) 455, arXiv:0711.4556.

[488] Belle collaboration, A. Bondar *et al.*, *Observation of two charged bottomonium-like resonances in Y(5S) decays*, Phys. Rev. Lett. **108** (2011) 122001, arXiv:1110.2251.

[489] E. J. Eichten, K. Lane, and C. Quigg, *Charmonium levels near threshold and the narrow state $X(3872) \to \pi^+\pi^- J/\psi$*, Phys. Rev. D **69** (2004) 094019, arXiv:0401210.

[490] R. Balest *et al.*, *Inclusive decays of B mesons to charmonium*, Phys. Rev. D **52** (1995) 2661.

[491] B. Aubert *et al.*, *Study of inclusive production of charmonium mesons in B decays*, Phys. Rev. D **67** (2003) 032002, arXiv:0207097.

[492] C.-H. V. Chang and W.-S. Hou, *Probing for the charm content of B and Υ mesons*, Phys. Rev. D **64** (2001) 071501, arXiv:hep-ph/0101162.

[493] S. Brodsky and F. Navarra, *Looking for exotic multiquark states in nonleptonic B decays*, Physics Letters B **411** (1997) 152 , arXiv:9704348.

[494] T. J. Burns *et al.*, *Momentum distribution of J/ψ in B decays*, Phys. Rev. D **83** (2011) 114029, arXiv:1104.1781.

[495] G. Eilam, M. Ladisa, and Y.-D. Yang, *Study of $B^0 \to J/\psi D^{(*)}$ and $\eta_c D^{(*)}$ in perturbative QCD*, Phys. Rev. D **65** (2002) 037504, arXiv:hep-ph/0107043.

[496] BaBar collaboration, B. Aubert *et al.*, *Evidence for $B^+ \to J/\psi p\overline{\Lambda}$ and search for $B^0 \to J/\psi p\overline{p}$*, Phys. Rev. Lett. **90** (2003) 231801, arXiv:0303036.

[497] Belle collaboration, Q. Xie *et al.*, *Observation of $B^- \to J/\psi\,\Lambda\overline{p}$ and searches for $B^- \to J/\psi\,\Sigma^0\overline{p}$ and $B^0 \to J/\psi\,p\overline{p}$ decays*, Phys. Rev. **D72** (2005) 051105, arXiv:hep-ex/0508011.

[498] LHCb collaboration, R. Aaij *et al.*, *First observation of the decay* $B_c^+ \to J/\psi\pi^+\pi^-\pi^+$, Phys. Rev. Lett. **108** (2012) 251802, arXiv:1204.0079.

[499] G. Altarelli, M. Mangano *et al.*, *Workshop on Standard Model Physics (and more) at the LHC*, Tech. Rep. 200-004, CERN Yellow Report, 2000.

[500] LHCb collaboration, R. Aaij *et al.*, *Measurement of relative branching fractions of B decays to* $\psi(2S)$ *and* J/ψ *mesons*, arXiv:1205.0918.

[501] Y.-N. Gao *et al.*, *Experimental prospects of the* B_c^+ *studies of the LHCb experiment*, Chin. Phys. Lett. **27** (2010) 061302.

[502] I. Gouz *et al.*, *Prospects for the* B_c *studies at LHCb*, Physics of Atomic Nuclei **67** (2004) 1559, arXiv:0211432.

[503] S. Godfrey, *Spectroscopy of* B_c *mesons in the relativized quark model*, Phys. Rev. **D70** (2004) 054017, arXiv:hep-ph/0406228.

[504] V. Kiselev, A. Likhoded, and A. Tkabladze, *B(c) spectroscopy*, Phys. Rev. **D51** (1995) 3613, arXiv:hep-ph/9406339.

[505] R. Dowdall, C. Davies, T. Hammant, and R. Horgan, *Precise heavy-light meson masses and hyperfine splittings from lattice QCD including charm quarks in the sea*, arXiv:1207.5149.

[506] LHCb collaboration, *Measurement of the masses of the* Ξ_b^- *and* Ω_b^-, LHCb-CONF-2011-060.

[507] C.-H. Chang, J.-P. Ma, C.-F. Qiao, and X.-G. Wu, *Hadronic production of the doubly charmed baryon* Ξ_{cc} *with intrinsic charm*, J. Phys. **G34** (2007) 845, arXiv:hep-ph/0610205.

[508] J.-W. Zhang *et al.*, *Hadronic production of the doubly heavy baryon* Ξ_{bc} *at LHC*, Phys. Rev. **D83** (2011) 034026, arXiv:1101.1130.

[509] R. McNulty, *LHCb: tools to incorporate LHCb data in fits*, Working Group on Electroweak precision measurements at the LHC, 2011.

[510] ALEPH collaboration, DELPHI collaboration, L3 collaboration, OPAL collaboration, SLD collaboration, LEP Electroweak Working Group, SLD Electroweak Group, SLD Heavy Flavour Group, *Precision electroweak measurements on the Z resonance*, Phys. Rept. **427** (2006) 257, arXiv:hep-ex/0509008.

[511] J. Rojo, *NNPDF2.3 and inclusion of the LHC data*, PDF4LHC meeting, 2012.

[512] LHCb collaboration, *Inclusive low mass Drell-Yan production in the forward region at* $\sqrt{s} = 7$ *TeV*, LHCb-CONF-2012-013.

[513] ATLAS collaboration, N. Besson *et al.*, *Re-evaluation of the LHC potential for the measurement of M_W*, Eur. Phys. J. **C57** (2008) 627, arXiv:0805.2093.

[514] CDF collaboration, T. Aaltonen *et al.*, *Evidence for a mass-dependent forward-backward asymmetry in top quark pair production*, Phys. Rev. **D83** (2011) 112003, arXiv:1101.0034.

[515] D0 collaboration, V. M. Abazov *et al.*, *Forward-backward asymmetry in top quark-antiquark production*, Phys. Rev. **D84** (2011) 112005, arXiv:1107.4995.

[516] CDF collaboration, Y. Takeuchi *et al.*, CDF Note 10398.

[517] CDF collaboration, T. Schwarz *et al.*, CDF Note 10584.

[518] CDF collaboration, S. Leone, Talk given at Moriond EWK, March 9, 2012.

[519] K. M. Zurek, *TASI 2009 Lectures: Searching for Unexpected Physics at the LHC*, arXiv:1001.2563.

[520] M. J. Strassler and K. M. Zurek, *Echoes of a hidden valley at hadron colliders*, Phys. Lett. **B651** (2007) 374, arXiv:hep-ph/0604261.

[521] L. M. Carpenter, D. E. Kaplan, and E.-J. Rhee, *Reduced fine-tuning in supersymmetry with R-parity violation*, Phys. Rev. Lett. **99** (2007) 211801, arXiv:hep-ph/0607204.

[522] M. J. Strassler and K. M. Zurek, *Discovering the Higgs through highly-displaced vertices*, Phys. Lett. **B661** (2008) 263, arXiv:hep-ph/0605193.

[523] P. Fileviez Perez, S. Spinner, and M. K. Trenkel, *The LSP Stability and New Higgs Signals at the LHC*, Phys. Rev. **D84** (2011) 095028, arXiv:1103.5504.

[524] F. de Campos, O. Eboli, M. Magro, and D. Restrepo, *Searching supersymmetry at the LHCb with displaced vertices*, Phys. Rev. **D79** (2009) 055008, arXiv:0809.0007.

[525] New Physics Working Group, G. Brooijmans *et al.*, *New Physics at the LHC. A Les Houches Report: Physics at TeV Colliders 2009 - New Physics Working Group*, arXiv:1005.1229.

[526] CDF collaboration, T. Aaltonen *et al.*, *Search for exclusive $\gamma\gamma$ production in hadron-hadron collisions*, Phys. Rev. Lett. **99** (2007) 242002, arXiv:0707.2374.

[527] CDF collaboration, T. Aaltonen *et al.*, *Observation of exclusive dijet production at the Fermilab Tevatron $p\bar{p}$ collider*, Phys. Rev. **D77** (2008) 052004, arXiv:0712.0604.

[528] D0 collaboration, V. M. Abazov *et al.*, *High mass exclusive diffractive dijet production in $p\bar{p}$ collisions at $\sqrt{s}$ = 1.96 TeV*, Phys. Lett. **B705** (2011) 193, arXiv:1009.2444.

[529] CDF collaboration, T. Aaltonen *et al.*, *Observation of Exclusive Charmonium Production and $\gamma\gamma \to \mu^+\mu^-$ in $p\overline{p}$ Collisions at $\sqrt{s} = 1.96$ TeV*, Phys. Rev. Lett. **102** (2009) 242001, arXiv:0902.1271.

[530] LHCb collaboration, *Central Exclusive Dimuon Production at $\sqrt{s} = 7$ TeV*, LHCb-CONF-2011-022.

[531] http://projects.hepforge.org/superchic.

[532] J. W. Lamsa and R. Orava, *Central Diffraction at the LHCb*, JINST **4** (2009) P11019, arXiv:0907.3847.

[533] FP420 collaboration, M. G. Albrow *et al.*, *The FP420 RD Project: Higgs and New Physics with forward protons at the LHC*, JINST **4** (2009) T10001, arXiv:0806.0302.

[534] L. Harland-Lang, V. Khoze, M. Ryskin, and W. Stirling, *Standard candle central exclusive processes at the Tevatron and LHC*, Eur. Phys. J. **C69** (2010) 179, arXiv:1005.0695.

[535] S. Heinemeyer *et al.*, *BSM Higgs Physics in the Exclusive Forward Proton Mode at the LHC*, Eur. Phys. J. **C71** (2011) 1649, arXiv:1012.5007.